Does levodopa affect endogenous and exogenous dopaminergic neuron survival?

This thesis is submitted for the degree of Doctor of Philosophy at

Cardiff University

by

Mengru Song

Supervised by

Emma Lane

Mariah Lelos

August 2022

Acknowledgements

Being in Cardiff University for almost 5 years, I feel I have gained so much through this period. I wish to express my gratitude to Emma Lane and Mariah Lelos for their help and support throughout my doctoral program. They gave me carefully, thoughtful and thorough guidance on my PHD projects. Their devotion to science and high-quality style of work benefits me a lot. They have provided me the motivation to move on in difficult times and complete my project.

I am happy to be a member of the Brain Repair Group and also want to say thank you to all the members in the group. Rachel Hills helped me and gave me advice on animal behavior work and also gave me induction in histological lab and microscopy room. She must have my special thanks to all her kind and friendly talks.

Emma Kidd and Youcef Mehellou kindly offered me advice on my paper writing. This helped me to shape my writing in the early stage of my PhD period and made it easier to improve my writing quality.

I would like to thank my family, who gave me so many supports to complete my study. Without their encouragement, it would not be possible for me to study in Cardiff and finish the project.

ABBREVIATIONS

·OH	hydroxyl radical
3-MT	3-methoxytyrosine
3-OMD	3-O-Methyldopa
5-HT	5-hydorxytyptamine or serotonin
6-OHDA	6-hydroxydopamine
AADC	aromatic L-amino acid decarboxylase
AIM	abnormal involuntary movement
ALDH1a1	aldehyde dehydrogenase 1 family, member A1
ATP13A2	the gene encoding a member of the P5 subfamily of ATPases
BBB	blood brain barrier
CB	carotid body
COMT	catechol-O-methyl transferase
CSF	Cerebrospinal fluid
D1 receptor	dopaminergic receptor 1
D2 receptor	dopaminergic receptor 2
DA	dopamine
DAB	3,3'-Diaminobenzidine
DAC	Dopaminochrome
DAergic	dopaminergic
DAT	dopamine transporter
DBS	deep brain stimulation surgery
DJ-1	gene encoding Parkinson disease protein 7
DHI	5,6-dihydroxylindole
DPX	distyrene plasticizer and xylene
EN1	homeobox protein engrailed-1
FOXA2	forkhead box protein A2
GABA	λ amino butyric acid
GDNF	glial cell line-derived neurotrophic factor
GFAP	Glial fibrillary acidic protein
GID	Graft induced dyskinesia
Glu	glutamate
GMP	good manufacturing practice
GPe	the external segment of the Globus Pallidus
GPi	the internal segment of the Globus Pallidus
GSH	glutathione
Hcy	homocysteine
hESCs	human embryonic stem cells
hiPSCs	human induced pluripotent stem cells

HLA	human leukocyte antigen
hPSCs	human pluripotent stem cells
Hunu	human nuclear
HVA	homovanillic acid
Iba1	Ionized calcium binding adaptor molecule 1
i.p.	intraperitoneal
LBs	Lewy bodies
L-DOPA	L-3,4-dihydroxyphenylalanine
LID	L-DOPA-induced dyskinesia
LMX1A	LIM homeobox transcription factor 1, alpha
LNs	Lewy neurites
LRRK2	leucine-rich repeat kinase 2
LS	left side striatum
MAO-B	monoamine oxidase-B
mDA	midbrain DAergic neurons
MHCII	major histocompatibility complex II
MPTP	N-methyl-4-phenyl-1,2,3,6-tetrahydropyridine
MSN	medium spiny neurons
NURR1	Nuclear receptor related 1 protein
$O2^{-\cdot}$	superoxide anion
OCPs	organochlorine pesticides
PARK1	PTEN-induced putative kinase 1
PD	Parkinson's disease
PFFs	pre-formed α-synuclein fibers
PIGD	postural instability/ gait difficulty
PITX3	pituitary homeobox 3
PPN	pedunculopontine nucleus
PQ2+	paraquat
PRKN	the gene encoding ubiquitin-E3-ligase
PSCs	pluripotent stem cells
PTEN	Phosphatase and tensin homolog
rAAV	recombinant adeno-associated virus
Rab7	Ras-related protein 7
ROS	reactive oxygen species
RS	right side striatum
s.c.	subcutaneous
SAH	S-adenosylhomocysteine
SAM	S-adenosylmethionine
SHH	Sonic hedgehog
SN	substantia nigra
SNc	substantia nigra pars compacta

SNCA	α-synuclein gene
SNpr	substantia nigra pars reticulata
SNr	substantial nigra pars reticulate
SOD	superoxide dismutase
SPECT	a single photon emission computed tomography
STN	subthalamic nucleus
TBS	tris-buffered saline
TFs	transcription factors
TH	tyrosine hydroxylase
UPDRS	Unified Parkinson's Disease Rating Scale
UPS	ubiquitin proteasome system
VMAT2	vesicular monoamine transporter 2
VTA	ventral tegmental area
ns	no significance
α-synβ	α-synuclein with β-sheet structure

Abstract

Parkinson's disease is a progressive neurodegenerative disease that has no cure to date. Fortunately, stem cell replacement therapy has now become a promising option that has the potential to greatly restore patient's motor function. However, efforts have to be paid to understand if current golden standard L-DOPA treatment will have negative impact on the novel therapy. Therefore, this study aims to evaluate the effects of L-DOPA on endogenous and exogenous dopaminergic cells.

To evaluate endogenous dopaminergic cells, the classical 6-OHDA rat model was used. The L-DOPA treatment plan was adjusted to faithfully reproduce clinical experiences of PD patients. Behavior and immunohistochemistry analysis were conducted for the evaluation of the results. Overall, the L-DOPA treatment showed no negative influences on the endogenous dopaminergic neuron survival.

Next, 6-OHDA model was used to observe if long-term L-DOPA treatment will influence the survival of exogenous human grafts. Again, the treatment plan was mimicking the real situation which includes the proper use of immunosuppressant and its withdrawal. The results reflected that L-DOPA did not negatively influence exogenous dopaminergic neurons in the absence of immunosuppression.

Lastly, an improved α-synuclein overexpression plus preformed α-synuclein fibril model was used, allowing the progressive feature of PD to be reproduced. This model still aimed to evaluate the impact of L-DOPA on the endogenous dopaminergic neurons, but it provides more information about the interplay between L-DOPA and the neurodegenerative feature of PD. Overall, the results

still indicated that L-DOPA has no negative impact on the dopaminergic neuron survival.

In conclusion, L-DOPA showed no detrimental effects to endogenous and exogenous dopaminergic neuron survival in any of these rat models mentioned above and this provides valuable information for further studies in this aspect.

Table of contents

1. Introduction

1.1. Overview

Parkinson's disease (PD) is a common progressive neurodegenerative disease that has affected more than 6.1 million people worldwide (Dorsey et al. 2018). The burden of PD in society is increasing significantly along with people's growing life expectancy and negative environmental changes (Rocca 2018). PD is also known as shaking palsy of which two major pathological features are defined: the first is the degeneration of dopaminergic (DAergic) neurons especially in the substantia nigra pars compacta (SNc) and the second is the formation of Lewy bodies in the brain, of which a major component is α-synuclein (Schneider and Obeso 2014). The loss of DAergic neurons leads to a dopamine (DA) deficit in the striatum which in turn causes dysfunction in the basal ganglia and is manifested by the patient as motor disorder symptoms (Mehler-Wex et al. 2006). To control the motor function symptoms, dopamine level in the brain must be restored by medication. However, current pharmacological treatments cannot modify disease progression and patients are suffering from various side effects in addition to the disease's symptoms of the disease (Singh et al. 2007).

One of the most pervading questions in Parkinson's, which has remained unresolved for more than 5 decades, is whether levodopa (L-DOPA, chemical name L-3,4-dihydroxyphenylalanine) affects disease progression and the overall survival of DAergic neurons (Ziv et al. 1997; Mytilineou et al. 2003; Sabens et al. 2010; Song et al. 2017). In the context of cell therapy, there is a further question: will L-DOPA affect the survival and differentiation of grafted

stem cells? L-DOPA is the most common and powerful drug currently available to control PD symptoms. Despite the existence of other available drugs, levodopa will eventually be given to nearly all patients with Parkinson's disease in the clinic (LeWitt 2009). This relationship between L-DOPA and DAergic neurons is therefore an unavoidable issue that needs urgent attention and forms the core of this project.

Sustained motor function recovery is becoming more of a reality by recent advances in pluripotent stem cell technology (Yasuhara et al. 2017). International corporations are preparing for large scale generation of stem cell derived grafts in replacement of the lost DAergic neurons in the brain of Parkinson's patients (Studer 2017). As one of the most advanced approaches for the treatment of Parkinson's disease, stem cell-based cell therapies require massive amount of work prior to its approval.

This thesis addresses these critical questions by examining the effect of L-DOPA in two models of Parkinson's disease and one model of cell transplantation of human embryonic stem cells to further understand the role of L-DOPA may play in disease progression and novel therapeutic strategies.

1.2. Parkinson's disease and treatment

Parkinson's disease is a progressive neurological disorder characterized by a series of Parkinsonian syndromes including bradykinesia (slowness of movement), tremor, dementia, progressive supranuclear palsy, multisystem atrophy, etc (Tolosa et al. 2006). Clinically, the diagnosis depends on the patients' manifestations as there is no single definitive test (Jankovic 2008). In fact, patient's syndromes can be quite divergent and there have been rising voices that Parkinson's disease should be more clearly divided into several

subtypes (Berg et al. 2014; Fereshtehnejad et al. 2017). This complication is likely to be caused by multiple underlying mechanisms that may be involved at different stages of Parkinson's disease pathology (Poewe et al. 2017). To date, the proposed mechanisms of cell death mainly include: prion-like behavior of α-synuclein (α-syn) (Kordower et al. 2008), malfunction of mitochondria (Winklhofer and Haass 2010), elevated level of oxidative stress and immune reactions (inflammation) that exacerbate the situation (Houser and Tansey 2017; Caggiu et al. 2019).

Unfortunately, new disease modifying drug candidates which are designed based on these relatively new theories are still under development (Shihabuddin et al. 2018). Currently clinically used drugs are still based on the restoration of the dopaminergic motor circuit, in combination with medication for the non-motor symptoms (psychiatric disorders, sensory malfunctions and autonomic disruptions) (Sveinbjornsdottir 2016).

Despite the decline in efficacy and ability to control symptoms over time, the classical pharmacological treatments remain the mainstream therapy for PD patients (Barker et al. 2015). This is quite important when considering novel treatments as the classical drugs could influence the efficacy. Novel therapies aim to have a long-term benefit for PD patients and improve their life quality. The most promising and achievable strategy is rebuilding the neuronal environment through gene or cell therapy (Hegarty et al. 2014). It can be achieved by nourishing the nigral DAergic neurons or facilitating the regeneration of the damaged axons with growth factors (Axelsen and Woldbye 2018; Niethammer et al. 2018), or by replacing the dead DAergic neurons with functional DAergic cells, which are capable of innervating the brain and restoring dopamine level (Adler et al. 2019; Barker et al. 2019).

1.2.1. Pathology of PD

PD is characterized by two unequivocal features in pathology: the degeneration of DAergic neurons in the SNc and formation of Lewy bodies (Forno 1981). The SNc is an important part of the basal ganglia, a complex that controls motor function. The degeneration of DAergic neurons in the SNc causes dysfunction of basal ganglia and leads to motor function disorders (Dauer and Przedborski 2003).

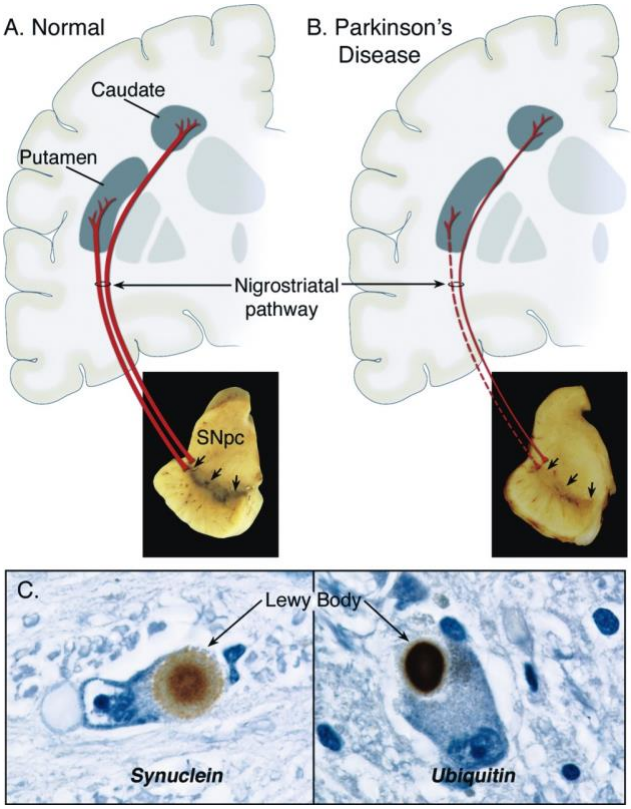

Figure 1-1 Features of PD (Dauer and Przedborski 2003)[1] DA degeneration in the SN(p)c and formation of Lewy bodies. (A) Normally, DAergic neurons in the SN(p)c project fibers to the striatum (putamen and caudate). (B) Under the condition of Parkinson's Disease, nigral DAergic neuron degenerates and DA level reduces in the striatum. (C) Lewy body's major component is α-synuclein but may also contain ubiquitin and other miscellaneous proteins.

[1] These two features must be both found to define a patient with PD, but neither feature is specific.

1.2.1.1. Basal ganglia dysfunction

DAergic neurons from the SNc innervate the putamen and caudate nuclei (striatum), synapsing on the direct and indirect pathways which play a key modifying role on motor activity (Figure 1-1). In the direct pathway, stimulation from the cortex excites the striatum and inhibits the internal segment of the globus pallidus (GPi). GPi suppresses the activity of the thalamus when there is no input from the striatum but releases the brake when the direct pathway gets activated. This allows the activation of the motor cortex and normal motor movements. In the indirect pathway, however, the external segment of the globus pallidus (GPe) is involved. The inhibition of GPe results in the excitement of subthalamic nucleus (STN) which stops the thalamus from sending excitatory signals to the cortex, thus limiting the overall locomotor activity and movement (Figure 1-2) (Calabresi et al. 2014).

The direct pathway and indirect pathway are mediated by GABAergic medium spiny neurons (MSN). They can be divided into MSNs that expresses D1 receptors (direct pathway) and MSN that expresses D2 receptors (indirect pathway) (Gerfen and Surmeier 2011). After DA is released into the cleft, DA acts both on D1 and D2 post synaptic receptors. DA excites D1 receptor-expressing MSCs while inhibits D2 receptor-expressing MSCs. For PD patients, the selective loss of the SNc neurons leads to a decrease of the dopamine level in the striatum and a reduction in the neural activity of the nigral-striatal dopaminergic system. Insufficient activation of D1 receptors reduces the stimulation of striatal input to the GPi in the direct pathway. Furthermore, in the indirect pathway, the inhibitory effect caused by the D2 receptors is increased, resulting in the hyperactivity of the indirect pathway. These pathological changes in the direct and indirect pathway lead to a loss of cortical output and reduced motor function (Cazorla et al. 2015).

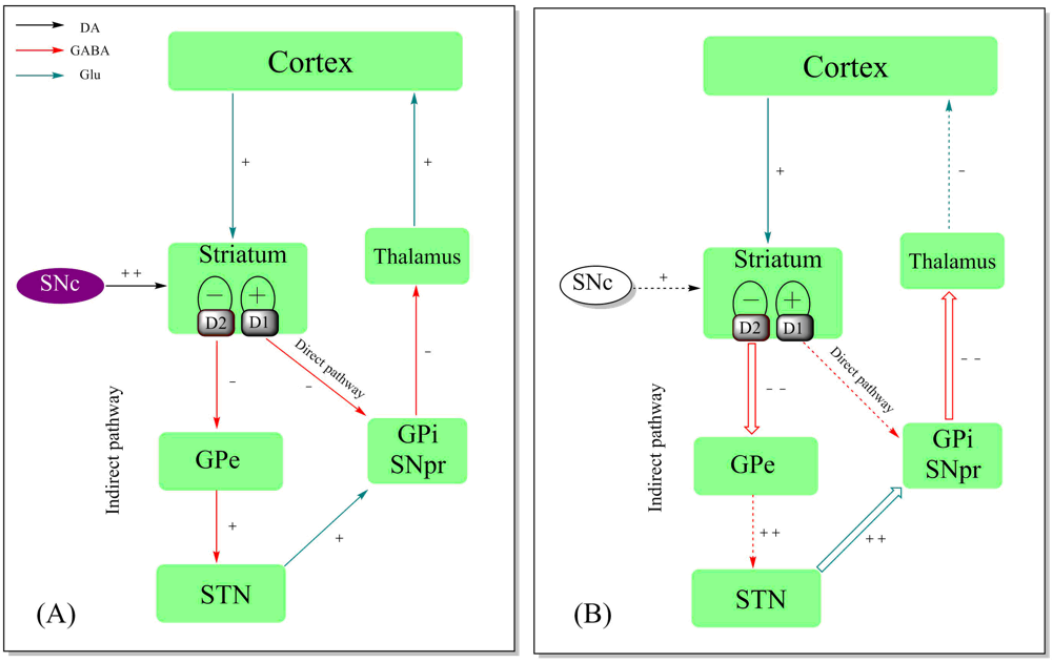

Figure 1-2 Circuit diagram of the direct pathway and indirect pathway of the basal ganglia. SNc can be regarded as filters that finely modulate stimulations from the cortex. Stimulation from the cortex triggers DA release from SNc to the striatum. Once triggered, the direct pathway outputs inhibitory signals to the GABAergic nuclei (GPi and SNpr), allowing motor signals to be sent from thalamus. Indirect pathway counteracts with direct pathway to avoid unwanted movements. (A) Normally, the two pathways are well-balanced. (B) For Parkinson's patient, the degeneration of DAergic neurons in the SNc part leads to DA deficit, resulting in the hyperactivity of the indirect pathway and hypoactivity of the direct pathway. As a result, thalamus receives unnecessary inhibition, and it causes difficulty for motor movements. SNc: substantia nigral pars compacta; GPe: the external segment of the Globus Pallidus; STN: subthalamic nucleus; GPi: the internal segment of the Globus Pallidus; SNpr: substantia nigra pars reticulata; DA: dopamine; GABA: γ-aminobutyric acid; Glu: glutamate; D1: dopaminergic receptor 1; D2: dopaminergic receptor 2. Figure drawn by Chemdraw.

1.2.1.2. Lewy bodies and α-synuclein

The formation of Lewy bodies and Lewy neurites (LNs) is a key pathological feature of PD. Lewy bodies have been found extensively in the central nervous system in Parkinson's patients including the cortex, substantia nigra, hypothalamus and brainstem, but not in the striatum or thalamus (Ohama and

Ikuta 1976; Iannuzzelli et al. 2020). According to Braak, this propagation of Lewy body indicates the progression of Parkinson's disease (Braak et al. 2003): It can be divided into 6 stages and each stage has distinct symptoms related to the nuclei that has been infected by the Lewy bodies (see Figure 1-3): In his theory, the formation of Lewy bodies starts from the enteric nerves system and/or olfactory system (stage 1: hyposmia (inability to smell) and gastrointestinal dysfunction), progresses through the medulla oblongata (stage 2: sleep disorder) and SNc (stage 3: motor function disorders). Then, gradually spreads to the cortex (stage 4: bilateral motor symptoms) and affects cognitive functions (stage 5 and 6: autonomic dysfunction and dementia) (Hawkes et al. 2010).

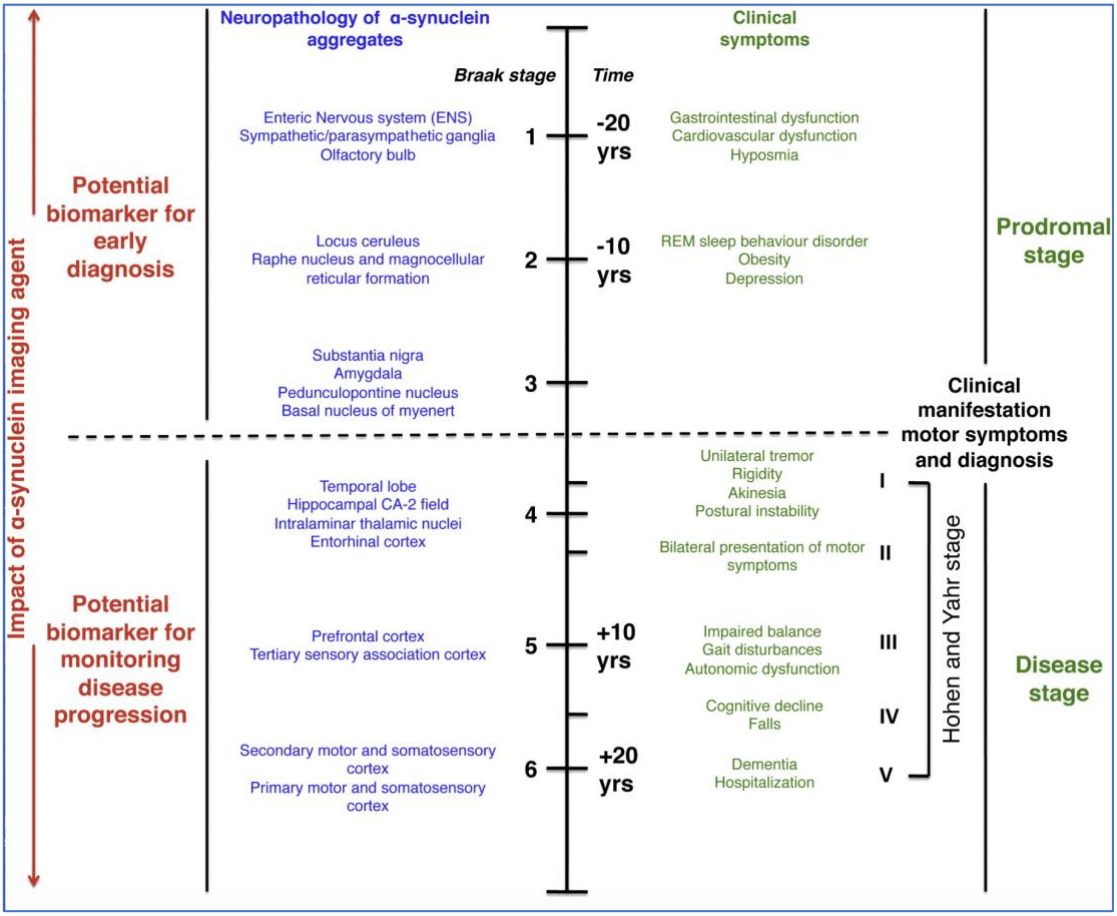

Figure 1-3 Pathology of Lewy bodies with PD development (Hawkes et al. 2010). The timeline of Parkinson's disease based on the distribution of Lewy bodies (abnormal α-synuclein aggregates) in the central nervous system.

This Braak PD stage model is supported by the observation that Lewy body can propagate through the brain (Brundin et al. 2008). Lewy bodies contain a mixture of compounds in which misfolded fibrillar α-synuclein protein is the main component (Uversky 2008). α-synuclein is a highly soluble protein consists of 140 amino acid residues and senses curvature in cell membrane (Snead and Eliezer 2014). Surprisingly, the normal function of α-synuclein under physiological conditions remains unclear. There are many guesses and postulations, but these views have further obscured the situation. Three completely different mainstream theories are: 1. α-synuclein modifies the speed of neurotransmission by acting on the synaptic vesicle transportation (Cheng et al. 2011). 2. α-synuclein forms a chaperone complex by binding to synaptobrevin-2 (Sun et al. 2019). 3. α-synuclein is a ferrireductase that reduces iron (III) to iron (II) (Davies et al. 2011).

Nevertheless, the forming of Lewy bodies appears unrelated to the normal function of a-synuclein. The core of Lewy body is misfolded α-synuclein with β-sheet structure (α-synβ). The misfolded α-synβ core has contagious, prion-like spreading property that can propagate through not only the natural brain tissues (Masuda-Suzukake et al. 2013) but also grafted tissues (Kordower et al. 2008). The marking of α-synβ inclusion by ubiquitin shows that the degradation mechanism failed to process misfolded α-synβ. Post-mortem studies have shown that the ubiquitin-proteasomal system which is normally designated to eliminate misfolded proteins had lost its function in PD (McNaught et al. 2003). Unable to be degraded, the α-synβ proteins can thereafter assemble to oligomers and fibers (Vargas et al. 2019). The exact process of Lewy bodies formation is unfortunately still unclear with even the composition being debated (Lashuel 2020). Consensus over the past few decades was that α-synuclein oligomers and fibers are interfering with their surrounding organelles and cell

membranes, snowballing into an indigestible multi-component complex and slowly killing the cells (Wakabayashi et al. 2007; Volpicelli-Daley et al. 2011; Volpicelli-Daley et al. 2014). Such assumptions were challenged recently by improved light and electron microscopy with super resolution technology and quantitative proteomic analyses. New insights include two major points: First, pre-formed α-synuclein fibers (PFFs) alone can act as seeds to induce Lewy bodies similar to those found in Parkinson's patient, but PFFs are not necessarily included in the Lewy body structure; Second, the formation of Lewy body is an active process that involves selective recruitment and exclusion of cell membrane segments and organelles, change of signaling pathways and alteration of gene expressions (Shahmoradian et al. 2019; Mahul-Mellier et al. 2020). The process depicted by the recent technologies revealed a much more complicated and dynamic process with clear stages and intertwined cellular mechanism than the previous assumed simple aggregation pattern of α-synuclein proteins. It is also one of the reasons why α-synuclein levels challenging to be used as a biomarker for the diagnosis of PD. In fact, α-synuclein levels especially in peripheral blood are found to be unrelated to the disease (Malek et al. 2014; Atik et al. 2016). The dynamic pathological cell environment should be regarded as an indispensable feature as suggested by the new findings.

From high resolution postmortem electron microscope (Figure 1-4), it can be clearly seen that mitochondria and lysosome constituted a part of Lewy body (Shahmoradian et al. 2019). The link between mitochondria and α-synuclein is probably parkin, encoded by PARK2 gene (Miklya et al. 2014). Parkin is an E3 ubiquitin ligase that recognizes synphilin-1, a protein that interacts with α-synuclein. The function of synphilin-1 is not fully understood but it has been shown that the forming of Lewy body inclusion can be assisted by this protein (Engelender et al. 1999). The fact is the ubiquitination of synphilin-1 by parkin

is one of the causes of the formation of Lewy body. All familial-linked mutations of parkin prevents the Lewy body from forming and, as a result, patients who have parkin mutations did not have Lewy bodies in the brain (Chung et al. 2001). The postulation is that α-synuclein aggregates are toxic to mitochondria, causing depolarization of mitochondria membrane (Nakamura et al. 2011). The stressed mitochondria recruit parkin to sit on the mitochondria outer membrane. Parkin then ubiquitinates synphilin-1 (Norris et al. 2015) and physically forms an association among α-synuclein, synphilin-1, parkin and mitochondria.

From Figure 1-4, it can be clearly seen that lysosomes are interacting not with α-synuclein but mitochondria. More precisely speaking, lysosomes are tethered to the mitochondria in the brains of PD patients. Such ‘tethering’ has been found recently as a physiological measure to maintain cellular homeostasis, which is different from mitophagy or lysosomal degradation (Wong et al. 2019). But tethering for an extended period causes problems in PD patients. The master regulator for the untethering mechanism is called Rab7 (Ras-related protein 7) that switches between two forms: Rab7-GTP binding state (active form) or Rab7-GDP binding state (inactive form) (Zhang et al. 2009). Sustaining the active state can be harmful and may result in disrupted mitochondria distribution, damaged mitochondria activity and eventually low ATP level (Kim et al. 2021).

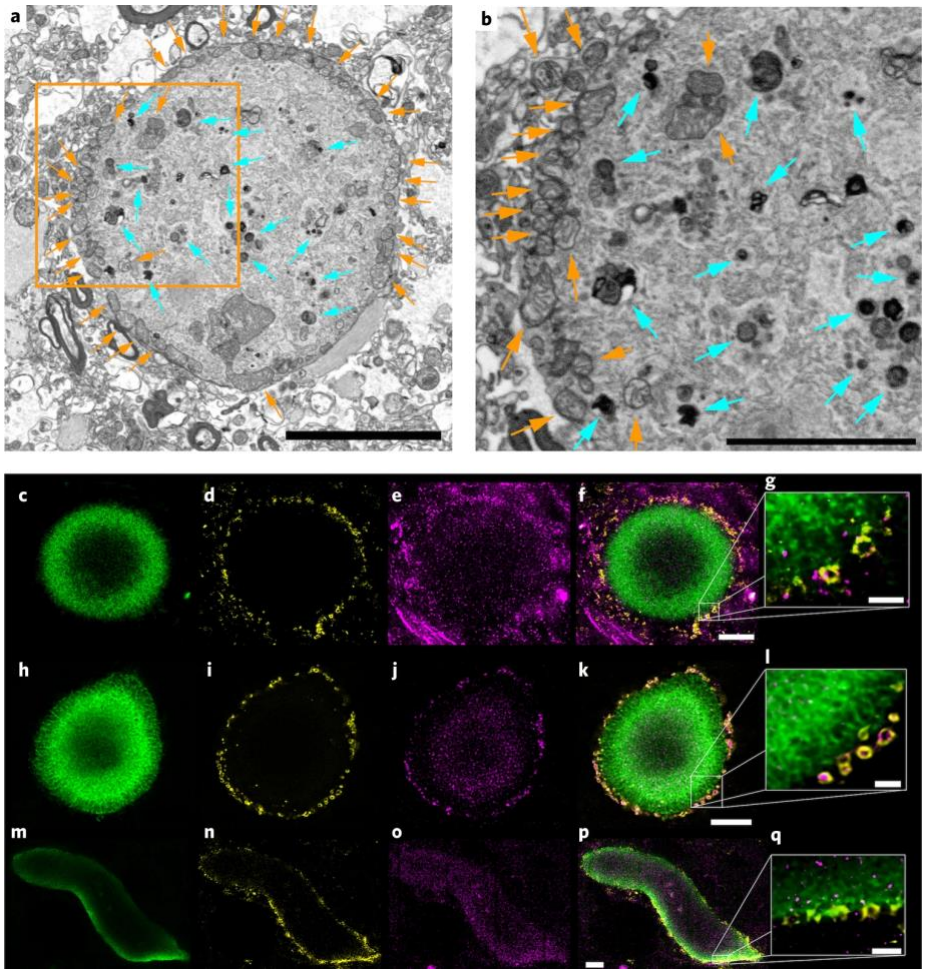

Figure 1-4 High resolution postmortem serial block-face scanning electron microscopic data from Shahmoradian et al. (Shahmoradian et al. 2019). (a, b) It showed that Lewy body included substantial number of mitochondria (orange arrows) and lysosomes (cyan arrows), indicating there is a link among α-synuclein, mitochondria and lysosomes. (c-q) Green fluorescence showed phosphorylated α-synuclein (pS129); Yellow fluorescence showed mitochondria (porin); purple fluorescence for lysosome (LAMP1).

From a recent PFF based *in vitro* study, it was observed that PFF causes Lewy body formation and the death of DAergic neurons started only after the formation of Lewy body. 70 genes related to cell death signaling pathway were upregulated, among which 24 genes were related to apoptosis (Mahul-Mellier et al. 2020). This is in line with postmortem experiment that Lewy body related diseases cause a much higher rate of apoptotic SNc neurons and apoptosis is likely to be the major contributor to sporadic neuronal loss (Tompkins et al.

1997).

To summarize this part, the core information about α-synuclein and Lewy body are listed below: α-synuclein (with β-sheet structure) has been widely recognized as a biomarker for the progression of Parkinson's disease. α-synuclein aggregates into tubular forms (fibers) and physically connects to synphilin-1, parkin, mitochondria and lysosome sequentially. This huge inclusion has a dynamic forming process and is called Lewy body that induces apoptosis to the surrounding neurons.

1.2.2. Etiology of PD

1.2.2.1. Age and gender

Based on the prevalence (the percentage of the population that are affected by PD at different ages) and incidence (the percentage of PD case occurring in one year) of PD, age and gender are the two main contributing factors (Ball et al. 2019). The prevalence and incidence rates significantly increase along with ageing after 55 years old. The prevalence of PD between age 70 and 79 (around 1%) is tenfold higher than that between 50 and 59 (around 0.1%) (Tysnes and Storstein 2017). On the other hand, age-standardized incidence rate between males and females also showed a significant difference, with the incidence and prevalence of male is 1.5 times higher than that of female (Myall et al. 2017).

1.2.2.2. Genetic factors

The percentage of patients with gene mutation(s) across the PD population is

about 10% (Klein and Westenberger 2012). Several genes are causative of familial PD, including SNCA (the gene encoding α-synuclein), LRRK2 (the gene encoding leucine-rich repeat kinase 2), PRKN (the gene encoding ubiquitin-E3-ligase), PARK1 (the gene encoding PTEN-induced putative kinase), DJ-1 (the gene encoding Parkinson disease protein 7) and ATP13A2 (the gene encoding a member of the P5 subfamily of ATPases). Most of the PD related genes are observed from familial PD patients but these genes can also play a key role in sporadic PD (Satake et al. 2009). PD induced by these gene mutations share similar phenotypes though some of them may bear slight differences in the onset age, cognitive deficit, and Lewy body formation (Simon-Sanchez et al. 2009) (Table 1-1) .

Table 1-1. Genes related to PD (Rimoin et al. 2013; Trinh et al. 2014; Funayama et al. 2015; Ishizu et al. 2016; Shulskaya et al. 2018; Youn et al. 2019)

Genetic region	Gene name	Autosomal dominant (D) or autosomal recessive (R)	Early onset (E) or late onset (L)	Gene location
PARK1	SNCA	D	E	4q21-q22
PARK2	Parkin	R	L	6q25.2-q27
PARK3	unconfirmed	D	L	2p13
PARK4	SNCA	D	E	4q21-q23
PARK5	UCHL1	D	L	4p13
PARK6	PINK1	R	E	1p35-p36
PARK7	DJ-1	R	E	1p36
PARK8	LRRK2	D	L	12q12
PARK9	ATP13A2	R	atypical	1p36
PARK10	USP24	D	L	1p32
PARK11	GIGYF2	D	L	2q36-q37
PARK12	unconfirmed	NA[2]	NA	Xq21-q25
PARK13	HTRA2	D	E	2p13
PARK14	PLA2G6	R	L	22q13
PARK15	FBXO7	R	E	22q12-q13
PARK16	unconfirmed	NA	NA	1q32
PARK17	VPS35	D	L	16q11.2
PARK18	EIF4G1	D	L	3q27.1
PARK19	DNAJC6	R	atypical	1p31.3
PARK20	SYNJ1	R	atypical	21q22.11
PARK21	DNAJC13	D	L	3q22.1
PARK22	CHCHD2	D	L	7p11.2
PARK23	VPS13C	D	E	15q22

[2] NA= not available.

1.2.2.2.1. SNCA (PARK1/4)

SNCA gene encodes α-synuclein (Polymeropoulos et al. 1997). Although it has a causal effect in PD (autosomal dominant), most studies have found that the mutations of this gene are rare in both familial and sporadic PD patients (Ahn et al. 2008; Sironi et al. 2010). Multiple forms of SNCA mutations were found and each form influenced the onset age and severity of the motor symptoms and whether non-motor symptoms were accompanied. These mutations include H50Q, A53T, A30P, E46K, duplication and triplication (Kasten and Klein 2013). However, current reports were mostly based on case studies. The phenotypes with SNCA mutation observed in the clinic vary to a considerable extent, ranging from the most classic PD symptoms to nontypical types (Singleton et al. 2013).

1.2.2.2.2. LRRK2 (PARK 8)

The LRRK2 (leucine rich repeat kinase 2, or dardarin) gene encodes a kinase related to the autophagy function of neuronal cells (Alegre-Abarrategui et al. 2009). Mutated LRRK2 (G2019S) abnormally binds to the lysosomal membrane protein LAMP2A and inhibits the association between lysosome and α-synuclein, slowing down the degradation of α-synuclein which facilitates the formation of α-synuclein aggregation (Orenstein et al. 2013). The abnormal LRRK2 gene was presented at a relative high proportion of PD patients, with the most common G2019S variant alone found around 4% in sporadic PD and 7% in familial PD (Paisán‐Ruiz 2009).

1.2.2.2.3. PINK1 (PARK6)

PINK1 encodes PTEN (Phosphatase and tensin homolog)-induced putative kinase, a mitochondrial serine/threonine protein kinase. 1% to 9% of PD cases was related to this gene despite a huge geographical difference between patients from different countries (Klein and Westenberger 2012). PINK1 monitors the membrane potential of mitochondria. Under stable conditions, PINK1 degrades upon entering mitochondria at a fast rate that stops PINK1 accumulation. In contrast, a decreased membrane potential stabilizes PINK1 and leads to parkin phosphorylation in below (PARK2) (Matsuda et al. 2010). PINK1 mutations have a causal effect for PD (Valente et al. 2004), but only homozygous or compound heterozygous mutations increase PD risk (autosomal recessive). Single heterozygous PINK1 variant did not show relationship to increased PD risk (Krohn et al. 2020).

1.2.2.2.4. PARKIN (PARK2)

The PARK2 gene encodes parkin, an E3 ubiquitin ligase. Unlike SNCA or LRRK2 gene, PARK2 is an autosomal recessive gene (Bonifati et al. 2002). More than a hundred mutations of PARK2 have been identified in PD patients, making it difficult to understand the link between specific mutations and PD pathology (Abbas et al. 1999). However, the relationship between parkin and PINK1 (PTEN-induced putative kinase 1) was long discovered. Depolarized mitochondria anchors PINK1 in their outer membrane, which phosphorylates parkin. Parkin then mediates ubiquitination and leads to the degradation of damaged mitochondria (mitophagy) (Park et al. 2006). Mutations of PARK2 or PINK1 gene may therefore disrupt the quality control of mitochondria and exacerbate PD. Unfortunately, this presumption has not been well-supported by *in vivo* or clinical evidence as PD patients with PARK2 or PINK1 mutations

are indistinguishable from sporadic PD patients in clinical symptoms or Lewy body formation (Lücking et al. 2000; Von Coelln et al. 2006).

1.2.2.2.5. DJ-1 (PARK7)

DJ-1 is a neuronal protective protein that responds to increased ROS (reactive oxygen species) levels in cells (Mitsumoto and Nakagawa 2001). One to 2% of sporadic early onset PD cases have been attributed to abnormal DJ-1 (autosomal recessive) (Singleton et al. 2013). A PD related DJ-1 mutation was found to be L166P (Bonifati et al. 2003). This point mutation changes the overall folding shape of DJ-1 and results in a non-functional monomer instead of the usual dimer (Anderson and Daggett 2008). DJ-1 with L166P mutation selectively accumulates in mitochondria, eliciting apoptotic signaling by dissociating apoptotic regulator Bax from Bcl-X_L (Ren et al. 2012). Therefore, the elevated cell death through mitochondrial impairment was thought to be the main contributor to PD pathogenesis in the case of DJ-1 mutation (Wang et al. 2012).

1.2.2.2.6. Other genetic factors

Apart from the most intensively studied genes above, other genes related to PD are also under extensive investigation and one recent Genome-Wide Association Study (GWAS) has revealed 70 genes that are considered as having potential causal effects in PD (Nalls et al. 2019). However, this work at the current stage can only serve as a platform for researchers to prioritize candidate genes and the functions of the majority of those genes remain unclear (Grenn et al. 2020). Furthermore, this meta-analysis identified variants within the non-coding regions. It will also take time to understand how these

loci contribute to the risk of PD (Spisák et al. 2015).

1.2.2.3. Environmental risk

A large cohort study of 143,325 individuals demonstrated that the incidence of PD in people who were exposed to pesticide or herbicide is 1.7% while that in the non-exposed pesticide or herbicide group the incidence is around 1%, which suggests that pesticide or herbicide exposure can increase the risk of PD (Ascherio et al. 2006). The relationship between specific types of pesticide/ herbicide and PD have been widely investigated. Exposure to paraquat, rotenone and organochlorine pesticides (OCPs) were highly suspected to be linked to increased risk of PD. Paraquat （$PQ2^+$, N,N′-dimethyl-4–4′-bipiridinium), is linked to the high prevalence of PD in the regions that used this particular herbicide (Hertzman et al. 1990; Liou et al. 1997). The mechanism of paraquat raising the risk of PD was proposed as follows: Paraquat is converted into PQ^+ before entering human cells. Then, PQ^+ is selectively delivered into DAergic neurons via DAT, which leads to accumulation of PQ^+ in DAergic cells. The accumulation of PQ^+ causes oxidative stress, and eventually DAergic neuron death (Rappold et al. 2011). Rotenone is a mitochondrial complex I inhibitor that can lead to mitochondrial dysfunction and oxidative stress (Testa et al. 2005), which may exacerbate the condition around the DA neurons. *In vivo* evidence shows that after long-term rotenone exposure, some features of PD can be replicated, such as DA neurodegeneration and ubiquitin and α-synuclein positive inclusions (Betarbet et al. 2000). A further experiment from the same group shows parkinsonism induced by rotenone may associate with its negative impacts on the DJ-1, α-synuclein, and the ubiquitin–proteasome system (Betarbet et al. 2006). 61.4% of PD people in a northern region of India region were found to have detectable blood levels of dieldrin, a pesticide in the category of OCP (Singh et al. 2013). *In vitro* and *in vivo* experiments suggest that the role of dieldrin in PD may associate with dieldrin induced oxidative

stress and mitochondrial damage (Kitazawa et al. 2001; Richardson et al. 2006; Schmidt et al. 2017).

1.2.3. PD treatment

1.2.3.1. Current treatment

Currently, most classical PD treatments are focusing on the replacement of DA by 1) replacing DA directly, 2) inhibiting DA metabolism or 3) mimicking the action of DA (Poewe et al. 2017). Accordingly, those categories are called: L-DOPA, MAO inhibitor and DA agonist (Figure 1-5).

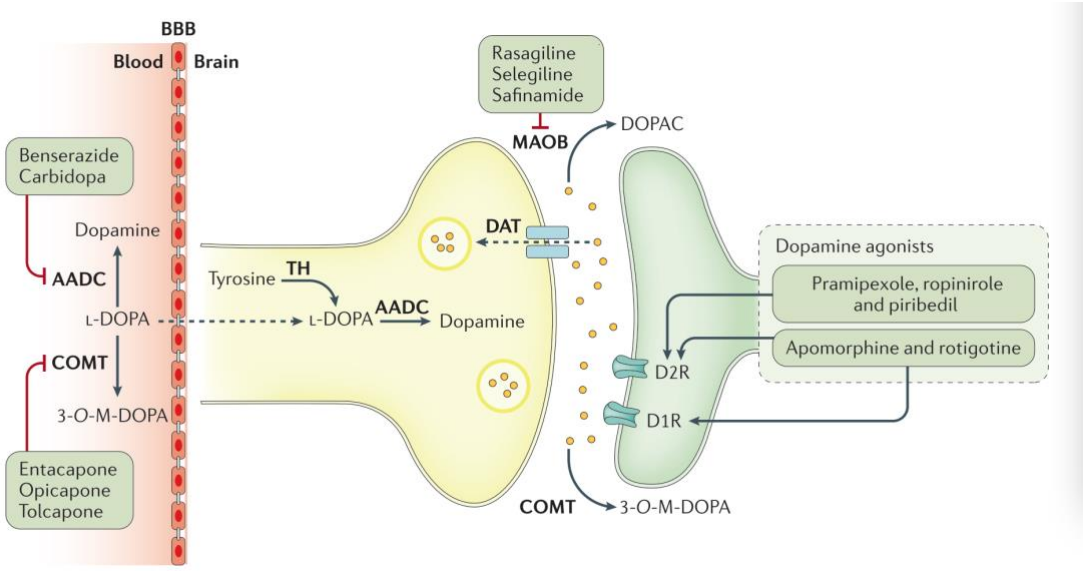

Figure 1-5 Mechanism and target of DA replacement treatment (Poewe et al. 2017). Viewing from left to right. (1) Inhibitors of AADC and COMT prevent L-DOPA breakdowns in the peripheral. Thus, this category promotes L-DOPA transportation through the blood-brain barrier (BBB) and builds up L-DOPA concentration in the brain. L-DOPA can be converted into DA by AADC in the pre-synapse of DA neurons. (2) MAO-B inhibitor allows more DA to be reabsorbed to pre-synapse by slowing down DA breakdown rate in the cleft. (3) DA agonists mimic the function of DA by exciting the DA receptors in the post-synapse. DAT: dopamine transporter; COMT: catechol-O-methyl transferase; MAOB: monoamine oxidase B; AADC: aromatic L-amino acid decarboxylase; D1R: D1 receptors; D2R: D2 receptors

L-DOPA has been used to treat PD since 1961 (Birkmayer and Hornykiewicz 2001). As the precursor of DA, it can be converted into DA by AADC in the brain (Fox et al. 2011). To avoid deactivation by AADC and COMT in the peripheral system, it is always used in combination with peripheral AADC inhibitors (e.g., carbidopa and benserazide) and COMT inhibitors (e.g., entacapone, opicapone and tolcapone)(Barbeau et al. 1972; Zoccolella et al. 2009). However, the efficacy of L-DOPA treatment does not last for long periods. Also, side effects like 'wearing off' effects[3] and L-DOPA induced dyskinesias (LID)[4] are likely to occur (Lane 2019).

DA receptor agonists (e.g., D2 receptor agonists Pramipexole, ropinirole and piribedil; non-selective DA receptors agonist apomorphine and rotigotine) directly act on DA receptors on MSNs to mimic the action of DA in the striatum. DA agonist monotherapy that is used at early stages can relieve PD symptoms and delay the need for L-DOPA treatment (Bonuccelli et al. 2009). The risk of dyskinesia is lower compared to L-DOPA at early stage of PD treatment (Holloway et al. 2004). It can also be used as an adjunctive therapy with L-DOPA to decrease L-DOPA dosage and reduce time of "off phenomenon" (a type of motor fluctuation, in the off-time, L-DOPA cannot control PD symptoms) at the late stage of PD (Stocchi 2009).

MAO-B inhibitors (e.g., selegiline, rasagiline and most recently safinamide) are

---

[3] Also known as "on and off phenomenon". During the "on time", L-DOPA can control PD symptoms while during the "off time", PD symptoms are out of control until the next dose of L-DOPA is given.

[4] A series of involuntary and uncontrollable movement after long-term L-DOPA treatment.

used as a monotherapy at the early stage or as an adjunctive therapy with L-DOPA at the more advanced stage of PD (Rabey et al. 2000). MAO-B is one of the main enzymes engaged in DA metabolism in the brain. After being released into the synaptic cleft, DA can be broken down by MAO-B or be transported back to pre-synapse by dopamine transporters (DAT). The inhibition of MAO-B activity increases DA reabsorption through DAT route and raises presynaptic DA concentration. Monotherapy of MAO-B inhibitors thus improves PD symptoms and delays the administration of L-DOPA (Teo and Ho 2013). At later stage of PD, add-on therapy of MAO-B to L-DOPA (a combination treatment consists of MAO-B inhibitor and L-DOPA) can relieve motor fluctuations and reduce the 'off' phenomenon (Ruggieri et al. 1986).

Deep brain stimulation (DBS) has also been used for the treatment of PD. Abnormal motor symptoms of PD have been considered to be a result from increased activity of the subthalamic nucleus (STN) in the basal ganglia. DBS targeted on the STN to inhibit neuronal activity of the STN via high frequency electrical stimulation and can therefore generate improvement in motor symptoms (Breit et al. 2004).

1.2.3.2. Limitations of current treatment

Unfortunately, most of the current therapies can induce a series of undesirable side effects and significantly influence the quality of life for PD patients. Furthermore, these drugs show less effect on non-motor symptoms control and cannot stop disease progression (Chaudhuri et al. 2006). With DAergic terminal losing over time, even motor symptoms will gradually run out of control (Giguère et al. 2018). Drug induced motor dysfunction also appears at the late stage of PD (Figge et al. 2016).

1.2.3.2.1. L-DOPA

L-DOPA showed benefits on PD symptom control but not for all motor symptoms, for example gait difficulty, tremor and imbalance symptom, which are linked with a loss of cholinergic neurons in the pedunculopontine nucleus (PPN; a brainstem locomotor center) rather than DAergic neuron in SNc (Hirsch et al. 1987; Bohnen et al. 2009; Karachi et al. 2010; Bohnen et al. 2013).

After long term L-DOPA administration, motor fluctuations often occur. These are largely caused by DAergic neuron deficit and the short half-life of L-DOPA (90 minutes) (Thanvi and Lo 2004). Striatal DAergic terminals will gradually lose their ability to store and release DA when PD progresses. Eventually, at the late stage of PD, the striatal DA level will be directly linked to plasma L-DOPA concentration, and this narrows down effective time window of L-DOPA. For PD patients, a gap will appear between two consecutive L-DOPA administrations. Within the effective time window, the symptoms can be controlled so it is called the “on” period; Out of the effective time window the PD symptoms can appear again, and it is called the “off” period (Mena et al. 2009).

LID is a more serious motor fluctuation that may occur in late-stage PD patients after long-term L-DOPA treatment. The occurrence of LID can be as high as 80% after 5 years L-DOPA treatment (Bastide et al. 2015). LID is characterized by a series of involuntary movements, including chorea, dystonia, and athetosis (Pandey and Srivanitchapoom 2017). Although monotherapy of DA receptor agonists and COMT inhibitors can substitute for L-DOPA in the early stages of PD, these drugs alone cannot control the symptoms as the disease progresses and eventually adjunctive L-DOPA is required. At late stage, patients still need to face the risk of LID.

There are two types of dyskinesia; one is peak dose dyskinesias which occurs in the peak plasma dose of L-DOPA; another one is diphasic dyskinesias which occurs at the beginning or the end of L-DOPA administration (Smith et al. 2003). Peak dose LID is associated with pulsatile stimulation of DA receptors by L-DOPA (Arai et al. 1994). It was argued that pre-synaptic and post-synaptic changes may contribute to the hyperstimulation of DAergic receptors. Pre-synaptic hypothesis claims that 5-HT (5-hydroxytryptamine or serotonin) neurons gradually replace the lost DAergic neurons to release DA. At the early stage of PD, the remaining DAergic neurons are still capable of storing and controlling DA release to avoid overstimulation of DAergic receptors in the striatum (regulated DA release; shown in Figure 1-6. A). DA reabsorption through DAT is regulated by D2 auto-receptors. As the disease progresses, the number of D2 auto-receptors in SNc reduces and the capability of DA neurons to convert L-DOPA into DA is similarly reduced. 5-HT neurons have to take over DAergic neurons' role to convert exogenous L-DOPA into DA and store it (Maeda et al. 2005). In this case, DA is accumulated in 5-HT neurons and vesicles, and the level of serotonin in 5-HT neurons is reduced. This causes a disrupted release of transmitters by the 5-HT cells. Under normal conditions, transmitter release is controlled by a negative feedback loop in which 5-HT1B receptors and 5-HT1A receptors senses serotonin release. When DA occupies 5-HT neurons, such feedback is abolished because those receptors can't recognize DA. The consequence is an uncontrollable, fast release of DA (Figure 1-6. B) (Björklund and Stenevi 1979; Perlow et al. 1979). 5-HT theory was supported by the fact that L-DOPA released can be modified by 5-HT1B agonist and 5-HT1A agonist (Figure 1-6. C) (Carta et al. 2007).

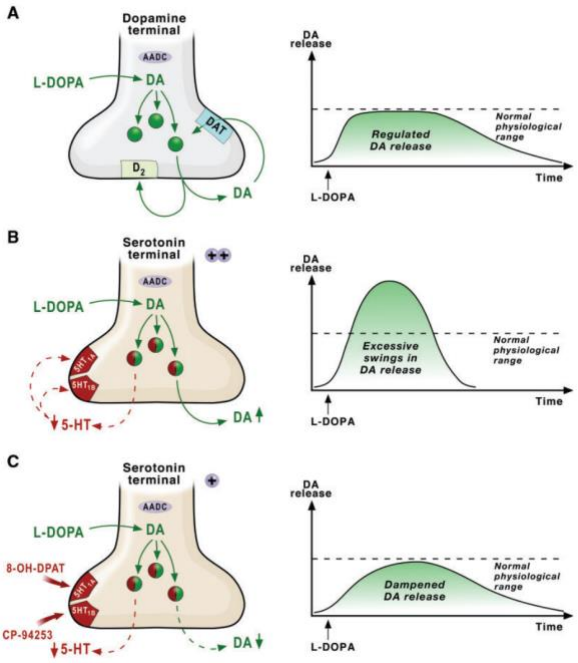

Figure 1-6 Mechanism underlying L-DOPA induced dyskinesia (Carta et al. 2007). (A) Normally, the storage and release of DA is regulated by D2 auto-receptor and DAT on the DAergic neurons. (B). At the late stage of PD, 5-HT neurons replace DAergic neurons and play a major role in DA generation, release and storage. However, there is no D2 auto-receptor or DAT on the 5-HT neurons to control DA release and storage. This results in an uncontrolled DA release (excessive swings). (C). 5-HT agonists (8-OH-DPAT and CP-94253) can activate 5-HT1A and 5-HT1B receptor that control the transmitter release, which reduces DA release in a short period and proved that 5-HT neuron's function.

For post-synaptic changes, with the degeneration of DAergic terminals, the density of D2 receptor increased and D1 receptors on MSN neurons overactivated. As a result, in response to a high level of striatal DA that is released after L-DOPA administration, the direct pathway is over-stimulated, and the indirect pathway is over-inhibited. The effect of L-DOPA on both the direct and indirect pathway eventually causes overactivation of the thalamus and abnormal involuntary movements (Berthet et al. 2009). To be noted, this over-simplified hypothesis did not receive general acceptance (Jenner 2008) and recently dyskinesia has been recognized as a result of PD progression instead of one of the side effects of L-DOPA (Espay et al. 2018).

1.2.3.2.2. L-DOPA metabolism in the brain

The metabolism of L-DOPA involves oxidative products that may negatively affect the surrounding cells. In the brain, there are three metabolic pathways of L-DOPA (Figure 1-7). After the metabolism of L-DOPA, the catecholic compounds can be oxidized into quinone species, which have been shown to be associated with oxidative stress.

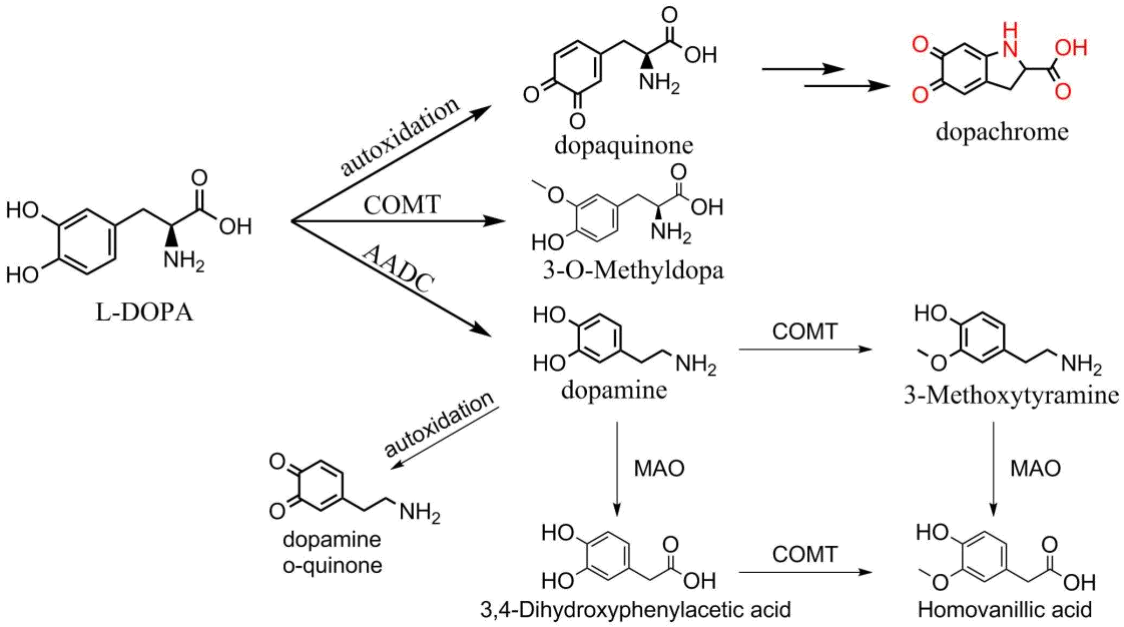

Figure 1-7 The process of L-DOPA metabolism in the brain. L-DOPA can be converted to DA by AADC or be converted to 3-O-Methyldopa (3-OMD) by COMT; DA metabolism mainly involves COMT and MAO. L-DOPA may undergo autoxidation and yield cytotoxic quinones (Graham 1978). DA can either be methylated into 3-methoxytyramine (3-MT) via COMT or oxidized into dihydroxyphenylacetic acid (DOPAC) by MAO. Enzymes are employed sequentially but either one can be used first. The final product of the two processes yields homovanillic acid (HVA) (Eisenhofer et al. 2004). DA may also undergo autoxidation and form toxic quinone species (Fornstedt et al. 1990). Figure drawn by Chemdraw.

Postmortem evidence showed that oxidation levels in the SN of patients with PD was higher than that in non-PD people (Dexter et al. 1989). The presence

of large amount of L-DOPA is suspected to be a contributing factor to the vulnerability of SN DAergic neurons (Lipski et al. 2011). Autooxidation of DA or L-DOPA can generate DA quinone and superoxide anion ($O_2^{-\cdot}$). $O_2^{-\cdot}$ can be catalyzed into H_2O_2 by superoxide dismutase (SOD) and further converted to harmless water by glutathione (GSH). However, in the condition of high level ROS or low level GSH, H_2O_2 are converted to hydroxyl radical (·OH) by metal ions (see Figure 1-8) (Emdadul Haque et al. 2003). All these radicals ($O_2^{-\cdot}$, ·OH) and superoxide (H_2O_2) are ROS and can damage lipids, proteins and DNA, causing cell impairment or death. Administration of L-DOPA therefore has the theoretical potential to increase oxidative stress in DAergic neurons and contribute to their dysfunction or death.

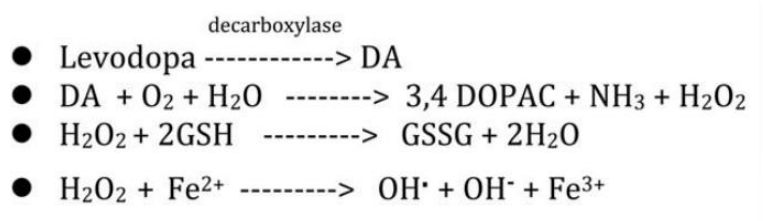

Figure 1-8 Generation of reactive oxidative species from L-DOPA (Olanow 2015). (1) L-DOPA can be converted to DA by decarboxylation. (2) DA may undergo autooxidation to generation H_2O_2. (3) H_2O_2 can be eliminated by glutathione (GSH). (4) DA neurons are rich in iron content which may further exacerbate oxidative stress by generating superoxidative radicals and hydrogen peroxide from Fenton reaction.

Furthermore, L-DOPA can be methylated into 3-O-Methyldopa (3-OMD) by COMT. 3-OMD can damage DAergic cells via oxidative stress, depolarization of mitochondrial membranes and inhibition of astrocyte-mediated dopaminergic neuroprotection (Lee et al. 2008; Asanuma and Miyazaki 2016). The situation maybe further exacerbated by the long half-life of 3-OMD (12-13 hours in the brain) that could lead to 3-OMD accumulation in the brain and cause more damage to brain tissues (Bartholini et al. 1970).

The administration of L-DOPA is also associated with unwanted peripheral

changes such as hyperhomocysteinemia. Although homocysteine (Hcy) acts as an essential intermediate in folate and activated methyl cycles inside cells, elevated extracellular Hcy has been considered a risk factor (Medina et al. 2001). When wrongly picked up during protein synthesis, Hcy can lead to impaired protein functions related to cardiovascular disease, neurodegenerative disease and other pathological changes in humans. Hcy may be generated from methionine after the methylation of L-DOPA or DA, a reaction catalyzed by catechol O-methyltransferase (COMT) (Kumar et al. 2017; Azzini et al. 2020). A clinical study that included 235 patients with PD showed that the increased concentration of Hcy in blood was the result of L-DOPA treatment and implied that it may link to increased risk of cardiovascular diseases, dementia, etc (Rogers et al. 2003). Another clinical investigation suggested that elevated Hcy level worsened the performance of PD patients on neuropsychometric assessment, and the patients were inclined towards depression (O'Suilleabhain et al. 2004b).

1.2.3.2.3. Other anti-Parkinson treatments

DA agonists generally have a longer half-life than L-DOPA so they can be used *de novo* to delay the L-DOPA administration or alongside L-DOPA to reduce the dose of L-DOPA and to prevent dyskinesia but at the same time they bring up other side effects: PD patients may suffer neuropsychiatric symptoms such as sleep disorder, mood changes, or even delusion and hallucination (Bonuccelli et al. 2009). Sleep disorders are also commonly experienced by patients taking COMT and MAOB inhibitors. Sleep attacks (the experience of suddenly falling asleep, even without feeling sleepy or any other signs) is a more serious side effect that can happened in some cases (Paus et al. 2003). Other side effects rarely appear but can be fatal; selegiline can cause hypertensive crisis (Ito et al. 2001) and tolcapone may cause severe liver failure (Borges 2003).

Deep brain stimulation (DBS) is a valuable additional tool alongside medications, especially for advanced Parkinson's experiencing complications associated with the medication. Although the exact underlying mechanism is still under investigation, inhibition of the subthalamic nucleus in the basal ganglia was found to be able to reduce PD symptoms in animal models as well as in humans (Benabid 2003). Similar to the current anti-parkinsons drugs, though, DBS has no effect on disease progression. Data from National Surgical Quality Improvement Program (NSQIP) in North America has even suggested a high rate (24.2%) of revision or removal of DBS devices (Moro 2016). The suboptimal positioning of DBS devices as well as the infections and skin erosions may seriously affect the overall life quality of the recipients and thus limit its usage.

Because of the short control period of PD symptoms and severe side effects of the current treatment, new treatments are in urgent need for PD patients. Gene therapy delivers vector virus which carries key enzyme genes related to DA synthesis into the brain and aims to restore DA level inside the brain to relieve PD motor symptoms (Azzouz et al. 2002; Kaplitt et al. 2007; Mittermeyer et al. 2012). Vector virus with genes encoding glial cell line derived grow factors was also reported to be able to protect the remaining DAergic neurons and slow down disease progression. But the effectiveness of gene therapy is still under debate (Kirik et al. 2017). On one hand, the viral vector may lead to severe immune reactions; On the other hand, modified host genome may increase the risk of abnormal cell development such as tumor (Isacson and Kordower 2008).

1.3. Cell therapy

Some of the key motor deficits of PD are caused by the loss of the midbrain DAergic neurons. Cell therapy directly addresses the problem by replacing the

lost DAergic neurons with transplanted cells. The hypothesis for this therapy is that the transplanted DAergic neurons in striatum can generate functional and histological reinnervation with striatum to rectify dysfunctions caused by deficit DA neurotransmission in the nigrostriatal system and thus relieve PD symptoms (Yasuhara et al. 2017). The year 1979 was the first time when researchers attempted to graft DAergic neuron rich tissues, dopaminergic neuroblasts, into damaged nigrostriatal systems in rat models of PD. The results showed partially restored function in the damaged brain (Perlow et al. 1979). The year 1985 was the first time when cell therapy went into clinical trials: Adrenal medullary tissues (a type of DAergic neuron rich tissue) were transplanted into two PD patients, but only limited clinical improvement was observed (Backlund et al. 1985). Since 1987, fetal midbrain tissue (DA neuron precursors or neuroblasts obtained from fetal midbrain tissues) has been used as the primary source of tissue to transplant into PD patients in clinical trials and has shown advantages over other types of cells like adrenal medulla peripheral nerve or carotid body (CB) glomus cells (Lindvall et al. 1988; Watts et al. 1997; Mínguez-Castellanos et al. 2007). However, serious issues (especially with morality) are bound with fetal midbrain tissues (as discussed in the following section) and limited their use.

1.3.1. Human fetal tissue transplantation

A large amount of data from clinical trials suggest that transplanted fetal tissues can survive, grow, and integrate with original tissues in the host striatum (Kordower et al. 1995). Successful transplantations can restore the function of the striatum and generate long-term clinical benefits, even after L-DOPA withdrawal (Ishii and Eto 2014). The reported case in 1999 showed a significantly relief of the classical PD symptoms (e.g. rigidity, hypokinesia and resting tremor) and drug induced side effects (e.g. ‘on-off’ fluctuations) (Piccini

et al. 1999). Long-term follow-up study also claimed that the clinical benefit had been persistently observed for 18 years in two clinical cases (Kefalopoulou et al. 2014).

Fluorodopa (^{18}F-DOPA) uptake and dopamine release level are indicators for the estimation of the capacity of DA storage. Both indicators were used in separate studies to follow and estimate the clinical outcome of PD patients and it was observed that the estimated DA level was restored to a normal range after receiving graft for around 10 years (Piccini et al. 1999). Furthermore, the development of grafted cells is directly observable from the postmortem cases. A patient who had received graft for 18 months showed the grafted DA neurons survived, developed and innervated to the dorsal half of the putamen (Kordower et al. 1995). The longest case study reported that the grafted cells survived for 24 years (Li et al. 2016).

However, the source of grafting fetal tissues hampers the pace for cell therapy. The fetal mesencephalic tissues from aborted fetuses are limited because of ethical issues and non-unified standards. In many countries and different religions, the use of fetal tissues is prohibited (Boer 1994). As for the quality control, fetal midbrain cells usually cannot meet high quality standards - only a small number of aborted fetuses can be used for transplantation for the following reasons: 1) The age of the embryo is critically important for the success of transplantation: The crown-rump length of embryo must be between 12mm and 28mm. If the crown-rump length of embryo is lesser than 12mm, removing non-neural tissue out can be difficult; If the crown-rump length of embryo is larger than 28mm, the survival rate of DAergic neurons significantly decrease. 2) Part of the midbrain tissues may be destroyed during the surgical termination of pregnancy. 3) For each transplantation surgery, 2-6 embryos are needed. 4) No evidence of sexually transmitted diseases in the mother,

adequate survival of the cells at the time of dissection (Brundin et al. 2010; Ye et al. 2017). All these factors have resulted in the short storage of fetal midbrain tissues and limited large-scale application. For example, many surgeries were planned to be conducted by TRANSEURO research consortium around 2010 while only 20 surgeries were completed due to the short supply (Barker et al. 2017).

1.3.2. Pluripotent stem cells

It was in 1981 when for the first time, ESCs were successfully derived from the mouse inner cell mass of pre-implantation blastocyst (Evans and Kaufman 1981). This type of pluripotent stem cells has shown potential to be induced into various cells under defined conditions while remain immortal if not differentiated (hold the ability to proliferate infinitely). After that, focus has been put to stem cells originated by human tissues. Human pluripotent stem cells (hPSCs) are more likely to become an alternative source for transplantation because of less issues about immunogenicity. Two types of hPSCs are under the consideration of large bio-companies to be used for clinical trials: They are human embryonic stem cells (hESCs) and human induced pluripotent stem cells (hiPSCs, also called reprogrammed adult somatic cells), see Figure 1-9 (Barker et al. 2017).

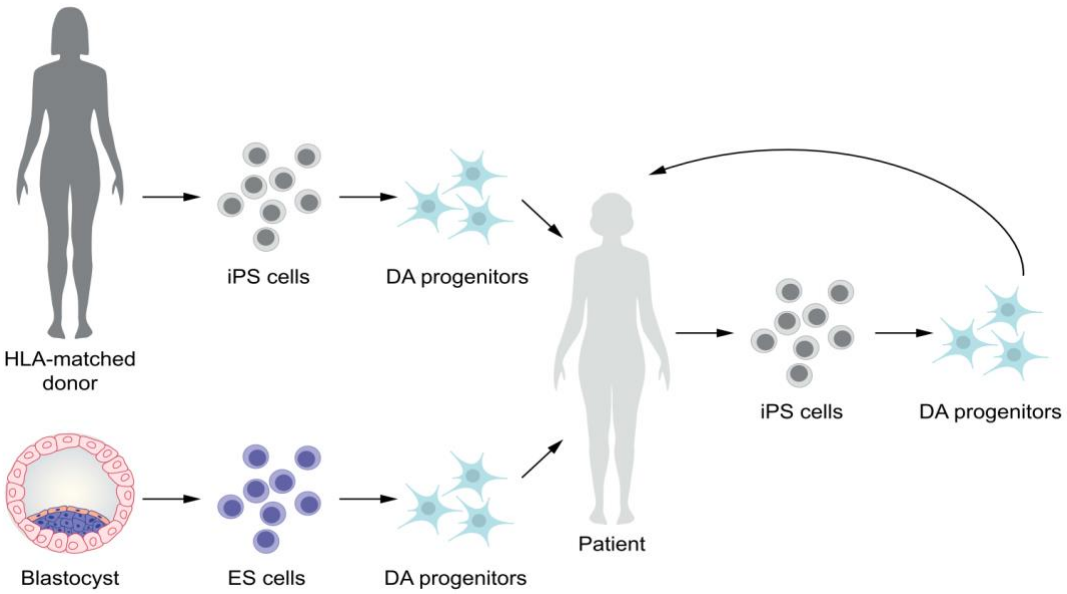

Figure 1-9 Stem cells for clinical trials (Barker et al. 2017). The DA progenitors can be derived from embryonic stem cells or pluripotent stem cells which are induced from HLA-matched donor or autologous cell.

1.3.2.1. hESCs-derived DAergic neurons

In 1998, hESCs were successfully derived from human blastocysts, which paved a way for hPSC based therapy (Thomson et al. 1998). But a successful and reliable induction of hESC into DAergic neurons was not found at the time. DAergic neurons are born and developed in the intermediate vicinity to the human midbrain floor plate and require a specific region where fibroblast growth factor 8 and sonic hedgehog signals overlap, which can be influenced by a bundle of transcription factors, growth factors, signaling pathways (Smidt and Burbach 2007), making it quite challenging to differentiate functional $FOXA2^{+}$ (floor plate marker)/TH^{+} DAergic neurons (Hynes et al. 1995; Kriks et al. 2011). In addition, those generated DAergic neurons must also express midbrain characteristics such as Lmx1a/b, Nurr1, En1 (developmental transcription factors) and electrophysiological properties (Xi et al. 2012). Long term survival of hESC-derived DAergic neurons in animal model was not reported until 2006.

The results showed the precursor of DAergic neurons were converted to DAergic neurons but only partially. It showed this protocol still had risks of tumor development or abnormal cell outgrowth (Roy et al. 2006). Studies that followed identified WNT1-LMX1A (LIM homeobox transcription factor 1, alpha) and SHH-FOXA2 (Sonic hedgehog-forkhead box protein A2) regulatory loops, which are the key pathways involved in the development of midbrain DAergic neurons (mDA). These loops can be manipulated to promote neural differentiation into mature phenotype (Yuan et al. 2015). Based on these, protocols that can reliably produce hESC-DAergic cells were developed. DAergic neuronal progenitors produced under these protocols provided cells with high level of TH and midbrain neuron markers (LMX1 and FOXA2) (Kriks et al. 2011; Kirkeby et al. 2012). Several hESC cell lines are now being produced following the standard protocols under good manufacturing practice (GMP) (Arabadjiev et al. 2010). The efficacy and safety of hESC-DAergic cells had no significant difference to fetal midbrain tissues in the aspects of their phenotypic features and the axonal interaction between grafts and striatum when tested in PD animal model (Grealish et al. 2014).

1.3.2.2. hiPSC-derived DAergic neurons

In 2006, mouse adult fibroblasts were reprogrammed into ESC-like cells, called induced stem cells, by selective expression of several genes (Takahashi and Yamanaka 2006). Four transcription factors Oct3/4, Sox2, c-Myc, and Klf4 in the somatic cells were found to play an important role in maintaining the pluripotency and controlling the expression of other genes (Adachi and Schöler 2012). The forced expression of these four genes can maintain the cells in the pluripotent state. Following this research many human somatic cells were reprogrammed into hiPSCs (Swistowski et al. 2010; Sánchez-Danés et al. 2012). The technique allows allogenic personalized dopaminergic neurons to

be unlimitedly produced from human somatic cells and can theoretically avoid immune reactions. Protocols that were developed by Kriks and Kirkeby have also been used in the induction of hiPSCs into DA neurons (Kriks et al. 2011; Kirkeby et al. 2012). To assess the safety (tumor risk) of the grafted neurons, the size of the graft was monitored in primate PD model. The result showed that the size of the graft had a tendency to increase for 6-9 months, then remained stable (i.e. without sign of overgrowth). The efficacy of grafted cells was assessed by monitoring the functional recovery: Function recovery was observed from month 1 to month 12 without any tumor formation (Kikuchi et al. 2017). In 2020, a case study in the clinic was reported. The patient received hiPSC implantation without the need for any immunosuppression. The graft growth was monitored by positron emission tomography (PET) and it was shown that the grafted cell survived for 2 years, with observable improvement in the motor functions. No adverse impact was found in this case study (Schweitzer et al. 2020). These studies provided persuasive evidence that hiPSC-derived DA neurons are efficacious and safe.

1.4. Animal models for PD

1.4.1. 6-OHDA animal model

Injecting 6-hydroxydopamine (6-OHDA) into nigrostriatal pathways has been the most classical way to build rodent models of PD that have functional deficits, for the study of symptomatic interventions. In 1968, Ungerstedt identified that 6-OHDA can cause the depletion of DA neurons in the brain selectively and this could be used to create animal models (Ungerstedt 1968; Luthman et al. 1989). DA neurons can be selectively targeted because 6-OHDA once injected into the brain will be transported into cell plasma via DA and noradrenaline (NA) transporter (Sauer and Oertel 1994; Stott and Barker 2014). The subsequent

depletion of DA neurons is likely to be caused by oxidative stress from 6-OHDA metabolites (Rodriguez-Pallares et al. 2007).

Unilateral lesion of nigrostriatal pathways is the most common way to build 6-OHDA animal models, while bilateral 6-OHDA lesion can increase risks of bradykinesia (slowness of movement), aphagia (inability to swallow) or adipsia (lack of thirst) (Deumens et al. 2002; Quiroga-Varela et al. 2017). Therefore, bilateral 6-OHDA lesioned rats need special care while post-surgically the unilateral lesioned rats experience no problems fulfilling their own basic needs (feeding and drinking), which is more desirable when creating or using animal models.

In the nigrostriatal dopaminergic pathway, the fibers of DA neurons are projected from the SNc, through medial forebrain bundle (MFB) and to dorsal striatum. Therefore, those three sites are commonly used for 6-OHDA lesions (Figure 1-10 and table 1-2): (1) 6-OHDA striatum lesioned animal model is a type of terminal lesion model that leads to retrograded degeneration of DAergic neurons. For example, administration of 6-OHDA (28μg) resulted in the DA fiber depletion first, then the degeneration of the cell body of DAergic neuron; Around 60% of DAergic neurons in the SNc can be lost at the end of two weeks (Walsh et al. 2011). (2) 6-OHDA MFB lesioned model is usually used as a complete lesion model that can be generated by the administration of high doses of 6-OHDA (e.g. 16μg and 12μg). If a partial lesion is desired, the dose of 6-OHDA need to be lower. (3) For the SNc 6-OHDA lesion model, the lesion degree of DAergic neurons in SNc is dose-dependent as well (Carman et al. 1991; Bruet et al. 2001; Datla et al. 2001). The advantage of using an MFB lesion is that neither striatum nor SNc will be physically damaged following the 6-OHDA injection, which is especially suitable for the study of cell therapies. Notably, although 6-OHDA lesioned model can mimic the decrease of DAergic fiber

density in dorsal striatum and the number of DAergic neurons in SNc, the mechanism of DAergic neuronal death is far different from the slow natural process of PD and cannot reproduce Lewy bodies formation (discussed in more details in Chapter 5) (Walsh et al. 2011).

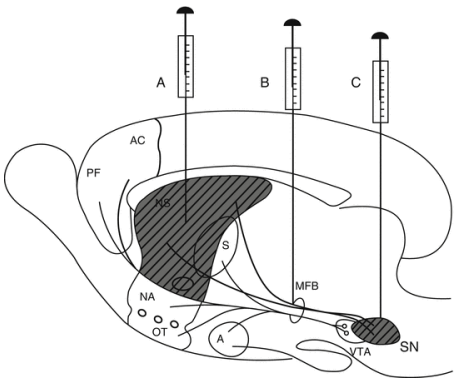

Figure 1-10 Three most common 6-OHDA lesioned sites (Walz 2016). A:striatum B: MFB; medial forebrain bundle C: SN; substantial nigra

Table 1-2 6-OHDA lesioned PD model

Lesion sites	Quantity/ volume	Species	DA neuron lost	References
Medial brain bundle	16μg/4μl	rat	Over 95% SN	(Truong et al. 2006)
	12μg/3μl	rat	Over 90% SN	(Walsh et al. 2011)
	8μg/4μl	rat	90% SN and 39%VTA	(Carman et al. 1991)
	8μg/4μl	rat	86% SN	(Truong et al. 2006)
	4μg /4μl	rat	35% SN	(Truong et al. 2006)
Striatum	28μg/12μl	rat	60% of SN	(Walsh et al. 2011)
Substantia nigra	8μg/4μl	rat	88% SN and 31% VTA	(Carman et al. 1991)
	8μg/4μl	rat	69% SN	(Datla et al. 2001)
	3μg/1μl	rat	40-60% SN	(Bruet et al. 2001)

The drug-induced rotation test is widely used to estimate the degree of lesion of individual animal in the unilateral 6-OHDA lesion models. Drug induced

rotation was at first observed in healthy rats in 1966 (Andén et al. 1966). The rotation of healthy rats was induced by high doses of amphetamine which stimulated DA release from the DAergic terminal in the striatum and lead to the activation of motor activity. The high dose of amphetamine causes unbalanced release of DA in striatum between two hemispheres (as there is a slight difference in the number of DAergic neurons from the two hemispheres in a healthy nigrostriatal system) and the unbalanced stimulation of striatum will finally lead to motor imbalance. Amphetamine and apomorphine-induced rotation in the unilateral lesion model were built on the same theory.

The mechanism of amphetamine induced rotation is shown in Figure 1-11: When the right-side nigrostriatal system is destroyed by 6-OHDA, the number of DA neurons in the lesioned side is decreased. After amphetamine (DA release stimulator) is given, the release of DA in the intact side will be much more than that in the lesioned side, driving motor activity and lead to a rotation bias towards the side ipsilateral to the lesion (Figure 1-11a).

The mechanism of apomorphine induced rotation (the case with low doses of apomorphine) is as follows: As the DA release in the right side is decreased, the D1 receptors on the ipsilateral striatum are upregulated. After apomorphine (DAergic receptor agonist) is given, the response of DAergic receptors to apomorphine in the lesioned side is therefore stronger that in the intact side and lead to a rotation towards the side contralateral to the lesion (Figure 1-11b).

A threshold was used to estimate the degree of SNc lesion (Torres et al. 2011). The number of rotations was recorded for 90 minutes after 2.5 mg/kg amphetamine was injected in rats. If rats show $\geq$6 full body turns/min towards one side (clock-wise or anti-clock wise), it indicates 90% of DA neurons in the SNc was lost (Volpicelli-Daley et al. 2011).

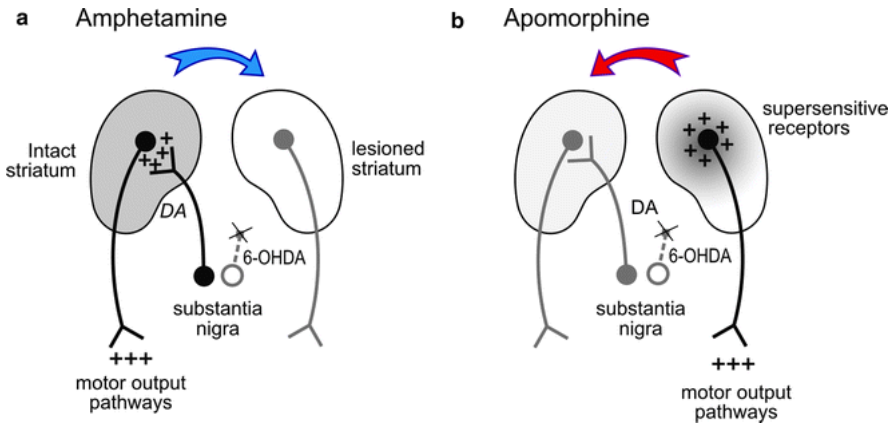

Figure 1-11 (a) Amphetamine induced rotation (Lindgren and Lane 2011): amphetamine induces DA efflux from DAergic terminal of intact side and induce a rotation towards the side ipsilateral to the lesion (b) apomorphine induced rotation: apomorphine directly stimulates supersensitive receptors on the lesioned side and induce a rotation towards the side contralateral to the lesion

1.4.2. α-Synuclein-based Animal Models of Parkinson's Disease

Ideally, a successful PD model should replicate not only PD symptoms but also key pathological features and accurately predict the effectiveness of treatment. Neurotoxin-based PD models contributed a lot in the past to predict the effectiveness of various treatments in the regard of motor symptoms control since the models were quite successful in the reproduction of PD motor symptoms by depleting DAergic neurons in the SNc. However, α-synuclein accumulation and Lewy body formation, an important feature of PD, cannot be reproduced by these models and this may contribute to the lack of translation of potential neuroprotective therapies from lab to clinical trial. For example, in the case of glial cell line-derived neurotrophic factor (GDNF) study, GDNF showed a protective action against 6-OHDA in a preclinical experiment by using toxin-based PD model, but this result is not consistent with the result from α-synuclein animal model and clinical trials (Decressac et al. 2011). Some promising results from open label studies were not replicated in placebo-controlled studies and no clinical improvements were seen from a more recent

trial (Marks et al. 2010; Whone et al. 2019). One possibility is that the overexpression of α-synuclein can block intracellular response to GDNF in DAergic neurons and neutralize the function of neuroprotective agent (Decressac et al. 2012). Collectively, recent reports suggest that neurotoxin-based PD model has its limitation in the application to novel PD treatments and it is essential to develop a more advanced α-synuclein-based PD model. There are currently two mainstream methods for building an α-synuclein PD model (Klein et al. 1998; Masliah et al. 2000):

(1) α-synuclein gene over-expression model using recombinant adeno-associated viruses (rAAV).
(2) α-synuclein fibril model using α-synuclein fibrils (theories were mentioned in introduction part 1.2.1.2.).

Mutation and multiplication of SNCA gene have been identified as causes of familial PD. Based on these discoveries, novel α-synuclein-based PD models were developed by the overexpression of mutated or wild-type SNCA gene. Recombinant adeno-associated virus (rAAV) is commonly used as a carrier to transduce mutated gene or wild-type gene into DAergic neurons in the midbrain. One advantage of rAAV is that rAAV can selectively deliver α-synuclein to the SNc (high tropism) (Ulusoy et al. 2010). α-synuclein A53T mutation can generate more insoluble inclusions and can cause more DAergic loss (~35% in 6 months) than wild-type α-synuclein gene and it's often used to produce a more severe PD model (Chen et al. 2015; Lu et al. 2015).

Unlike neurotoxin-based PD models, α-synuclein overexpression models cause progressive degeneration of the DAergic neuron body and axons (Kirik et al. 2002; Klein et al. 2002). While a progressive PD model is desirable, the variability in the results impeded the use of such models. Early data suggest that the nigral cell lose observed from rats in the group receiving nigral induction

of AAV-mediated α-synuclein gene were between 30% to 80% at 8 weeks after injection, while the behavior impairment was only found in the rats with at least 50-60% of DAergic neuron lost (Kirik et al. 2002). The failure to induce stable DAergic neuron lose in these models led to non-reproducible motor performances and limited their usage. Fortunately, recent studies have improved the method and satisfactory results were obtained. For instance, the intra-nigral injection of rAAV2/7-mediated A53T α-synuclein caused 80% of DAergic neuron lose in the SNc after 6 weeks (Van der Perren et al. 2016).

1.5 Aims and objectives

Despite the efforts to replicate the features of Parkinson's disease in animal models, the preclinical settings were usually unable to reflect the clinical situation. To more precisely evaluate the impact of L-DOPA on the endogenous and exogenous DAergic neurons and to provide useful information more related to PD patients with long-term L-DOPA treatment, this thesis aims to explore the effect of L-DOPA on DAergic neuron survival on improved 6-OHDA and α-synuclein PD rat models. The dosage and frequency of L-DOPA treatment were reconsidered to better mimic clinical L-DOPA usage in all experimental chapters, alongside with other improvements (like immunosuppression regimen in Chapter 4).

The hypothesis of the thesis is that L-DOPA may affect endogenous and exogenous DAergic neuronal survival and has been addressed by the following objectives:

Chapter 3 – Aims to characterize the effects of bidaily L-DOPA in our 6-OHDA lesioned rat model

- To assess the effects of L-DOPA on both the intact side and lesioned

side of the midbrain following twice daily L-DOPA in the 6-OHDA rat model.

- To assess if this L-DOPA regimen induces striatal inflammatory responses.
- To assess the change of Hcy levels in the peripheral system in response to L-DOPA.

Chapter 4 - Aims to determine the effect of bidaily L-DOPA on the survival of hESC derived cell transplants in the absence of immunosuppression.

- To assess the impact of the graft on motor and behavioral recovery in the presence and absence of L-DOPA.
- To assess the impact of the graft on the severity of LID.
- To characterize the histological features of the graft and the endogenous DAergic neurons in the presence and absence of L-DOPA.
- Utilizing MRI scanning to allow visualization of the graft prior to withdrawal of immunosuppression and determine the viability of this approach to detecting surviving grafts.
- To assess the immune response induced by the graft after the withdrawal of immunosuppression in the presence and absence of L-DOPA.

Chapter 5 – Aims to determine whether twice daily L-DOPA treatment influences the toxicity of α-synuclein in α-synuclein viral vector rat model and α-synuclein viral vector + preformed fibril combined model.

- To assess and compare the impact of L-DOPA on DAergic neuron survival in both models.
- To assess the behavioral changes in both models.
- To assess if L-DOPA treatment influences the immune responses in the brain.

2. General methods

2.1. Animals and materials

Adult Sprague Dawley rats (Charles River, UK) were housed in groups of three to four per cage and maintained on a 12: 12-h light/dark cycle. The room temperature was controlled at 20 °C. Rats had free access to food and water during the experiment. All experiments were conducted in compliance with the UK Animals (Scientific Procedures) Act 1986 under Home Office License No. 30/3316 and with the approval of the local Cardiff University Ethics Review Committee. 6-OHDA hydrobromide (H116-5mg), L-DOPA (D1507-5GM) and benserazide (B7283-5GM) were obtained from Sigma. Sodium pentobarbital was obtained from Merial, UK. Isoflurane (P1274) was from Thermofisher Scientific. ABC protein assay kit (A-11037) was from Thermofisher Scientific, Homocysteine (Hcy) ELISA Kit (ABIN457241) was from Antibodies.com.

2.2. Surgical procedure

All the surgeries were carried out under 2-5% isoflurane anesthesia (4-5% for induction; 2-3% for maintenance) which was carried by a mixture of oxygen and nitrous oxide in a proportion of 2:1. After incisions were sutured by Vicyl 4-0 sutures, 30 µl Metacam (5 mg/ml, Boehringer Ingelheim, Germany) and 5ml 0.9% saline containing glucose (20%) were subcutaneously injected into the rats to alleviate pain and prevent postoperative dehydration respectively. Then, the rats were placed in heated chambers (30°C) for recovery. When the rats could right themselves, they were moved back to cages. The health condition and weight change of the rats were monitored daily for one week and then twice per week till the end of the experiment.

2.2.1. Stereotaxic surgery

A stereotaxic frame is a tool used to accurately locate the discrete regions of the brain by knowing their spatial relationships to visible landmarks (JoVE Science Education Database, 2018). It allows us to make lesions or other acts by using three dimensional axes. There are three set of axes to describe the direction of the brain, anterior-posterior, medial-lateral and dorsal-ventral. The stereotaxic frame is consisted of the main frame, the micromanipulators and the probe holder. Incisor and ear bars in the main frame are used to fix the head of an animal. The movement of surgical drill can be precisely controlled by the micromanipulator to targeted coordinates. The sliding Vernier scales on the micromanipulator is used for exact distance measures in three dimensions.

After the shaved rats were held and placed on the stereotaxic frame, front teeth were placed in the incisor bars followed by the ear bars were placed in the ears of rats. The anteroposterior coordinate was measured from landmarks on the skulls. Orientation of target is based on stereotaxic atlas and landmarks. Bregma and lambdoid are the most common landmarks, they are formed by intersections of bone plates. Bregma is the point of intersection of the sagittal suture with the coronal suture. Lambda is at the posterior of the skull and is the point of intersection of sagittal suture and lambdoid suture.

The skull was exposed after the skin was incised with a scalpel. The bregma is used as a landmark and medio-lateral and antero-posterior coordinates were measured. Based on the target coordinates from brain atlas, the target coordinates were calculated. This position was marked on the skull and a drill was used to carefully make a hole in the bone. After dura was found under the skull, the driller was replaced by an injection needle. The tip of the needle placed on the micromanipulator arm was placed on the surface of dura, and the

dorsoventral coordinate was recorded. Finally, the tip of needle was placed into the position to the target dorsoventral coordinate, followed by injection.

2.2.2. 6-OHDA lesioned surgery

Sham and 6-OHDA lesioned surgery were conducted on stereotaxic instrument. 3 µl of 4 µg/µl 6-OHDA or saline (0.9% NaCl) was perfused into medial forebrain bundle (Anteroposterior：−4.4 mm from bregma, Lateral：−1.0 mm from bregma, Dorsoventral: −7.8 mm below dura) of the right hemisphere by using a 10 µl Hamilton Syringe (Hamilton, Germany) at a rate of 1µl/min with a 30-gauge metal cannula. 6-OHDA solution was kept in foil covered tubes on ice. After injection of 6-OHDA or saline into the MFB, the cannula was left in the tissue for 2 minutes for 6-OHDA diffusion.

2.3. L-DOPA treatment

L-3,4-Dihydroxyphenylalainine Methylester (L-DOPA) plus benserazide hydrochloride in saline (0.9% NaCl) was injected into L-DOPA treated group twice a day subcutaneously. The doses of L-DOPA and benserazide were described in the method of each chapter. The saline treated group received daily injection with saline twice a day (0.9%, 1 ml/kg) subcutaneously.

2.4. Behavior assessment

2.4.1. Amphetamine induced rotation

Amphetamine-induced rotations were recorded by automated rotometer bowls

for 90 minutes immediately after 2.5 mg/kg methamphetamine hydrochloride injection via i.p. (Sigma-Aldrich, UK). Two to three weeks after 6-OHDA lesions, rats that showed ≥6 full body turns per min towards the direction that was ipsilateral to the lesion were selected for the following steps. Data are presented as average full body rotations (Ungerstedt and Arbuthnott 1970).

2.4.2. Apomorphine rotation test

Apomorphine induced rotations were recorded by automated rotometer bowls for 60 minutes after fresh apomorphine solution (0.05 mg/kg in saline; Sigma–Aldrich) was injected via subcutaneously (s.c.). Data are presented as average full body rotations (Ungerstedt and Arbuthnott 1970).

2.4.3. Stepping test

The stepping test is used to assess to asymmetry forelimb motor function. The assessment was conducted in a flat surface of a bench. At the start of this test, a rat was lifted on the bench for 3 seconds. The body and hind limb were held and supported by the researcher to allow the tested forelimb rat to touch on the table. The rats were forced to move forwards and backwards at a distance of 1 meter over 10 seconds. The number of forelimb touch on the surface was recorded accordingly (Olsson et al. 1995).

2.4.4. Whisker test

Whisker test is used to assess the asymmetry ability of forelimb in response to touch stimulation. The sensorimotor function of contralateral side to lesion was damaged after 6-OHDA infusion. During the test, the body and hind limbs of a rat were held by a researcher. An untested forelimb was restrained, and a tested

forelimb was allowed to hang freely. The rat was moved slowly upwards from bench and let whisker brush the edge of bench. The trial was repeated 10 times on each side of whisker. An ipsilateral paw was flexibly placed on the bench top in response to stimulation of whisker. Success placements of the lesioned paw were counted (Schallert et al. 2000).

2.4.5. Cylinder test

Cylinder test is used to test paw preference in a novel environment. A rat was placed inside a perspex cylinder with a diameter of 33.5 cm and a height of 19 cm. Two mirrors were placed behind the cylinder at 60° to create a 360° view for observer. The whole process was recorded by camera. In the first 20 times of paw touch, the number of paw use from lesioned side and intact side was recorded (Schallert et al. 2000).

2.4.6. Abnormal involuntary movement rate scales（AIMs）

After L-DOPA injection, the rat was put into an activity box and observed for 3 hours. AIMs is used to evaluate the degree of L-DOPA induced dyskinesia (Breger 2013). AIMs were measured twice a week throughout the L-DOPA administration period. The AIMs were evaluated by observing the maximum severity and duration of abnormal movement of body axis, forelimb, orofacial muscle and hindlimb over a 1-minute observation period every 20 minutes (Figure 2-1). A scoring system (from 0 to 4) was used to represent the degree of severity and duration of dyskinesia, see table 2-1. The maximum severity and duration of body axis, forelimb, orofacial muscle and locomotion were recorded respectively.

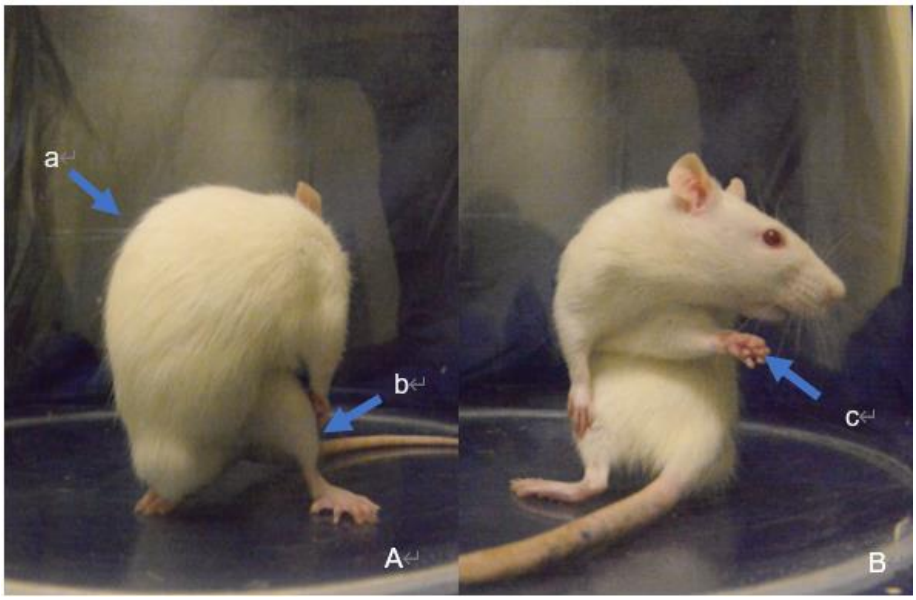

Figure 2-1 the typical posture of rat with L-DOPA induced dyskinesia A(back) and B(front). a. Abnormally twisted body, showing axial dyskinesia. b. Stretched hind limb. c. Translocation of left forelimb.

Table 2-1 The AIM scale is described by Breger (Breger 2013).

AIM subtype	Amplitude Score Locomotive	Duration score
Locomotive	None	0 = absent 1 = occasional (<30 seconds) 2 = frequent (>30 seconds) 3 = continuous but interrupted by sensory distraction 4 = continuous, severe, not interrupted by sensory distraction
Axial dystonia	1 = lateral deviation of head and neck (<30°) 2 = lateral deviation of head and neck (30°-60°) 3 = lateral deviation or torsion of head, neck and upper trunk (60°- 90°) 4 = torsion of neck and trunk at (>90°), causing the rat to lose balance	
Orolingual dyskinesia	1 = jaw movements, facial grimacing 2 = tongue protrusion	
Forelimb dyskinesia	1 = tiny oscillatory movements of the paw and the distal forelimb around a fixed position 2 = movements of low amplitude but causing visible translocation of both distal and proximal limb 3 = translocation of the whole limb with visible contraction of shoulder muscles 4 = vigorous limb and shoulder movements of maximal amplitude	
Hindlimb dyskinesia	1 = abnormal posturing of limb 2 = sustained posturing of limb, mildly extended in abnormal posture 3 = severely hyperextended in abnormal position 4 = hind limb fully extended, causing the rat to lose balance	

2.5. Tissue preparation

Rats were terminally anesthetized with 100mg/kg of sodium pentobarbital (i.p., Euthatal, Merial, UK). The thoracic cavity of the rats was opened to expose the heart. Blood was collected by 5ml syringe (26 g) from the hearts. The collected blood was stored in the EDTA-containing tube on ice. After ascending aorta was clamped and the rats were perfused with prewash solution (1.8% Di-Sodium hydrogen phosphate, 0.9% sodium chloride in distilled water; PH 7.3) for 2 minutes and 4% paraformaldehyde (4% PFA in prewash solution; PH7.3) for 4 minutes. Brains were collected and post-fixed with 4% PFA for 4 hours, followed by incubation in 25% sucrose solution (25% sucrose in prewash solution; PH7.3) for dehydration and cryoprotection. Then, the brains were sectioned into 30 μm-thick coronal sections in 1:12 series using a freezing microtome. The brain sections were successively transferred into 1ml tubes with anti-freeze solution (5.45% di-sodium hydrogen orthophosphate anhydrous, 1.57% sodium dihydrogen phosphate in a mixed solution contains 40% distilled water, 30% ethylene glycol and 30% glycerol; PH 7.4) and stored at 4°C until required. The whole blood was divided into supernatant and blood cells by centrifuge (3500 rotation/min for 10 minutes, 4°C). The supernatant was rapidly separated and frozen at -80°C.

2.6. DAB-immunohistochemistry

Free-floating brain sections were washed with tris-buffered saline (TBS) to remove anti-freeze, and with quench solution (3% hydrogen peroxide and 10% methanol in distilled water) for 5 minutes to clear peroxidases in the sections. Then, the sections were washed in TBS 3 times (each time for 10 minutes). The sections were blocked with 3% serum (the same species from which the secondary antibody was derived) in TXTBS solution (0.2% Triton-X in TBS, pH

7.4) for 1 hour. These blocked sections were incubated with the primary antibody in TXTBS with 1% normal serum overnight at room temperature. On the second day, the sections were washed with TBS 3 times (10 minutes each) and incubated in the secondary antibody in TBS solution with 1% normal serum for 3 hours. The sections were washed in TBS 3 times (10 minutes each) before incubating with the streptavidin–horseradish peroxidase complex (ABC kit) in TBS with 1% serum for 2 hours. The sections were washed with TBS 3 times (10 minutes each) and with TNS (tris-buffer; 0.6% Trizma base in distilled water, PH 7.4) twice (5 minutes each). The washed sections were placed into diaminobenzidine tetrahydrochloride (DAB) in TNS containing 25% hydrogen peroxide solution until sections turned to light brown and the staining was stopped by TBS washing. The stained tissues were mounted on gelatinized slides, air dried and then dehydrated in sequentially increasing concentration of 70%, 90% and 100% ethanol for 5 minutes. The dehydrated sections were cleared in the xylene for 5 minutes, then cover-slipped with distyrene plasticizer and xylene (DPX). The list of primary antibodies and secondary antibodies was shown in table 2-2.

Table 2-2 list of primary antibodies and secondary antibodies used in DAB-immunohistochemistry

antibody	Target	Host	Working dilution	Source and catalogue number
Tyrosine hydroxylase (TH)	Dopaminergic neurons	Rabbit	1:2000	Millipore, AB152
Glial fibrillary acidic protein (GFAP)	astrocyte	rabbit	1:1000	Agilent Technologies, Z0334
Anti-human nuclear (Hunu)	Human nuclear	Mouse	1:200	Millipore, MAB 1281
Ionized calcium binding adaptor molecule 1 (Iba1)	microglia	Goat	1:8000	Fujifilm Wako, 011-27991
Biotinylated anti-mouse	mouse IgG	Goat	1:200	Vector, BA-9200
Biotinylated anti-rabbit	rabbit IgG	Goat	1:200	Vector, BA-1000

2.7. Immunofluorescence

Free-floating sections were washed with TBS to remove anti-freeze, 3 times TBS wash (each time for 10 minutes). The sections were blocked with 3% serum in TBS with 0.05% Triton-X (pH 7.4) for 1 hour. These blocked sections were incubated with the primary antibody in TBS with 1% normal serum and 0.01% Triton-X at room temperature for 4 hours. Then, (all the operations were in the dark), the sections were washed with TBS 3 times (each time 10 minutes) and incubated in the secondary antibody in TBS solution with 1% normal serum and 0.01% Triton-X for 2 hours. The sections were washed in TBS 3 times (10 minutes each) before in TBS for 5 minutes. The sections were washed with TBS 3 times (10 minutes each). The stained tissues were mounted on gelatinized slides, air dried overnight and then cover-slipped with Dako

immunofluorescence mounting solution. The list of primary antibodies and secondary antibodies was shown in table 2-3.

Table 2-3 List of primary antibodies and secondary antibodies used in immunofluorescence

Antibody	Target	Host	Working dilution	Manufacturer and catalogue number
G protein-activated inward rectifier potassium channel 2 (GIRK2)	GIRK2 on dopaminergic neurons	Rabbit (polyclonal)	1:200	Alomone, APC-006
Tyrosine hydroxylase	Dopaminergic neurons in VTA and SNc	Mouse (monoclonal)	1:500	Millipore, MB318
Calbindin-D-28k	Calbindin on dopaminergic neurons	Mouse (monoclonal)	1:1000	Sigma, C9848
Tyrosine hydroxylase	Dopaminergic neurons in VTA and SN	Rabbit (polyclonal)	1:1000	Millipore, AB152
anti-rabbit alexa fluor 594	Rabbit Ig	goat	1:200	Invitrogen, A11037
anti-mouse alexa fluor 488	Mouse Ig	goat	1:200	Invitrogen, A11029

2.8. ELISA test for serum Hcy analysis

Homocysteine Enzyme Immunoassay Kit (ABIN457241, Antibodies-online) was used to measure the concentration of homocysteine in serum. The experiment was conducted following manufacturer's protocol. Hcy Standard was dissolved in sample diluent into 50 nmol/ml as a stock solution. Hcy

standard solution was prepared from stock solution to different concentrations: [50, 25, 12.5, 6.25, 3.12, 1.56, 0.78 ,0] nmol/ml. Antibody pre-coated 12×8-well-plate was used. 100ul of Hcy standard solutions were added into the wells and incubated for 2 hours at 37 °C. After the liquid was removed from wells, biotin-conjugated antibody was added into each well and incubated for 1 hours at 37 °C. Excess antibody was washed away by 200µl Wash Buffer 2 times. 100µl avidin conjugated Horseradish Peroxidase was added to the each well and incubate for 1hour at 37 °C. 90µl TMB Substrate was added to each well for 15-30 minutes at 37 °C. 50ul stop solution was added to each well. The absorbance of standard solutions was measured by UV spectrometer at 450 nm and 540 nm. The optical density was determined by subtracting the reading at 540 nm from reading 450 nm. Calibration curve was drawn by the corrected reading at 450 nm to Hcy standard concentration.

Sample solutions were made by adding 62.5µl to 62.5µl of sample diluent solution. The absorbances were measured in the same method as Hcy standard solution, and the concentration of Hcy was calculated based on calibration curve.

2.9. Histological quantification

2.9.1. Substantia nigra DAergic neuron lose quantification

In chapter 4, to quantify the number of remaining dopaminergic cells in SNc after 6-OHDA infusion, the TH-positive neurons were counted via an Olympus B 50 Stereology microscope equipped with a motorized stage and Leica attachment (40× objective) (Hedreen 1998). Counting was implemented using the Visopharm software. 1 section from a 1:12 series were analyzed for each brain. The number of DAergic neurons in the SN that both contralateral and

ipsilateral to the lesion was counted. The lesion degree was presented as percentage of the number of the losing DAergic neuron in ipsilateral side over the number of DAergic neuron in contralateral side to the lesion.

2.9.2. Stereological cells counting

Optical fractionator sampling was carried out on an Olympus B 50 Stereology microscope equipped with a motorized stage and Leica attachment (40×objective) (Hedreen 1998). Sampling was implemented using the Visopharm software. Based on anatomical landmarks, the regions of VTA, SNc and SNr were separated and marked. Unbiased sampling regions were selected by the software at a uniform step length on X-axis and Y-axis within a region of interest. The fractionator is used for counting the cell in the frame (West 2002): if cells within the frame or on acceptance line (on the top and right) of the frame without on the forbidden, the cells were counted; If the cells are on forbidden line (left and bottom line) of the counting frame, the cells were not counted.

In the chapter 3 and 5, to estimate the total number of DAergic neurons in the midbrain, 6-7 sections from a 1:6 series were analyzed for each brain. Counting frame information: counting frame width (X) was 55.90 μm, height (Y) was 44.72 μm. Counting frame size was set roughly 2 to 5 neurons were counted per frame and was maintained across all regions sampled were counted per sections. System randomly selected samples within defined regions.

To estimate the total number of grafted human cells, 1:6 series were analyzed for each brain. All sections with grafts were included. Counting frame information: counting frame width (X) was 35.36 μm, height (Y) was 28.28 μm. Counting frame size was set roughly 5 were counted per frame and was

maintained across all regions sampled were counted per sections. System randomly selected samples within defined regions.

$$N = \sum\left\{n * \frac{A}{a * S} * F * \frac{T}{T + D}\right\}$$

N= the total estimated cell number; n= counted cells within the counting frame; A= the defined region; a = the area of frame; F = series frequency; S = the number of frames in defined region; T = section thickness; D = cell diameter

2.9.3. Graft volume

In chapter 4, to estimate graft volume, a 1:6 series were analyzed for each brain. The surface area of Hunu$^+$ staining was used to estimate graft volume and was carried out on an Olympus B 50 Stereology microscope equipped with a motorized stage and Leica attachment (5×objective). $\text{Graft volume} = \sum\{a * F * T\}$ where a = surface area; F = series frequency; T = section thickness.

2.9.4. Optical density by ImageJ

The optical density was analyzed by ImageJ. Firstly, the optical density calibration was conducted following official ImageJ instructions (Hartig 2013). Then, the mean gray value of region of interest were analyzed. Finally, the optical density was calculated via this formula by ImageJ: $\text{optical denstity} = \log_{10}(255/(mean\ gray\ value\ )$. In this experiment, the real optical density was used as final optical density: The real optical density= the optical density of region of interest - the optical density of background control.

For optical density of TH$^+$ fibers in chapter 5, two images (Bregema +1.60 and Bregema +0.480) from each rat were collected by an Olympus B 50 Stereology

microscope equipped with a motorized stage and Leica attachment (5× objective). Samples from cortex in each side was used as background control. The data was presented as the optical density of lesioned side over that of intact side.

For optical density of $IBA1^+$ neurons in chapter 3, one striatal image from each rat were collected by an Olympus B 50 Stereology microscope equipped with a motorized stage and Leica attachment (5× objective). Samples from cortex in each side was used as background control. The data was presented as the optical density of lesioned side over that of intact side.

For optical density of striatal TH^+ fibers in chapter 5, one striatal image from each rat were collected by an Olympus B 50 Stereology microscope equipped with a motorized stage and Leica attachment (5× objective). Striatum from each hemisphere was divided into two areas, medial and lateral parts of the striatum. Samples from cortex in each side was used as background control. The data was presented as the optical density of lesioned side over that of intact side.

For optical density of microglia and astrocyte, one section of striatum from each rat were obtained by an Olympus B 50 Stereology microscope equipped with a motorized stage and Leica attachment (20× objective). In the chapter 3 and chapter 5, medial and lateral striatum from intact and lesioned sides were chosen as regions of interest. The data was presented as the optical density of lesioned side over that of intact side. In the chapter 3 and 5, one VTA site and two SN sites were chosen as regions of interest. Samples from each side were used as background control.

2.9.5. The density of microglia and astrocyte analysis

To estimate the density of $GFAP^+$ cells in the striatum, 1 section from a 1:12 series were analyzed for each brain. In the chapter 3 and 4, each hemisphere was divided into three areas, medial, central, and lateral parts of the striatum. In the chapter 5, each hemisphere was divided into two areas, medial and lateral parts of the striatum. Counting frame information: counting frame width (X) was 100 μm, height (Y) was 100 μm. System randomly select 5 samples within defined areas. Counting frame was maintained across all regions sampled were counted per sections.

To estimate the density of $IBA1^+$ cells in the striatum, 1 section from a 1:12 series were analyzed for each brain. The morphological features used to characterize microglia: (1) Resting microglia: a small cell body with long and extended processes. (2) Activated microglia: an enlarged and round shaped (ameboid) cell body with shorter and thicker processes. (3) Round microglia: a round soma without any process (Jonas et al. 2012). In the chapter 3 and 4, each hemisphere was divided into three areas, medial, central, and lateral parts of the striatum. In the chapter 5, each hemisphere was divided into two areas, medial and lateral parts of the striatum. Counting frame information: counting frame width (X) was 200 μm, height (Y) was 200 μm. 1 sample within defined areas was counted.

2.10. Statistical analysis

Statistical analyses were performed in SPSS Statistics 25 (IBM Corp., Armonk, USA) and GraphPad Prism 9. The results were represented as group mean ± standard error of the mean (SEM). Histological data was analyzed by univariate analysis (one-way) ANOVA analysis or multivariate analysis (two-way) ANOVA

analysis. An unpaired T-test was used when compared the means of two independent groups. Post-hoc test was used to compare significant differences between different groups. If 95% (*P <0.05) is deemed to significant, if 99% (**P <0.01) 99.9% (***P <0.001) is regarded as highly significant or 99.99% (****P <0.0001) is regarded as extremely high significant.

Chapter 3. Impact of L-DOPA on intact endogenous DAergic neurons in 6-OHDA lesioned rats

3.1. Introduction

L-DOPA has been the golden standard treatment for PD for more than half a century. While in the 1990-2000, alternative dopaminergic medications (e.g., dopamine agonists) were preferred for early PD treatment, follow-up studies in the clinic found that delaying L-DOPA treatment for PD showed no long-term benefits (Katzenschlager et al. 2008; Gray et al. 2014). It was stated in the report from Katzenschlarger et al. that the "*Initial treatment with the dopamine agonist…did not reduce mortality or motor disability and the initially reduced frequency in motor complications was not sustained. We found no evidence of a long-term benefit or clinically relevant disease-modifying effect with initial dopamine agonist treatment* (Katzenschlager et al. 2008)." The general consensus currently is that L-DOPA is still the most effective drug to alleviate motor symptoms in PD and has an irreplaceable role in current clinical practice (Murata 2009). Given that L-DOPA remains the most widely prescribed medication for people with PD, understanding its potential contribution to disease pathogenesis and impact on DAergic neurons in the brain is fundamental. While L-DOPA clinically is commonly administered up to 5 times a day, in animal models this is routinely a once daily administration. This chapter therefore explores the effect of L-DOPA on endogenous DAergic neuron survival in an improved 6-OHDA PD model that tries to more closely replicate the conditions of a PD patient in the clinic.

3.1.1. L-DOPA's impact on endogenous DA cell survival *in vitro*

Most *in vitro* studies suggest that L-DOPA could have a toxic effect on DAergic neurons (Cheng et al. 1996). The toxicity of L-DOPA is dose dependent: Only

relatively high levels of L-DOPA treatment (0.25 x 10^{-4} M or larger) causes DAergic cell death (Godwin-Austen et al. 1969) (Table 3-1). L-DOPA induced toxicity can be reversed by antioxidants, suggesting ROS is a key contributing factor to L-DOPA's toxicity (Pardo et al. 1995). ROS is most probably generated by mitochondrial dysfunction as discussed in chapter 1.2.1.2 and has been considered to be the main mechanism leading to L-DOPA's toxicity (Bose and Beal 2016). The malfunction of mitochondria has also been related to defective ubiquitin-proteasome system (UPS) and subsequently accumulation of misfolded proteins (see chapter 1.2.1.2.). Misfolded proteins may further cause inflammatory responses related to microglia activation, release of cytokines and other inflammatory factors (Winklhofer and Haass 2010). Those inflammatory responses may further increase the generation of ROS and thus form a vicious cycle (Soliman et al. 2002).

Treatment	Result(s)	References
DAergic cells + L-DOPA	Low dosage: L-DOPA inhibited proliferation of DAergic neuron High dosage (0.25 x 10^{-4} M or larger): L-DOPA can reduce total cell number.	(Godwin-Austen et al. 1969; Mena et al. 1992; Mena et al. 1993; Basma et al. 1995; Pardo et al. 1995; Walkinshaw and Waters 1995; Cheng et al. 1996)
DAergic cells + Antioxidative agent	Protect DAergic neuron against L-DOPA induced neurotoxicity	(Mena et al. 1993; Pardo et al. 1993; Cheng et al. 1996)
DAergic neuron + glial cells	Protect DAergic neuron against L-DOPA induced neurotoxicity	(Han et al. 1996)

Table 3-1. Most early *in vitro* studies suggest that L-DOPA is toxic to DAergic neurons, and this is most probably due to the generation of ROS. However, such toxicity was not seen in the presence of glial cells.

Other than oxidative stress theory, there are also emerging hypotheses concerning how L-DOPA generates toxicity towards DAergic neurons. L-DOPA resembles the structure of L-tyrosine and therefore maybe mistakenly taken by cells for protein synthesis, which usually results in misfolded proteins, alteration of mitochondrial function and activation of ubiquitin-lysosomal system (Giannopoulos et al. 2019). L-DOPA may also trigger ERK1/2-c-Jun signaling pathway by increasing cAMP concentration inside DAergic cells and turn on apoptotic process that affects DAergic cell viability (Park et al. 2016).

3.1.2. The impact of L-DOPA on endogenous DA cell survival *in vivo*

Importantly, however, in stark contrast to *in vitro* studies, most *in vivo* data (including rat and primate models) indicate that L-DOPA treatment has minimal, if any, negative impact on DAergic neuron survival, with once daily administration of L-DOPA into animals (dosage ranged from 80 to 170 mg/kg/day) for 3-26 weeks (Dziewczapolski et al. 1997; Murer et al. 1998; Ferrario et al. 2003). Usually, DAergic cells (TH^+) were counted both on the intact and lesioned side. The cell survival rate was often expressed as the DAergic cells in the lesioned side over DAergic cells in the intact side (% intact). Toxicity has only observed when the dosage administered into animal surpassed clinically relevant levels for extended periods (200 mg/kg/day L-DOPA treatment for 27 weeks) (Blunt et al. 1993) (Table 3-2).

From these *in vivo* studies, it could be clearly seen that there is no standard dose to be used in such experiments (table 3-2). The duration for these experiments and the pre-treatment methods that could result in different degree of stress varies to an astonishing extent, making it hard to reach a consensus over the topic. It is therefore essential to establish an animal model that closely mimic the realistic condition of a PD patient and evaluate L-DOPA's effect in

this more clinically relevant model.

DAergic neurons counting has been used most widely to assess the survival rate as this is the most obvious and persuasive indicator for evaluation and comparison. It worth noting that most studies only compare the lesioned side with intact side, expressing the data as the percentage loss compared to the intact side, thus assuming that the intact side was not receiving any impact from L-DOPA. This may not be necessarily the case. Therefore, in the experiments presented within this chapter, the approach that was taken included both control lesioned groups, as well as a true naïve control, which will allow us to conclusively study the impact of L-dopa on the lesioned and intact hemispheres simultaneously following twice daily administration of L-DOPA.

Publication	Dose (mg/kg/day)	Duration (weeks)	Animal model	Impact on cell viability
(Blunt et al. 1993)	200	27	6-OHDA MFB lesioned rats	Cell lost in the VTA of the lesioned side
(Ferrario et al. 2003)	170	3	6-OHDA striatal lesioned rats	No impact
(Dziewczapolski et al. 1997)	170	26	6-OHDA MFB lesioned rats	No impact
(Murer et al. 1998)	170	26	6-OHDA MFB lesioned rats	No impact
(Lyras et al. 2002)	80	13	Non-lesioned primates	No impact
(Perry et al. 1984)	100	17	Non-lesioned rats	No impact

Table 3-2. *In vivo* studies provided opposite views to those observed in cell cultures. *In vivo* studies suggest that L-DOPA is non-toxic in normal dosage. Toxicity was only observed with extremely high dosage (200 mg/kg/day) and long-term administration (27 weeks).

A possible explanation for the difference in effects between the *in vivo* and *in vitro* studies is that for *in vivo* studies, the host brain has a more complex cellular environment. Glial cells, for example, could protect DAergic neurons from oxidative stress mentioned above (Iwata-Ichikawa et al. 1999).

3.1.3. L-dopa and PD progression *in PD patients*

This has been addressed in clinical studies seeking to determine whether the progression of PD can be hastened after L-DOPA treatment. The most common evaluation is based on observations for practicability. For example, Unified Parkinson's Disease Rating Scale (UPDRS) has been used to measure the severity of PD symptoms (Goetz et al. 2008). In a large scale well-designed randomized, double-blinded study, 361 early-stage PD patients who received different dosage (ranging from 0 (placebo) to 600 mg) of L-DOPA treatment were followed for 40 weeks and then 2 weeks after withdrawal. The UPDRS in those patients who received higher dosage was significantly lower than that in PD patients receiving lower dose of L-DOPA or placebo (Fahn et al. 2004). It gave strong evidence that L-DOPA appears not to be altering the course of the disease.

However, using clinical evaluation to estimate disease progression can be misleading as the symptoms may still under the control of L-DOPA for a long time after L-DOPA withdrawal. It has been observed that UPDRS is elevated for up to 15 days after L-DOPA withdrawal, and this recorded daily change proved that UPDRS may not precisely reflect the true progression of PD (Hauser et al. 2000). The kinetics of this long duration response caused by repetitive administration of L-DOPA is not well understood and changes with the disease progression (Albin and Leventhal 2017). Other than that, it was also

pointed out that the age and severity of the disease connects with L-DOPA's response. In general, older patients had poorer L-DOPA response and higher UPDRS score (Virameteekul et al. 2021). But age is not the only determinant of the score. Vascular diseases for example may also affect the final outcome (Malek et al. 2019). So far, the factors that could impact on the score were not fully explored and it will be challenging to disentangle.

3.1.4. Limitations of current research

In vitro experiments have certain limitations. Firstly, cell cultures cannot completely mimic the complex condition of the brain. Cell cultures lack the protective factors such as growth factors and glial cells that are presented in normal brain (Mena et al. 1997). Secondly, it is difficult to correlate the dosage used in cell experiment to the clinical dosage for PD patients. Extrapolating results from cell experiments to the clinic is difficult and the clinical outcome might be quite different from what was observed from *in vitro* studies (Olanow 2015).

For *in vivo* experiments, most studies in the past were restricted to the classical 6-OHDA lesioned PD model and classical biomarkers such as TH or DAT that marks all DAergic neurons without considering the subtypes. However, the subtypes, as well as the accompanied immune responses caused by neuronal loss are crucial for the evaluation of PD progression. Today, for instance, $Girk2^+/TH^+$ and $Calbindin^+/TH^+$ double staining is the mainstream immuno-histological methods that are widely used for distinguishing A9 and A10 subtypes of midbrain DAergic neurons *in vivo* and transcriptomic and proteomic analyses are defining ever more markers of these subtypes. (Thompson et al. 2005; Reyes et al. 2012).

One essential pathological change that was neglected in the early studies about L-DOPA is the immunological changes in the brain. Nearly all PD etiological propositions suggest that PD progression is accompanied by inflammation (Rogers et al. 2007). Neuroinflammation can be regarded as a result of cell content leakage. Neuromelanin, for example, triggers the activation of microglia (Zhang et al. 2013). As the most abundant population of immune cells in the SNc region, microglia are in charge of inflammatory response. It could be a major contributing factor for the death of SNc cells (Vivekanantham et al. 2015), but the relationship has not been fully understood. Recent rat models suggest that the key immune cell population that helps the forming of α-synuclein inclusion (and therefore the death of DAergic neurons) might be recruited from the peripheral system. The innate microglia in the brain were merely involved to increase the expression of MHCII (major histocompatibility complex II), which was previously correlated to α-synuclein inclusions (Imamura et al. 2003; Harms et al. 2017). In this view, α-synuclein deposits were caused by a mixed interaction of innate and adaptive immunity and the recruitment of peripheral immune cells was pivotal in the whole process. If this theory holds true, then the number of microglia might not be so important as their function in the forming of α-synuclein were limited to the expression of HLA (human leukocyte antigen) gene. In contrast, whether microglial is activated or not becomes crucial as only activated microglial can be involved (Tan et al. 2020).

Astrocyte was also reported to be closely linked to PD conditions. It is well understood that astrocytes protect and repair the brain through various mechanisms including reducing oxidative burden in the brain that may explain the controversial results from *in vitro* and *in vivo* experiments concerning oxidative stress (Dringen et al. 2000; Bylicky et al. 2018). But to be noted, a neurotoxic subtype of astrocyte termed A1 astrocyte was also found and may relate to PD (Liddelow et al. 2017). The A1 subtype can also be induced by

activated microglia. The blockage of such process was proved to be neuron protective in PD animal models (Yun et al. 2018).

Another aspect of astrocyte changes during PD progression relates to glutamate levels in the extracellular space. Normally, astrocytes control glutamate uptake in the central nervous system and maintain glutamate level in a balanced homeostasis (Mahmoud et al. 2019). However, some PD mutations (for instance in PARK7 or SNCA genes) can reduce the capability of glutamate uptake by astrocytes. As a result, glutamate levels in the extracellular space were raised. High extracellular glutamate is known to cause excitotoxicity and this can in turn cause neurodegeneration (Booth et al. 2017).

Potentially, peripheral T cell population may also be linked to PD progression as there is mounting evidence in recent years that the peripheral immune system is affected by PD (Booth et al. 2017; MacMahon Copas et al. 2021). The exact mechanism of T cell entry into the CNS is still debated but since BBB disruption has been extensively found both *in vivo* animals, and in post-mortem studies, the infiltration of T cells into the CNS is quite possible (Gray and Woulfe 2015). Using $CD4^{-/-}$ and $CD8^{-/-}$ mice, it was found that $CD4^{+}$ T cells may take the major role in neurodegeneration (Brochard et al. 2009). However, without additional compromise to the BBB in the rat model, the infiltration process may take an exceptionally long time to achieve. Therefore, peripheral T cell monitoring was only explored in Chapter 4 where the animals were kept for 25 weeks after treatment.

3.1.5. Peripheral changes in response to L-DOPA treatment

L-DOPA has systemic effects on the body, and it is reasonable to hypothesize that there may be peripheral changes associated with chronic L-DOPA

exposure. The amino acid homocysteine (Hcy) is generated as a product of protein metabolism (Figure 3-1): When L-DOPA is methylated by COMT, S-adenosylmethionine (SAM), the donor of the methyl group, is converted into S-adenosylhomocysteine (SAH) which can be further hydrolyzed into Hcy. The blood samples collected from PD patients who received L-DOPA treatment had a higher level of plasma Hcy than healthy people (Zoccolella et al. 2009). This is supported by rat studies in which L-DOPA treatment raised Hcy levels to twice those of control rats (Daly et al. 1997; O'Suilleabhain et al. 2004a; Valkovic et al. 2005). These are sound evidence that the administration of L-DOPA increases the level of plasma Hcy. Abnormal Hcy level is often observed in the non-alcoholic fatty liver patients (Dai et al. 2016) or in fatty rats (Bravo et al. 2011) which leads to the hypothesis that Hcy may contribute to fatty liver. In 6-OHDA rats who received long-term L-DOPA treatment (16 weeks), hepatic steatosis (fat deposits) was indeed observed but the relationship with Hcy was not fully established (Elabi 2017). To confirm the link between Hcy and hepatic steatosis and further the relationship between L-DOPA and fatty liver, this experiment set naïve and sham group (surgical control) as control groups to rule out the influences from diet imbalance or surgical injury itself.

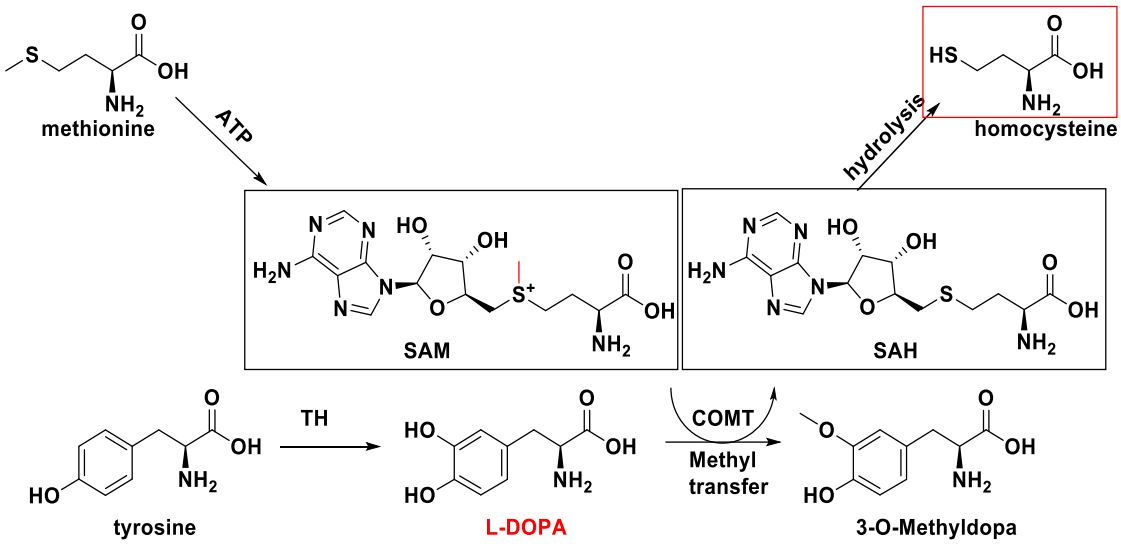

Figure 3-1. Generation of Homocysteine in L-DOPA metabolism. Homocysteine is generated in two steps: The first step is usually reversible and mainly caused by the attack from ATP to methionine. The S-adenosylmethionine (SAM) generated in the first step can transfer its methyl group to L-DOPA and release homocysteine upon hydrolysis. Excess L-DOPA is thought to push the second step forward as there are more receptors of the methyl group.

3.1.6. Aims of the chapter

The hypothesis in this chapter is that L-DOPA may have a negative effective on endogenous DAergic neuron survival.

This thesis aims to understand more about the effects of L-DOPA in the rodent model, but the first step is to ensure that the model being used reflects the most important features of PD patients for this purpose. Most studies to date have used once daily L-DOPA injections and relatively short periods of L-DOPA exposure. Histological analysis of the post-mortem tissue calculates DAergic neurons depletion on the lesioned side as a percentage of the intact side, failing to take into account any possible effects of L-DOPA on the intact side. This study sets out to clarify:

1. What the effects of L-DOPA are on the intact side of the midbrain in this model?
2. Does longer term L-DOPA treatment affect inflammatory responses?
3. Are Hcy levels increased in the peripheral system?

3.2. Experiment design and method

3.2.1. Experiment design

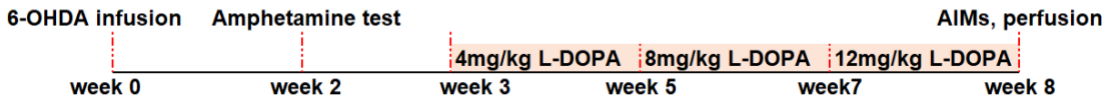

Figure 3-2 Timeline of the experiment

The total number of rats was 30. A naïve group (n=5) did not receive any surgery or treatment. After two weeks' acclimatization, a subset of rats (n=15) received unilateral 6-OHDA lesions to the medial forebrain bundle and another subset of rats (n=10) received saline infusion to the medial forebrain bundle. After two weeks' recovery, all rats underwent amphetamine-induced rotation assessment to evaluate the degree of lesion. Successfully lesioned animals and sham surgical animals were divided into two groups respectively: one group underwent L-DOPA treatment and the other groups received saline treatment (see table 3-3). The four treated groups were injected with saline or L-DOPA for 6 weeks via subcutaneous injection. During the administration period, abnormal involuntary rate scales (AIMs) were tested twice a week. 14 hours after the last L-DOPA or saline treatment, all rats were sacrificed via transcardiac perfusion (Figure 3-2). The brains were collected for further assessment (Brain: immunohistochemistry and immunofluorescence).

Named Groups	The condition of treatment and surgery
Naïve control (n=5)	no surgical or drug administration
Sham saline (n=5)	saline infusion, saline treatment
Sham L-DOPA (n=5)	saline infusion, L-DOPA treatment
6-OHDA saline (n=7)	6-OHDA lesion, saline treatment
6-OHDA L-DOPA (n=8)	6-OHDA lesion, L-DOPA treatment

Table 3-3. Details of each experimental group

3.2.2. L-DOPA treatment

Two weeks following surgery, L-DOPA plus Benserazide (in 0.9% saline) was administered to the L-DOPA treated groups, twice a day, subcutaneously. The doses of L-DOPA were gradually increased over 6 weeks, starting from 4mg/kg in the 1st and 2nd weeks, to 8mg/kg in the 3rd and 4th weeks, and finally 12mg/kg in the 5^{th} and 6^{th} week. Benserazide was given at a fixed dose (15mg/kg) (Breger 2013). The saline treated group received daily injection with saline twice a day (0.9%, 1 ml/kg) subcutaneously during the 6 weeks.

3.3. Results

3.3.1. Amphetamine induced rotation

The 6-OHDA lesioned rats all achieved over 6 ipsilateral full body turns/minute following i.p. administration of 2.5mg/kg amphetamine two weeks after surgery. The rotating frequency of 6-OHDA lesioned groups was significantly higher than the sham lesioned groups ($F_{(3,20)}$ =23.06, P<0.0001). Rats were divided into sham saline group, sham L-DOPA group, 6-OHDA saline group and 6-OHDA L-DOPA group. The standard for grouping was to ensure there were no statistical differences between sham saline group and sham L-DOPA group; Also, matched groups were created to ensure there were no statistical differences between 6-OHDA saline group and 6-OHDA L-DOPA group on the amphetamine-induced rotation test (Figure 3-3).

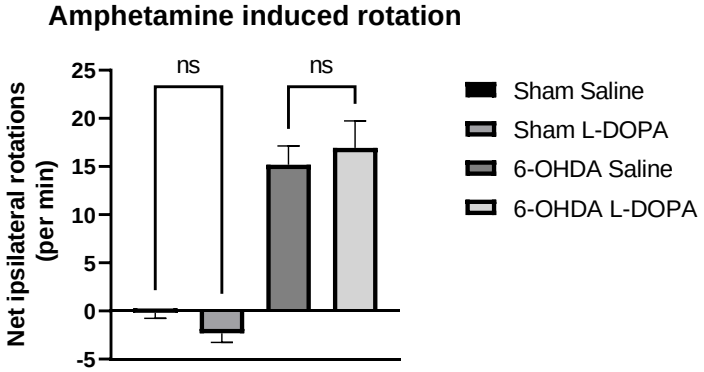

Figure 3-3 Amphetamine-induced rotational bias of different groups of rats. Mean full body rotations per minute were recorded for rats after injected with 2.5 mg/kg methamphetamine via i.p. The data were presented as mean rotation ± standard error of the mean (SEM); Error bars = ± SEM. One-way ANOVA was used to test statistical significance with Bonferroni post-hoc analysis.

3.3.2. Abnormal Involuntary Movement Score (AIMs)

AIMs are a measure of L-DOPA induced dyskinesia. The 6-OHDA L-DOPA group developed abnormal involuntary movement after L-DOPA treatment. AIM was scored by observing the severity of axial, orolingual, forelimb and hindlimb AIMs. Time course and amplitude of AIM were the two factors used for the judgement. Higher dose of L-DOPA resulted in higher AIM score while naïve group, sham saline group and 6-OHDA saline group did not show any AIM during the time course of the assessment (Severity: $F_{(2, 21)} = 10.32$, $P=0.0008$), duration: $F_{(2, 21)} = 7.673$, $P=0.0032$, Amplitude: $F_{(2, 21)} = 12.53$, $P=0.0003$) (Figure 3-4).

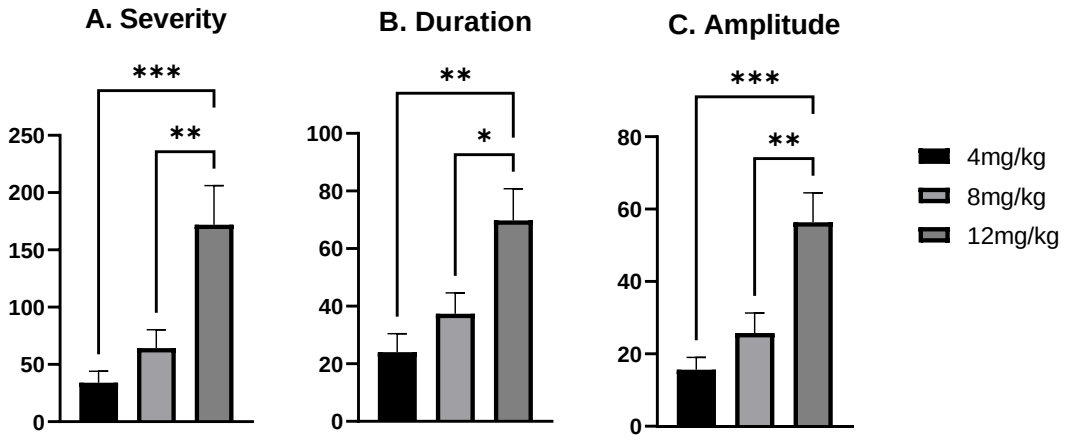

Figure 3-4 The degree of L-DOPA induced dyskinesia was determined by AIMs. AIMs score for Lesion L-DOPA group under different L-DOPA dosage (4mg/kg, 8mg/kg and 12 mg/kg). A. AIMs score of severity ($F_{(2, 21)} = 10.32$, $P=0.0008$). B. AIMs score of duration ($F_{(2, 21)} = 7.673$, $P=0.0032$). C. AIMs score of amplitude ($F_{(2, 21)} = 12.53$, $P=0.0003$). Severity was evaluated based on the score of duration and amplitude. AIMs are presented as mean score ± standard error of the mean (SEM); Error bars = ± SEM. One-way ANOVA was used to test statistical significance with Bonferroni post-hoc analysis. *P<0.05, **P<0.01, ***P<0.001, and ****P<0.0001.

3.3.3. Immunohistochemistry results

3.3.3.1. The impact of intracerebral 6-OHDA infusion on the TH^+ DAergic neurons and the impact of L-DOPA treatment on TH^+ DAergic neuron survival

TH expression (TH^+) cell loss was confirmed by immunocytochemistry. 30µm coronal sections of rat's brain were stained by DAB-staining to visualize tyrosine hydroxylase (see methods 2.7.), the enzyme responsible for L-DOPA production under physiological conditions. 6-OHDA saline group and 6-OHDA L-DOPA group lost most of their DAergic neurons in the lesioned side which was clearly shown by DAB staining (Figure 3-5). TH^+ cell number was quantified by unbiased stereological counting. TH^+ cells on the lesioned side were almost depleted in the SNc ($F_{(4, 24)} = 75.63$, $P<0.0001$) and TH^+ cell number was largely reduced in VTA for 6-OHDA saline group and 6-OHDA L-DOPA group ($F_{(4, 24)} = 19.03$, $P<0.0001$) and this model can therefore be regarded as complete lesion model for Parkinson's disease (Figure 3-6).

L-DOPA treatment produced no effect on the TH^+ DAergic neuron survival (Figure 3-6). No statistical significance was found between sham saline and sham L-DOPA group or between 6-OHDA saline and 6-OHDA L-DOPA group (SNc：$F_{(4, 24)} = 0.8175$，$P=0.5266$, SNr: $F_{(4, 24)} = 1.030$, $P=0.4122$), VTA: $F_{(4, 24)} = 0.3280$, $P=0.8564$).

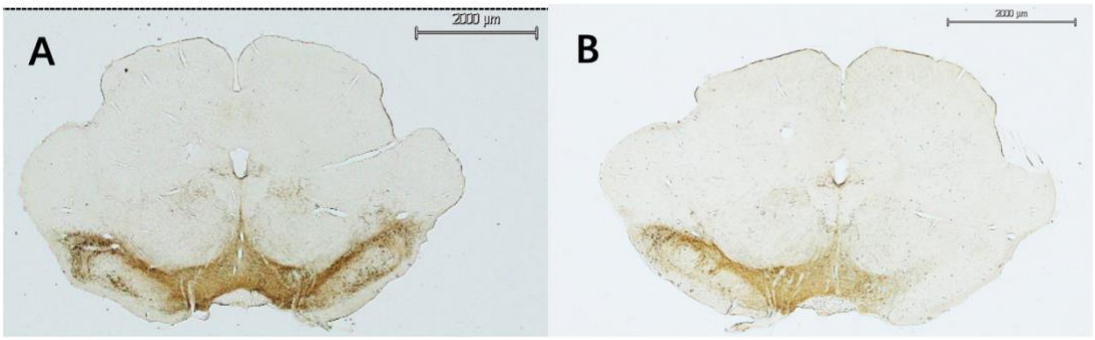

Figure 3-5 The impact of intracerebral infusion of 6-OHDA on tyrosine hydroxylase immuno-reactive cell bodies in the SN and VTA areas. (A) Representative image from naïve control group. (B) Representative image from 6-OHDA saline group. The neurons are visualized by their TH immunoreactivity with DAB (dark brown signal). Scale bar: 2000µm.

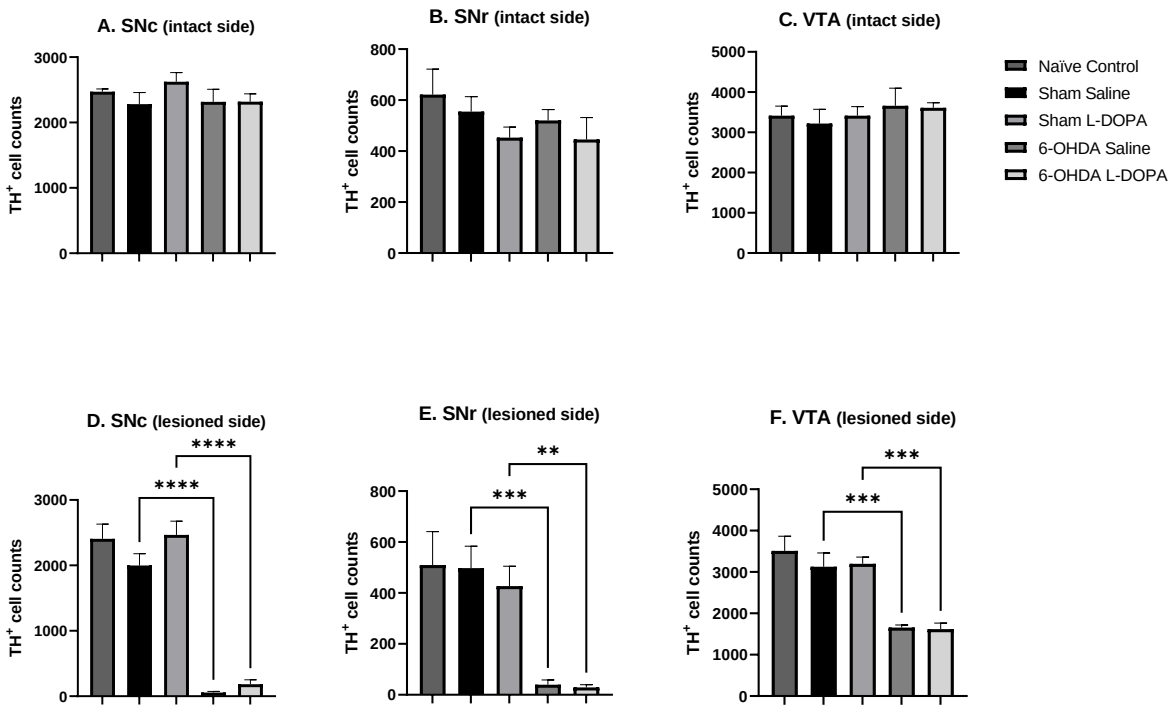

Figure 3-6 The mean number of TH^+ expressing cells counted in different regions of the lesioned side. (D-F). TH^+ cells were depleted in the 6-OHDA groups in SNc ($F_{(4, 24)} = 75.63$, $P<0.0001$), SNr ($F_{(4, 24)} = 13.67$, $P<0.0001$) and VTA ($F_{(4, 24)} = 19.03$, $P<0.0001$). The number of DAergic neurons are presented as mean ± standard error of the mean. One-way ANOVA and Bonferroni post-hoc analysis was used to examine statistical significance. *$P<0.05$, **$P<0.01$, ***$P<0.001$, and ****$P<0.0001$.

3.3.3.2. Inflammatory Response

3.3.3.2.1. GFAP$^+$ astrocytes

Negligible changes in GFAP$^+$ astrocytes were observed (Figure 3-7). No statistical differences of GFAP$^+$ astrocytes were found between naïve group and every other group in striatum both in the intact ($F_{(4, 24)}$ = 0.4636, P=0.7617) and the lesioned side ($F_{(4, 24)}$ = 0.09576, P=0.9828) (Figure 3-8. A and B). Also, this trend was universal to medial ($F_{(4, 24)}$ = 0.03046, P=0.9981), central ($F_{(4, 24)}$ = 0.1435, P=0.9641) and lateral striatum ($F_{(4, 24)}$ = 0.6638, P=0.6232) though the average number of GFAP$^+$ astrocytes in the lateral part was less than medial and central striatum (Figure 3-8. C, D, E, F, G and H) (Figure 3-8).

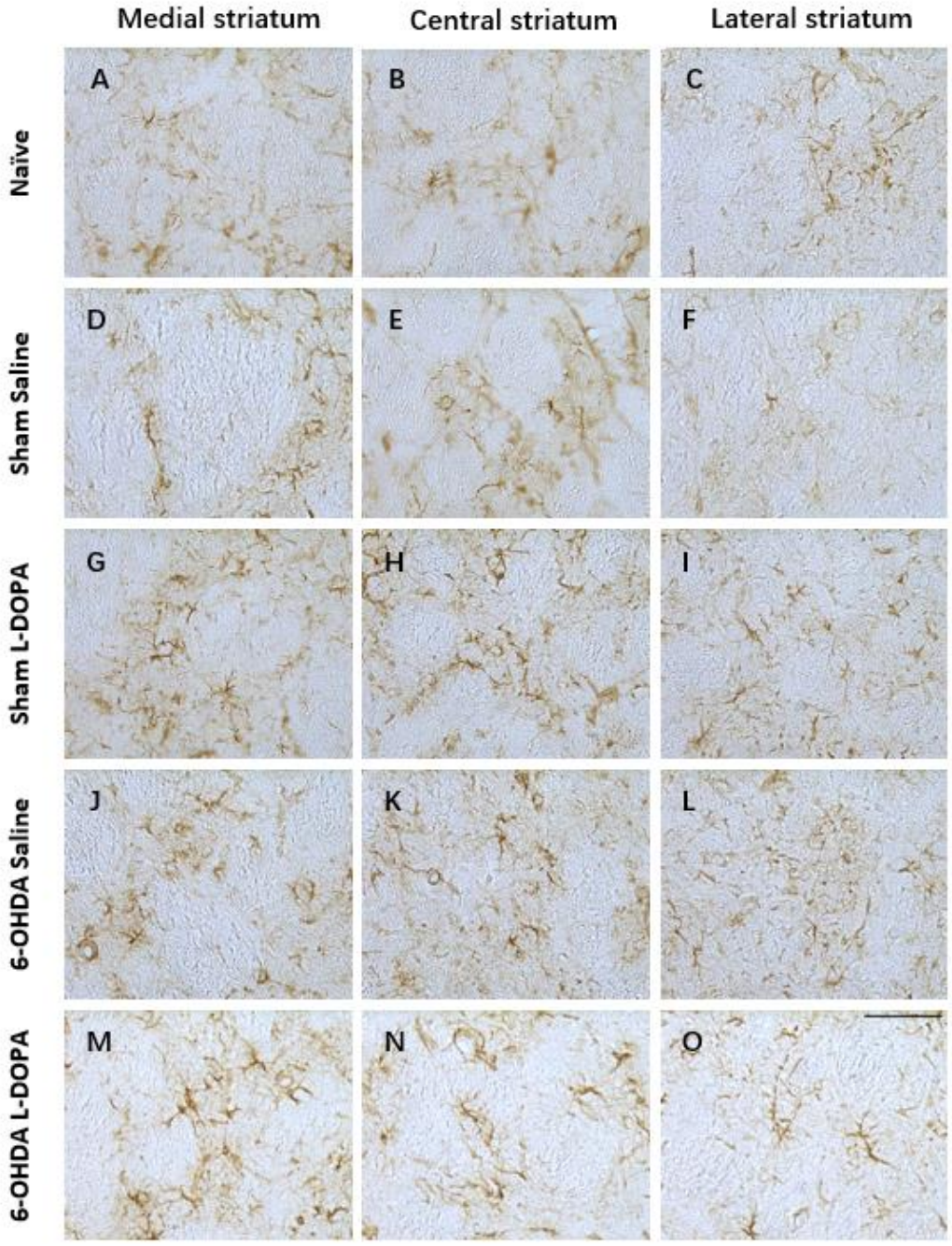

Figure 3-7 Representative images of GFAP staining were presented for each group. Astrocytes was labelled by GFAP antibody. Images were taken at 20 x magnification. Scale bar: 85μm

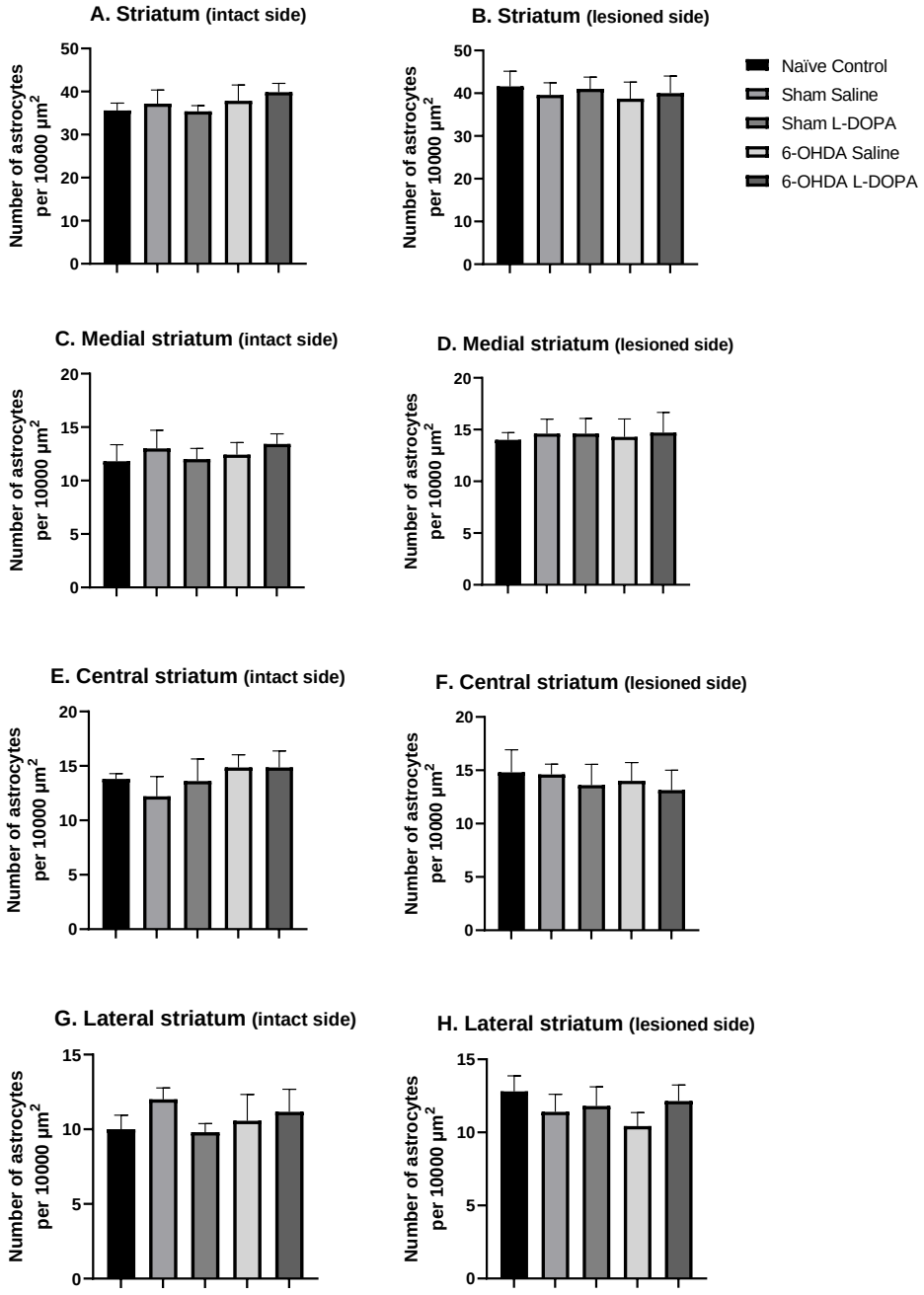

Figure 3-8. Number of GFAP$^+$ cells per 10000 µm^2 were presented as mean ± standard error of the mean. One-way ANOVA and Bonferroni post-hoc analysis was used to examine statistical significance.

3.3.3.2.2. IBA1$^+$ microglial cells

In the intact side of striatum, activated IBA1$^+$ microglial cells increased significantly in 6-OHDA saline group (medial striatum: $F_{(4, 17)} = 3.130$, $P=0.0423$, dorsal striatum: $F_{(4, 18)} = 8.777$, $P=0.0004$)) compared to naive control group and sham saline group. L-DOPA treatment reduced the number of activated IBA1$^+$ microglial in 6-OHDA L-DOPA group when compared to the 6-OHDA saline group but did not reach statistical significance. Statistically, the elevation of activated IBA1$^+$ microglial cell number was more remarkable in dorsal striatum and medial striatum (Figure 3-9).

In the lesioned side of the striatum, activated IBA1$^+$ microglial cells also increased significantly in 6-OHDA saline group (medial striatum: $F_{(4, 18)} = 9.418$, $P=0.0003$, dorsal striatum: $F_{(4, 18)} = 15.27$, $P<0.0001$)) (Figure 3-10 and Figure 3-11). Unlike the intact side, L-DOPA's effect of reducing IBA1$^+$ microglial cell increase was statistically significant in dorsal striatum compared to 6-OHDA saline group.

IBA1$^+$ microglial cell density reflects the total number of IBA1$^+$ microglial cells and both results (optical density or unbiased counting) showed that the total number of IBA1$^+$ microglial cells had no difference among all groups in dorsal striatum (Figure 3-12) (intact side: $F_{(4, 18)} = 1.921$, $P=0.1505$, lesioned side: $F_{(4, 18)} = 2.278$, $P=0.1009$) and medial striatum (intact side: $F_{(4, 18)} = 1.242$, $P=0.3286$, lesioned side: $F_{(4, 18)} = 1.462$, $P=0.2551$).

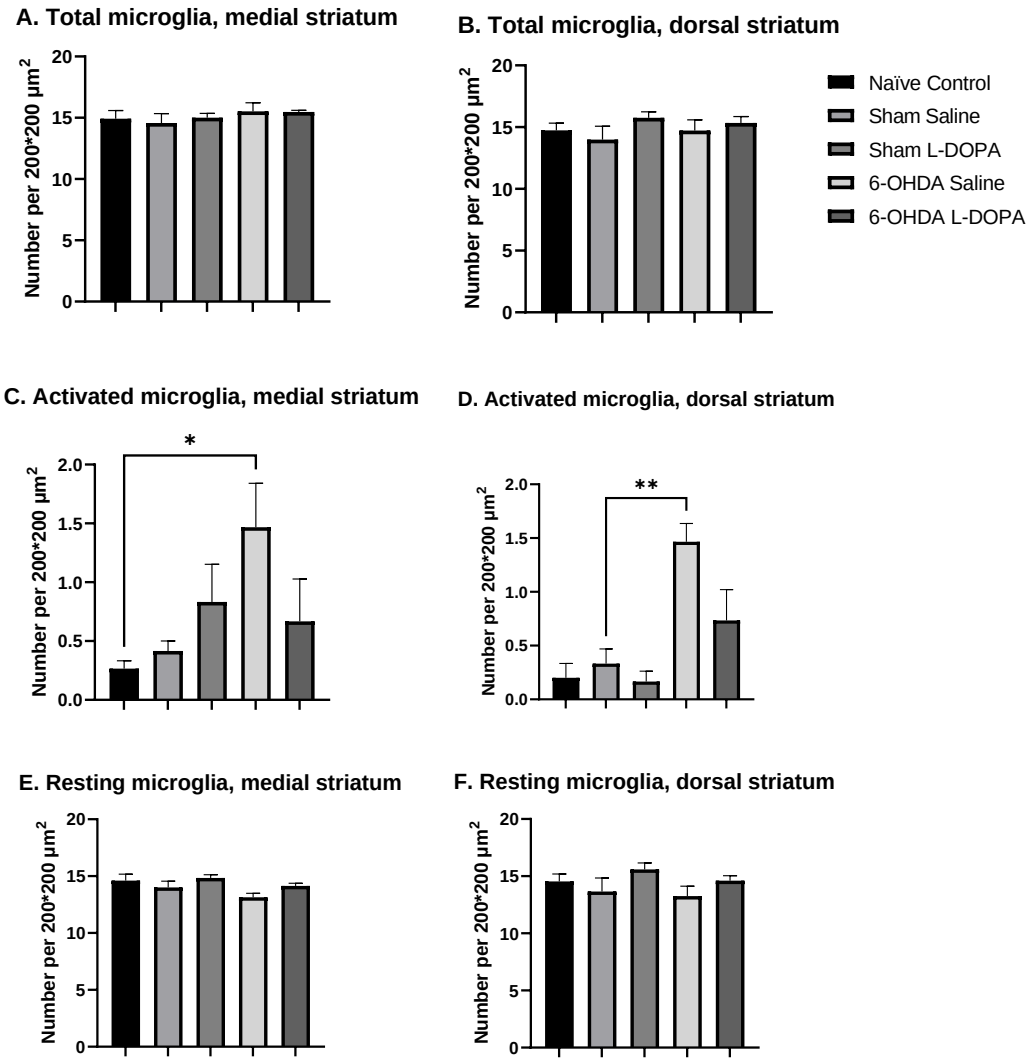

Figure 3-9 Number of IBA1^{+} cells per 200*200 µm^2 in the intact side were presented as mean ± standard error of the mean. Activated microglia were increased in medial ($F_{(4, 17)}$ = 3.130, P=0.0423) and dorsal striatum ($F_{(4, 18)}$ = 8.777, P=0.0004). One-way ANOVA and Bonferroni post-hoc analysis was used to examine statistical significance. *P<0.05, **P<0.01, ***P<0.001, and ****P<0.0001.

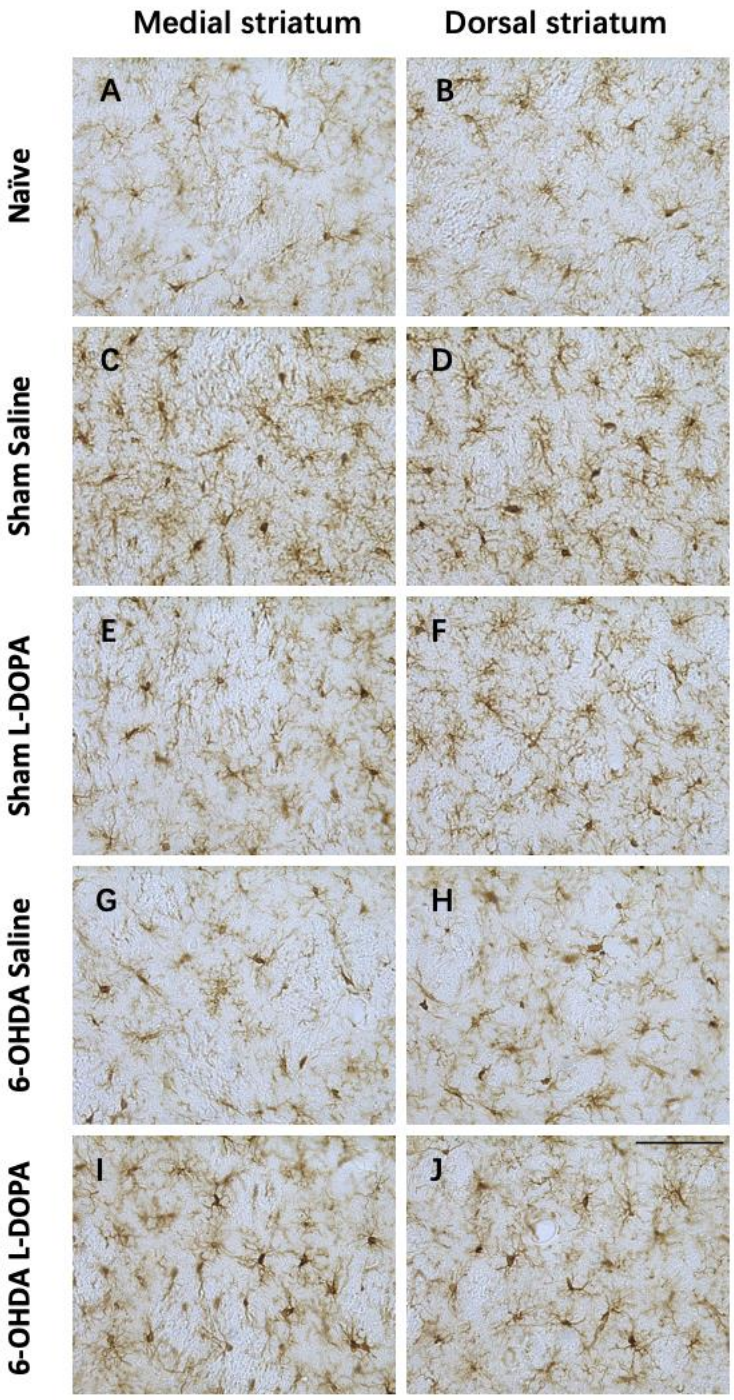

Figure 3-10 Inflammatory response in the striatum in the lesioned side. Representative images of IBA1 staining were presented for each group. Microglia cells were labelled by IBA1 antibody. Images were taken at 20 x magnification. Scale bar: 85μm

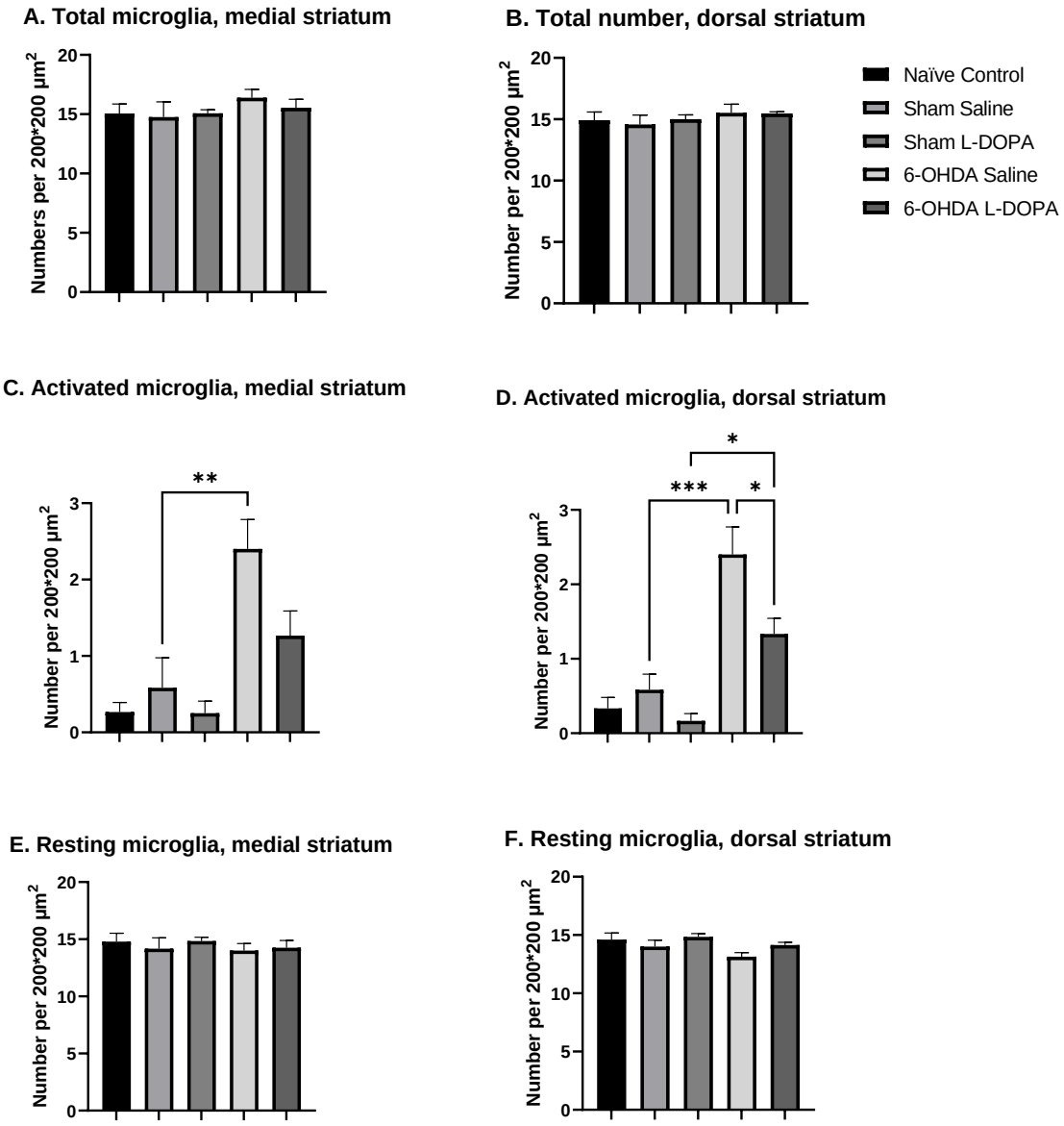

Figure 3-11 Number of IBA1^{+} cells per 200*200 µm^2 in the lesioned side were presented as mean ± standard error of the mean. Activated microglia were increased in medial ($F_{(4, 18)}$ = 9.418, P=0.0003) and dorsal striatum ($F_{(4, 18)}$ = 15.27, P<0.0001). One-way ANOVA and Bonferroni post-hoc analysis was used to examine statistical significance. *P<0.05, **P<0.01, ***P<0.001, and ****P<0.0001.

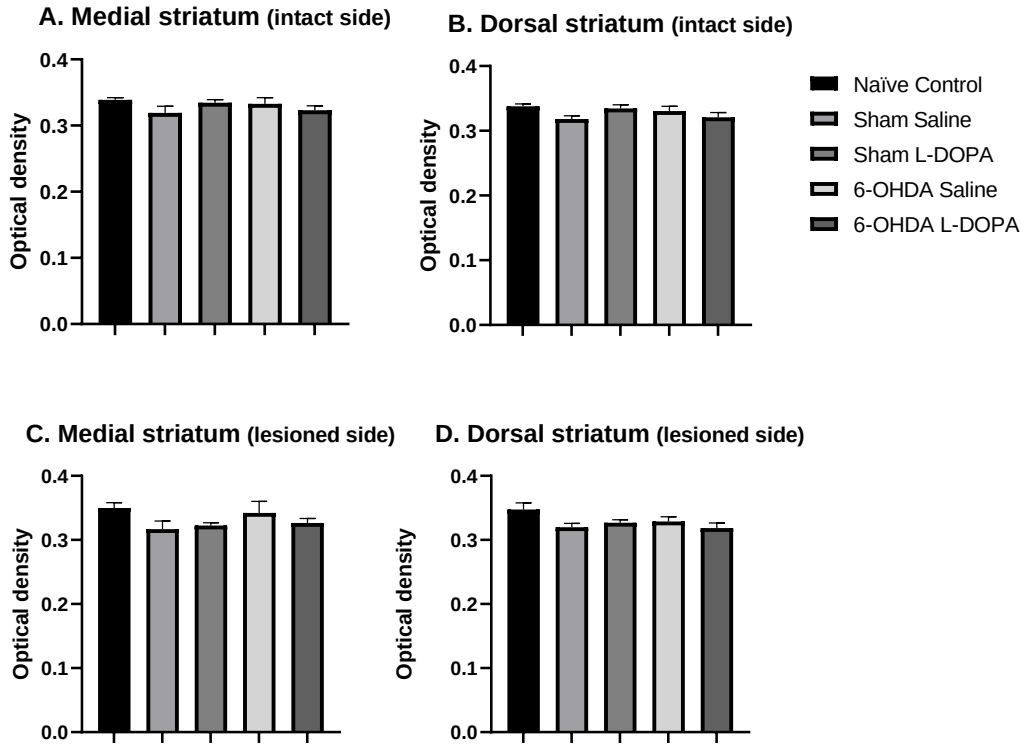

Figure 3-12 Optical density of IBA1⁺ cells in the intact and lesioned side were presented as mean ± standard error of the mean. One-way ANOVA and Bonferroni post-hoc analysis was used to examine statistical significance. *P<0.05, **P<0.01, ***P<0.001, and ****P<0.0001.

Representative images of IBA1⁺ microglial cells in the midbrain are shown in Figure 3-13. The optical density of IBA1⁺ microglial cells showed that the total number of IBA1⁺ microglial cells had no difference among all groups in SNc areas in the midbrain (SNc1 in the intact side: $F_{(4, 18)} = 2.145$, P=0.1170, SNc2 in the intact side: $F_{(4, 18)} = 0.5034$, P=0.7337, SNc1 in the lesioned side: $F_{(4, 18)} = 1.897$, P=0.1548, SNc2 in the lesioned side, $F_{(4, 18)} = 1.192$, P=0.3481. In the VTA, the optical density of IBA1⁺ microglial cell in the sham L-DOPA was significantly lower than that in the naïve control group (intact side: $F_{(4, 18)} = 3.226$, P=0.0367) lesioned side: $F_{(4, 18)} = 4.698$, P=0.0090) (Figure 3-13 and Figure 3-14).

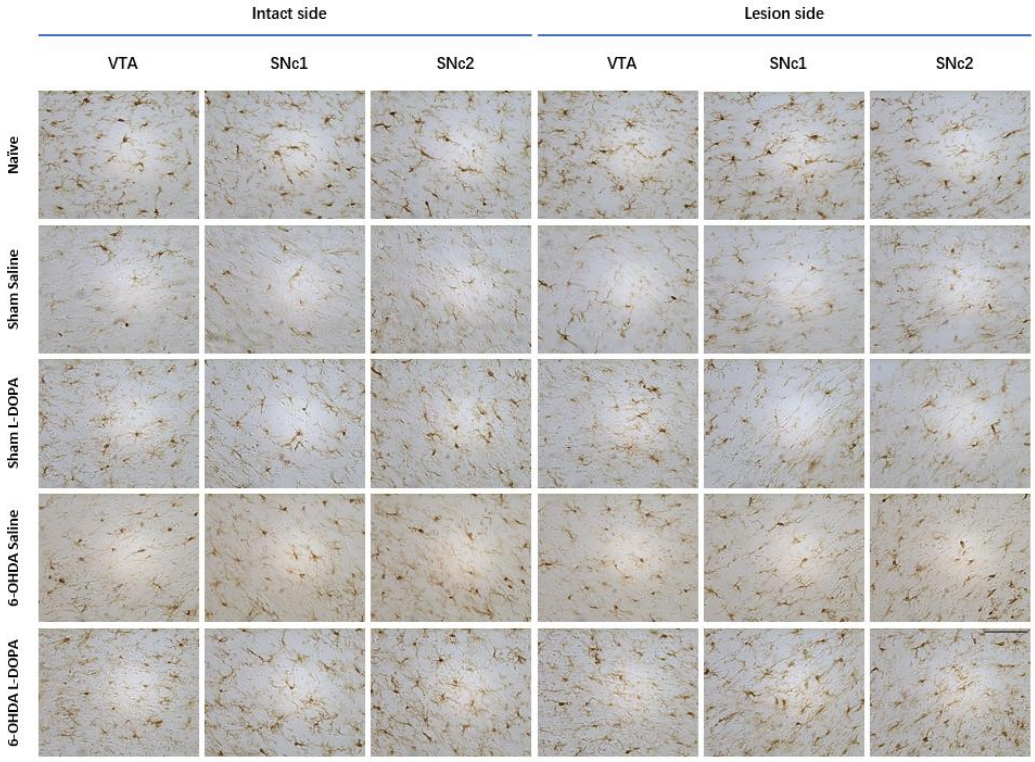

.

Figure 3-13 Inflammatory response in the midbrain. Representative images of IBA1 staining were presented for each group. Microglia cells were labelled by IBA1 antibody. Images were taken at 20 x magnification. Scale bar: 85μm

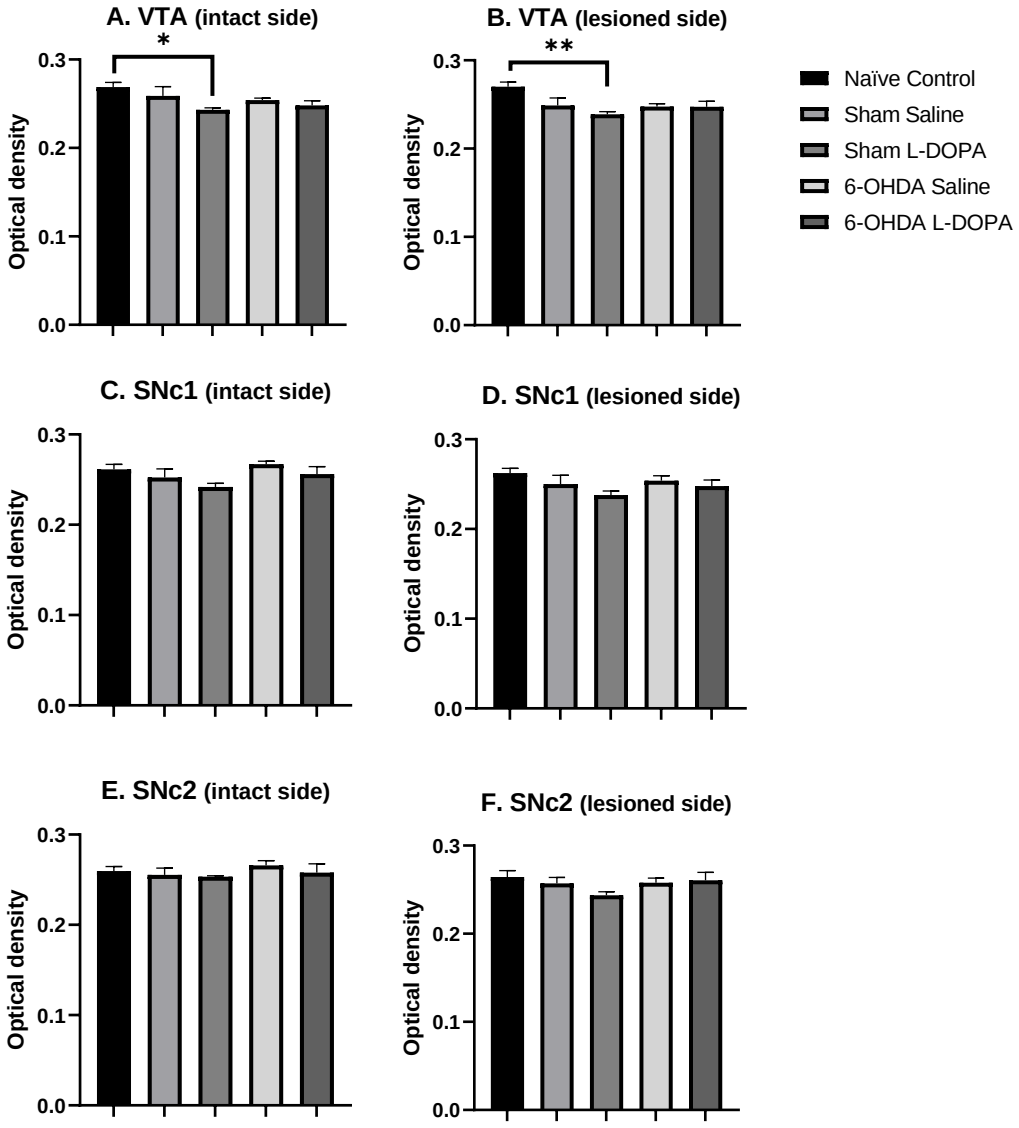

Figure 3-14 Optical density of IBA1$^+$ cells in the midbrain were presented as mean ± standard error of the mean. One-way ANOVA and Bonferroni post-hoc analysis was used to examine statistical significance. The optical density of IBA1$^+$ cells in VTA were increased in both intact (F (4, 18) = 3.226, P=0.0367) and lesioned side ($F_{(4, 18)}$ = 4.698, P=0.0090).

3.3.3.3. The impact of L-DOPA on the subtypes of DAergic neurons (A9/A10)

The DAergic neurons were double stained for TH/Girk2 and TH/Calbindin. Girk2 is a marker previously reported for identifying A9 nigral subtype of dopamine neurons; Calbindin in combination with TH is used to identify A10 subtype of dopamine neurons (Thompson et al. 2005). Girk2 expression were found in almost all the TH^+ (TH expressing neurons) cells in SNc (93.86%，SEM 0.49%) and VTA (88.54%， SEM 1.33%)(Figure 3-16). $Calbindin^+$ neurons were mainly found in the (49.22%, SEM 3.36%) TH^+ neurons in VTA; Only a few of the TH^+ /$Calbindin^+$ neurons were found in SNc (21.33%, SEM 1.97%) (Figure 3-15).

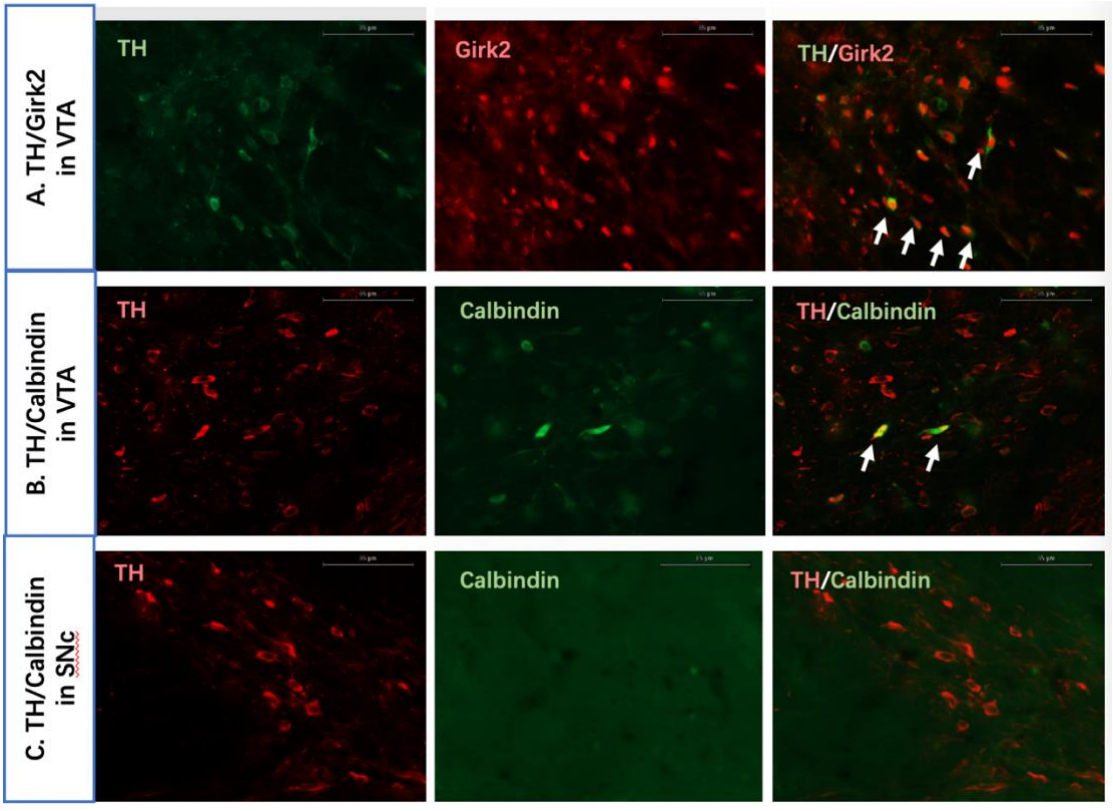

Figure 3-15 Calbindin and Girk2 expression in TH expressing neurons. A. $Girk2^+/TH^+$ cells in VTA. Neurons co-expresses both protein markers are pointed by white arrows. B. Calbindin expression within TH expressing neurons ($calbindin^+/TH^+$) in VTA. Neurons co-expresses both protein markers are pointed by white arrows. C. Calbindin expression within TH expressing cells in SNc. Scale bars: 85 μm.

The fact that GIRK2 expression was universally found in almost all TH^+ cells made it impossible to distinguish A9 subtype and study A9 related differences.

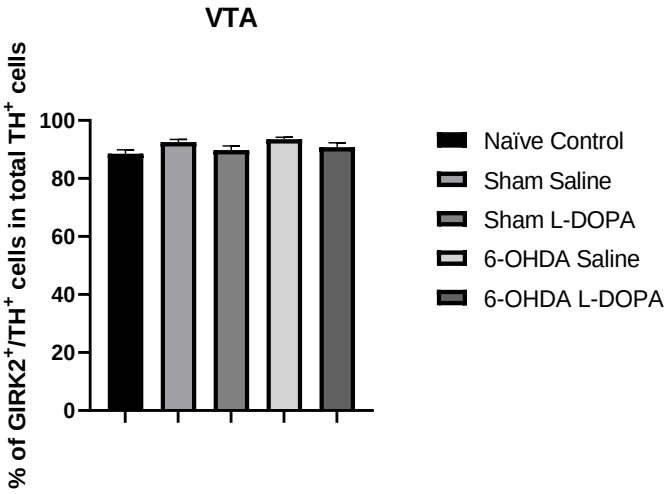

Figure 3-16 Percentage of $GIRK2^+/TH^+$ cells in total TH^+ cells. The number of DAergic neurons were presented as mean ± standard error of the mean. One-way ANOVA and Bonferroni post-hoc analysis was used to examine statistical significance. *P<0.05, **P<0.01, ***P<0.001, and ****P<0.0001.

For the A10 DAergic neurons, no differences were found on the intact side among all groups in the SNc ($F_{(4, 14)}$ = 1.748, P=0.1955) and the VTA ($F_{(4, 14)}$ = 0.3002, P=0.8729) (Figure 3-17 A and B).

On the lesioned side, the number of A10 neurons between sham groups and 6-OHDA groups was significantly different in the SNc ($F_{(4, 14)}$ = 31.00, P<0.0001) and the VTA ($F_{(4, 14)}$ = 8.620, P=0.001) because most TH^+ cells were depleted by the toxicity of 6-OHDA (Figure 3-17 C and D).

Comparing 6-OHDA saline and 6-OHDA L-DOPA group, it showed that L-DOPA treatment did not cause a statistically significant change to A10 cell populations, but on the lesioned side, there was a trend that L-DOPA administration led to

elevated A10 cells.

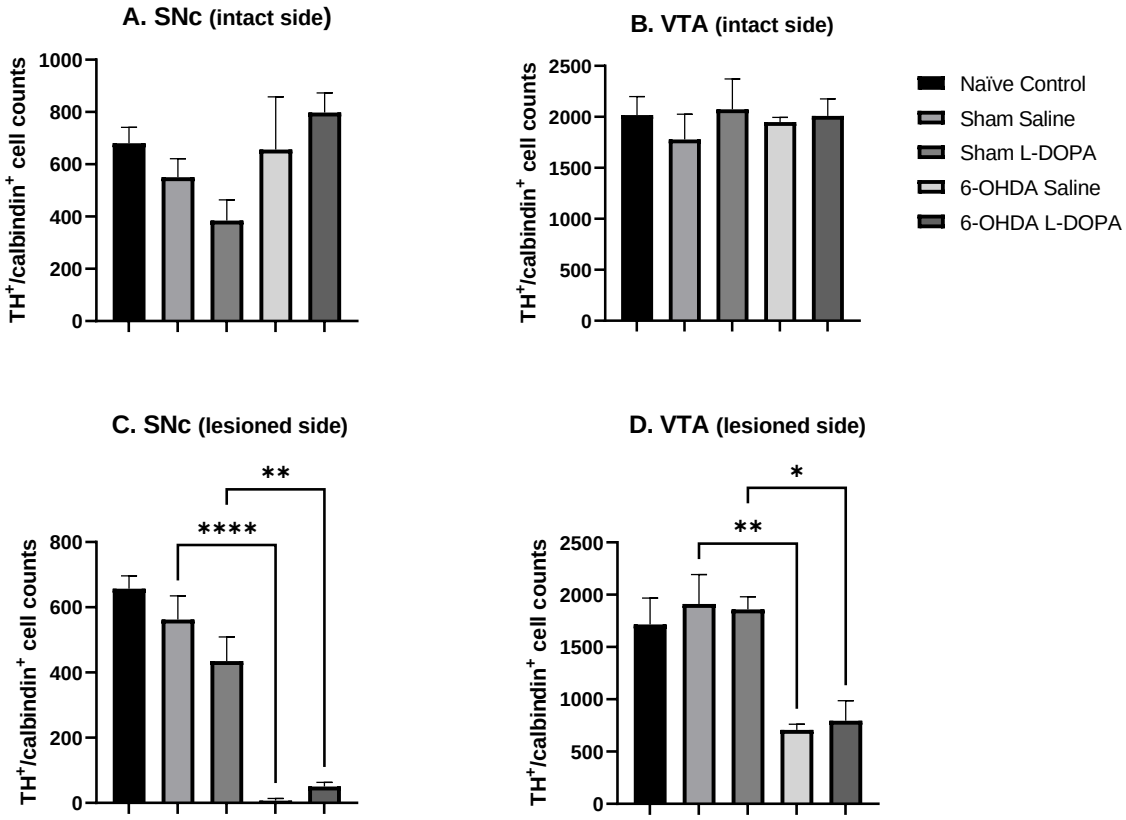

Figure 3-17 the mean number of TH^+ and $TH^+/Calbindin^+$ expressing cells counted in different regions on the intact side and the lesioned side. The number of DAergic neurons were presented as mean ± standard error of the mean. The trend in double staining were the same as TH^+ staining. $TH^+/Calbindin^+$ expressing cells were depleted in SNc ($F_{(4, 14)}$ = 31.00, P<0.0001) and VTA ($F_{(4, 14)}$ = 8.620, P=0.0010) in the lesioned side. One-way ANOVA and Bonferroni post-hoc analysis was used to examine statistical significance. *P<0.05, **P<0.01, ***P<0.001, and ****P<0.0001.

3.3.4. The impact of L-DOPA on the concentration of Hcy

The concentration of Hcy in the serum was measured (Figure 3-18). There was a significant difference of the concentration of Hcy between naïve group and lesioned groups ($F_{(4, 24)}$ = 11.30, P<0.0001). The level of Hcy in saline control group showed significant difference to lesion control group but not to lesion L-DOPA group. However, when comparing lesion control with lesion L-DOPA

group, no statistical difference can be found.

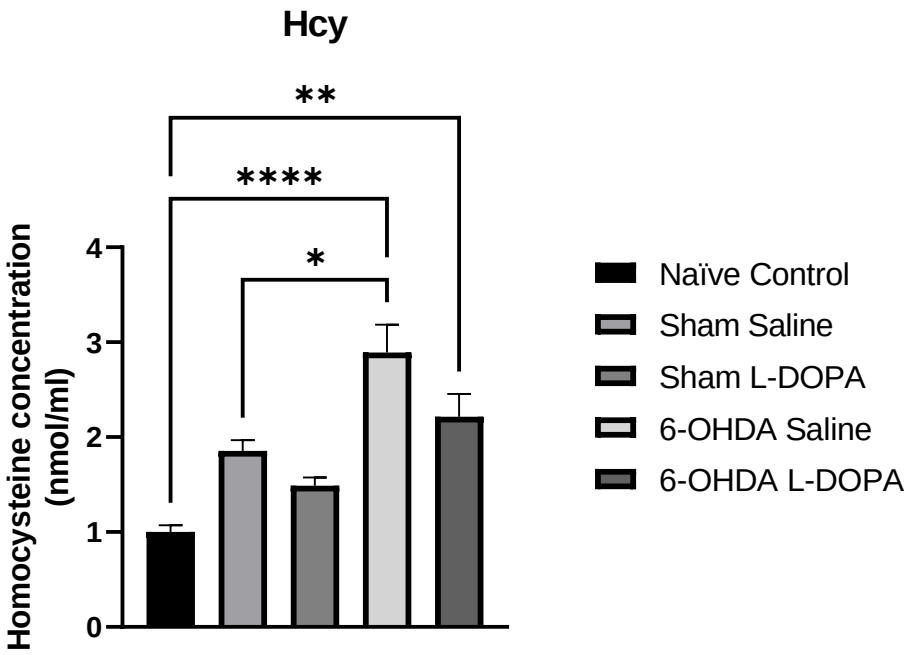

Figure 3-18 The concentration of homocysteine in different groups. The concentration of homocysteine for each group are presented as mean ± standard error of the mean. Naïve (n=5), saline control (n=5), saline L-DOPA (n=5), lesion control (n=7) and lesion L-DOPA (n=7). Hcy level significantly increased in 6-OHDA treated groups ($F_{(4, 24)}$ = 11.30, P<0.0001). One-way ANOVA and Bonferroni post-hoc were used for analysis. *P<0.05, **P<0.01, ***P<0.001, and ****P<0.0001.

3.4 Discussion and conclusion

3.4.1. General discussion

The aim of this experiment was to examine the effect of L-DOPA on endogenous DAergic cells in rat model. The results revealed that L-DOPA was not affecting the survival of DAergic neurons both in the intact and lesioned side. Also, immune response and peripheral Hcy level were not negatively influenced after chronic L-DOPA treatment.

The study of L-DOPA's impact on both disease progression and impact of L-DOPA on the survival of TH neurons in the rodent brain have been repeatedly addressed, each not satisfactorily. Critically, it was important for the rest of this thesis to be able to determine how the model behaves in our hands and also to address the issue that the dosage and frequency of L-DOPA treatment were not reflective of the actual situation of people with PD. In practice, PD patients receive escalating dose of L-DOPA to cope with disease progression. The gradual loss of DA cells makes DA release uncontrollable, which may result in wear-off effect and L-DOPA induced dyskinesia (Stocchi 2006). Previous *in vivo* experiments seldom look into this common feature of PD patients and L-DOPA's effect on LID was barely investigated. Therefore, to better understand L-DOPA's influence in the clinical setting, this chapter established and characterized a bi-daily long-term L-DOPA treatment model based on the classical 6-OHDA lesioned rat model.

Chronic treatment of L-DOPA often results in LID, a movement complication that appears in the majority of people with PD after receiving L-DOPA treatment (Grandas et al. 1999). A good correlation between the dosage of L-DOPA and

the severity of LID in rat model was found by Putterman et al. (Putterman et al. 2007). It was pointed out that 4 mg/kg of L-DOPA treatment is the lowest dosage to evoke LID in the 6-OHDA rat model. Clinical studies suggest that twice daily L-DOPA treatment is most suitable for clinical practice in early disease (Hinson et al. 2009) and it is more practically and ethically allowed to administer L-DOPA in this frequency. Therefore, twice daily 4 mg/kg L-DOPA treatment was set as the best compromise in the animal model and should be more representative than once daily dosing. In the clinic, the dosing strategy is to increase L-DOPA dose after chronic use as L-DOPA's effect wears off alongside with gradual DA neuron loss (Brooks 2008). This escalating dose was also reflected by increasing L-DOPA's dose from 4mg/kg to 8mg/kg, then finally 12mg/kg. From reports by Cenci and colleagues, it can be extrapolated that increasing dosage of L-DOPA is correlated with increasing AIMs (Winkler et al. 2002; Peng et al. 2019). A significant difference was found between 4mg/kg and 8mg/kg, and between 4mg/kg and 12mg/kg, proving that L-DOPA treatment was affecting the LID level.

This mild to more disabling LID symptoms was set to mimic patients with long-term L-DOPA treatment. Since the behavior changes reflected by AIMs matches the experiment expectation, the next step was to analyze and compare the L-DOPA's impact on both the intact side and lesioned side by immunohistological measures.

3.4.2. Discussion over findings from immunohistology

First of all, the DAB staining showed that 6-OHDA had depleted most TH cells in the lesioned side, which means the 6-OHDA lesion was successful (Torres and Dunnett 2011). No impact of L-DOPA was found on both intact and lesioned side in regard to DA cell survival, which is in agreement with most *in vivo* studies

that L-DOPA is non-toxic to DA neurons (Mytilineou et al. 2003). This data supports other findings and differences between *in vivo* and *in vitro* findings and could be two-fold: the dose is likely to be significantly lower *in vivo* with L-DOPA having very low bioavailability and secondly possibly the complex cell environment that cannot be easily replicated *in vitro*. As shown in the result, 6-OHDA mainly damaged the DA neurons in the SNc and SNr but did not affect the number of astrocytes. the loss of DA did not change the number of reactive astrocytes in the striatum (including naïve group), showing that the damage is specific to neurons. It also shows specificity of the immune response in that microglia were activated but astrocytes not recruited. It is important to note that the cell death in response to the lesion would be stable as this occurred at 1-2 weeks post lesion. However, no residual astrocyte response was evident. Astrocytes supply antioxidants that are protective to oxidative stress (Rangasamy et al. 2010) and express neurotrophic factors that are neurorestorative to DA neurons (Wang et al. 2002; Fernandez-Fernandez et al. 2012). The dose of L-DOPA in this improved 6-OHDA model is small (4 mg/kg to 12 mg/kg bidaily) compared with similar L-DOPA related tests (80-200 mg/kg daily. See Table 3-1). Therefore, the oxidative species produced by L-DOPA metabolism is unlikely to exceed the capacity of the protective cells and antioxidants in this rat model.

It was argued that A9 subtype of DA neurons were of great importance to the motor function of PD subjects (Grealish et al. 2010) but, in the meanwhile, were the most vulnerable of their species in ventral midbrain (Hegarty et al. 2013). Therefore, this study used double staining to evaluate if L-DOPA selectively causes cell death on a specific subtype of DA neuron. The results in 3.3.3.3. showed that calbindin/TH co-staining successfully marked A10 cells while Girk2/TH co-staining marked almost all TH^+ cells in SNc and VTA, failing to selectively mark A9 cells. Most studies suggest that it's feasible to prepare high

A9 component graft tissue from fetal ventral midbrain or hESC-derived source (Grealish et al. 2014) and Girk2 can be used in those studies for calculating A9 subtype percentage (Grealish et al. 2010). However, for endogenous rat DA cells, such reports were unseen. The Girk2 expression in adult rat brain may hamper the use of Girk2 to selectively mark A9 cells. mRNA study in rat showed that Girk2 expression in both SNc and its neighboring VTA region were extremely high (Karschin et al. 1996). Therefore, it may worth trying to stain A9 subtype with other markers such as ALDH1a1 (aldehyde dehydrogenase 1 family, member A1), PITX3 (pituitary homeobox 3), NURR1 (Nuclear receptor related 1 protein), LMXA1 (LIM homeobox transcription factor 1, alpha), or EN1 (homeobox protein engrailed-1) (McCaffery and Dräger 1994; Garitaonandia et al. 2012; Decressac et al. 2013). Overall, neither Girk2/TH nor calbindin/TH co-staining showed that L-DOPA had any impact on the survival of DA neuron subtypes.

Beside the direct influence of L-DOPA on DA neurons, this study also investigated if L-DOPA changed immune responses in the PD rat model. As previously discussed (see section 3.1.4), the immune system plays an important role in DA neuron degeneration and post-mortem data showed that microglial cells were extensively activated in PD patients' brain (Gerhard et al. 2006). Therefore, this study counted the $IBA1^+$ microglial cell number and density in the striatum, SNc and VTA. The results in striatum showed that following 6-OHDA lesion, the immune cells in both intact and lesioned side of the rat brain were activated. This is in line with recent consensus that microglia activates in all areas following neuronal loss with or without the presence of cell death (Ferreira and Romero-Ramos 2018). In terms of L-DOPA's effect, it was surprising to see that L-DOPA decreased the number of activated microglia, revealing an anti-inflammatory effect in this model.

The results showed no impact of L-DOPA to astrocytes in the striatum. Astrocytes were believed to be neuroprotective and neurotrophic to DA neurons in people with PD, though recent views proposed that astrocytes should be divided into detrimental A1 subtype and protective A2 subtype (Miyazaki and Asanuma 2020). Investigating these different phenotypes might yield slightly different results to the inactivated/activated distinction considered here. However, the subtypes were not considered in this study for many reasons: The most prominent issue is most commonly used marker for astrocytes: GFAP. The marking of a specific neuron cell is quite difficult as those proteins may be expressed by other cell types and also the expression level is highly dependent on the cell environment as well as their activation status (Jurga et al. 2021). Fortunately, astrocytes have a characteristic morphological change when activated which is distinct enough to be counted as different populations, which will be otherwise quite challenging due to lack of specificity (Kimelberg 2004). Nevertheless, we found no report suggesting that this morphological feature can be relied on to further distinguish the subtypes of astrocytes. In fact, those subtypes were so named after gene signature but even those signatures were found not very specific in recent studies (Sarkar and Biswas 2021). Further works are still needed to determine whether astrocyte's heterogeneity is to be finely classified.

Combining with the results of microglial cells, the overall influence of L-DOPA to immune response in the brain were mainly about $IBA1^+$ cells. The unexpected reduction of $IBA1^+$ cells showed L-DOPA may have an anti-inflammatory effect when DA cells were damaged by neurotoxins (mechanism is based on attacks from free radicals). Inflammation was always considered as a detrimental factor to the overall survival of DA neurons in PD patient's brain (Pajares et al. 2020). The results from this 6-OHDA rat model were showing that since L-DOPA is not exacerbating inflammatory responses in the brain and,

more importantly, not affecting DA neuron survival, the chronic L-DOPA treatment should be considered unharmful to the tested subjects in this model.

3.4.3. No impact of L-DOPA on the peripheral Hcy level was found in this model

Other than the CNS, L-DOPA treatment might have impact on the peripheral Hcy concentration, which in turn, may negatively affect cognitive functions of PD patient (Licking et al. 2017). However, previous research also suggested that Hcy level in PD patients received only minor influence from L-DOPA treatment (Kocer et al. 2016). This experiment therefore compared the Hcy level in each group to see if this impact is significant. The result showed that while 6-OHDA lesion led to a significant increase of Hcy level in rat peripheral blood, L-DOPA had no impact on both saline sham and 6-OHDA lesioned groups. The reason why 6-OHDA affects Hcy level is unknown. No studies investigating this effect were identified in the literature.

3.4.4. Conclusion

This experiment built a 6-OHDA PD rat model that closely reproduced the real situation of people with PD. L-DOPA's effect on both intact and lesioned side of the rat brain were evaluated based on DA neuron survival and immune response. L-DOPA was not affecting DA neuron survival in this situation, but it attenuated the microglial response in the striatum.

Chapter 4. Impact of L-DOPA on human embryonic stem cell derived dopaminergic neuron transplantation in the 6-OHDA rat model of PD

4.1. Introduction

In the previous chapter, the impact of L-DOPA on the classical 6-OHDA model was investigated. The results confirmed that L-DOPA had no impact on DA neuron survival when the dosage more closely mimicked PD patient's condition, neither did long term L-DOPA specifically exacerbate the inflammatory response in contrast to other studies. The next goal is to investigate the impact of L-DOPA on hESC-derived grafted cells, the cells that are poised to enter clinical trials, and to similarly consider what factors need to be replicated to more closely represent the patient experience of transplantation and medication.

It has taken many years for stem cell therapies to enter clinical trials. Many institutions such as Lund and Cambridge Universities and Sloan-Kettering Institute are driving hESC-based cell therapies from the bench to the clinic (Grealish et al. 2014; Kirkeby et al. 2017; Tiklová et al. 2020). Preclinical studies show that hESC derived DA neurons can have the same level of therapeutic value when compared to the classical fetal tissue transplanted but have fewer moral and legal issues associated with their development. In addition, high quality production pipelines are now ready to produce hESC for transplantation en mass. These efforts ensured the safety, efficacy and industrial future for the hESC therapy (Liu and Cheung 2020; Parish and Thompson 2021).

As described in Chapter 1 currently people with PD are living with not only the disease itself but also significant side effects from the dopaminergic medications. Cell replacement is novel intervention that may offer some advantages compared to pharmacotherapy. In the case of transplanted cells, DA supplied by the graft is released directly into the striatum in the basal ganglia. this may reduce the need for escalating dosage of DA medication and thus

alleviate the side effects associated with peripheral dopamine supply (Tomishima and Kirkeby 2021).

Looking back into the history of the related studies, the source of graft cells and the method for the study of L-DOPA's impact has been changed significantly, alongside with attitude towards L-DOPA treatment. From 1980s to 2000s, the source for most *in vivo* experiments was solid fetal midbrain tissues. Those brain tissues were grafted into the striatum and L-DOPA treatment were given immediately after transplantation to study L-DOPA's effect on the graft. Most results from such experiments concluded that L-DOPA treatment had a negative effect on the survival and functional recovery of DAergic neurons (Steece-Collier et al. 1990; Blunt et al. 1991; Yurek et al. 1991). In the same period, there was significant refinement of the preparation of the tissue and suspended cell suspensions of fetal cells, rather than tissues pieces, were used to reduce immunogenicity. L-DOPA studies with improved methodology reached opposite conclusions to those with solid tissues, finding that in this paradigm, L-DOPA had no impact on the graft survival (Blunt et al. 1991,1992; Steece-Collier et al. 2009). The most plausible explanation is that large solid tissue pieces may contain more antigens from the original source and thus triggers more severe immune responses, while graft cell suspension is generally purer cells due to their preparation protocol and induces a lower level of activation of immune cells (Mendez et al. 2005). These studies were conducted using syngeneic rat to rat transplants, for whom the cell suspension methods significantly reduce the immune response. These studies have not been replicated for any human cell to rat host transplants. It is known that immune responses differ greatly from rodent model to human, and the translation of hESC technology from rat models to human may not exclude problems of immunogenicity (Mestas and Hughes 2004). However, the strict rules and management (GMP protocols are needed for the providers of clinical

grade graft) for producing hESC cells will at least avoid impurities such as blood vessels etc. in tissue pieces (Kirkeby et al. 2017).

In the clinic, as a common problem with transplantations, without immunosuppression, there was very little benefit/cell survival seen after graft surgery (Freed et al. 2001). The biggest immunological risk is immediately after transplantation when the brain-blood barrier (BBB) is compromised. Immunosuppression over this time might mitigate the excessive response that occurs after transplantation. Thus, administration of immunosuppressive drug at the time of the transplantation is critical for enhancing the graft survival rate (Kordower et al. 1995; Mendez et al. 2005). When given, these immunosuppressive drugs have been withdrawn variously at 6-24 months post graft (Mendez et al. 2008; Barker et al. 2019). The most common theory currently is that the blood brain barrier then offers some degree of protection once the brain has healed from the surgery (Chodobski et al. 2011). Although immunosuppressive regimens are changing, one of the most widely used immunosuppressant is cyclosporine A. To replicate the situation after graft surgery, it was used in this chapter as immunosuppressive agent.

Drawing conclusions from immune responses in animal models in transplant studies can be problematic because of the need to transplant across species. The transplantation of exogenous human cells into rodents without immunosuppression would result in immune rejection and death of the transplanted cells in a relatively short period of time (2 to 4 weeks) (Sloan et al. 1991; Heuer et al. 2016). In order to study hESC *in vivo*, this issue needs to be managed carefully. In this study one of the aims is to determine whether L-DOPA has an additional impact on immune response to the graft. Currently, most *in vivo* studies utilize one of the three methods listed below, each has their advantages and disadvantages:

(1) The usage of immunosuppressive agent alone. Daily administration of Cyclosporine A is the most common way to attenuate immune response but after chronic use (between 20 and 30 weeks in the rat) it may cause drug induced toxicity which includes organ damage and microbial infection (Graham 1994; Gijtenbeek et al. 1999; Christians et al. 2011). The severe side effects limit long term usage of cyclosporine A. Therefore, cyclosporine A alone is not considered to be the most appropriate plan for the hESC based animal model in this project, as the duration would ideally exceed 30 weeks to record the fully matured neurite development and changes (Heuer et al. 2016).

(2) Using athymic nude rats, the immunocompromised animal for the experiment. Athymic nude rat is an alternative choice to study long term xenograft transplantation without interference from immunosuppressive drugs (Rolstad 2001). These rats have a genetic defect (rnu gene) which compromises their thymus development and education of functional T cells (Rolstad 2001). However, the laboratory conditions for handling the animals become more demanding due to the animal's compromised immune system. The rats have to be transferred between different rooms for surgery, maintenance, behavioral testing and drug administration. All processes can increase the risk of infection (Grealish et al. 2014). On top of the rigorous sterile conditions for keeping the animals, this method also compromises the possibility to examine the immune response to the graft since immunity is altered artificially in this case, which doesn't resemble the condition of a real PD patient.

(3) A pre-exposure rat model. Exposing rat pups to human cells early in the post-natal period largely reduces rejections from the immune system in their adulthood. During immune system development, the circulating cells will be recognized as self-cell and acquire tolerance from the rats' immunity. This more naturalistic approach avoids high dose of immunosuppressive drugs

and allows long term studies (Kelly et al. 2009). The original study and similar studies provided evidence that the desensitized rats do not need additional immunosuppression for the xenograft (hESC) survival (Heuer et al. 2016). But one of the aims of this study is to investigate the immunological changes after immunosuppressant withdrawal to mimic the clinical conditions of PD patients. Therefore, additional immunosuppressant (cyclosporin A) was still given to fulfill this purpose.

As described above, immunosuppressants were typically used in human clinical trials for 6-24 months and then withdrawn with good survival shown in post-mortem studies many years after immunosuppression withdrawal. The duration of the use of immunosuppressant, however, cannot be directly taken from the clinical standard. Animal welfare had to be considered in this long-term study and to get a more accurate representation of the role of L-DOPA in the absence of immunosuppression, it was important to consider how inflammatory responses could be studied without their presence. Therefore, MRI was introduced at week 20. 20 weeks is the maximum duration for cyclosporine A model according to previous studies. Beyond this point, animals generally start to fail, and studies are commonly terminated (Diehl et al. 2017; Coblentz et al. 2020). The goal was to demonstrate survival of the graft cells prior to withdrawal of the immunosuppression such that we could then determine whether L-DOPA impacted in the absence of immunosuppression.

Long-term L-DOPA treatment may influence the immune environment through DA (Sarkar et al. 2010). In the brain, the most relevant immune population to the aim of the thesis is microglial cells, which express D1 and D2 receptors. Human microglia migrated *in vitro* when co-cultured with human SH-SY5Y cells charactering DA phenotypic features (Mastroeni et al. 2009). A more recent *in vitro* study with mouse microglial cells showed that DA stimulates resting microglia while inhibits activated microglia. It is worth noting that p38MAPK

activation caused by DA could not be inhibited by DA receptor inhibitors such as Spiperone but DAT antagonist, indicating that DA receptors may not be involved in some of the activation process (Fan et al. 2018).

One previous study (Elabi et al 2022) exposed hESC derived dopaminergic grafts to L-DOPA *in vivo*. This was a once daily dose in the presence of immunosuppression showing that L-DOPA treatment (12 mg/kg for 3 weeks, then 6 mg/kg for 18 weeks) had no influence on graft survival. Nonetheless, for human participants in clinical trials they may be receiving L-DOPA up to 5 times daily and receive around 6 months immunosuppression before this is stopped. It is therefore important to understand the possible role of L-DOPA in a study that more closely parallels the clinical experience. Herein, L-DOPA administration was designed to be given twice daily as the best compromise when considering animal welfare, practicability and experimental objectives. The immunosuppression plan was also considered to best reflect clinical situation after hESC transplantation to allow monitoring of immune responses under the influence of long-term L-DOPA treatment.

4.1.1 Aims of this chapter

In order to demonstrate the impact of L-DOPA in the absence of immunosuppression, it was important to withdraw the immunosuppression. Therefore, a hybrid model was used in which immunosuppressant was administered to neonatally desensitized animals before being withdrawn at a later time point. Brain imaging using MRI was intended to capture the graft prior to and following immunosuppressant withdrawal.

The hypothesis is that bidaily L-DOPA administration in the absence of immunosuppression may affect the development and survival of hESC-derived DAergic neurons.

The aim of this chapter is therefore to determine the impact of long-term, bidaily L-DOPA treatment on the development and survival of hESC-derived DAergic neurons following withdrawal of immunosuppression.

Objectives:

- Assess the impact of the graft on motor and behavioral recovery in the presence and absence of L-DOPA.
- Assess the impact of the graft on the severity of LID.
- Characterize the histological features of the graft and the endogenous DAergic neurons in the presence and absence of L-DOPA.
- Utilize MRI scanning to allow visualization of the graft prior to withdrawal of immunosuppression and determine the viability of this approach to detecting surviving grafts.
- Assess the immune response induced by the graft after the withdrawal of immunosuppression in the presence and absence of L-DOPA.

4.2. Experimental design

Pups from Sprague Dawley dams (n=48) were desensitized by injecting day 16 hESC dopaminergic progenitors (produced by the lab of Prof Parmar from Lund University) on post-natal day(p) p1 or p2. Eight weeks after desensitization, all rats (n=41, 16 males, 25 female) received a unilateral 6-OHDA lesion to the right medial forebrain bundle. After two-week recovery, all rats underwent an amphetamine-induced rotation assessment to test the lesion extent, followed by baseline stepping test and vibrissae (whisker) tests. The successfully lesioned rats were further divided into four equal groups based on the results of amphetamine induced rotation, stepping test and Whisker test (table 4-1). Then the rats began to receive either saline or L-DOPA treatment depending on their group, starting from four weeks prior to transplantation and continued post-transplantation until the termination of the study, one saline group and one L-DOPA group received an intra-striatal graft of hESC derived cells whilst the other two groups had a sham saline infusion. The four groups were as described in table 4-1: Sham/Saline (n=10, 3 male, 7 female), Sham/L-DOPA (n=10, 4 male, 6 female), graft/Saline (n=10, 4 male, 6 female) and graft/L-DOPA (n=11, 5 male, 6 female). 24 hours before grafting, all rats received cyclosporine A treatment (i.p.). AIMs were conducted weekly to monitor LID. The two graft groups then received hESC-derived DAergic neural progenitors. Amphetamine induced rotation and behavior tests (including stepping test and Whisker test) started at 6 weeks post transplantation and all rats were assessed every six weeks and also one week before perfusion which was at 25 weeks post transplantation. MRI T2 scans were conducted at 18 weeks post transplantation to confirm the survival of the grafted cells to that point. At 20 weeks post transplantation, cyclosporine A was withdrawn. At 25 weeks post transplantation the rats were perfused, and the brains and livers removed for further analysis. Cardiac blood was also sampled and spun for PBMC isolation

(Figure 4-1).

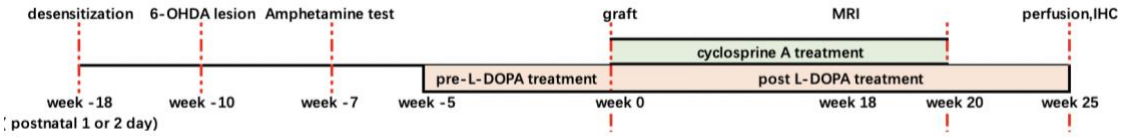

Figure 4-1 Timeline of the experiment. IHC: Immunohistochemistry.

Table 4-1 grouping information

Name of group	Surgical group	Drug treatment group
Sham saline (n=10)	saline infusion	saline
Sham L-DOPA (n=10)	saline infusion	L-DOPA
Graft saline (n=10)	Graft	saline
Graft L-DOPA (n=11)	Graft	L-DOPA

4.3. Methods

4.3.1. Treatment

L-DOPA 6mg/kg plus Benserazide 12mg/kg in 0.9% saline was injected into L-DOPA treated group twice a day subcutaneously from 4 weeks prior to transplantation until the rats were perfused. The saline treated group received daily injection with saline twice a day (0.9%, 1 ml/kg) subcutaneously. 10 mg/kg Cyclosporine-A in 0.9% saline was given (i.p.) to all the rats 24 hours before transplantation and was withdrawn at the end of week 20 post transplantation.

4.3.2. Preparation of differentiated ESC cells for desensitization and transplantation

Day 16 hESC dopaminergic progenitors were provided by Kirkeby and Parmar group from Lund University and stored at -80°C (Nolbrant et al. 2017). Before use, the frozen cells were thawed by following steps. 10% human serum albumin was dissolved in DMEM/F12 (Dulbecco's Modified Eagle Medium/Nutrient Mixture F-12) into 1% as a washing medium. HBSS/DNase solution was prepared from Hanks balanced salt solution (HBSS, Thermo Fisher, cat. no. 14175095) and DNase (Pulmozyme, Dornase Alpha, Roche, cat. no. 11899) in a ratio of 1:6 as a stock solution keeping at 4°C. A vial containing frozen cells was removed from -80 °C freezer and was transferred to Thawstar. After thawing was completed, 1 ml washing medium was added dropwise into the vial. The cells in medium were moved to 15 ml tube and the empty vial was re-washed by 1 ml washing medium and the washing medium was combined to the same 15 ml tube containing cells. Then, 8 ml washing medium was added to the 15 ml tube, the 11ml cell suspension was centrifuged at 400xg for 5 minutes. The medium was removed from the tube with 10 ml pipette. The cell pellet was resuspended in 1 ml HBSS/DNase solution and 100 µl wash medium. 10 µl cell suspension was stained by 0.04% trypan blue solution, the number of cells were counted under the microscope. The number of cells in the vial was calculated (Total number of cells in the vial = cell density x 1.1 ml). Cells suspension was centrifuged at 400xg for 5 minutes. After the medium was removed, the cell pellet was resuspended in HBSS/DNase solution to yield a final concentration of 100,000 cells/µl. The vial containing the cell suspension was kept on ice throughout the surgical procedure.

4.3.3. Induction of neonatal desensitization

The dam was moved to an anesthesia induction chamber and was anesthetized with 3% isoflurane which was carried by a mixture of oxygen and nitrous oxide in a proportion of 1:2. Before pups were handled, disposable nitrile gloves were worn and were scrubbed thoroughly with bedding material under the cage to avoid the transition of strange odours to the pups. Pups were checked that they had fed from the dam (milk in the stomach is visible externally). Pups were injected i.p. with 1ul of 100,000 cells/µl cell suspension containing immature neural progenitors (day 16 of differentiation, prepared as described above 4.3.2) via i.p on the post-natal day 1 or 2, delivered via 10 µl Hamilton Syringe with 26-gauge needle. After all the pups were injected, the dam was returned to the home cage with pups. There were no instances of rejection of the pups following the procedure.

4.3.4. Cell transplantation

Two deposits (1 µl per deposit) were infused into one site of striatum (Anteroposterior：-0.5 mm from bregma, Lateral：−3.0 mm from bregma, Dorsoventral: −5 mm and -4mm below dura) by using a 10 µl Hamilton Syringe infusing at the rate of 1 µl/ 90 second with 23-gauge stainless steel cannula. After DAergic progenitors (day 16 of differentiation, prepared as described above 4.3.2) were grafted into striatum, the cannula was left in the tissue for 3 minutes to prevent the cell solution from refluxing up the tract.

4.3.5. Peripheral blood mononuclear cells (PBMC) isolation

2.5ml RPMI 1640 medium was added to dilute a 3.5 ml blood sample to a total

volume of 6ml. 5ml Histopaque 1083 solution was added into 15ml falcon tube in advance. The diluted 6ml blood sample was gently layered on the top of the Histopaque layer and were centrifuged at 400G for 30 minutes without brakes. PBMC layer were transferred into a fresh 15ml falcon tube with 10ml RPMI media. The mixed solution was centrifuged for 10 minutes at 400G with normal brake setting. After the solution were removed, PBMC pellets were re-suspend by trituation and were performed Trypan Blue cell counting at 0.4%. The remaining PBMC suspension was measured and centrifuged for 10 mins at 400G with normal brake settings. Supernatant were removed to make a suspension of 40,000 cells per µl by adding 1:1 RPMI medium and ice cold 20% DMSO in RPMI medium. The PBMCs were frozen for further analysis.

4.3.6. qPCR

RNA from PBMCs was isolated by using PureLink™ RNA Mini Kit (12183018A, Invitrogen) based on manufacturer's instructions. The concentration and purification of RNA were measured by nanodrop spectrometer. The Applied Biosystems High Capacity Reverse Transcription Kit (4368814, Applied Biosystems) were used for converting from RNA to cDNA based on manufacturers' instructions. qPCR was run on StepOnePlus™ Real-Time PCR System by using Prime time Gene expression master mix (1055772, integrated DNA technologies) and PrimeTime qPCR Primer Assay (integrated DNA technologies). The PCR condition consist of 50^{o}C for 2 mins, followed by 95^{o}C for 10 mins. Then, samples underwent 40 cycles of 95^{o}C for 15s and 60^{o}C for 1 minute. Cycle threshold (Ct) values were collected from the real-time qPCR for further calculation. The relative changes in gene expression were analyzed by using the $2^{-\Delta\Delta CT}$ method. The following PrimeTime Std® qPCR Primer Assay (integrated DNA technologies) were used: CTLA4 (Rn.PT.58.37464261), C3(Rn.PT.58.8086490), CD8a (Rn.PT.58.38249657), CD86 (Rn.PT.58.46141668), CD3g (Rn.PT.58.6607345), CD59 (Rn.PT.58.37936128),

CD4 (Rn.PT.58.12759565), FoxP3 (Rn.PT.58.37804009), Cd11b (Rn.PT.58.23882443), CD68 (Rn.PT.58.7890131.gs). Housekeeping genes: TBP(Rn.PT.39a.22214837) and PPIA (Rn.PT.39a.22214830).

4.3.7. MRI scanning

MRI scans were conducted at 18 weeks post transplantation. Animals were anesthetized with 1-2% isoflurane which was carried by a mixture of oxygen and nitrous oxide in a proportion of 1:2. Incisor and ear bars in the stereotaxic frame are used to fix the head of the rat. During scanning a heat pad was used to maintain the body temperature at 37 °C and breath rate was monitored. T2 rare and SWI scans were conducted. The data was analyzed by MATLAB@2021.

4.4. Results

4.4.1. Behavior results

4.4.1.1. Amphetamine induced rotations and apomorphine-induced rotation

Amphetamine-induced rotations were performed pre-graft, then 6 weeks, 12 weeks, 18 weeks and 25 weeks post-graft (Figure 4-2. A). Before transplantation, there was no significant difference in the number of rotations among these four groups ($F_{(12, 140)} = 1.374$, $P=0.1853$). At 18 weeks post-transplantation, there was a slight decrease in the number of amphetamine-induced rotations for grafted groups when compared to sham groups. The number of amphetamine rotations of the two grafted groups (graft L-DOPA and graft saline) remained at the same level ($P>0.9999$). At 25 weeks post-transplantation, the number of amphetamine-induced rotation of grafted groups showed a slight increase though the changes were not statistically significant ($P>0.9999$). Apomorphine-induced rotation was performed at 6 weeks, 12 weeks, 18 weeks and 25 weeks post-graft (Figure 4-2. B). There was no difference between each of the groups at these time points ($P=0.0439$).

4.4.1.2. Stepping test and whisker test

Stepping test was performed pre-graft, 6 weeks, 12 weeks, 18 weeks and 25 weeks post-graft (Figure 4-2. C and D). Before transplantation, 6-OHDA induced significant motor deficit in both stepping test and whisker test. For the stepping there was no difference in backhand steps during the whole period ($F_{(12, 140)} = 0.8787$, $P=0.5701$), so the results presented below are all forehand. From 12 weeks post-transplantation there was an increasing trend in the

percentage of contralateral forehand stepping in graft saline group. A significant difference appeared between graft saline and graft L-DOPA rats ($F_{(12, 140)}$ = 3.124, P=0.0006) at week 12 post-graft (P=0.0063) and week 18 post-graft (P=0.0224).

Whisker test was also performed at the week pre-graft and at weeks 6,12, 18 and 25 post-graft (Figure 4-2. E). No difference was found between the four groups from pre-graft to 25 weeks post transplantation ($F_{(12, 140)}$ = 0.6408, P=0.8044).

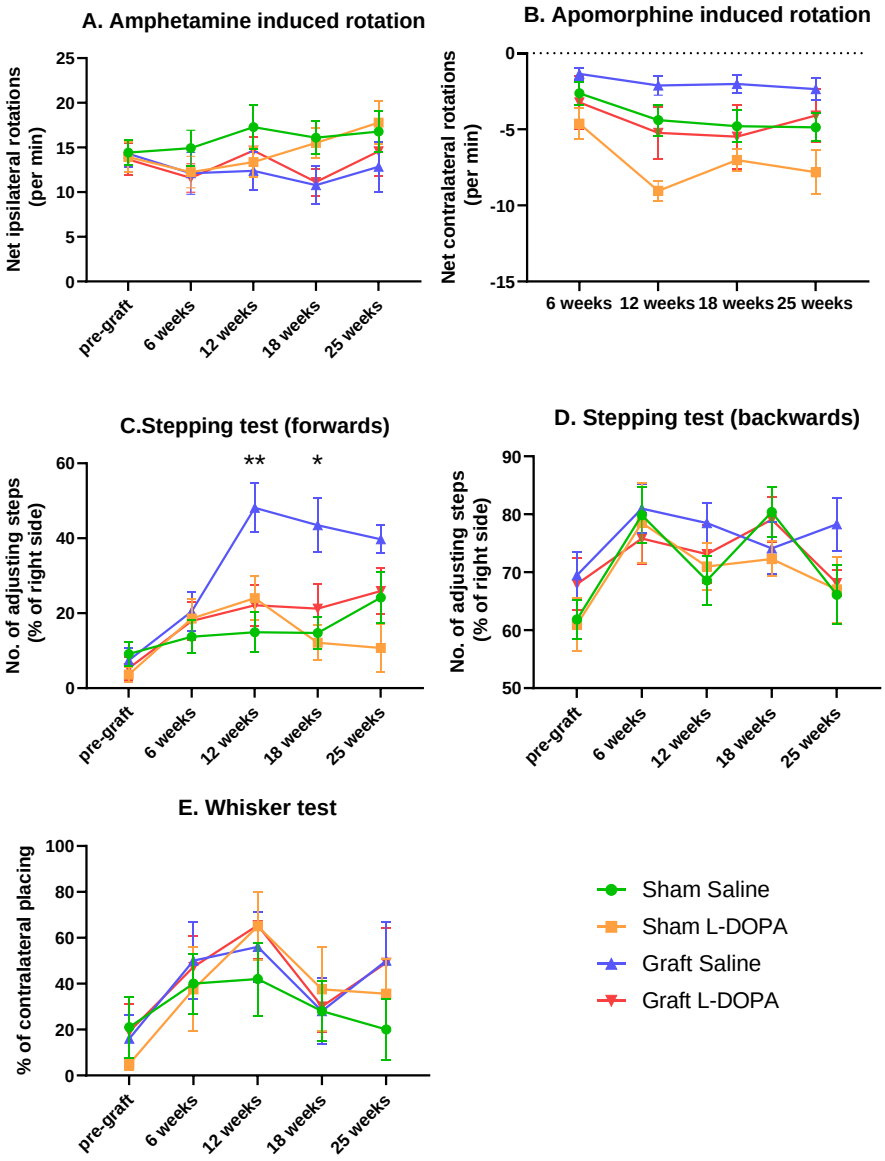

Figure 4-2 (A) Amphetamine-induced rotational bias of different groups. Mean full body rotations per minute were recorded for rats after injected with 2.5 mg/kg methamphetamine via i.p.. Data were presented as mean rotation ± standard error of the mean (SEM); Error bars = ± SEM. (B) Apomorphine-induced rotational bias of different groups. Mean full body rotations per minute were recorded for rats after injected with 0.05 mg/kg Apomorphine via i.p. Data were presented as mean rotation ± standard error of the mean (SEM); Error bars = ± SEM. (C-E) stepping test and whisker test. Data were represented as percentage change to the ipsilateral side. Significance was found in stepping forward test ($F_{(12, 140)}$ = 3.124, P=0.0006). Data were presented as mean score ± standard error of the mean (SEM); Error bars = ± SEM. Two-way ANOVA was used to test statistical significance with Bonferroni post-hoc analysis. *P<0.05, **P<0.01, ***P<0.001, and ****P<0.0001.

4.4.1.3. L-DOPA induced AIMs

A rapid increase in the AIMs was observed after rats received L-DOPA treatment for 5 weeks. The level of AIMs reached a peak 5 weeks after L-DOPA administration in both sham L-DOPA and graft L-DOPA groups. The AIMs decreased at 20 weeks post-graft in the graft L-DOPA group, but this trend was not statistically significant ($F_{(3,\ 68)}$ = 0.7892, P=0.5041). L-DOPA-induced rotational behavior was tested weekly. At week 20 post-graft, there was a slight decrease in the number of contralateral rotations in the graft L-DOPA group while with no statistical significance ($F_{(3,\ 68)}$ = 0.3259, P=0.8066) (Figure 4-3).

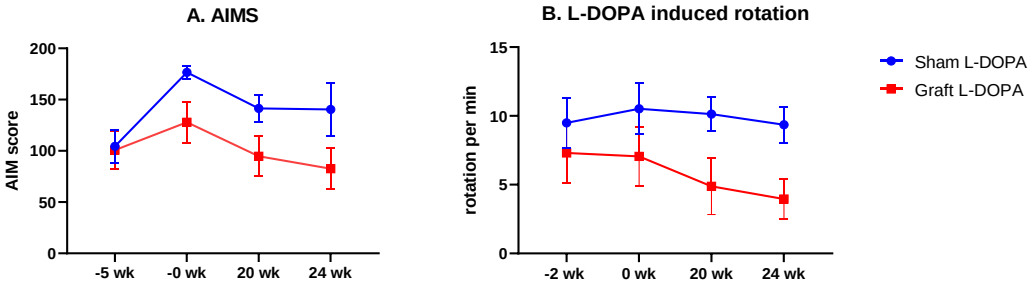

Figure 4-3 A. The degree of L-DOPA induced dyskinesia was determined by AIMs. B. The degree of L-DOPA induced rotations. AIMs were presented as mean score ± standard error of the mean (SEM); Error bars = ± SEM. L-DOPA induced rotations were presented as mean full body rotation ± standard error of the mean (SEM); Error bars = ± SEM. Two-way ANOVA was used to test statistical significance with Bonferroni post-hoc analysis.

4.4.2. Histological analysis

4.4.2.1. Nigral TH-cell loss

DAergic neurons in the SNc were visualized by DAB-staining of tyrosine hydroxylase. TH-DAB staining showed the unilateral MFB 6-OHDA injections caused DAergic neuron loss in the SNc. Histological analysis showed 95% of

DAergic neurons in the SNc on lesioned side were lost when compared to that in the SNc on the intact side in all groups. There was no difference in the percentage of TH cell number loss among the four groups ($F_{(3, 35)}$ = 2.419, P=0.0826), suggesting that the late-stage PD models were successfully built (Figure 4-4).

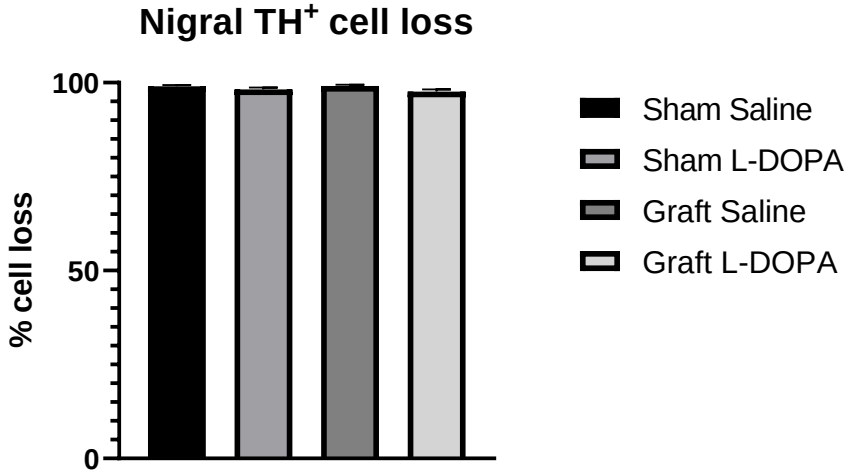

Figure 4-4 The impact of MFB infusion of 6-OHDA on tyrosine hydroxylase immuno-reactive cell bodies in the SN. Percentage of lost DAergic neurons in SN in the lesion side, relative to the intact side. The data are presented as mean ± standard error of the mean. One-way ANOVA analysis and Bonferroni post-hoc analysis was used to compare between groups.

4.4.2.2. The impact of L-DOPA treatment on graft survival

Striatal graft survival was assessed by histological analysis. TH-DAB staining was used to label the DAergic neurons in the striatum (Figure 4-5). The survival rate of TH^+ cells in the graft L-DOPA group was more than that in graft saline group but with no statistical significance ($t_{(19)}$=1.437, P=0.1670) (Figure 4-6.A). The A9 subtype of DA neurons were identified with $GIRK2^+$. All the $GIRK2^+$ cell express TH markers so Girk2 DAB staining was used to measure the level of Girk2 in the graft, see Figure 4-7. The number of $GIRK2^+$ followed the same trend as TH^+ cells but not reaching significance ($t_{(17)}$= 1.460, P=0.1626) (Figure

4-6.B). HuNu-staining was used to mark the nuclei of all the grafted human cells. Again, no significant difference in the number of HuNu$^+$ cells was found between graft L-DOPA and graft saline group ($t_{(19)}$=1.478, P= 0.1557) (Figure 4-6 C).

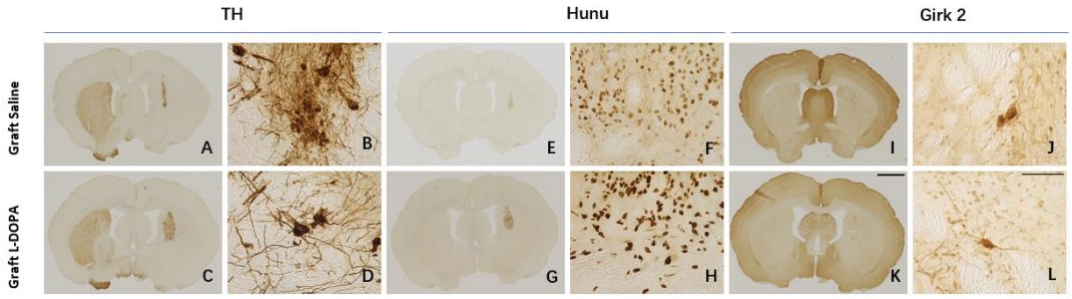

Figure 4-5 Representative images of hESC-derived DAergic neurons in the 6-OHDA model. (A-D) DAergic neurons were labelled by TH staining. (E-F) Human cells were labelled by Hunu staining. (I-L) A9 DAergic neurons were labelled by Girk2 staining. A, C, E, G, I and K were 5 x magnification. B, D, F, H, J and L were taken at 20 x magnification. Figure A, C, E, G, I and K scale bar 2000μm. Figure B, D, F, H, J and L scale bar: 85μm

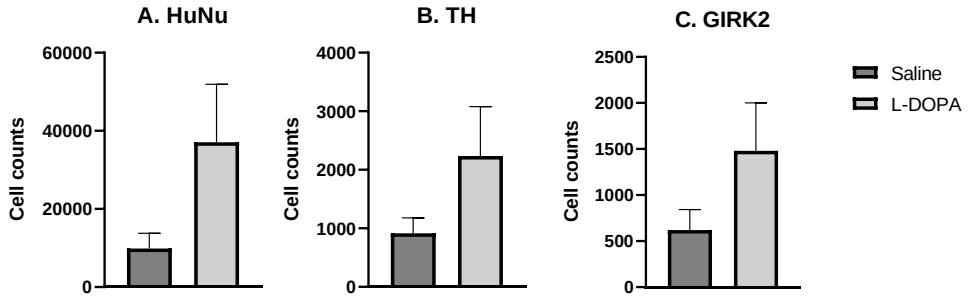

Figure 4-6 Hunu$^+$, TH$^+$ and GIRK2$^+$ cells count in the striatum. The number of Hunu$^+$ cells, TH$^+$ cells and GIRK2$^+$ cells were presented as mean ± standard error of the mean. Unpaired t test was used to examine statistical significance.

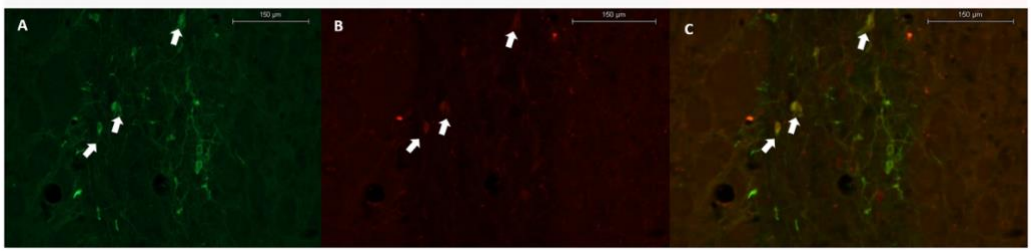

Figure 4-7 Representative images of TH (green), GIRK2 (red) staining and merged picture. Arrows point to GIRK2$^+$/TH$^+$ cells, showing examples of A9 DAergic cells. Scale bar 150μm

4.4.2.3. The impact of L-DOPA treatment on immune response

Immunological response in the striatum was assessed using a microglia marker (Iba1) and an astrocyte marker (GFAP).

4.4.2.3.1. Impact on IBA1$^+$ microglia

The number of IBA1$^+$ microglia on the lesioned side was counted, and their morphological features were considered. It was clear that the graft was inducing IBA$^+$ cell activation on the lesioned side. The resting state IBA$^+$ cells were depleting ($F_{(3, 35)} = 7.668$, $P=0.0005$) while the activated state (activated ($F_{(3, 35)} = 5.703$, $P=0.0027$) and round ($F_{(3, 35)} = 5.066$, $P= 0.0051$) IBA$^+$ cells were increasing significantly. In contrast, the areas away from the graft showed no sign of IBA$^+$ cell activation ($F_{(3, 35)} = 0.4130$, $P=0.7447$). The results also showed a sign of chemotaxis that the total number in the graft saline group were significantly higher than other groups ($F_{(3, 35)} = 5.899$, $P=0.0023$). L-DOPA showed an anti-inflammatory effect here that lowered the number of activated IBA$^+$ cells in graft L-DOPA group and stopped the chemotaxis around the graft site (Figure 4-8 and Figure 4-9).

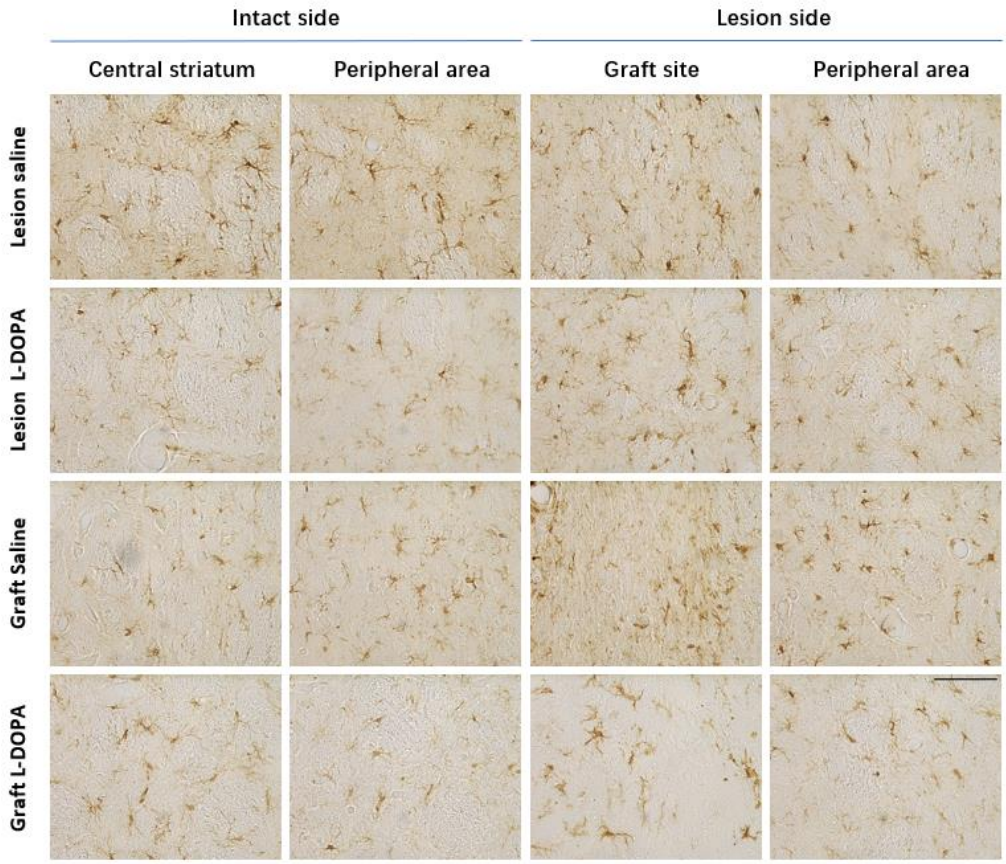

Figure 4-8 Microglia was labelled by Iba1 staining. Images were taken at 20 x magnification scale bar: 85μm

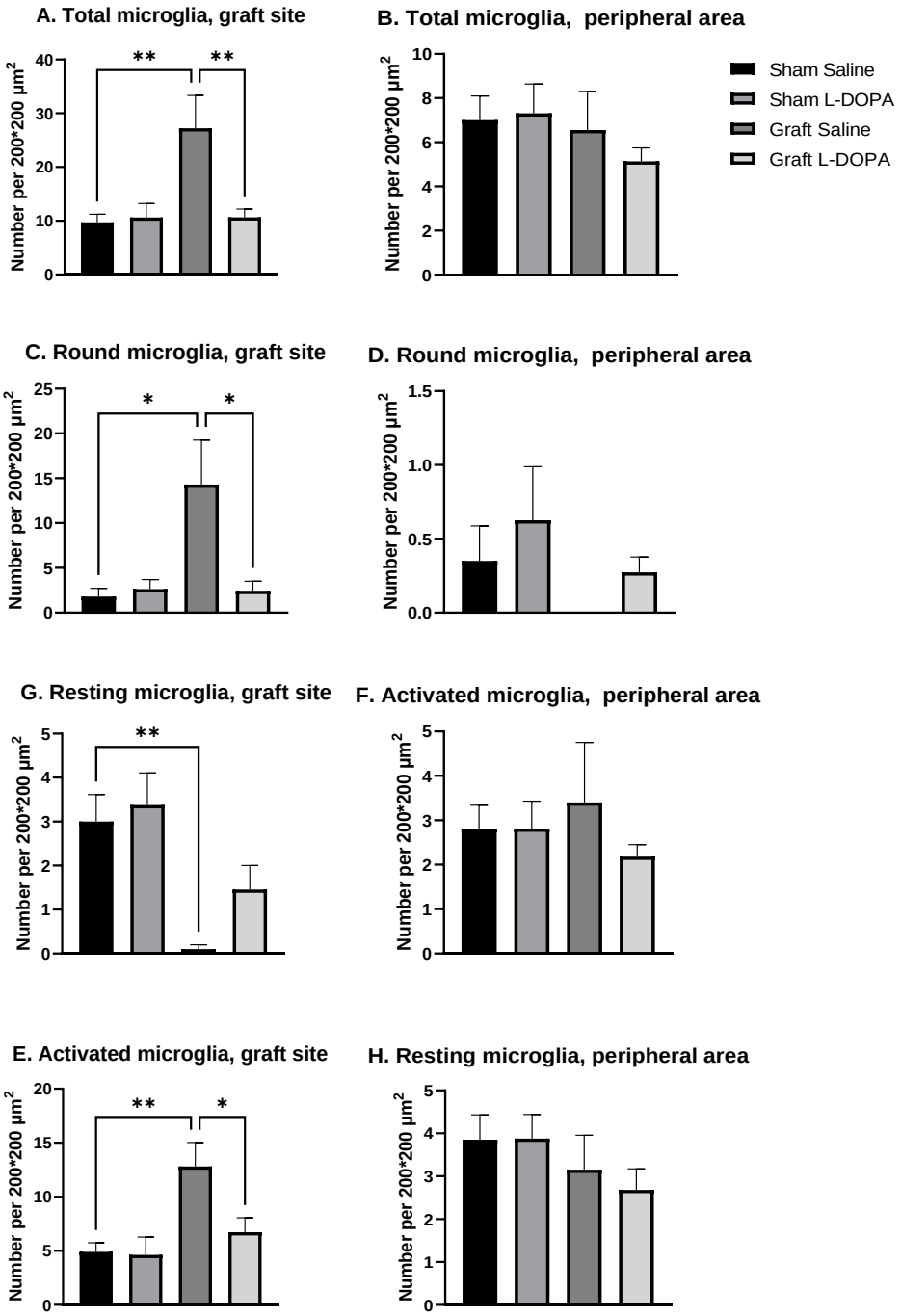

Figure 4-9 IBA1$^+$ cells count per 200*200 in the striatum of lesioned side. The number of IBA1$^+$ cells were presented as mean ± standard error of the mean. The number of resting microglia were significantly reduced *($F_{(3, 35)}$ = 7.668, P=0.0005)* while the number of activated microglia (including activated ($F_{(3, 35)}$ = 5.703, P=0.0027) and round ($F_{(3, 35)}$ = 5.066, P=0.0051) and the total number of microglia ($F_{(3, 35)}$ = 5.899, P=0.0023) were significantly increased in graft saline group at the graft site. One-way ANOVA and Bonferroni post-hoc analysis is used to compare between groups. *P<0.05, **P<0.01, ***P<0.001, and ****P<0.0001.

4.4.2.3.2. Impact on GFAP$^+$ astrocyte

The number of GFAP$^+$ astrocytes in different areas of striatum was counted for each group. On the intact side, there was no statistical difference in the number of GFAP$^+$ cells between each group ($F_{(4,39)}$ =0.6263, P=0.6028). On the lesioned side, there was also no significant difference between each group ($F_{(4,39)}$ =1.664. P=0.1925) (Figure 4-10 and Figure 4-11).

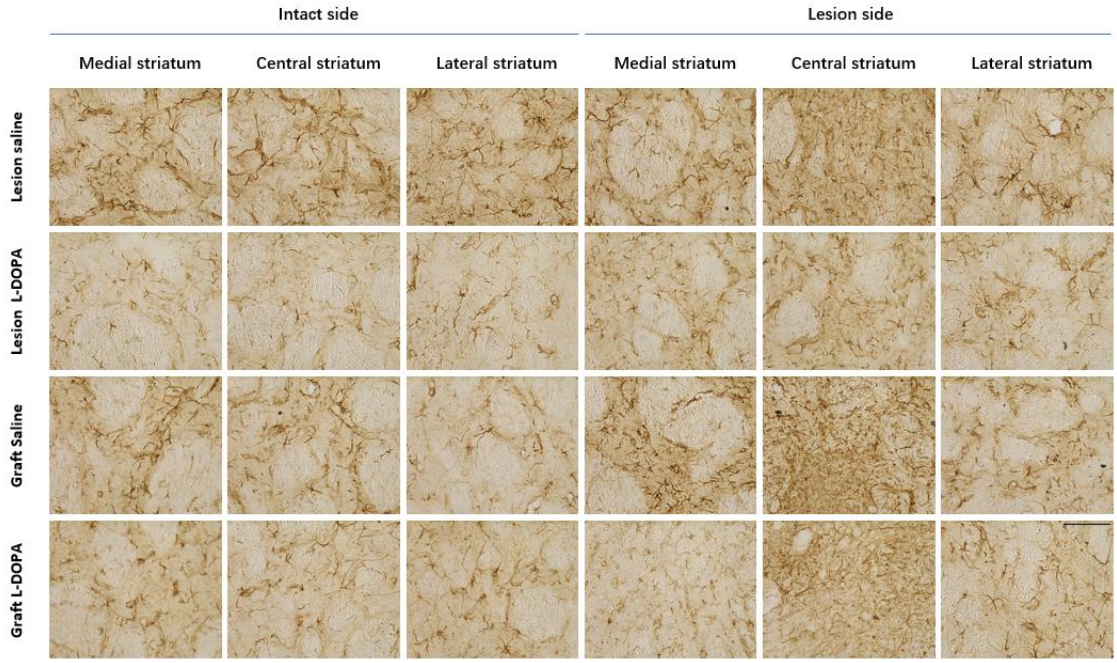

Figure 4-10 Astrocyte was labelled by GFAP staining. Images were taken at 20 x magnification. Scale bar: 85μm

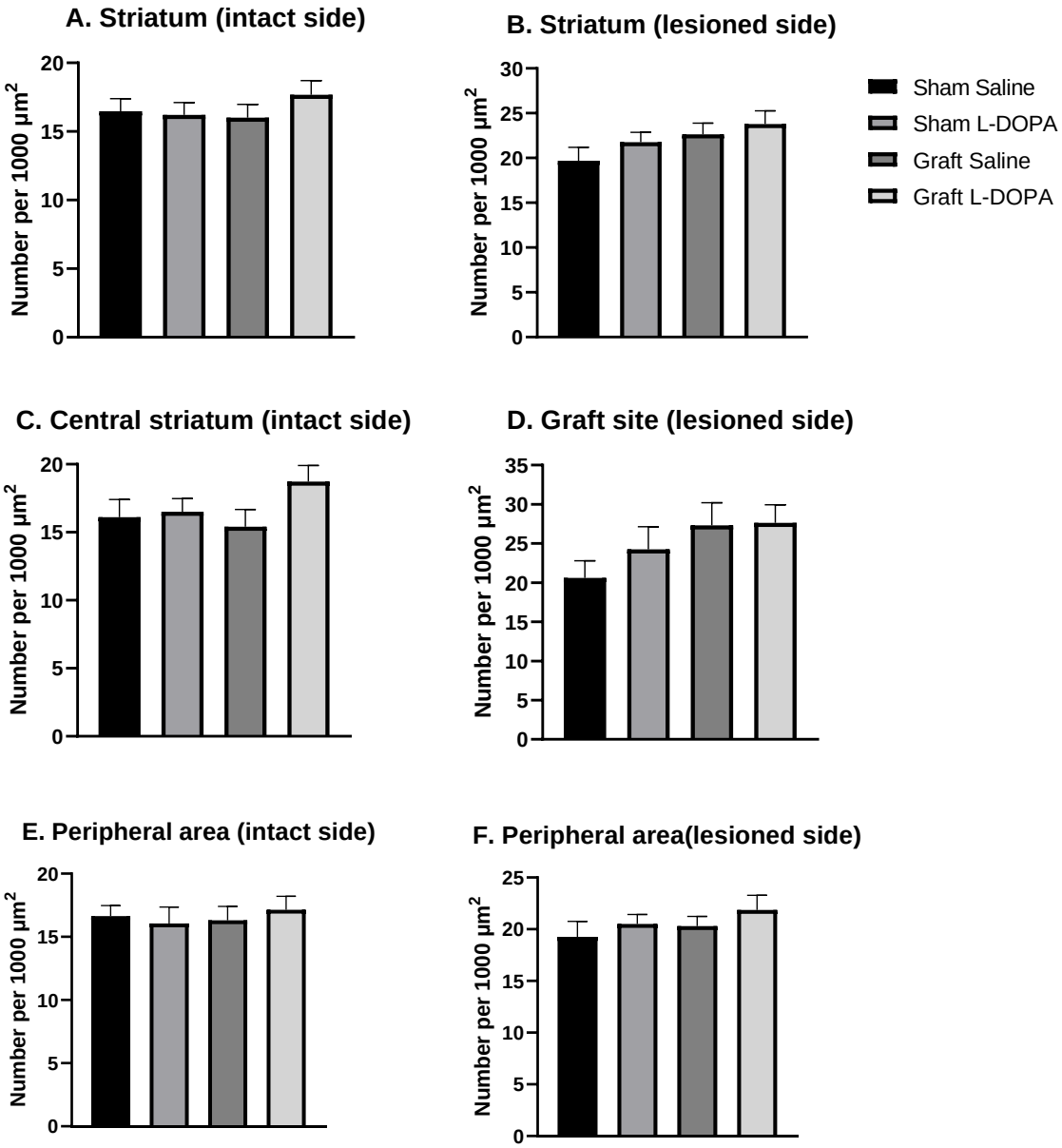

Figure 4-11 The density of astrocyte in the striatum. The number of astrocytes were presented as mean ± standard error of the mean. One-way ANOVA and Bonferroni post-hoc analysis was used to examine statistical significance.

4.4.2.3.3. Impact on the peripheral immune system[5]

Though it is quite difficult to understand the role L-DOPA was playing in the peripheral immune system as immunosuppression was used, preliminary data may still give some insight on these changes. Common biomarkers for the peripheral immune system activation were used to monitor the changes. Significance was found on Itgam, CD59 and FOXP3 but not on other markers (Figure 4-12).

[5] The RCR analysis test and data analysis were done by Jeremie Costales.

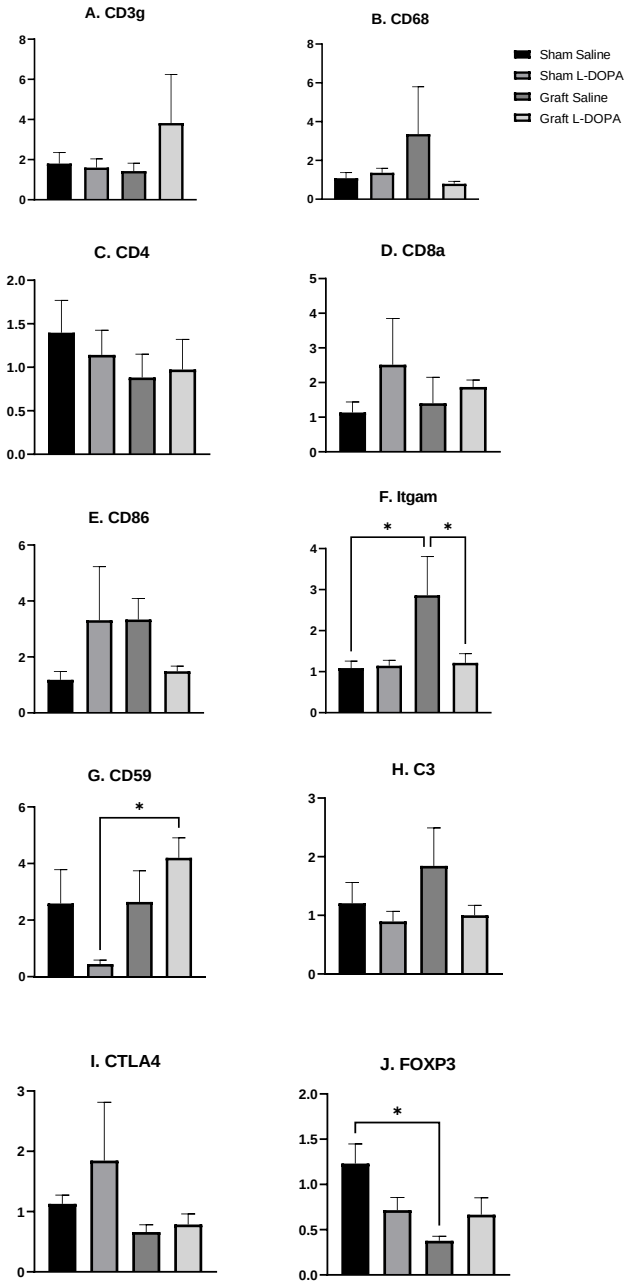

Figure 4-12. Common biomarkers for the peripheral immune system were used to compare the impact of treatment in each group. Data were presented as mean fold change in gene expression. (A-B) CD3g and CD68 are related to T cell activation. (C) CD4 marks T helper cells. (D) CD8a marks antigens for T killer cells. (E-F) CD86 and Itgam (CD11b) are related to innate immunity. (G-H) CD59 and C3 are related to complement system. (I-J) CTLA4 is an immune checkpoint and FOXP3 is related to Treg cells. High expression of CTLA4 and activation of Treg inhibit immune system. Data were presented as mean ± standard error of the mean. One-way ANOVA and Bonferroni post-hoc analysis was used to examine statistical significance.

4.4.3. MRI data

4.4.3.1. T2 imaging and cross matching volume of graft against TH

To fully monitor the change of the graft, MRI scanning technique was applied. The volume of the graft showed that before the immunosuppressive drug withdrawal, there were no difference between saline and L-DOPA group ($t_{(19)}$ =0.4720, P=0.6423). After immunological staining, it showed that the mean volume of the graft was larger in L-DOPA group though not statistically different ($t_{(19)}$ =1.082, P=0.4634) (Figure 4-13 and Figure 4-14).

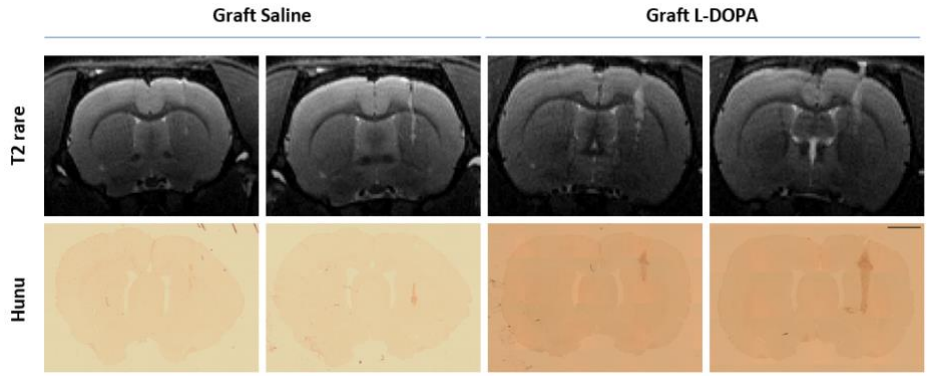

Figure 4-13 Graft was visualized by T2 rare prior to IS withdrawal. Hunu volume was used to estimate the graft volume after IS withdrawal (Scale bar: 2000μm).

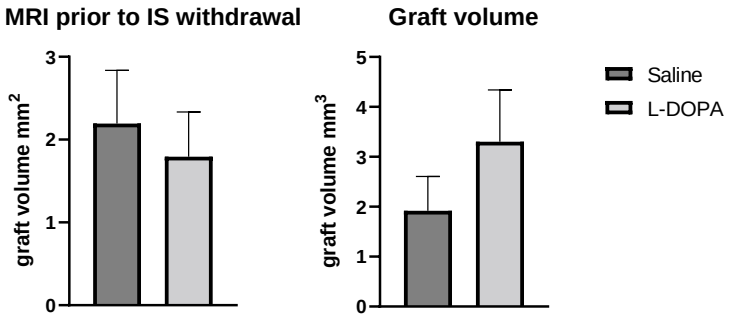

Figure 4-14. A. MRI data showed no statistical difference between saline and L-DOPA group regarding the graft volume. B. Immuno-histological staining result of graft survival. Data were presented as mean ± standard error of the mean. T-test was used to examine statistical significance. *P<0.05, **P<0.01, ***P<0.001, and ****P<0.0001.

4.4.3.2. DWI scan data

The DWI data provided three parameters for the graft survival. FA is related to the integrity and the arrangement of the graft cells; high MD is more relevant to cellular damage; and high RD indicates demyelination (Zhang and Burock 2020). The results showed a low MD and RD value, meaning the graft was not damaged. There was no significant difference found between saline and L-DOPA group for FA ($t_{(17)}$ =0.7349, P=0.4724), MD ($t_{(17)}$ =0.8187, P=0.4243) and RD values ($t_{(17)}$ =0.9457, P=0.3575). This indicates that L-DOPA had no impact on the graft growth and the graft survival (Figure 4-15).

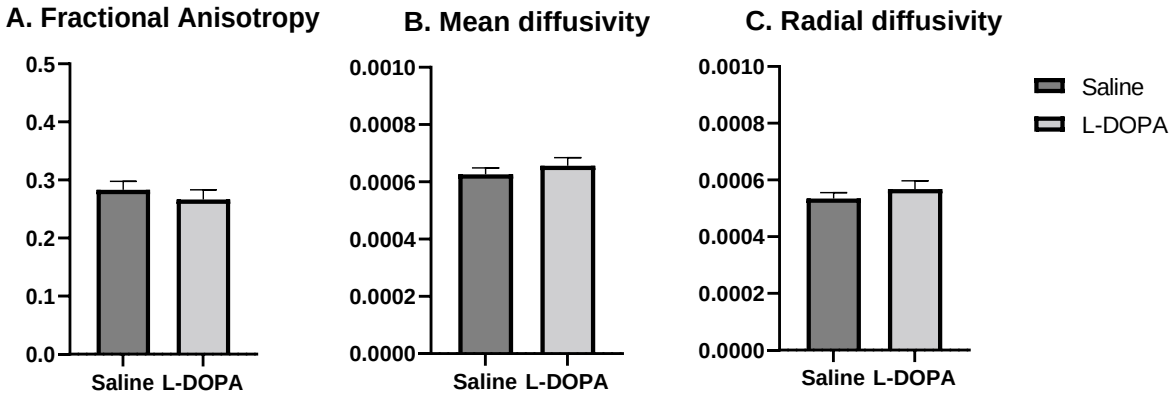

Figure 4-15. Fractional anisotrophy (FA), mean diffusivity (MD) and radial diffusivity (RD) data showed no difference between saline and L-DOPA group. FA is related to the integrity and the arrangement of the graft cells; high MD is more relevant to cellular damage; and high RD indicates dysmyelination. Data were presented as mean ± standard error of the mean. T-test was used to examine statistical significance.

4.5. Discussion and conclusion

There is very limited data on the impact of L-DOPA on hESC-derived DAergic neurons when transplanted, especially in the absence of immunosuppressive drugs. In this study, the impact of L-DOPA treatment on the development of ESC-derived DAergic progenitor after a period of withdrawal from immunosuppression was investigated.

The behavior tests overall showed an improvement of motor functions of all groups except sham saline group which was set as a control. The optimal functional recovery was observed at week 12, before the withdrawal of immunosuppressant, suggesting that immune response may play an important role in motor functions. No sex differences were observed during behavior tests. The MRI and immunohistochemistry (Hunu, TH and Girk2 staining) suggest the volume of the graft in L-DOPA and saline group were not different. Also, the graft attenuated LID in graft L-DOPA group compared to saline group, showing that the graft was buffering the release of DA and therefore lowered the AIMs. Importantly, these data suggest that L-DOPA was not affecting the overall survival of exogenous DAergic neurons.

The MRI data combined with IHC results showed that L-DOPA may help to reduce the immune response in the rat's brain and promote the survival of the graft cells (although this didn't reach statistical significance) but would be consistent with a published study (Elabi et al). Histological analysis showed a trend of TH^+, $GIRK2^+$ and $HuNu^+$ number to be higher in the grafted L-DOPA treated group although not reaching statistical significance. It suggested L-DOPA has no negative impact on the graft survival or development, or in the number of $GFAP^+$ cells. The lack of differences in GFAP suggest that the immune responses are minimally impacted by L-DOPA, at least within the

timeframe of this project. Evidence from other groups suggest that the immune response may need to take an exceptionally long time to respond to the graft. $GFAP^+$ astrocytes were found gathering around both the 12-year and the 16-year graft in one patient. While after 22 years, another patient showed no accumulation of astrocytes and very few $IBA1^+$ microglial cells (Kurowska et al. 2011).

The lack of statistical significance is in part due to the variability of the grafts which may in turn be due to the complex multistage approach that has been used in an attempt to evaluate the effect of L-DOPA in the absence of immunosuppression. There are likely to be individual differences of rats in the rate of producing immune rejection and also how fast the graft cells may be impacted by the immune system. there is little published data on the effect of immunosuppression withdrawal in rats after graft surgery, but this is the most common treatment protocol for a human patient (Wenning et al. 1997). Cyclosporin A can be used alone as a monotherapy or be used in combination with azathioprine and steroids (Lindvall et al. 1990; Lindvall 2016). The best regimen for cell transplantation is still under debate but if we consider the side effects of each drug in this combination, the triple therapy is not the optimal option as the dose especially for steroids in the clinic is high (40mg/kg in the first 3-4 months) (Barker et al. 2019).

Although the brain was regarded as an immune privileged organ (immune privilege, a hypothesis that the brain can tolerate antigens and does not induce an inflammatory reaction) decades ago (Harris et al. 2014), immune responses can still be triggered after exogenous graft implantation surgery (Piquet et al. 2012). Interestingly, despite the fact that daily administration of cyclosporin A is detrimental for the animals added to the nephrotoxic effects of long-term immunosuppression, there are very few studies looking at immunosuppression

withdrawal in animals (Tamburrino et al. 2015). Previous clinical studies on the withdrawal of immunosuppression following neural transplantation of fetal tissues found that graft survival is not affected within 3 weeks of immunosuppressive drug withdrawal (Lindvall et al. 1989). Longer withdrawal periods also did not affect the graft survival, but the immunological changes were not tested in these clinical trials (Piccini et al. 2005). Certainly, in clinical trials immunosuppression withdrawal has been successfully achieved with maintained survival of grafts (Li et al. 2016) but these were allogenic human to human fetal grafts. Here human to rats grafts are xenogeneic and therefore the profile of rejection likely to be different. Here to try to extend this window, we worked on a baseline of early post-natal xenograft induced tolerance to hopefully allow evaluation of L-DOPAs effects in the absence of acute immunosuppression. We had evidence of good graft survival at the end point although inflammatory responses were high (activated IBA1$^+$ cells were significantly increased in graft saline group). This supports the validity of the experiment design with delayed immunosuppression withdrawal. However, to establish a relationship between L-DOPA treatment and graft survival after immunosuppressant withdrawal, further work and improvements on the rat model is needed. A key improvement would be on the reduction of individual differences at the immunosuppressant withdrawal point. As inflammation is related to GID and graft surgery outcome, a better model should finely regulate the causes for that. Other real-time measurements should also be applied, if possible, to increase the understanding of changes before and after the immunosuppressant withdrawal point, in addition to the MRI technique. Grafts in athymic rats can survive without triggering microglial (Iba1$^+$) response (Grealish et al. 2014). In contrast, in this experiment, Iba1$^+$ cells in the CNS were activated following immunosuppressant withdrawal. This contrast correlated the peripheral immune environment (especially T cell population) with the CNS.

Importantly, this experiment found L-DOPA led to a significant reduction of activated IBA1^{+} population on the lesioned side in graft L-DOPA group. It is possible that L-DOPA treatment is creating to a less inflammatory environment which promotes the recovery of DA neurons (Dutra et al. 2012). This effect is consistent with the findings in Chapter 3 showing effect to the lesioned side in 6-OHDA rat model. The effect of L-DOPA to the immune environment was strong enough to compete with the immune response caused by graft itself. In addition, the affected population may be influenced by the dosage and duration of L-DOPA treatment. Interestingly, postmortem data from a patient who received graft for 24 years showed no sign of immune response to the graft and had been under L-DOPA treatment throughout (Li et al. 2016). In this case, the immunosuppressive drug was withdrawn 5 years after graft surgery. It is possible that L-DOPA contributed to the adjustment of the immune response after the immunosuppressant withdrawal. This remains to be fully established as there is not enough post-mortem transplantation data to be sure of the effect of L-DOPA, but it is certainly conclusive and consistent with previous studies that L-DOPA is not toxic to transplanted cells of hESC origin.

For the peripheral immune system, CD68, CD3g, CD4 and CD8a showed no difference between each group, suggesting that the T cell population were not altered by the treatment (Miceli and Parnes 1991; Hameed et al. 1994; Torres et al. 2002). However, the expression of Itgam (CD11b), CD 59 and FOXP3 were changed. This might mean that the innate immunity, the complement system as well as Treg cells were influenced by cyclosporin A and L-DOPA (Kmieciak et al. 2009; Schnabolk et al. 2014; Schmid et al. 2018). But the trend was very unclear. Treg cells are a type of T cells that help to reduce autoimmunity in animal and humans. Cyclosporin A affects the whole T cell population including Treg cells which, to some degree, compromises its

suppressive role in the immune system (Wang et al. 2006; Levite et al. 2017). Interestingly, Treg cells also express DA receptors and their function can be suppressed by DA (Arce-Sillas et al. 2019). In this experiment, both cyclosporin A and L-DOPA treatment should reduce the activity of Treg and, in this case, the effective T cells (Teff) should be more active. After the withdrawal of cyclosporin A, the effect of L-DOPA should be more dominant, and this could be the main contribution to the final Treg cell number change. However, there were a few factors that could affect the analysis of the PCR data. First, the sample size for the peripheral system was quite small: Some animals died before the end point of the experiment due to peripheral infections. Those rats were removed before data collection. Second, the raw data (not shown) suggest the variability between individuals were extremely high even within the same group. Given the long-term duration of this experiment and complicated treatment the rats received, the results may not faithfully indicate the impact of L-DOPA on each group. To better understand the relationship, there might need a model that requires no administration of immunosuppressants.

Significant motor function recovery was observed after transplantation in graft saline group, based on the stepping test and whisker test. This function recovery maybe directly linked to the survival of grafted DAergic neuron. The previous study from Elabi et al. suggested that 1,000 surviving hESC-DAergic neurons can generate a motor function recovery (Elabi 2017), while in this study, it showed the number needed for a significant motor function recovery may be less. It's hard to conclude why other behavior tests did not show significance for the recovery but the innervation could be a contributor to the cause (Cardoso et al. 2018). For graft L-DOPA group, the motor function recovery was complicated by inhibitory effect of L-DOPA itself. It was observed in the mid-1990' that reversible inhibition of the motor function recovery could occur when 50 mg/kg L-DOPA was given twice a day (Steece-Collier et al. 1995). Though

the dose is far higher than the dose in this experiment, it may still be the most significant contributing factor to the significant difference between graft saline and graft L-DOPA group in the aspect of those two tests.

In addition to motor function recovery, grafted DAergic neurons may relieve L-DOPA-induced dyskinesia, reflected by the trend shown in L-DOPA induced rotations and AIMs. These findings are consistent with previous experiments that even a small size of graft can relieve L-DOPA induce dyskinesia (Breger et al. 2017; Elabi 2017). Two of the rats in the saline treated graft group developed post-transplant dyskinesia in the absence of any intervention (‘‘off-drug” dyskinesia, graft induced dyskinesia, GID), which were observed at the week 18 post-graft but not seen at week 21 post-graft (one week after cyclosporine A withdrawal). Spontaneous rotation behavior was observed in both rats with a mild upper limb dyskinesia after the rats were put into observation bowls. These abnormal behaviors can be easily disturbed when observer approaches the rats, and it could be one of the reasons why GID is rarely observed in previous animal models. One of the rats showed a twisted body under anesthetized condition during the MRI scanning, a similar posture when a rat suffering L-DOPA induced dyskinesia were under anesthesia, which further confirmed the existence of graft induced dyskinesia.

Graft induced dyskinesia is a series of abnormal involuntary movements that would occur in the grafted patients when anti-Parkinson medication is absent, which has significantly affected the life quality of grafted PD patients (Olanow et al. 2009). While the cause for GID was thought to be graft-derived 5-HT hyperinnervation and high level of 5-HT/DA transporter ratio (Politis et al. 2011), recent findings from hESC grafted rat models were debating against it. Those hESC cells were 5-HT free thanks to the advancement in stem cell technique. Also, the saline treated group in this recent study did not receive L-DOPA

treatment, indicating that neither 5-HT nor L-DOPA treatment is a prerequisite condition for inducing GID (Lane et al. 2022).

In conclusion, this is the first study to look at twice daily administration of L-DOPA and its effects in the absence of immunosuppression. Withdrawal of immunosuppression after 20 weeks in neonatally desensitized animals allowed for sustaining transplantation survival up to 5 weeks after withdrawal. The improved outcomes in the L-DOPA treated group indicate that that ongoing L-DOPA treatment may be of benefit to the transplant and offers no indication that it will have negative effects.

Chapter 5. Impact of L-DOPA on the survival of endogenous dopaminergic neurons in a α-synuclein based rat PD model

5.1. Introduction

The presence of Lewy bodies is one of the hallmarks of Parkinson's disease and the main component is α-synuclein. The identification of mutated α-synuclein gene related familial cases of Parkinson's disease and Braak's studies (introduced in 1.2.1.2) showed that α-synuclein pathology are closely linked to DAergic neurons degeneration in the SNc (Krüger et al. 1998; Braak et al. 2003; Zarranz et al. 2004). It is commonly believed that α-synuclein aggregation causes a series of pathological changes including inflammation, ubiquitin-proteasome system abnormality and eventually DA neuron death (Riederer et al. 2019).

Theoretically, L-DOPA or DA is not involved in the forming process of α-synuclein fibrils (components of α-synuclein fibrils were introduced in 1.2.1.2, Figure 1-4). However, when testing anti-parkinsonism drugs against the aggregation process of α-synuclein, a Japanese group discovered that orthoquinone structures had considerable affinity to free α-synuclein units and destabilized the consequent 3D structures of α-synuclein aggregation (Ono et al. 2007). Orthoquinone structures can be derived from L-DOPA or DA through simple redox reactions which is not rare under stressed neuronal environments (Surmeier et al. 2011; Sbodio et al. 2019). Therefore, it is hypothesized here that L-DOPA may ameliorate the damage from α-synuclein induced toxicity through its interaction with α-synuclein.

In the previous chapters (Chapter 3 and Chapter 4), 6-OHDA lesioned models produced a stable level of DAergic neuron loss and led to similar motor function deficits seen in PD patients. However, the mechanism of this model for producing DAergic neuron loss is quite different from PD pathology. 6-OHDA lesion is caused by acute attack from free radicals (Glinka et al. 1997) while the

more complex neural environment in PD patients are more progressive, with the presence of α-synuclein pathology and chronic inflammatory response. This complex environment may directly affect the condition for DAergic neuron survival and these three important features can be reproduced in the presence of α-synuclein pathology (Duffy et al. 2018). Therefore, α-synuclein models would be the preferred neural environment to mimic PD pathology.

However, the majority of α-synuclein models used in the 2010s had deficiencies. Those models were based on α-synuclein overexpression technique while it has been proved recently that the α-synuclein overexpression technique alone cannot reproduce structural and morphological changes found in post-mortem source (Mahul-Mellier et al. 2020). One key feature of PD is the presence of Lewy bodies. Lewy bodies own intricate structures and dynamically interact with their surrounding cellular environment (more details in 1.2.1.2.). In contrast, the α-synuclein overexpression technique produces only loosely connected α-synuclein fibers with no uniformed organizations and cannot functionally fully reproduce the features of Lewy body. On the other hand, the newly developed PFF models have produced similar Lewy body structures to those found in real patients (Duffy et al. 2018). This newly developed model has provided us with the opportunity to study L-DOPA's effect in a more realistic environment and hopefully the results can more precisely depict the influences of L-DOPA to DA neuron survival.

α-synuclein in fibrillar form is the main architecture of α-synuclein in Lewy body (Spillantini et al. 1998) and it has been reported that α-synuclein fibril alone induces features representative of those found post-mortem in patient with Parkinson disease (Shimozawa et al. 2019). However, human α-synuclein fibrils may not induce the same level of α-synuclein pathology in rat brain. Indeed, both the fibril-based models and the α-synuclein overexpression PD

models have deficiencies, such as slow pathology development and unreliable DAergic neuron loss (ranged from 30%-80% within the same group, the variability is too large to be accepted in most scientific studies) (Thakur et al. 2017). To speed up the pathological processes and to produce reliable DAergic neuron loss, a more precise model that replicates the pathology found in the human PD patients is needed. To address this need, a rat model that contains both fibrils and α-synuclein over-expression gene has been developed. Fibrils and virus that carries α-synuclein over-expression gene were injected via two separate surgeries respectively in the model developed in 2017 (two-step procedures), and a satisfactory result with stable DAergic neuron deficits was obtained (60~70%) (Thakur et al. 2017). Afterwards, the two-step procedures were simplified to one step by using mixed α-synuclein and FPP injection (Hoban et al. 2020). This rat model is ideal for the purpose of this chapter and the result was compared with the more classical α-synuclein overexpression PD model (pros and cons of different models were discussed in 1.4.2).

As the model is relatively new and the DAergic cell loss was only partial (60~70% TH cell loss) (Hoban et al. 2020), the remaining TH cells is unlikely to be influenced by L-DOPA in the dosage that showed no impact on the full lesion model (6-OHDA lesion) in the last two chapters (Chapter 3: escalating dose from 4 mg/kg to 12 mg/kg; Chapter 4: 6 mg/kg). For this reason, the dose (15 mg/kg) in this chapter was set to exceed the maximal dose for the LID induction as tested in Chapter 3.

5.1.1. Aims and objectives

There is a need for a more degenerative model and a model more aligned with clinical PD. Clinical PD is neuronal loss, plus α-synuclein and arguably the presence of L-DOPA/dopamine replacement. The aim of this experiment is to understand the interplay between L-DOPA and degenerative feature of PD. The hypothesis is L-DOPA may decrease the toxicity caused by α-synuclein in the neurodegenerative process.

Objectives:

To determine the impact of twice a day L-DOPA treatment on the DAergic neuron survival in α-synuclein based rat models that include

1) α-synuclein viral vector rat model and
2) α-synuclein viral vector and preformed fibril combined model

The experiments on the classical α-synuclein viral vector rat model will make the results from this study more comparable to the results from the last two decades and also will make a good comparison to the findings from the new α-synuclein+PFF model.

5.2. Experiment design

Before lesion, 47 Sprague Dawley female rats (180-200g) were food restricted and pretrained on staircase task over a period of 3 weeks. Rats received unilateral lesion by injection of human WT α-synuclein viral vector alone (n = 30) or a mixture of human WT α-synuclein viral vector and preformed fibrils (n= 11) into three sites of the midbrain. 6 naïve animals were selected from those who did not train on the staircase test, and they received no further treatment afterwards. After 4 days of surgery recovery, the rats received twice a day either L-DOPA treatment or saline treatment for 8 weeks post-surgery (see Table 5-1). At 3rd and 8th week post lesion, the staircase test, cylinder test, stepping test, vibrissae test and amphetamine-induced rotations were assessed. AIMs were assessed at 5th and 7th post lesion. After 8-week L-DOPA treatment, the rats were perfused for immunohistochemical analysis (Figure 5-1).

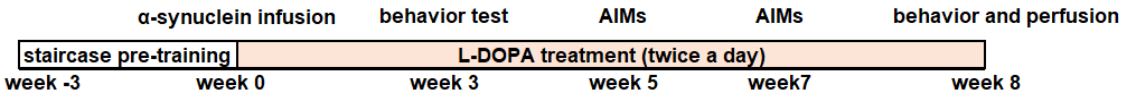

Figure 5-1 Timeline of the experiment.

Table 5-1 Grouping information

Groups	The condition of surgery and treatment
Naïve control	No lesion or drug treatment (n=6)
α-synuclein-AAV only saline (αSynAAV +Saline)	α-synuclein viral vector alone, saline (n=15)
α-synuclein AAV only L-DOPA (αSynAAV + L-DOPA)	α-synuclein viral vector alone, L-DOPA (n=15)
α-synuclein+fibrils saline (αSynAAVFib + Saline)	α-synuclein viral vector plus preformed fibrils, saline (n=5)
α-synuclein+fibrils L-DOPA (αSynAAVFib + L-DOPA)	α-synuclein viral vector plus preformed fibrils, L-DOPA (n=6)

5.3 Method

5.3.1. Preparation of virus

AAV6-α-synuclein-human wild type virus (tier:1.4E+14) was provided by Lund University. Details concerning the virus was published by Hoban et al (Hoban et al. 2020). The AAV6 -human wild type α-synuclein virus were diluted into 20% virus in DPBS (working concentration) as a stock. The 20% stock were kept in glass tubes at 4 °C.

5.3.2. Preparation of PFF

An aliquot of 5 mg/ml fibrils (batch:013119) were obtained from Kelvin Luk, University of Pennsylvania and was stored at -80 C. The aliquot of 5 mg/ml fibrils was thawed at room temperature before use. The thawed fibrils were sonicated with the QSonica machine (Model Q55) with probe arm (Model CL-188) in the fume hood. Before sonication, the probe arm was wiped with 70% ethanol and then with distilled water. The amplitude was set at 20 and the sonicator was turn on. The probe went down along the wall of Eppendorf into the fibril solution for a pulse of 5 seconds and this pulse process were repeated for 6 times to avoid the overheating and the generation of frothing. After sonication, the arm was cleaned by 70% ethanol and distilled water. The cap was closed, and the Eppendorf were centrifuged by a minicentrifuge to allow any spills on the wall down to the bottom. The volume of sonicated fibrils was measured by a pipette. The sonicated fibrils were mixed with equal volume of virus stock. After preparation, contaminated surface or in-disposable instruments was placed in 1% sodium dodecyl sulfate in distilled to water effectively inactive the α-synuclein fibrils (Fenyi et al. 2018).

5.3.3. α-synuclein surgery

AAV-α-synuclein and a combination of AAV–α-synuclein and PFF lesion surgeries were carried out under 2-5% isoflurane anesthesia (4-5% for induction; 2-3% for maintenance) which was carried by O_2. The surgery was conducted on a stereotaxic instrument (Kopf stereotaxic instrument, model 900LS). Once the rats were held on the stereotaxic frame, Metacam was given to the rats at the dosage of 2ul/kg via s.c. (5 mg/ml, Boehringer Ingelheim, Germany). The tooth bar was set at -3.5. α-synuclein viral vector or a combination of α-synuclein viral vector plus preformed fibrils were infused into VTA (Anteroposterior：−5.3 mm from bregma, Lateral：−0.8 mm from bregma, Dorsoventral: −7.0 mm below dura), medial SN (SN1) (Anteroposterior：−5.3 mm from bregma, Lateral：−1.6 mm from bregma, Dorsoventral: −7.2 mm below dura) , dorsal SN (SN2) (Anteroposterior：−5.3 mm from bregma, Lateral：−2.6 mm from bregma, Dorsoventral: −6.7 mm below dura) of the right hemisphere. Before drawing up the solution, the cannula was washed by following steps: 2 minutes 3% H_2O_2 in H_2O, 1 time 70% ethanol in water washing and 2 times DPBS washing. The cannula was covered with α-synuclein viral vector or a combination of α-synuclein viral vector plus preformed fibrils for 1 minutes before the syringe was filled with α-synuclein viral vector or a combination of α-synuclein viral vector plus preformed fibrils for infusion. For αSynAAV animals, 0.5µl, 1µl and 1µl α-synuclein viral vector were infused into VTA, SN1 and SN2 respectively. For αSynAAVFib animals, 1ul, 2ul and 2ul of a solution containing α-synuclein viral vector plus preformed fibrils were infused into VTA, SN1 and SN2 respectively. The infusion of α-synuclein was performed by using a 10µl Hamilton Syringe (Hamilton, Germany) with a 30-gauge metal cannula at a rate of 0.2 µl/min by using a minipump. After infusing toxin into each site, the cannula was left in the tissue for 2 minutes for diffusion. After suture, 5ml of a 5% glucosaline solution was administered

subcutaneously to the rats to prevent postoperative dehydration. Then, the rats were placed in heated chambers (30°C) for recovery till the rats can right themselves. They were moved back to cages. The health condition and weight change of the rats were monitored daily for one week and then twice per week till the end of the experiment.

5.3.4. Treatment

The L-DOPA/saline treatment was started 4 days after surgery and continued until the end of the experiment. A mixture of L-DOPA (15 mg/kg) and Benserazide (12mg/kg) in 0.9% saline was administered to the L-DOPA treated rats by s.c.. The saline treated group received twice a daily saline (0.9%, 1 ml/kg) treatment subcutaneously.

5.3.5. Staircase test (skilled reaching test)

The training was conducted prior to the lesion. 5 days before a training procedure, all rats were food restricted and the sucrose pellets (TestDiet,1811155, Cambridge university) were put in home cages once a day. During food restriction, the weight of the rats was monitored to ensure no less than 85% of the weight of free food access. The training on the staircase test was conducted for a period of 2 weeks (5 days per week) under food restriction to obtain a stable baseline. During training, after food deprived rats were placed in the chamber of the Montoya Staircase box, the first stair with pellets on each side were placed into the Montoya Box (Figure 5-2). Two sucrose pellets were placed in each of the 7 wells per side. After 15 minutes, the first stair was removed from the box. The second stair with sucrose pellets was placed into the Montoya box for 15 minutes. The pellets dropped on the floor and remaining

on the floors from each side were recorded separately. In the testing procedure, staircase testing was conducted at 3rd week and 8th post-lesion. One day before test, the food was withdrawn from the cages (overnight food restriction). The data was conducted the same way as in the training procedure. The data were recorded as the number of eaten pellets and the level of the stair. In the test, some of the rats could use a paw from one preferred side to grab and retrieve the pellets and some rats only lick and eat the pellets on the top 1st floor. Taken these factors into consideration, only the rats with at least two empty wells were included into the experimental group. The rats were divided into αSynAAV +Saline group, αSynAAV + L-dopa group, αSynAAVFib +Saline group and αSynAAVFib+L-DOPA group based on the left paw performance on the finial pretraining test. The rats didn't perform well were grouped into Naïve control group; data was not presented in the figures (Montoya et al. 1991; Barnéoud et al. 2000; de Souza Pagnussat et al. 2009).

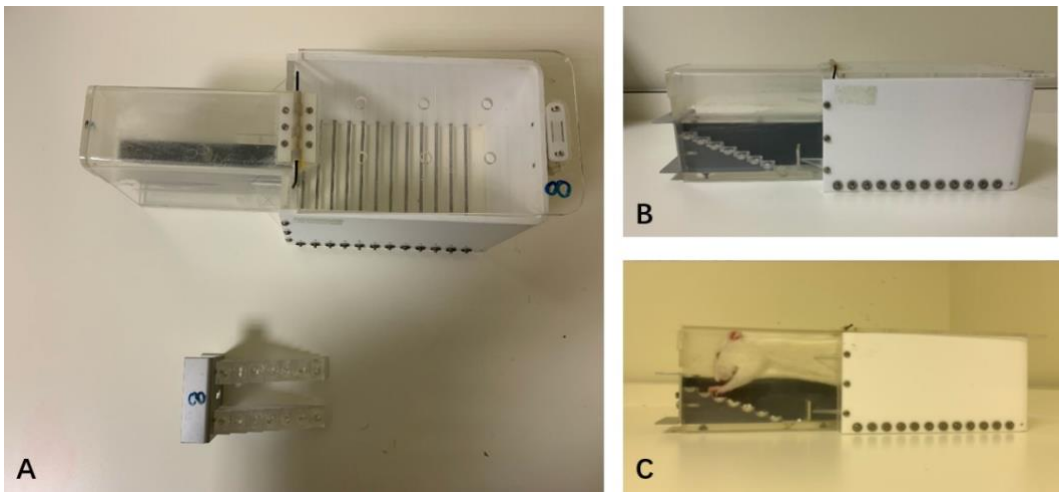

Figure 5-2 A. Montoya Staircase box and stair with pellets B. Stair placed in the Montoya Staircase box. C. A rat was grabbing the pellets on the floor.

5.4. Results

5.4.1. Behavior assessment

Stepping test: For stepping test (forwards), the adjusting steps of the contralateral forehand paw was presented as a percentage of the adjusting steps of the ipsilateral forehand paw (Figure 5-3 A). The percentage has a wide range from 127% to 50% and this wide variation was observed in lesioned groups. The overall trend showed an impairment of the performance of the contralateral paw in all α-synuclein based lesioned groups. However, no significance was shown by two-way repeated ANOVA. For stepping test (backwards), the adjusting steps of the contralateral forehand paw was presented as a percentage of the adjusting steps of the ipsilateral forehand paw[6] and there was not impairment on this measure Figure 5-3 B).

Whisker-induced touch test: In Whisker test, the number of vibrissae-elicited contralateral forehand paw placings were presented as a percentage of the number of vibrissae-elicited ipsilateral forelimb placings (Figure 5-3 C). The rats' response showed no significant difference among groups.

Cylinder test: For cylinder test, Contralateral paw contact number with the cylinder wall was presented as a percentage of the total number of contacts with both paws (Figure 5-3 D). The paw preference was not significant at 3 weeks post-lesion with all groups showed a tendency to use both paws equally (percentage near 50%). But at 8 weeks post-lesion the percentage dropped by

[6] The percentage of the adjusting steps largely eliminates the biases brought in by the size of the rats. This way of presenting the data of stepping test and Vibrissae-induced touch test is commonly seen in publications.

approximately 10% in all α-synuclein based lesioned groups. Two-way repeated ANOVA ($F_{(4, 42)}$ = 1.892, P=0.1297) showed αSynAAV L-DOPA rats were impaired on limb placement compared to the naïve control (P=0.0155). For Amphetamine induced rotation, α-SynFib groups showed a slight increase in rotations per min but with no statistical significance with other groups.

Amphetamine induced rotations test: The data was presented as net ipsilateral rotations per minutes . The test was run at week 3 and week 8. There was no statistical significance between each group.

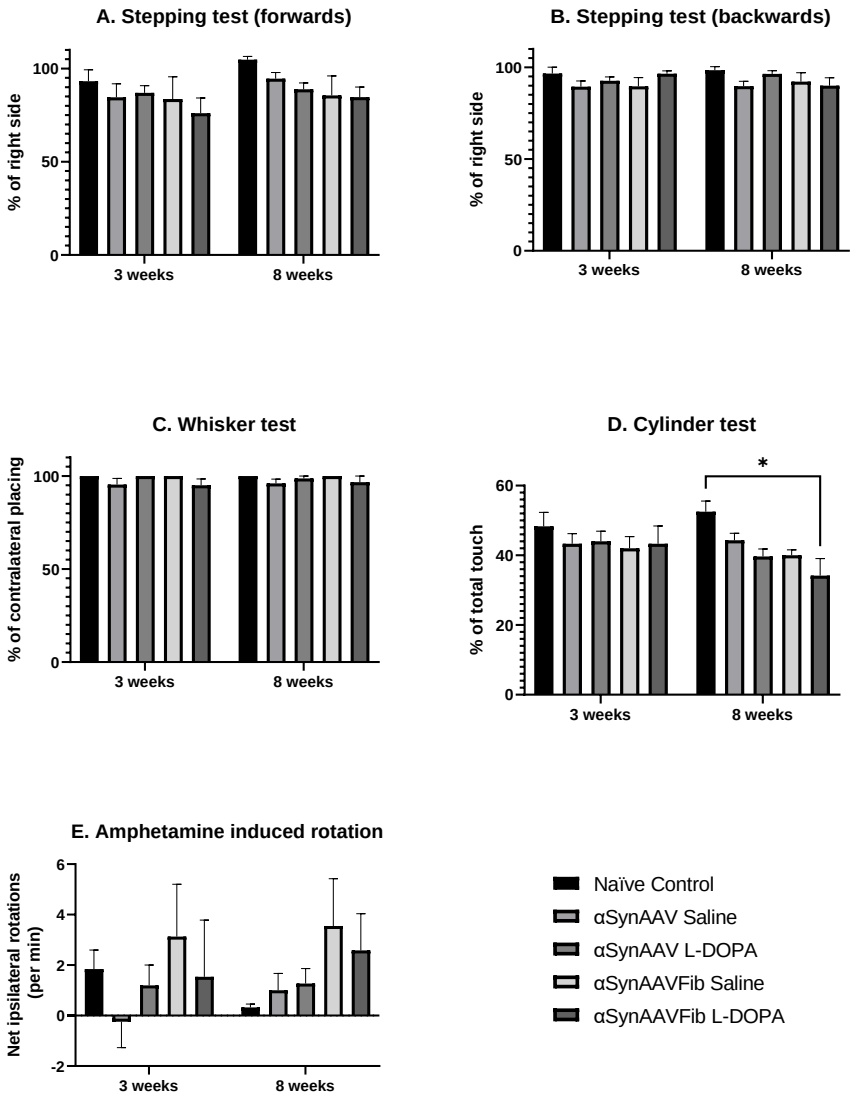

Figure 5-3 A. stepping test (forwards). B. stepping test (backwards). C. Whisker test. D. Cylinder test. αSynAAVFib group showed less touch compared to naïve group at week 8 post-surgery ($F_{(4, 42)} = 1.589$, $P=0.1951$). E. Amphetamine induced rotation. Data were presented as mean ± standard error of the mean. Two-way repeated measure ANOVA and Bonferroni post-hoc analysis was used to examine statistical significance. *P<0.05, **P<0.01, ***P<0.001, and ****P<0.0001.

Staircase test: The results of the staircase test are presented as the number of eaten pellets eaten grabbed by each hand and the level of floor can be reached (Figure 5-4). The left paw was affected by the lesion. Two-way repeated ANOVA was used to analyze the data. From the pre-training day 1 to day 7, the number of eaten pellets eaten, and the reached maximal floor was slightly increased but no difference. Comparing the last day of pre-training, 3 weeks and 8 weeks, there was no difference between each group.

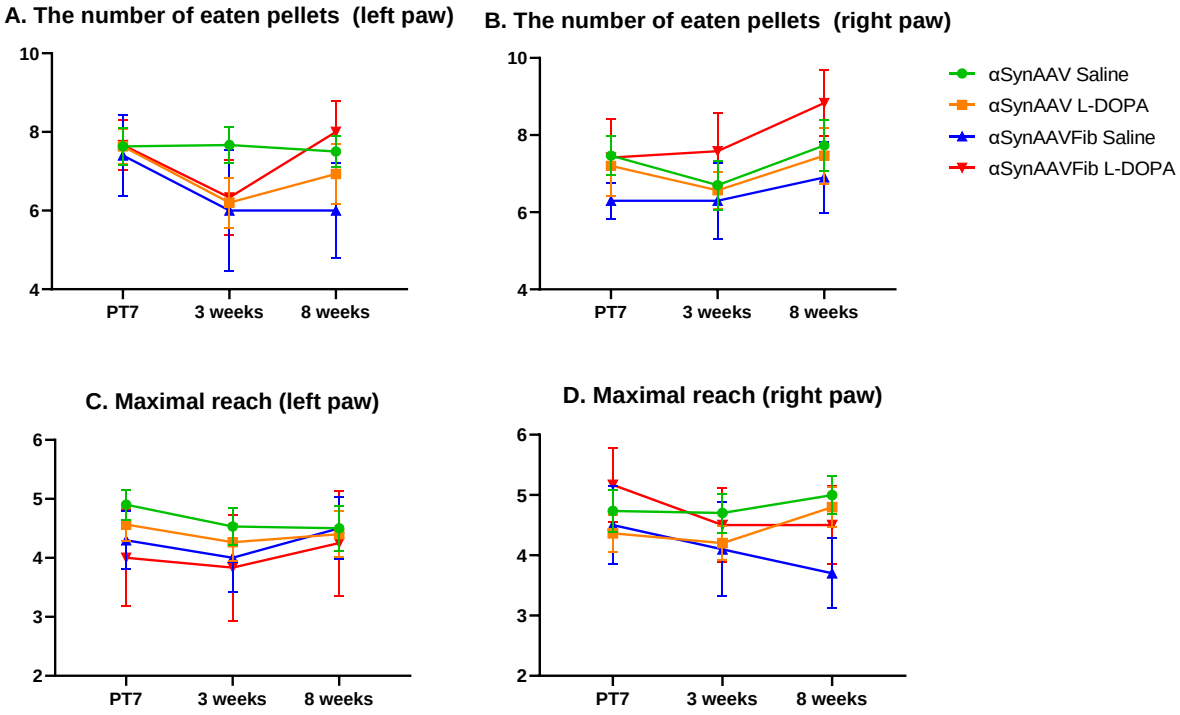

Figure 5-4. A and B showed the number of eaten pellets grabbed by right paw and left paw respectively. C and D showed the maximal level of floor reached by paw. Data were presented as mean ± standard error of the mean. Two-way repeated ANOVA and Bonferroni post-hoc analysis was used to examine statistical significance. *P<0.05, **P<0.01, ***P<0.001, and ****P<0.0001.

5.4.2. Immunohistochemistry results

5.4.2.1. Impact on DAergic neuron survival

At week 8 post-lesion, the αSynAAV groups showed only a mild, partial lesion of midbrain DAergic cells. In the SNc area, the αSyn viral vector alone caused ~50% TH^+ neuron loss ($F_{(2, 32)} = 10.53$. $P=0.0003$) and the neuron loss in SNr was insignificant ($F_{(2, 32)} = 2.231$, $P=0.1238$). αSynAAV L-DOPA group showed significant difference to naïve control in VTA area while αSynAAV saline group did not ($F_{(2, 32)} = 3.467$, $P=0.0434$). In contrast, αSynAAVFib groups showed about 80% neuron loss in the SNc area ($F_{(4, 41)} = 17.72$, $P<0.0001$) and around 50% neuron loss in SNr ($F_{(4, 41)} = 2.868$, $P=0.0349$) and VTA areas ($F_{(4, 41)} = 12.66$, $P<0.0001$). L-DOPA treatment showed no impact on either the αSynAAV or the αSynAAVFib models on DAergic neuron survival (Figure 5-5). The images were shown in Figure 5-6.

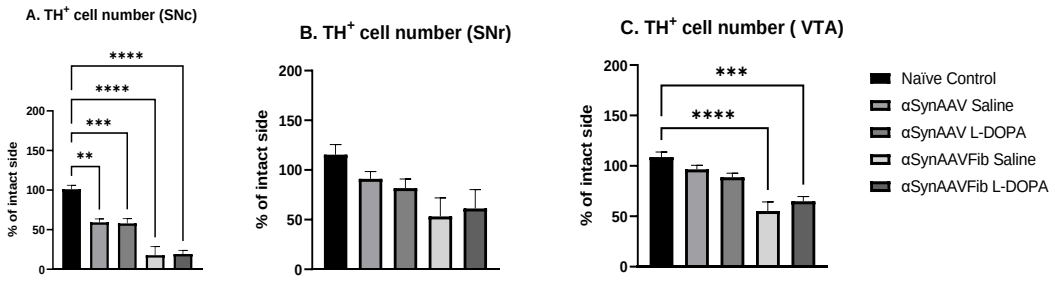

Figure 5-5 Percentage of TH^+ expressing cells counted in SNc, SNr and VTA regions (lesioned side over intact side). Significant neuronal loss was found between αSynAAVFib groups and naïve groups in SNc ($F_{(4, 41)} = 17.72$, $P<0.0001$) and VTA ($F_{(4, 41)} = 12.66$, $P<0.0001$). Data are presented as mean ± standard error of the mean. One-way ANOVA and Bonferroni post-hoc analysis was used to examine statistical significance. *$P<0.05$, **$P<0.01$, ***$P<0.001$, and ****$P<0.0001$.

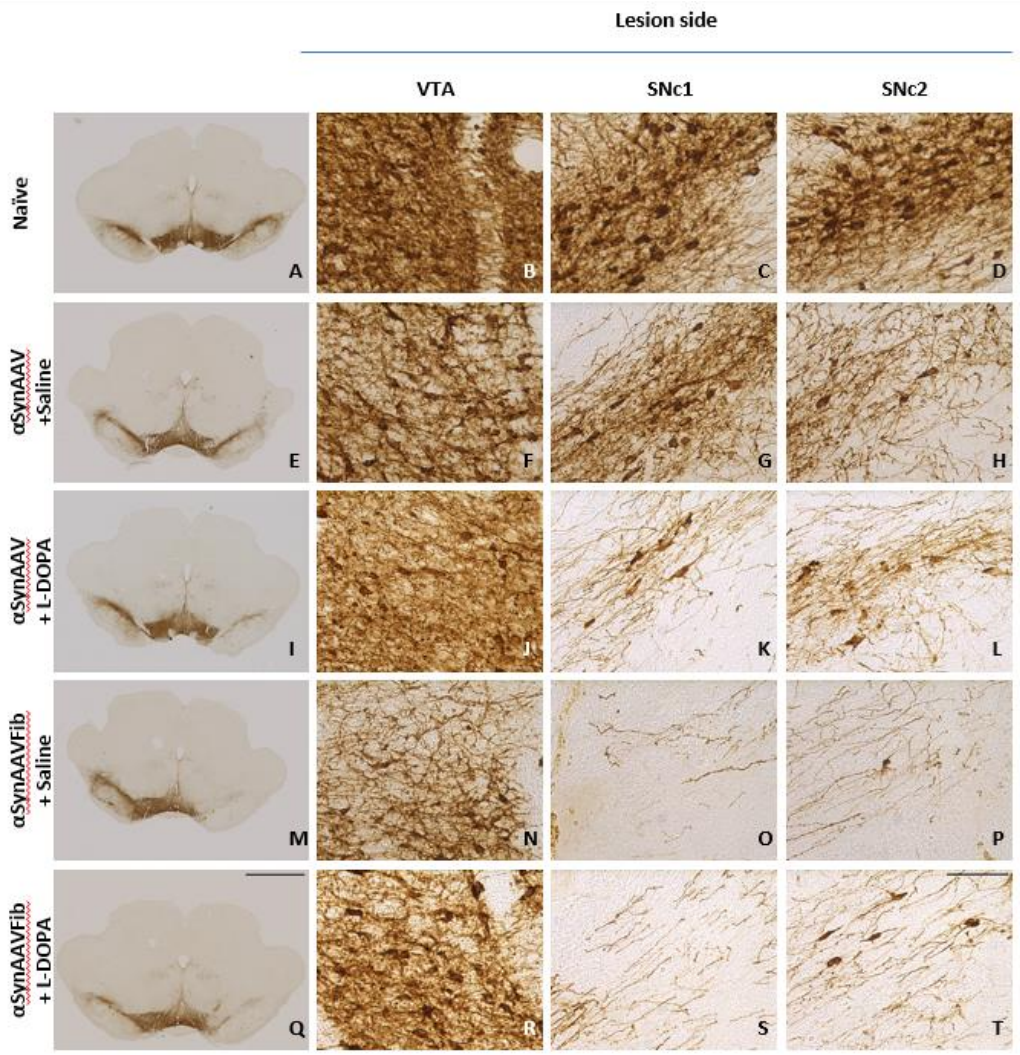

Figure 5-6 Representative images of TH DAB staining were presented for each group in VTA and two sites in SNc. A, E, I, M and Q scale bar: 2000μm. B, C, D, G, H, J, K, L, N, O, P, R, S and T scale bar: 85μm.

Measurement of TH^+ fiber density in the striatum followed the same trend of cell number counting but L-DOPA was showing more rescuing effect at bregma 1.60. Overall, TH^+ fiber density in the striatum showed a significant difference between the classical αSynAAV model and the more recent αSynAAVFib model at Bregma 1.60 ($F_{(4, 41)}$ = 13.44, P<0.0001) and Bregma 0.48 ($F_{(4, 42)}$ = 16.09, P<0.0001). However, at Bregma 1.60 (further than Bregma 0.48 from the injection site) the difference between αSynAAV L-DOPA and αSynAAVFib L-DOPA group was not significant. Medial and dorsal striatum were similarly

influenced by the method applied here (Figure 5-7).

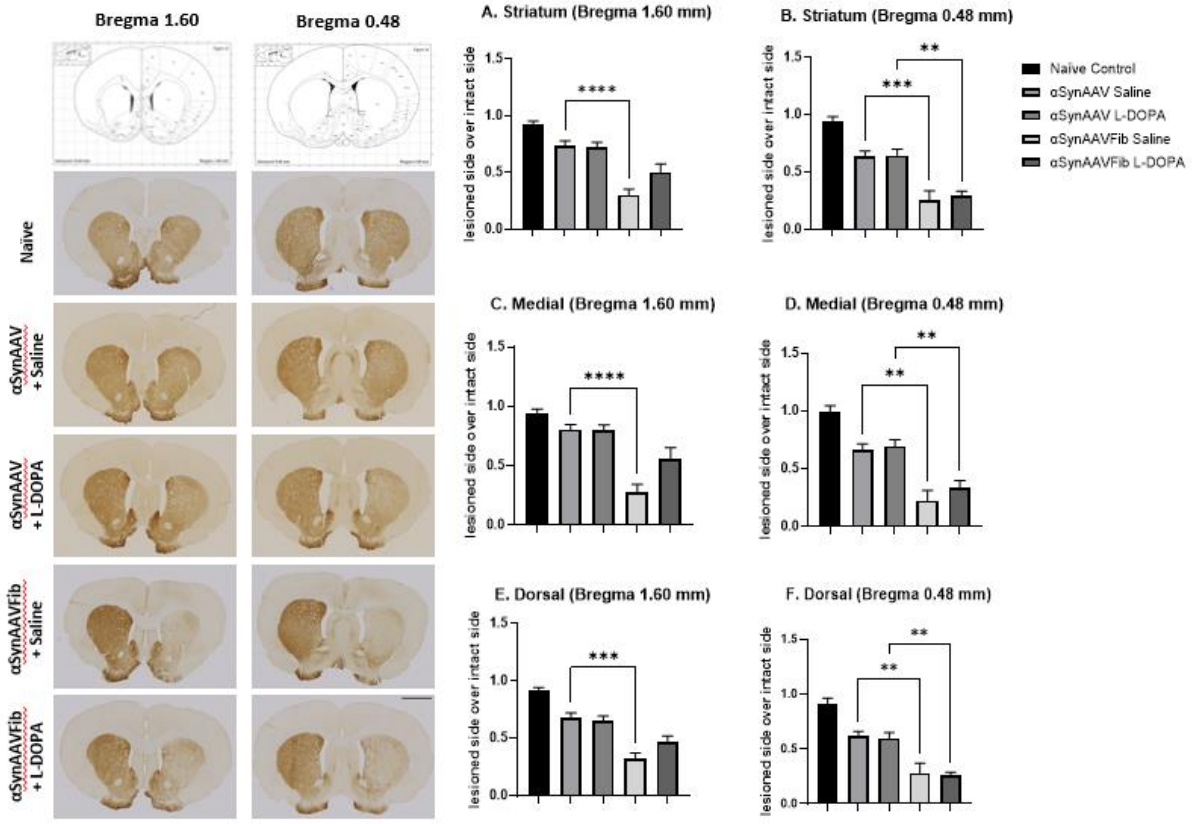

Figure 5-7 (Left) Representative images of TH DAB staining were presented for each group in the striatum at Bregma 1.60 and Bregma 0.48 (scale bar:2000μm). (A-B) Percentage of TH^+ expressing cells counted in the striatum at Bregma 1.60 ($F_{(4, 41)}$ = 13.44, P<0.0001) and Bregma 0.48 ($F_{(4, 42)}$ = 16.09, P<0.0001) (lesioned side over intact side). (C-D) Percentage of TH^+ expressing cells counted in medial striatum (Bregma 1.60: ($F_{(4, 41)}$ = 12.86, P<0.0001)，Bregma 0.48: $F_{(4, 42)}$ = 14.91, P<0.0001). (E-F) Percentage of TH^+ expressing cells counted in dorsal striatum (Bregma 1.60: $F_{(4, 41)}$ = 11.90, P<0.0001, Bregma 0.48: $F_{(4, 42)}$ = 14.32, P<0.0001). One-way ANOVA and Bonferroni post-hoc analysis was used to examine statistical significance. *P<0.05, **P<0.01, ***P<0.001, and ****P<0.0001.

5.4.2.2. Impact on $IBA1^+$ microglia

In the striatum, both αSynAAV saline group and αSynAAVFib saline group showed insignificant microglial reaction. In contrast, the inflammatory response was significant in the SNc ($F_{(4, 42)}$ = 13.91, P<0.0001) and VTA ($F_{(4, 42)}$ = 12.36, P<0.0001) for αSynAAVFib groups, while this was not seen for the αSynAAV groups. L-DOPA treatment showed no impact on both αSynAAV and

αSynAAVFib groups in the striatum (Figure 5-8 and Figure 5-9).

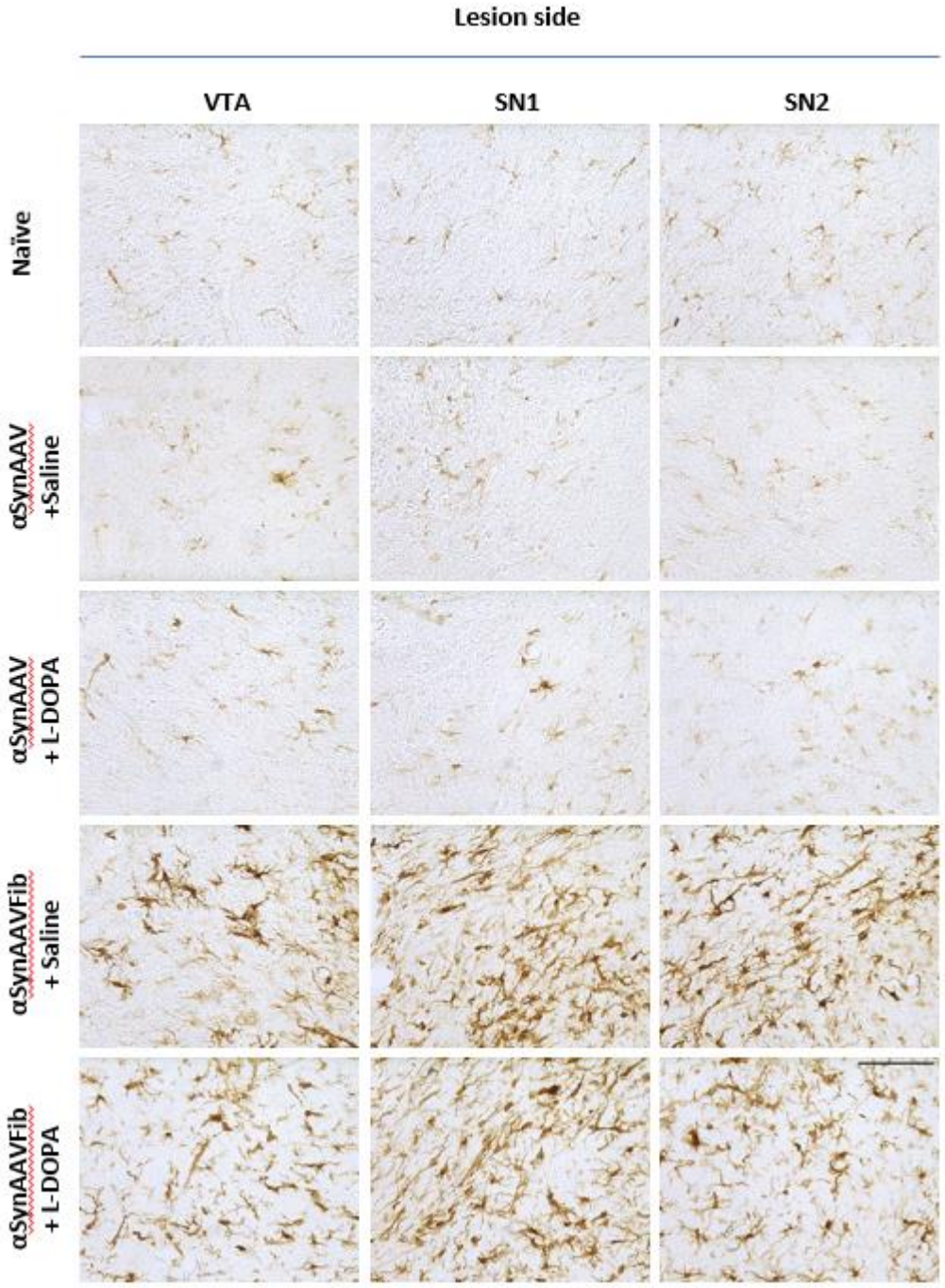

Figure 5-8 Inflammatory response in the midbrain on the lesioned side. Representative images of IBA1 staining were presented for each group. scale bar: 85μm

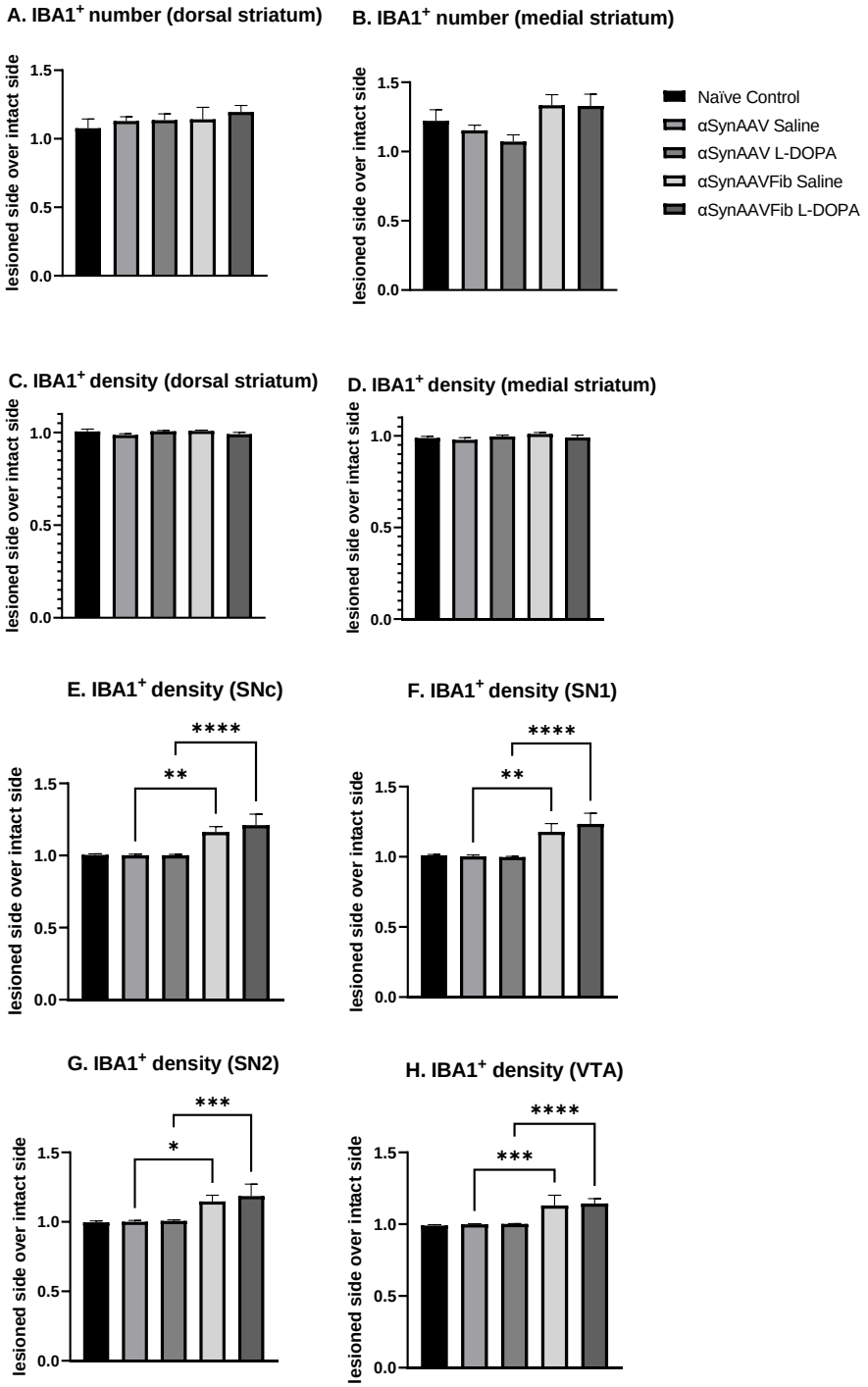

Figure 5-9 The results of relative IBA1$^+$ cells count in the striatum and midbrain on the lesioned side over intact side. The data were presented as mean ± standard error of the mean. The density of IBA1$^+$ cells were higher in the SNc ($F_{(4, 42)} = 13.91$, $P<0.0001$) and VTA areas ($F_{(4, 42)} = 12.36$, $P<0.0001$) in αSynAAVFib groups than naïve group. One-way ANOVA analysis and Bonferroni post-hoc analysis is used to compare between groups. *$P<0.05$, **$P<0.01$, ***$P<0.001$, and ****$P<0.0001$.

5.4.2.3. Impact on GFAP$^+$ astrocyte

GFAP$^+$ astrocytes were significantly increased in the αSynAAVFib saline group in SNc ($F_{(4, 42)}$ = 4.054, P=0.0072). This increase was seen in both SN1 and SN2 but only the SN2 showed statistical significance ($F_{(4, 42)}$ = 4.658, P=0.0033). This effect was confined only to SNc and was not seen in VTA, nor the striatum. αSynAAV groups on the other hand, also showed a trend of increasing level of GFAP$^+$ astrocytes but was statistically insignificant. L-DOPA treatment was weakening this effect and the GFAP$^+$ astrocyte density in αSynAAVFib L-DOPA group was not statistically different from that of naïve control group. This attenuating effect of L-DOPA was also confined to SNc only and was not seen in VTA or striatum (Figure 5-10 and Figure 5-11).

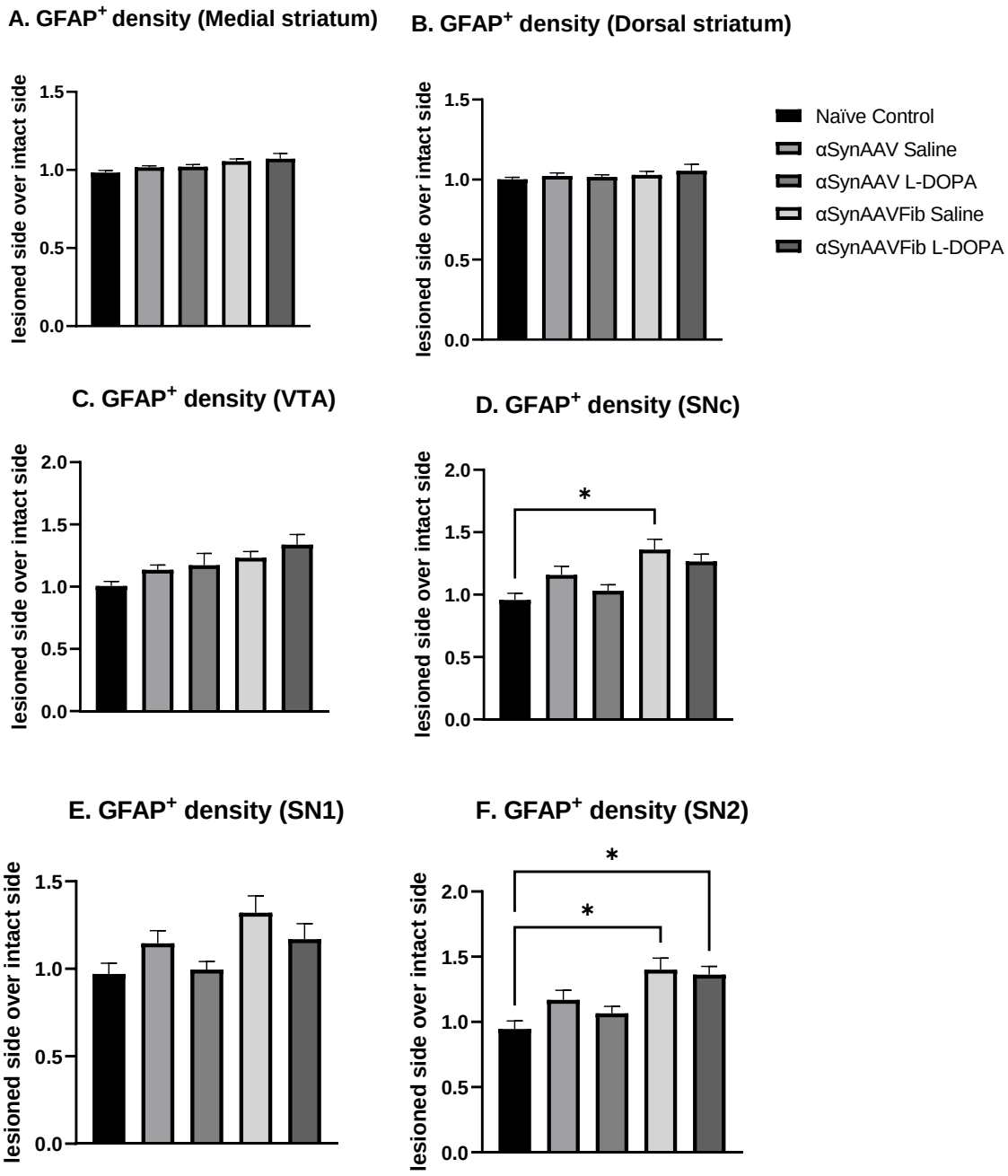

Figure 5-10. The results of relative optical density of GFAP⁺ cells in different areas in the brain. Data were presented as mean ± standard error of the mean. GFAP density significantly increased in SNc in αSynAAVFib saline group compared to naïve group ($F_{(4, 42)}$ = 4.054, P=0.0072). This is closer to SN2 site ($F_{(4, 42)}$ = 4.658, P=0.0033) while SN1 site showed no difference. One-way ANOVA and Bonferroni post-hoc analysis was used to examine statistical significance. *P<0.05, **P<0.01, ***P<0.001, and ****P<0.0001.

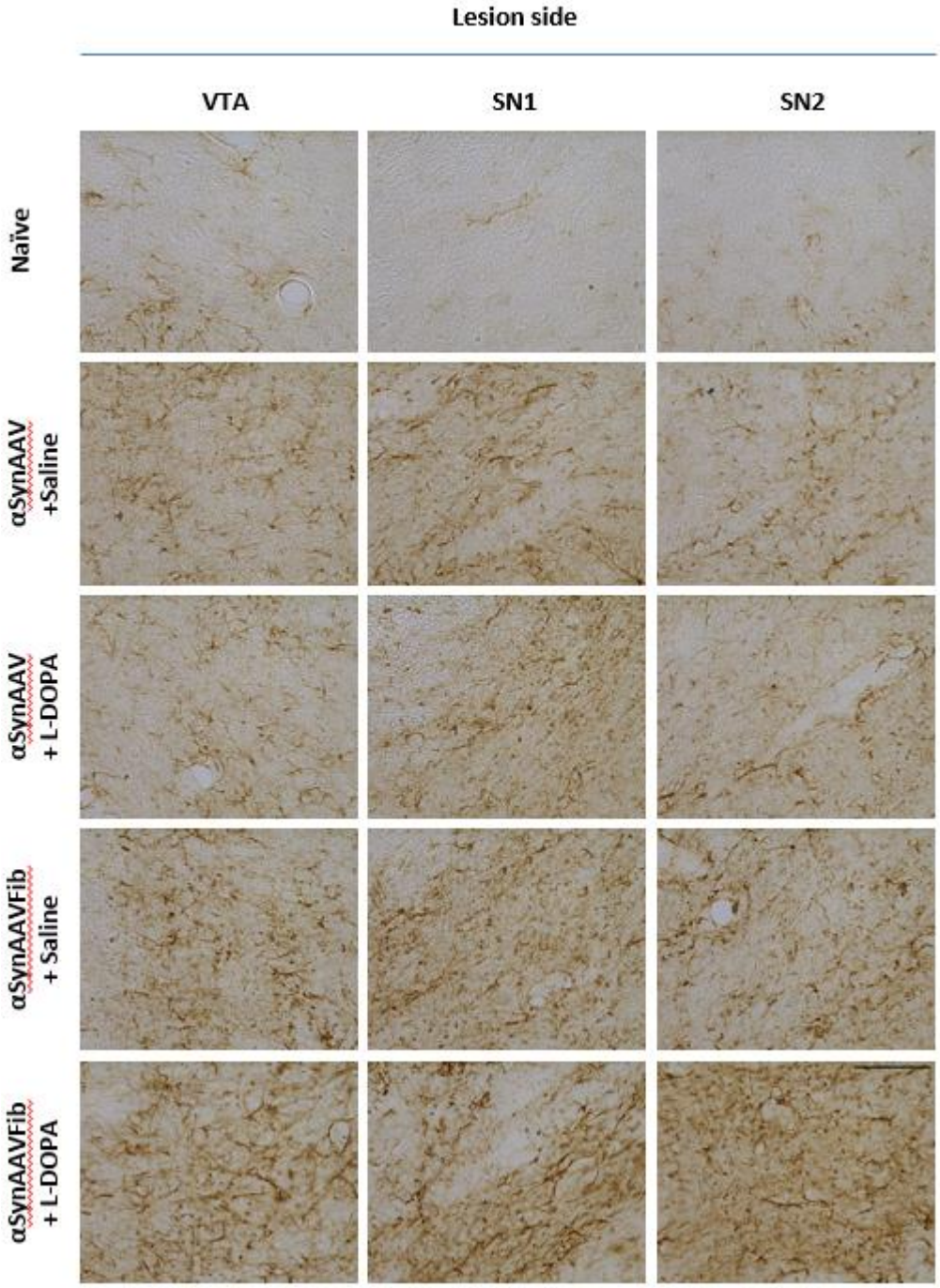

Figure 5-11 Inflammatory response in the midbrain on the lesioned side. Representative images of GFAP staining were presented for each group. scale bar: 85μm

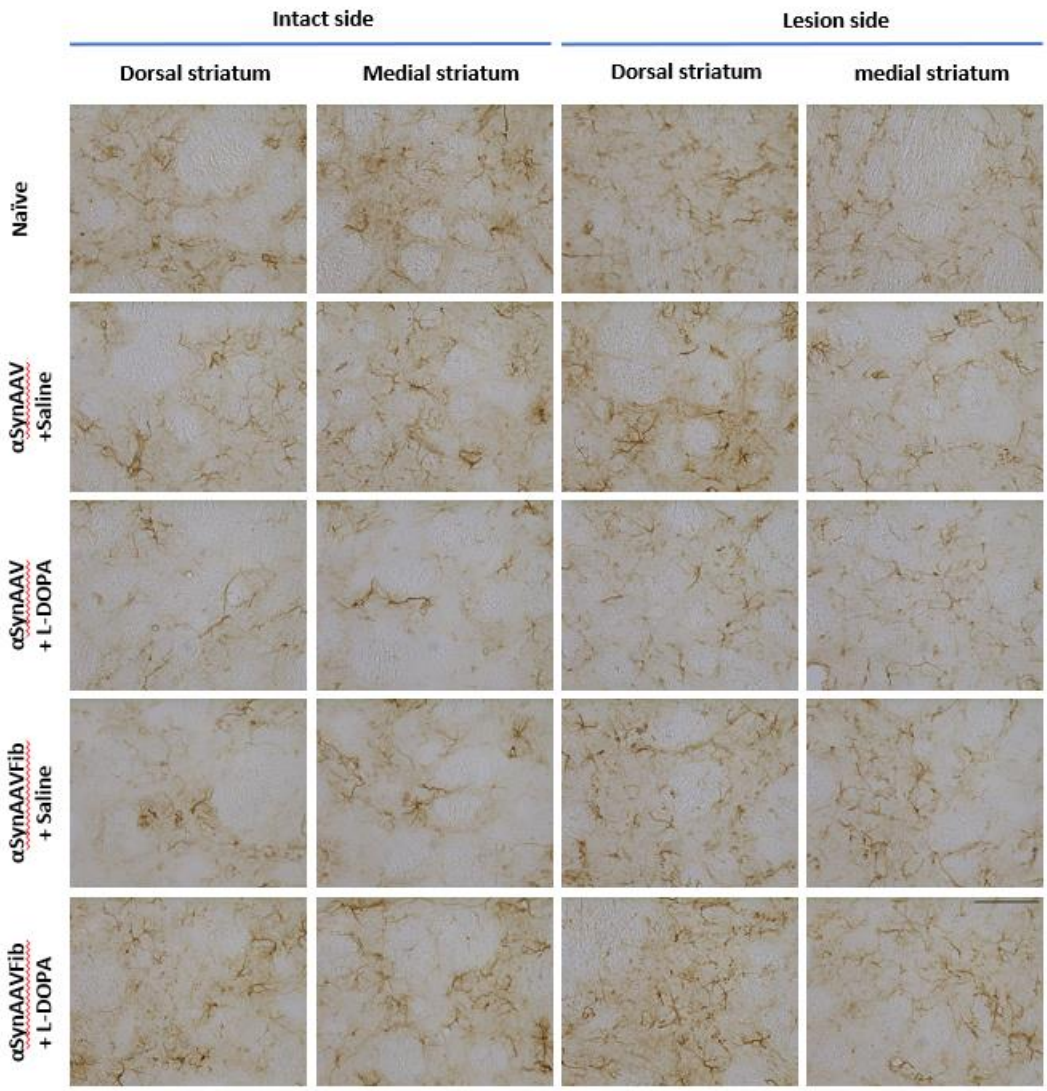

Figure 5-12 Inflammatory response in the striatum on the lesioned side. Representative images of GFAP staining were presented for each group. scale bar: 85μm

5.5. Discussion and conclusion

In chapter 3 and 4, the overall conclusion about L-DOPA's effect on DAergic neuron survival was that the administration of L-DOPA was not affecting the overall survival of DAergic neurons nor exacerbating the immunological environment following 6-OHDA lesion in the brain. In this chapter, the cause of the lesion was altered to α-synuclein/ α-synuclein fibers. This representative feature in PD may help to better illustrate the interactions between L-DOPA and the brain environment. The results were found to be slightly different from the 6-OHDA models but, pertaining to the main point, the overall survival of DAergic neurons was again not affected.

This indicates that although L-DOPA was suspected to attenuate the damage from α-synuclein, the effect may not be strong enough to influence the overall survival of the DAergic cells. A study conducted on female rhesus monkeys in 2021 obtained very similar results and clearly stated that twice a day L-DOPA treatment (20mg/kg) did not cause significant differences regarding DAergic neuron survival (Deffains et al. 2021).

The rat's behavior test data were also not significantly influenced by L-DOPA treatment, including one additional evaluation compared to chapter 3 and 4. The staircase test evaluates forelimb movements with little influences from other parts of the body, which is in contrast to cylinder test (Montoya et al. 1991). This test has been widely used in LID studies and can provide specific information restricted to the forelimbs, which may help reveal L-DOPA's influence in the partial lesion model more precisely (Winkler et al. 2002; Shin et al. 2014). One possible explanation for the behavior result is that the progressive loss of DAergic cells maybe more hidden than the usual neurotoxin lesioned model. Extending the observing period may eventually result in

significance between groups as reported by Hoban et al., which continued for 16 weeks post lesion, as opposed to 8 weeks in this experiment (Hoban et al. 2020).

Through TH^+ cell counting, the data here showed a clear trend that the mixed α-synuclein and FPP (α-SynFib) model induced a much more severe lesion (~80%) than the classical α-synuclein overexpression (α-Syn) PD model (~50%), the percentage of neuronal loss in the latter model was in line with similar studies (Mochizuki et al. 2006). 80% DA neuronal loss has been considered to be the threshold for the development of PD symptoms in the clinic (Masato et al. 2019) . Therefore, this new model is more representative of the situation of PD patients. Only 50% neuronal loss was achieved by Thakur's two-step virus+fiber model. The protocol was laborious and demanding, which might introduce more variability to the according results (Thakur et al. 2017). The subsequent one-step model developed by Shrigley refined the protocol and produced a model with 70%~75% neuronal loss (Hoban et al. 2020). In Thakur's model, there were three injection sites: two in SNc and one in VTA. While in Shrigley's model, only two injection sites in the SNc remained. Herein, the new model took Thakur's approach with three injection sites and successfully increased the toxicity.

Transgenic mouse and α-synuclein gene overexpression mouse have been used as models of α-synuclein degeneration to study DA or L-DOPA impact on the DAergic neurons survival. Although the α-synuclein gene (mutated or wild-type) and protocols for producing α-synuclein pathology were different among these studies, an increased level of DA led to more DAergic neurons loss. In the presence of increased daily DA dosage, a significant decrease in the number of DAergic neurons were observed with A53T mutant human α-synuclein transgenic mice (Mor et al. 2017). Similar results were obtained in the

rAAV6 human wildtype α-synuclein gene mouse model. When the level of DA was increased via decreasing vesicular storage of DA, there was a significant DAergic neuron loss compared to wildtype mouse (Ulusoy et al. 2012). These findings suggest that the increased cytosolic DA level can increase α-synuclein mediated toxicity. Like studies of DA, L-DOPA was reported to increase α-synuclein induced toxicity in mutant α-synuclein model. L-DOPA (daily 30 mg/kg, 90 days) administered to A30P α-synuclein (one of the common mutations found in PD patients) transgenic MPTP lesioned mice induced more DAergic neuron loss than saline treated A30P α-synuclein transgenic MPTP lesioned mice (Szego et al. 2012), indicating the administration of L-DOPA might increase α-synuclein induced toxicity.

However, recent studies have proved that the α-synuclein overexpression model used in such experiments failed to reproduce some of the key PD features found in post-mortem brain tissues (Mahul-Mellier et al. 2020). It is therefore necessary to retest L-DOPA's impact on this more advanced model.

Immunological results suggested more inspiring findings about this model. In the previous chapters, 6-OHDA was injected into the MFB (Deumens et al. 2002) and produced an extensive neuronal loss with over 95% of DA neuron destructed. The striatum had a significant increase of $IBA1^+$ cells because of the immune responses following the lesion and it was shown that L-DOPA was exerting an anti-inflammatory effect against $IBA1^+$ cell activation. However, in this model, the α-synuclein induced toxicity was still progressive. It did not cause a huge surge of the number of $IBA1^+$ cells in the striatum and, therefore, the previously seen anti-inflammatory effect was not observed in the α-SynFib model. Unlike the striatum, the immune responses in the SNc and VTA were strong in the α-SynFib model. $IBA1^+$ cells and $GFAP^+$ cells were increasing significantly in the SNc; and $IBA1^+$ cells were also increasing in the VTA part.

L-DOPA was exhibiting no effect to the immune responses in this α-SynFib model. This huge disparity between 6-OHDA and α-SynFib model was possibly due to the different timepoint for the dissection of the rat brain. 6-OHDA lesion was complete in two weeks after toxin injection (Thiele et al. 2012). By the time of dissection, the rat's brain was already lesioned completely for more than 6 weeks (in Chapter 3) and 33 weeks (in Chapter 4). In contrast, the α-SynFib model was a progressive model (Dehay and Fernagut 2016). The immune responses caused by this progressive damage was still active by the time of perfusion. The difference between acute-lesion and progressive model of immune defense may explain why L-DOPA was creating a less inflammatory environment in 6-OHDA lesioned model while had no effect on the α-SynFib model. It was also noted that the affected region in the brain were different. Acute lesion caused immunity was mainly found in the striatum while progressive lesion seems to affect the immune environment in SNc and VTA. Though still need to be confirmed, the preliminary conclusion was summarized in table 5-2.

Increasing number of publications are suggesting that L-DOPA helps to attenuate pathological changes caused by α-synuclein pathology (Shimozawa et al. 2019; Deffains et al. 2021). Previous report showed L-DOPA might have an epigenetic effect on SNCA gene and represses neuronal SNCA expression (Schmitt et al. 2015). This only explains the model based on α-synuclein overexpression but not on α-synuclein fibril. The result in this chapter also showed that the rescuing effect of L-DOPA were more apparent in α-SynFib model but not in α-Syn model (though insignificant). It indicates that there might be another underlying mechanism for L-DOPA's effect against α-synuclein pathology and this mechanism is unlikely to be immune system related since immune responses were not changed by L-DOPA in this model.

Table 5-2 summary of 6-OHDA model and α-SynFib model

	Lesion type	Time of brain dissection	Affected region	Affected cell type	L-DOPA's effect
6-OHDA model	Complete lesion (over 95% neuron loss)	At least 6-weeks post lesion	Striatum	Mainly IBA1+ cells	Anti-inflammatory
α-SynAAVFib model	Progressive lesion (~80%)	Continuous damage from α-Syn	SNc and VTA	IBA1+ cells and GFAP+ cells	No significant effect
α-SynAAV model	Progressive lesion (~50%)	Continuous damage from α-Syn	None	None	No significant effect

Chapter 6. General discussion

6.1. Summary

L-DOPA has been the golden standard treatment for PD for over half a century yet the effects of L-DOPA on DAergic neuron survival remains a debated issue even now (Lane 2019). Understanding the question becomes an urgent task as stem cell therapies are advancing and entering clinical trials worldwide (Parmar et al. 2020). Assessing L-DOPA's effect on a clinically relevant rat model would provide valuable information to future clinical studies and facilitate the application of relevant works.

This study firstly reassessed L-DOPA's effect on endogenous DAergic neuron survival on a classic 6-OHDA based neurotoxin model. A key feature of the model is the stability of toxin induced neuronal loss. As one of the most commonly applied models, the data is less variable, and the results are more robust (Schober 2004).

The first endogenous rat model is quite successful in terms of:
(1) the DAergic neuron loss that had been generated. The percentage of SNc cell loss was in line with most other 6-OHDA based rat model and provided support for the reproducibility of the study.
(2) the LID symptoms that are usually seen after long-term L-DOPA administration in the clinic. This indicator proves that the L-DOPA dosage used in this experiment was clinically relevant and the dose of L-DOPA could be set as a baseline for the rest of the rat models in this study.
(3) replicating the activated immune system accompanying DAergic neuron loss. Extensive activation of the immune system is a universal feature found in

people with PD (Tan et al. 2020). This model provided the opportunity to study L-DOPA's effect on the altered immune system. Overall, this ensured a thorough characterization of the model in my hands before beginning any other manipulations.

The model considered the bidaily administration of L-DOPA, a more relevant dosing schedule to PD prescribing and also took the impact on the intact side into account, which has been largely neglected in similar studies. In addition, peripheral Hcy concentration was investigated to understand if L-DOPA produces toxicity outside CNS. The results showed no correlation between L-DOPA treatment and toxicity inside or outside CNS, adding evidence to support the hypothesis that L-DOPA is not accelerating the DAergic cell loss in the brain (Parkkinen et al. 2011).

Building on the same 6-OHDA rat model, with confidence that any changes were as a result of L-DOPA impacting the graft and not the host model, exogenous graft cells were added to allow the investigation of L-DOPA's effect on human DAergic cells. This add-on of human stem cells, although cannot directly reflect the true human brain environment, depicts the possible influence of L-DOPA to the future clinical stem cell therapy.

The second study attempted to closely replicate the regimen and procedures from past surgical experiences, including the long-term usage of immunosuppressant, long-term L-DOPA treatment and the immune responses generated under such complex environment. The graft survival rate was in agreement with other studies and was confirmed by MRI technology. Recovery shown in the behavior test was also proving that the graft was helping to restore the functions of DA neurons.

L-DOPA treatment, first of all, exhibited no toxicity to the exogenous hESC graft. The immunological analyses even gave insight that L-DOPA treatment resulted in a less inflammatory environment compared to saline controls in this rat model. The situation may be better in the human brain as an allograft causes less immune response than xenograft transplantations (Piquet et al. 2012).

Since no detrimental effect of L-DOPA was found in the 6-OHDA based rat models, this study set out to further study L-DOPA's effect in a more refined pre-clinical model. Inspired by recent improvements in α-synuclein involved rat model, this study then slightly adopted the model to fit the general status of people with PD.

The three-site combination of α-synuclein delivered through AAV and preformed fibrils generated an unprecedented 80% DAergic neuron loss, which is ideal for modelling late stage, symptomatic PD. Once again, the results were supporting the use of L-DOPA as no toxicity was found in this improved α-synuclein based rat model.

Future works need to further evaluate the effect of L-DOPA on the same α-synuclein based model but with exogenous hESC graft. The second 6-OHDA based graft model provides a nice template for graft procedure and handling of immune rejections. It is expected to see how the graft survival will be affected by L-DOPA under this setting and whether immune responses will be influenced.

6.2. General discussion

6.2.1. Animal models for the evaluation of the effect of L-DOPA: advantages and limitations

With the progression of stem cell-based replacement therapies, clinically oriented studies are in dire need. Guidelines on the use of L-DOPA treatment before and after stem cell replacement surgeries are not fully established and the debates are still ongoing in the regard of L-DOPA's toxicity.

In vitro studies from the past several decades confirmed the toxicity of L-DOPA is dose dependent, but it's hard to monitor long-term toxicity from such studies. On the contrary, clinical studies are more suitable for this purpose. Subjects can be followed through several years to a few decades, depending on the nature of experimental design. However, it takes exceptionally long time for such studies to be conducted and it is also difficult to rule out influences from other non-PD treatments or impact from lifestyle.

To make it more predictable for a promising therapy that is yet to be applied in broad scale, animal models seem to be the best compromise between *in vitro* and clinical evaluations. On one hand, (within limits) the treatment can be adjusted to best fit drug regimen for PD. On the other hand, the monitoring of treatment effect is much easier, and the duration of the whole study is more controllable.

One thing to be noticed before animal studies were designed is whether the model will reflect the crucial features of PD, especially the pathological features that would usually take years to form. It would be most impractical to build a model in a life span. Even if it is possible to obtain animals in senile age, their body conditions could bring too many uncontrollable factors for behavior testing

or immunostaining and so on. Therefore, it must be aware that current studies were not conducted in physiologically aged brains, and this means the immunological environment, the rate of metabolism and gene expression could be quite different from those from PD, especially in late stage.

Unable to fully recapitulate the key features of PD, most current strategies are concentrating on the degeneration of DAergic cells and so on (Konnova and Swanberg 2018). Admittedly, these models such as 6-OHDA model are useful in reproducing symptoms and for testing new drugs, but the translation from these results to the clinic is often poor (Potashkin et al. 2010). It worth thinking of optimizing current models for new focuses, besides developing new models. In other words, more closely mimicking a PD regimen in animal models may help to better illustrate the drug effect even if the models hold differences to people with PD.

For instance, it is long known that the administration frequency and the dosing strategy of L-DOPA is closely related to the side effects such as LID. At early stages, when the majority of DAergic cells are still functioning, the L-DOPA release is buffered, and the motor fluctuations are less likely to happen. But when there is a severe DAergic cell loss, then the trough of L-DOPA level can lead to some side effects, like dyskinesia. Though there are still some debatable points in the mechanism for dyskinesia, it has been proved in the clinic that dyskinesia can be drastically offset by continuous L-DOPA infusion (Stocchi 2005).

If side effects like LID are caused by dosing strategy, which is more of a pharmacokinetic problem instead of intrinsic toxicity properties of L-DOPA, then is it possible that some other negative alterations reported in early publications were also due to the same reason? In 2016, Mulas et al. applied a continuous

L-DOPA delivery technique in 6-OHDA rat models which showed that not only were the LID symptoms completely offset by the continuous L-DOPA infusion, but also that the LID was not necessarily related to immune response induction (Mulas et al. 2016). In fact, continuous L-DOPA administration in this experiment caused no immune responses while the classic pulsatile administration did.

Adjusting doses of L-DOPA in animal models may not be as easy as it seems. Dividing doses to more than three times a day for animals is against the welfare of animals as well as for researchers. It will be difficult to fit the plan into daily working hours in most places. Also, continuous intrajejunal apparatus are not universally applied for every PD patient nor are they readily available in every lab. Although the future trend might be that continuous intrajejunal infusion of levodopa to be recommended for most PD cases given the benefits shown in the clinical study (Olanow et al. 2014), it is still not yet representative enough to design rat models solely based on this delivery system.
After all, animal models are still going to be used for the evaluation of on-going cell replacement therapies for PD. Lots of efforts were paid to the improvements of reproducing the DAergic neuron loss in these models, while it may be worthwhile to also acknowledge the impact from dosing strategies. Clinically relevant dosage may markedly change the outcomes and make the results more informative.

As opposed to early research which claimed that L-DOPA (ranged from 80 mg/kg to 200 mg/kg, mostly once a day) exacerbated the immune responses (discussed in Chapter 3), the lower dose of L-DOPA (ranged from 4 mg/kg to 15 mg/kg, bidaily) in this study has put this into debate. The majority of data to the interest of this study showed that clinically relevant dose of L-DOPA had no impact on the immune system, both inside and outside the central nervous

system of rats. Coincidently, a similar in vivo experiment published in 2020 investigated the impact of L-DOPA (20 mg/kg, bidaily) on the MPTP rhesus monkey model. The GFAP+ astrocytes in this study also supported the view that L-DOPA treatment do not significantly affect at least GFAP+ astrocytes (Deffains et al. 2021). More clinically oriented in vivo studies are needed before drawing a conclusive remark, but the current preliminary result from this study favors the use of relatively low dosage of L-DOPA when considering immune responses.

6.2.2. Influences of L-DOPA on PD pathology

There is a very interesting question: Is L-DOPA influencing the overall PD pathology? Different to the focus of the thesis, which is mainly considering DAergic neuron survival, PD pathology is more related to Lewy body and its component α-synuclein (Yates 2019). Albeit L-DOPA's effect was debatable when discussing DAergic neuron survival, the attitudes towards its effect on PD pathology is surprisingly clear. Mechanistically, L-DOPA is most likely to play a role against Lewy body formation, though the effect may not be clinically evident.

A Japanese group was focusing on the effect of L-DOPA to PD pathology for more than a dozen years. They showed firstly *in vitro* that physiologically relevant dose of L-DOPA as well as DA inhibit both α-synuclein fiber formation and aggregation process (Ono et al. 2013). More importantly, those filament structures, when formed under the presence of L-DOPA or DA, appeared to be less stable than the usual α-synuclein fibril structures. Their hypothesis was that the orthoquinone structures can be generated from the di-hydroxy groups on the benzene ring (catechol) after oxidation of L-DOPA or DA in an oxidizing chemical environment (Yen and Hsieh 1997). These orthoquinones have specific binding affinity to free α-synuclein units and thus inhibit α-synuclein

aggregation and also destabilize the toxic β-sheet structures of α-synuclein fibril in three-dimensional space (Ono and Yamada 2006; Ono et al. 2007).

To further confirm their theory, mouse α-synuclein plus α-synuclein fibrils were injected into one side of WT mice brain and successfully induced α-synuclein pathology. L-DOPA/benserazide treatment (200 mg/kg/75 mg/kg daily) significantly reduced the amount of $PS129^{+}$ (an anti-α-synuclein antibody) aggregates and it also showed a rescuing effect to TH^{+} cells. While the number of TH^{+} cells decreased in the no L-DOPA treatment group (the lesioned side compared to the intact side), the L-DOPA treated group showed no such difference (Shimozawa et al. 2019). This experiment resembles the study discussed in Chapter 5, though the source of α-synuclein was different (mouse α-synuclein instead of human α-synuclein). Emphasis might be better placed on the toxicity of α-synuclein when tested cross species, because in chapter 5, when human α-synuclein was used, L-DOPA treated group did not show any difference to saline control group.

Similar results were obtained from primate model. 1-methyl-4-phenyl-1,2,3,6-tetrahydropyridine (MPTP) model is the most classical primate model for PD and can reproduce α-synuclein pathology through the whole brain tissue (Porras et al. 2012). When treated with L-DOPA (20 mg/kg, bidaily for ~3 months), the intensity of immunofluorescence of α-synuclein was significantly reduced when compared to no L-DOPA treatment group (Deffains et al. 2021). These *in vivo* results strongly support the hypothesis that L-DOPA has an inhibitory effect towards α-synuclein pathology.

Nevertheless, as discussed in part 6.2.1, the translation from *in vivo* model to the clinic is not very promising. Albeit α-synuclein is a major part of Lewy body formation and L-DOPA treatment should greatly affect PD pathology according

to the *in vivo* results, the clinical outcome spoke differently. In the clinic, 96 cases with recorded L-DOPA treatment history were investigated and the statistics showed no connections between L-DOPA dose and Lewy body density (Parkkinen et al. 2011).

It is hard to make assertions at the current stage. PD pathology may involve multiple systems and organelles. Immune system for example was suspected to play an important role in PD progression (Joshi and Singh 2018) and was carefully examined in all the experimental chapters in this study. However, as shown in the results, immune responses to L-DOPA differed in different models (6-OHDA or α-synuclein). The immune response is possibly entangled with other factors like α-synuclein, DAergic cell loss, mitochondria, lysosome and so on, which makes the situation more difficult for further research (Stojkovska et al. 2015; Navarro-Romero et al. 2020; Wallings et al. 2020; Su and Zhou 2021).

Did L-DOPA show any positive influences in the clinical studies? The answer is yes but might be sex specific. The influence of L-DOPA may not be strong enough to resist PD progression, but it is offering extra help to the neuron environment other than DA supplement. A comparison of the peripheral blood samples between the sporadic PD patients and healthy controls showed that post-transcriptional process may be influenced by the disease. PD patients showed a lower level of methylation of SNCA intron 1, and such epigenetic alteration may increase the SNCA gene expression. Increased dosage of SNCA gene was also seen with growing age and was associated with PD progression (more details about SNCA gene on 1.2.2.2.1.) (Singleton et al. 2003; Sharma et al. 2012). Nevertheless, male PD patients who received L-DOPA treatment showed increased SNCA methylation compared to those who did not. Though for female PD patients, the SNCA methylation was decreased (Schmitt et al. 2015). This clinical study indicates that at least L-DOPA treatment might be

more beneficial to men as it down-regulates SNCA expression. Such benefit was not seen for women maybe partly due to the fact that the methylation of SNCA was naturally higher in women than men (Jowaed et al. 2010). The exact underlying mechanism is unfortunately not explored yet.

6.2.3. Trend of L-DOPA treatment: L-DOPA and the current and future therapies

L-DOPA treatment has been treated as the golden standard for PD in the past, present and will still be used for considerably long in the future unless a cure to be found. The influence of L-DOPA treatment to the current and future therapies then becomes an unavoidable topic that worth attention.

Among all the side effects, LID has remained to be an unresolved problem that seriously impaired the life quality of people with PD. The majority of patients develop LID within 10 years and this motor implication introduced by L-DOPA severely undermined its benefits for controlling motor dysfunctions from PD (Encarnacion and Hauser 2008). One of the main causes for LID was believed to be connected with striatal 5-HT innervation, neurons which cannot store and release DA properly in an DAergic cell depleted environment (Carta et al. 2007). This view is not comprehensive though. Emerging evidence suggests that both pre-synaptic and post-synaptic activities are involved in the pathogenesis of LID, accompanying non-DAergic neurotransmitter system changes (Yang et al. 2021).

Such complexity in structural and cellular changes hampers the understanding of the cause of dyskinesia but a few points were summarized based on current observations: (1) The preset environment for the induction of dyskinesia

comprises two major factors: Depletion of DAergic cells in the substantia nigra (must be over 50%) and pulsatile dopamine that triggers dyskinesia. (2) Once established, dyskinesia can also be triggered by DA agonists (Jenner 2008).

At present, the best way to delay LID is improving pharmacokinetic profiles of L-DOPA alongside the usage of selective D_2 DA agonists. Extended or controlled release of L-DOPA is achievable through development of advanced formulations or prodrug strategies (despite L-DOPA itself is already a prodrug of DA, additional masking group can still be conjugated to provide extended drug release) (Tambasco et al. 2018). Improved drug profiles offer more continuous DA stimulation which resembles the physiological state of DA receptors and greatly avoids pathological changes in the basal ganglia circuit (Grace 1995; Jenner 2004).

Preclinically, LID was proved to be more related to D_1 receptors than D_2 receptors. 6-OHDA lesioned mice with D_1 receptor knockout lacked LID features compared to wildtype mice, including behavior changes and phosphorylation of signaling pathways such as ERK. But D_2 receptor knockout mice showed no difference with wildtype (Darmopil et al. 2009). This suggest that selective D_2 agonists maybe used in adjunct with L-DOPA to lower the dosage of L-DOPA and further delay LID. D_2 agonists alone were reported still eliciting LID but this could be due to unwanted stimulation of D_1 receptor (Luquin et al. 1992).

Preclinical LID can be alleviated in many ways. Counteracting with changes in the brain helps to alleviate this side effect. For instance, mTOR and ERK pathways were found hyperactive in animal studies and genetically contribute to LID (Santini et al. 2007; Santini et al. 2009; Martín-Flores et al. 2019). Inhibiting these two pathways consequently reduced the severity of LID

(Decressac and Björklund 2013; Ryu et al. 2018). In the same way, aberrant glutamate receptor activities induced by LID can be modulated by MPEP (2-methyl-6-(phenylethynyl) pyridine), an allosteric antagonist for mGlu5 (Morissette et al. 2022). A glutamate N-methyl-D-aspartate (NMDA) receptor antagonist 4-chlorokynurenine (AV-101) has already been tested in primates and proceeded in clinical trial for anti-dyskinesia activity (Di Paolo et al. 2020). Other potential therapeutics in clinical trials includes 5-HT agonists, 3-hydroxy-3-methylglutaryl-coenzyme A (HMG-CoA) reductase inhibitors, D_3 receptor antagonist, and even herbal medicines (Huot et al. 2022). It remains to be seen whether any of these can provide relief from clinical LID.

In short, the current mainstay anti-parkinsonism therapy still revolves around L-DOPA for motor symptoms (Rizek et al. 2016). In addition to L-DOPA itself, the classical peripheral dopamine decarboxylase inhibitors such as Carbidopa has to be used to increase the bioavailability and decrease the plasma clearance of L-DOPA (Nutt et al. 1985). To delay LID, DA agonists or monoamine oxidase-B (MAO-B) may also be prescribed, especially in early-onset PD (Armstrong and Okun 2020). The combination of these three types of drugs unfortunately does not prevent LID. Therefore, the trend might be that the patients to be given extra anti-LID drugs after long-term L-DOPA treatment as mentioned above.

The current regimen is apparently not ideal and may have negative impact on the patient's compliance, considering that they may also need drugs to control non-motor symptoms. Novel therapeutic interventions such as stem cell therapy was then introduced to overcome this problem (Ahmad et al. 2022). Hope has been given to pluripotent stem cells for several advantages such as good availability, low immunogenicity and high survival rate as evidenced by most studies (Stoker 2018). However, past experiences from fetal transplantations did not rule out the use of L-DOPA. In fact, with relatively short

term of L-DOPA free period (L-DOPA was withdrawn for more than 2 years after successful transplantation), the motor symptoms reappeared, and L-DOPA had to be reintroduced in one of the most well-observed cases in Sweden (Li et al. 2016). Other problems involve graft induced dyskinesia which was observed clinically in the past and also shown in Chapter 4. Does this mean that more preclinical studies, such as those shown in this thesis, necessary for future guidance? Or is it best for the clinicians to learn directly from clinical trials? How can clinicians best manage patients post transplantation to get best efficacy from the transplant? All these questions need to be answered before PD patients can truly benefit from novel therapeutic approaches.

7. Bibliography

Abbas, N. et al. 1999. A wide variety of mutations in the parkin gene are responsible for autosomal recessive parkinsonism in Europe. *Human molecular genetics* 8(4), pp. 567-574.

Adachi, K. and Schöler, H. R. 2012. Directing reprogramming to pluripotency by transcription factors. *Curr Opin Genet Dev* 22(5), pp. 416-422. doi: 10.1016/j.gde.2012.07.001

Adler, A. F. et al. 2019. hESC-derived dopaminergic transplants integrate into basal ganglia circuitry in a preclinical model of Parkinson's disease. *Cell reports* 28(13), pp. 3462-3473. e3465.

Ahmad, J. et al. 2022. Novel therapeutic interventions for combating Parkinson's disease and prospects of Nose-to-Brain drug delivery. *Biochemical Pharmacology* 195, p. 114849. doi: https://doi.org/10.1016/j.bcp.2021.114849

Ahn, T.-B. et al. 2008. α-Synuclein gene duplication is present in sporadic Parkinson disease. *Neurology* 70(1), pp. 43-49.

Albin, R. L. and Leventhal, D. K. 2017. The missing, the short, and the long: Levodopa responses and dopamine actions. *Annals of neurology* 82(1), pp. 4-19. doi: 10.1002/ana.24961

Alegre-Abarrategui, J., Christian, H., Lufino, M. M., Mutihac, R., Venda, L. L., Ansorge, O. and Wade-Martins, R. 2009. LRRK2 regulates autophagic activity and localizes to specific membrane microdomains in a novel human genomic reporter cellular model. *Human molecular genetics* 18(21), pp. 4022-4034.

Andén, N. E., Dahlström, A., Fuxe, K. and Larsson, K. 1966. Functional role of the nigro-neostriatal dopamine neurons. *Acta Pharmacol Toxicol (Copenh)* 24(2), pp. 263-274. doi: 10.1111/j.1600-0773.1966.tb00389.x

Anderson, P. C. and Daggett, V. 2008. Molecular basis for the structural instability of human DJ-1 induced by the L166P mutation associated with Parkinson's disease. *Biochemistry* 47(36), pp. 9380-9393. doi: 10.1021/bi800677k

Arabadjiev, B., Petkova, R., Chakarov, S., Momchilova, A. and Pankov, R. 2010. Do we need more human embryonic stem cell lines? *Biotechnology & Biotechnological Equipment* 24(3), pp. 1921-1927.

Arai, R., Karasawa, N., Geffard, M., Nagatsu, T. and Nagatsu, I. 1994. Immunohistochemical evidence that central serotonin neurons produce dopamine from exogenousl-DOPA in the rat, with reference to the involvement of aromaticl-amino acid decar□ylase. *Brain Research* 667(2), pp. 295-299. doi: https://doi.org/10.1016/0006-8993(94)91511-3

Arce-Sillas, A. et al. 2019. Expression of Dopamine Receptors in Immune Regulatory Cells. *Neuroimmunomodulation* 26(3), pp. 159-166. doi: 10.1159/000501187

Armstrong, M. J. and Okun, M. S. 2020. Diagnosis and Treatment of Parkinson Disease: A Review. *Jama* 323(6), pp. 548-560. doi: 10.1001/jama.2019.22360

Asanuma, M. and Miyazaki, I. 2016. 3-O-Methyldopa inhibits astrocyte-mediated dopaminergic neuroprotective effects of L-DOPA. *BMC Neurosci* 17(1), p. 52. doi: 10.1186/s12868-016-0289-0

Atik, A., Stewart, T. and Zhang, J. 2016. Alpha-Synuclein as a Biomarker for Parkinson's Disease. *Brain Pathol* 26(3), pp. 410-418. doi: 10.1111/bpa.12370

Axelsen, T. M. and Woldbye, D. P. 2018. Gene therapy for Parkinson's disease, an update. *Journal of Parkinson's disease* 8(2), pp. 195-215.

Azzini, E., Ruggeri, S. and Polito, A. 2020. Homocysteine: Its Possible Emerging Role in At-Risk Population Groups. *Int J Mol Sci* 21(4), doi: 10.3390/ijms21041421

Azzouz, M. et al. 2002. Multicistronic lentiviral vector-mediated striatal gene transfer of aromatic L-amino acid decarboxylase, tyrosine hydroxylase, and GTP cyclohydrolase I induces sustained transgene expression, dopamine production, and functional improvement in a rat model of Parkinson's disease. *The Journal of neuroscience : the official journal of the Society for Neuroscience* 22(23), pp. 10302-10312. doi: 10.1523/jneurosci.22-23-10302.2002

Backlund, E. O. et al. 1985. Transplantation of adrenal medullary tissue to striatum in parkinsonism. First clinical trials. *J Neurosurg* 62(2), pp. 169-173. doi: 10.3171/jns.1985.62.2.0169

Ball, N., Teo, W.-P., Chandra, S. and Chapman, J. 2019. Parkinson's disease and the environment. *Frontiers in neurology* 10, p. 218.

Barbeau, A., Mars, H., Botez, M. I. and Joubert, M. 1972. Levodopa combined with peripheral decarboxylase inhibition in Parkinson's disease. *Can Med Assoc J* 106(11), pp. 1169-1174.

Barker, R. A., Drouin-Ouellet, J. and Parmar, M. 2015. Cell-based therapies for Parkinson disease—past insights and future potential. *Nature Reviews Neurology* 11(9), pp. 492-503. doi: 10.1038/nrneurol.2015.123

Barker, R. A. et al. 2019. Designing stem-cell-based dopamine cell replacement trials for Parkinson's disease. *Nature Medicine* 25(7), pp. 1045-1053. doi: 10.1038/s41591-019-0507-2

Barker, R. A., Parmar, M., Studer, L. and Takahashi, J. 2017. Human Trials of Stem Cell-Derived Dopamine Neurons for Parkinson's Disease: Dawn of a New Era. *Cell stem cell* 21(5), pp. 569-573. doi: 10.1016/j.stem.2017.09.014

Barnéoud, P., Descombris, E., Aubin, N. and Abrous, D. N. 2000. Evaluation of simple and complex sensorimotor behaviours in rats with a partial lesion of the dopaminergic nigrostriatal system. *European Journal of Neuroscience* 12(1), pp. 322-336.

Bartholini, G., Kuruma, I. and Pletscher, A. 1970. Distribution and metabolism of L-3-O-methyldopa in rats. *Br J Pharmacol* 40(3), pp. 461-467. doi: 10.1111/j.1476-5381.1970.tb10627.x

Basma, A. N., Morris, E. J., Nicklas, W. J. and Geller, H. M. 1995. L-dopa cytotoxicity to PC12 cells in culture is via its autoxidation. *J Neurochem* 64(2), pp. 825-832. doi: 10.1046/j.1471-4159.1995.64020825.x

Bastide, M. F. et al. 2015. Pathophysiology of L-dopa-induced motor and non-motor complications in Parkinson's disease. *Prog Neurobiol* 132, pp. 96-168. doi: 10.1016/j.pneurobio.2015.07.002

Benabid, A. L. 2003. Deep brain stimulation for Parkinson's disease. *Curr Opin Neurobiol* 13(6), pp. 696-706. doi: 10.1016/j.conb.2003.11.001

Berg, D. et al. 2014. Time to redefine PD? Introductory statement of the MDS Task Force on the definition of Parkinson's disease. *Movement Disorders* 29(4), pp. 454-462.

Berthet, A., Porras, G., Doudnikoff, E., Stark, H., Cador, M., Bezard, E. and Bloch, B. 2009. Pharmacological analysis demonstrates dramatic alteration of D1 dopamine receptor neuronal distribution in the rat analog of L-DOPA-induced dyskinesia. *The Journal of neuroscience : the official journal of the Society for Neuroscience* 29(15), pp. 4829-4835. doi: 10.1523/jneurosci.5884-08.2009

Birkmayer, W. and Hornykiewicz, O. 2001. The effect of l-3,4-dihydroxyphenylalanine (= DOPA) on akinesia in parkinsonism. 1961. *Wien Klin Wochenschr* 113(22), pp. 851-854.

Björklund, A. and Stenevi, U. 1979. Reconstruction of the nigrostriatal dopamine pathway by intracerebral nigral transplants. *Brain Res* 177(3), pp. 555-560. doi: 10.1016/0006-8993(79)90472-4

Blunt, S. B., Jenner, P. and Marsden, C. D. 1991. The effect of L-dopa and carbidopa treatment on the survival of rat fetal dopamine grafts assessed by tyrosine hydroxylase immunohistochemistry and [3H]mazindol autoradiography. *Neuroscience* 43(1), pp. 95-110. doi: 10.1016/0306-4522(91)90420-s

Blunt, S. B., Jenner, P. and Marsden, C. D. 1992. Motor function, graft survival and gliosis in rats with 6-OHDA lesions and foetal ventral mesencephalic grafts chronically treated with L-dopa and carbidopa. *Exp Brain Res* 88(2), pp. 326-340. doi: 10.1007/bf02259108

Blunt, S. B., Jenner, P. and Marsden, C. D. 1993. Suppressive effect of L-dopa on dopamine cells remaining in the ventral tegmental area of rats previously exposed to the neurotoxin 6-hydroxydopamine. *Movement disorders : official journal of the Movement Disorder Society* 8(2), pp. 129-133. doi: 10.1002/mds.870080202

Boer, G. J. 1994. Ethical guidelines for the use of human embryonic or fetal tissue for experimental and clinical neurotransplantation and research. Network of European CNS Transplantation and Restoration (NECTAR). *J Neurol* 242(1), pp. 1-13. doi: 10.1007/bf00920568

Bohnen, N. I. et al. 2013. Gait speed in Parkinson disease correlates with cholinergic degeneration. *Neurology* 81(18), pp. 1611-1616. doi: 10.1212/WNL.0b013e3182a9f558

Bohnen, N. I., Müller, M. L., Koeppe, R. A., Studenski, S. A., Kilbourn, M. A., Frey, K. A. and Albin, R. L. 2009. History of falls in Parkinson disease is associated with reduced cholinergic activity. *Neurology* 73(20), pp. 1670-1676. doi: 10.1212/WNL.0b013e3181c1ded6

Bonifati, V. et al. 2002. Autosomal recessive early onset parkinsonism is linked to three loci: PARK2, PARK6, and PARK7. *Neurological Sciences* 23(2), pp. s59-s60.

Bonifati, V. et al. 2003. Mutations in the DJ-1 gene associated with autosomal recessive early-onset parkinsonism. *Science* 299(5604), pp. 256-259. doi: 10.1126/science.1077209

Bonuccelli, U., Del Dotto, P. and Rascol, O. 2009. Role of dopamine receptor agonists in the treatment of early Parkinson's disease. *Parkinsonism Relat Disord* 15 Suppl 4, pp. S44-53. doi: 10.1016/s1353-8020(09)70835-1

Booth, H. D. E., Hirst, W. D. and Wade-Martins, R. 2017. The Role of Astrocyte Dysfunction in Parkinson's Disease Pathogenesis. *Trends Neurosci* 40(6), pp. 358-370. doi: 10.1016/j.tins.2017.04.001

Borges, N. 2003. Tolcapone-related liver dysfunction: implications for use in Parkinson's disease therapy. *Drug Saf* 26(11), pp. 743-747. doi: 10.2165/00002018-200326110-00001

Bose, A. and Beal, M. F. 2016. Mitochondrial dysfunction in Parkinson's disease. *Journal of neurochemistry* 139, pp. 216-231.

Braak, H., Del Tredici, K., Rüb, U., De Vos, R. A., Steur, E. N. J. and Braak, E. 2003. Staging of brain pathology related to sporadic Parkinson's disease. *Neurobiology of aging* 24(2), pp. 197-211.

Bravo, E. et al. 2011. High fat diet-induced non alcoholic fatty liver disease in rats is associated

with hyperhomocysteinemia caused by down regulation of the transsulphuration pathway. *Lipids Health Dis* 10, p. 60. doi: 10.1186/1476-511x-10-60

Breger, L. S., Kienle, K., Smith, G. A., Dunnett, S. B. and Lane, E. L. 2017. Influence of chronic L-DOPA treatment on immune response following allogeneic and xenogeneic graft in a rat model of Parkinson's disease. *Brain, behavior, and immunity* 61, pp. 155-164. doi: 10.1016/j.bbi.2016.11.014

Breit, S., Schulz, J. B. and Benabid, A.-L. 2004. Deep brain stimulation. *Cell and tissue research* 318(1), pp. 275-288.

Brochard, V. et al. 2009. Infiltration of CD4+ lymphocytes into the brain contributes to neurodegeneration in a mouse model of Parkinson disease. *J Clin Invest* 119(1), pp. 182-192. doi: 10.1172/jci36470

Brooks, D. J. 2008. Optimizing levodopa therapy for Parkinson's disease with levodopa/carbidopa/entacapone: implications from a clinical and patient perspective. *Neuropsychiatric disease and treatment* 4(1), pp. 39-47. doi: 10.2147/ndt.s1660

Bruet, N., Windels, F., Bertrand, A., Feuerstein, C., Poupard, A. and Savasta, M. 2001. High frequency stimulation of the subthalamic nucleus increases the extracellular contents of striatal dopamine in normal and partially dopaminergic denervated rats. *J Neuropathol Exp Neurol* 60(1), pp. 15-24. doi: 10.1093/jnen/60.1.15

Brundin, P., Barker, R. A. and Parmar, M. 2010. Neural grafting in Parkinson's disease Problems and possibilities. *Prog Brain Res* 184, pp. 265-294. doi: 10.1016/s0079-6123(10)84014-2

Brundin, P., Li, J.-Y., Holton, J. L., Lindvall, O. and Revesz, T. 2008. Research in motion: the enigma of Parkinson's disease pathology spread. *Nature Reviews Neuroscience* 9(10), pp. 741-745.

Bylicky, M. A., Mueller, G. P. and Day, R. M. 2018. Mechanisms of Endogenous Neuroprotective Effects of Astrocytes in Brain Injury. *Oxid Med Cell Longev* 2018, p. 6501031. doi: 10.1155/2018/6501031

Caggiu, E., Arru, G., Hosseini, S., Niegowska, M., Sechi, G., Zarbo, I. R. and Sechi, L. A. 2019. Inflammation, infectious triggers, and Parkinson's disease. *Frontiers in neurology* 10, p. 122.

Calabresi, P., Picconi, B., Tozzi, A., Ghiglieri, V. and Di Filippo, M. 2014. Direct and indirect pathways of basal ganglia: a critical reappraisal. *Nature neuroscience* 17(8), pp. 1022-1030.

Cardoso, T. et al. 2018. Target-specific forebrain projections and appropriate synaptic inputs of hESC-derived dopamine neurons grafted to the midbrain of parkinsonian rats. *J Comp Neurol* 526(13), pp. 2133-2146. doi: 10.1002/cne.24500

Carman, L. S., Gage, F. H. and Shults, C. W. 1991. Partial lesion of the substantia nigra: relation between extent of lesion and rotational behavior. *Brain Res* 553(2), pp. 275-283. doi: 10.1016/0006-8993(91)90835-j

Carta, M., Carlsson, T., Kirik, D. and Björklund, A. 2007. Dopamine released from 5-HT terminals is the cause of L-DOPA-induced dyskinesia in parkinsonian rats. *Brain* 130(Pt 7), pp. 1819-1833. doi: 10.1093/brain/awm082

Cazorla, M., Kang, U. J. and Kellendonk, C. 2015. Balancing the basal ganglia circuitry: a possible new role for dopamine D2 receptors in health and disease. *Movement disorders : official journal of the Movement Disorder Society* 30(7), pp. 895-903. doi: 10.1002/mds.26282

Chaudhuri, K. R., Healy, D. G. and Schapira, A. H. 2006. Non-motor symptoms of Parkinson's disease: diagnosis and management. *Lancet Neurol* 5(3), pp. 235-245. doi: 10.1016/s1474-4422(06)70373-8

Chen, L., Xie, Z., Turkson, S. and Zhuang, X. 2015. A53T human α-synuclein overexpression in transgenic mice induces pervasive mitochondria macroautophagy defects preceding dopamine neuron degeneration. *The Journal of neuroscience : the official journal of the Society for Neuroscience* 35(3), pp. 890-905. doi: 10.1523/JNEUROSCI.0089-14.2015

Cheng, F., Vivacqua, G. and Yu, S. 2011. The role of alpha-synuclein in neurotransmission and synaptic plasticity. *Journal of chemical neuroanatomy* 42(4), pp. 242-248.

Cheng, N.-n. et al. 1996. Differential neurotoxicity induced by l-DOPA and dopamine in cultured striatal neurons. *Brain Research* 743(1), pp. 278-283. doi: https://doi.org/10.1016/S0006-8993(96)01056-6

Chodobski, A., Zink, B. J. and Szmydynger-Chodobska, J. 2011. Blood–Brain Barrier Pathophysiology in Traumatic Brain Injury. *Translational Stroke Research* 2(4), pp. 492-516. doi: 10.1007/s12975-011-0125-x

Christians, U., Klawitter, J., Klawitter, J., Brunner, N. and Schmitz, V. 2011. Biomarkers of immunosuppressant organ toxicity after transplantation: status, concepts and misconceptions. *Expert Opin Drug Metab Toxicol* 7(2), pp. 175-200. doi: 10.1517/17425255.2011.544249

Chung, K. K. K. et al. 2001. Parkin ubiquitinates the α-synuclein–interacting protein, synphilin-1: implications for Lewy-body formation in Parkinson disease. *Nature Medicine* 7(10), pp. 1144-1150. doi: 10.1038/nm1001-1144

Coblentz, J. et al. 2020. The effect of different cyclosporine A doses in a 20-week animal model of uveal melanoma. *Investigative Ophthalmology & Visual Science* 61(7), pp. 3613-3613.

Dai, H., Wang, W., Tang, X., Chen, R., Chen, Z., Lu, Y. and Yuan, H. 2016. Association between

homocysteine and non-alcoholic fatty liver disease in Chinese adults: a cross-sectional study. *Nutr J* 15(1), p. 102. doi: 10.1186/s12937-016-0221-6

Daly, D., Miller, J. W., Nadeau, M. R. and Selhub, J. 1997. The effect of L-dopa administration and folate deficiency on plasma homocysteine concentrations in rats. *The Journal of Nutritional Biochemistry* 8(11), pp. 634-640.

Darmopil, S., Martín, A. B., De Diego, I. R., Ares, S. and Moratalla, R. 2009. Genetic Inactivation of Dopamine D1 but Not D2 Receptors Inhibits L-DOPA–Induced Dyskinesia and Histone Activation. *Biological Psychiatry* 66(6), pp. 603-613. doi: https://doi.org/10.1016/j.biopsych.2009.04.025

Datla, K. P., Blunt, S. B. and Dexter, D. T. 2001. Chronic L-DOPA administration is not toxic to the remaining dopaminergic nigrostriatal neurons, but instead may promote their functional recovery, in rats with partial 6-OHDA or FeCl(3) nigrostriatal lesions. *Movement disorders : official journal of the Movement Disorder Society* 16(3), pp. 424-434. doi: 10.1002/mds.1091

Dauer, W. and Przedborski, S. 2003. Parkinson's disease: mechanisms and models. *Neuron* 39(6), pp. 889-909.

Davies, P., Moualla, D. and Brown, D. R. 2011. Alpha-synuclein is a cellular ferrireductase. *PloS one* 6(1), pp. e15814-e15814. doi: 10.1371/journal.pone.0015814

de Souza Pagnussat, A., Michaelsen, S. M., Achaval, M. and Netto, C. A. 2009. Skilled forelimb reaching in Wistar rats: evaluation by means of Montoya staircase test. *Journal of Neuroscience Methods* 177(1), pp. 115-121.

Decressac, M. and Björklund, A. 2013. mTOR inhibition alleviates L-DOPA-induced dyskinesia in parkinsonian rats. *J Parkinsons Dis* 3(1), pp. 13-17. doi: 10.3233/jpd-120155

Decressac, M., Kadkhodaei, B., Mattsson, B., Laguna, A., Perlmann, T. and Björklund, A. 2012. α-Synuclein-induced down-regulation of Nurr1 disrupts GDNF signaling in nigral dopamine neurons. *Sci Transl Med* 4(163), p. 163ra156. doi: 10.1126/scitranslmed.3004676

Decressac, M., Ulusoy, A., Mattsson, B., Georgievska, B., Romero-Ramos, M., Kirik, D. and Björklund, A. 2011. GDNF fails to exert neuroprotection in a rat α-synuclein model of Parkinson's disease. *Brain* 134(Pt 8), pp. 2302-2311. doi: 10.1093/brain/awr149

Decressac, M., Volakakis, N., Björklund, A. and Perlmann, T. 2013. NURR1 in Parkinson disease—from pathogenesis to therapeutic potential. *Nature Reviews Neurology* 9(11), pp. 629-636. doi: 10.1038/nrneurol.2013.209

Deffains, M., Canron, M. H., Teil, M., Li, Q., Dehay, B., Bezard, E. and Fernagut, P. o. 2021. L-DOPA regulates α-synuclein accumulation in experimental parkinsonism. *Neuropathology and Applied Neurobiology* 47(4), pp. 532-543.

Dehay, B. and Fernagut, P.-O. 2016. Alpha-synuclein-based models of Parkinson's disease. *Revue neurologique* 172(6-7), pp. 371-378.

Deumens, R., Blokland, A. and Prickaerts, J. 2002. Modeling Parkinson's Disease in Rats: An Evaluation of 6-OHDA Lesions of the Nigrostriatal Pathway. *Experimental Neurology* 175(2), pp. 303-317. doi: https://doi.org/10.1006/exnr.2002.7891

Dexter, D. T. et al. 1989. Basal lipid peroxidation in substantia nigra is increased in Parkinson's disease. *J Neurochem* 52(2), pp. 381-389. doi: 10.1111/j.1471-4159.1989.tb09133.x

Di Paolo, T., Bourque, M. and Snodgrass, R. eds. 2020. *4-Chlorokynurenine inhibits L-Dopa-induced dyskinesias in non-human parkinsonian primates*. *Movement Disorders.* WILEY 111 RIVER ST, HOBOKEN 07030-5774, NJ USA.

Diehl, R., Ferrara, F., Müller, C., Dreyer, A. Y., McLeod, D. D., Fricke, S. and Boltze, J. 2017. Immunosuppression for in vivo research: state-of-the-art protocols and experimental approaches. *Cellular & molecular immunology* 14(2), pp. 146-179. doi: 10.1038/cmi.2016.39

Dorsey, E. R. et al. 2018. Global, regional, and national burden of Parkinson's disease, 1990–2016: a systematic analysis for the Global Burden of Disease Study 2016. *The Lancet Neurology* 17(11), pp. 939-953.

Dringen, R., Gutterer, J. M. and Hirrlinger, J. 2000. Glutathione metabolism in brain metabolic interaction between astrocytes and neurons in the defense against reactive oxygen species. *Eur J Biochem* 267(16), pp. 4912-4916. doi: 10.1046/j.1432-1327.2000.01597.x

Duffy, M. F., Collier, T. J., Patterson, J. R., Kemp, C. J., Fischer, D. L., Stoll, A. C. and Sortwell, C. E. 2018. Quality Over Quantity: Advantages of Using Alpha-Synuclein Preformed Fibril Triggered Synucleinopathy to Model Idiopathic Parkinson's Disease. *Frontiers in Neuroscience* 12, doi: 10.3389/fnins.2018.00621

Dutra, M. F., Jaeger, M., Ilha, J., Kalil-Gaspar, P. I., Marcuzzo, S. and Achaval, M. 2012. Exercise improves motor deficits and alters striatal GFAP expression in a 6-OHDA-induced rat model of Parkinson's disease. *Neurol Sci* 33(5), pp. 1137-1144. doi: 10.1007/s10072-011-0925-5

Dziewczapolski, G., Murer, G., Agid, Y., Gershanik, O. and Raisman-Vozari, R. 1997. Absence of neurotoxicity of chronic L-DOPA in 6-hydroxydopamine-lesioned rats. *Neuroreport* 8(4), pp. 975-979. doi: 10.1097/00001756-199703030-00031

Elabi, O. 2017. *The effect of L-dopa and neuroprotective agents on cell replacement therapy for Parkinson's disease.* Cardiff University.

Emdadul Haque, M., Asanuma, M., Higashi, Y., Miyazaki, I., Tanaka, K.-i. and Ogawa, N. 2003.

Apoptosis-inducing neurotoxicity of dopamine and its metabolites via reactive quinone generation in neuroblastoma cells. *Biochimica et Biophysica Acta (BBA) - General Subjects* 1619(1), pp. 39-52. doi: https://doi.org/10.1016/S0304-4165(02)00440-3

Encarnacion, E. V. and Hauser, R. A. 2008. Levodopa-induced dyskinesias in Parkinson's disease: etiology, impact on quality of life, and treatments. *Eur Neurol* 60(2), pp. 57-66. doi: 10.1159/000131893

Engelender, S. et al. 1999. Synphilin-1 associates with α-synuclein and promotes the formation of cytosolic inclusions. *Nature Genetics* 22(1), pp. 110-114. doi: 10.1038/8820

Espay, A. J. et al. 2018. Levodopa-induced dyskinesia in Parkinson disease: Current and evolving concepts. *Ann Neurol* 84(6), pp. 797-811. doi: 10.1002/ana.25364

Evans, M. J. and Kaufman, M. H. 1981. Establishment in culture of pluripotential cells from mouse embryos. *Nature* 292(5819), pp. 154-156. doi: 10.1038/292154a0

Fahn, S. et al. 2004. Levodopa and the progression of Parkinson's disease. *N Engl J Med* 351(24), pp. 2498-2508. doi: 10.1056/NEJMoa033447

Fan, Y., Chen, Z., Pathak, J. L., Carneiro, A. M. D. and Chung, C. Y. 2018. Differential Regulation of Adhesion and Phagocytosis of Resting and Activated Microglia by Dopamine. *Front Cell Neurosci* 12, p. 309. doi: 10.3389/fncel.2018.00309

Fenyi, A., Coens, A., Bellande, T., Melki, R. and Bousset, L. 2018. Assessment of the efficacy of different procedures that remove and disassemble alpha-synuclein, tau and A-beta fibrils from laboratory material and surfaces. *Sci Rep* 8(1), p. 10788. doi: 10.1038/s41598-018-28856-2

Fereshtehnejad, S.-M., Zeighami, Y., Dagher, A. and Postuma, R. B. 2017. Clinical criteria for subtyping Parkinson's disease: biomarkers and longitudinal progression. *Brain* 140(7), pp. 1959-1976. doi: 10.1093/brain/awx118

Fernandez-Fernandez, S., Almeida, A. and Bolaños, J. P. 2012. Antioxidant and bioenergetic coupling between neurons and astrocytes. *Biochem J* 443(1), pp. 3-11. doi: 10.1042/bj20111943

Ferrario, J. E. et al. 2003. Effects of orally administered levodopa on mesencephalic dopaminergic neurons undergoing a degenerative process. *Neurosci Res* 47(4), pp. 431-436. doi: 10.1016/j.neures.2003.08.001

Ferreira, S. A. and Romero-Ramos, M. 2018. Microglia Response During Parkinson's Disease: Alpha-Synuclein Intervention. *Front Cell Neurosci* 12, p. 247. doi: 10.3389/fncel.2018.00247

Figge, D. A., Eskow Jaunarajs, K. L. and Standaert, D. G. 2016. Dynamic DNA Methylation Regulates Levodopa-Induced Dyskinesia. *The Journal of neuroscience : the official journal of the Society for*

Neuroscience 36(24), pp. 6514-6524. doi: 10.1523/jneurosci.0683-16.2016

Forno, L. S. 1981. Pathology of Parkinson's disease.*Movement Disorders*. Elsevier, pp. 25-40.

Fox, S. H. et al. 2011. The Movement Disorder Society Evidence-Based Medicine Review Update: Treatments for the motor symptoms of Parkinson's disease. *Movement disorders : official journal of the Movement Disorder Society* 26 Suppl 3, pp. S2-41. doi: 10.1002/mds.23829

Freed, C. R. et al. 2001. Transplantation of embryonic dopamine neurons for severe Parkinson's disease. *N Engl J Med* 344(10), pp. 710-719. doi: 10.1056/nejm200103083441002

Funayama, M. et al. 2015. CHCHD2 mutations in autosomal dominant late-onset Parkinson's disease: a genome-wide linkage and sequencing study. *Lancet Neurol* 14(3), pp. 274-282. doi: 10.1016/s1474-4422(14)70266-2

Garitaonandia, I. et al. eds. 2012. *The Application of A9 Dopaminergic Neurons Derived from Human Parthenogenetic Stem Cells for the Treatment of Parkinson's Disease*. *MOLECULAR THERAPY.* NATURE PUBLISHING GROUP 75 VARICK ST, 9TH FLR, NEW YORK, NY 10013-1917 USA.

Gerfen, C. R. and Surmeier, D. J. 2011. Modulation of striatal projection systems by dopamine. *Annual review of neuroscience* 34, pp. 441-466.

Gerhard, A. et al. 2006. In vivo imaging of microglial activation with [11C](R)-PK11195 PET in idiopathic Parkinson's disease. *Neurobiol Dis* 21(2), pp. 404-412. doi: 10.1016/j.nbd.2005.08.002

Giannopoulos, S., Samardzic, K., Raymond, B. B. A., Djordjevic, S. P. and Rodgers, K. J. 2019. L-DOPA causes mitochondrial dysfunction in vitro: A novel mechanism of L-DOPA toxicity uncovered. *The International Journal of Biochemistry & Cell Biology* 117, p. 105624. doi: https://doi.org/10.1016/j.biocel.2019.105624

Giguère, N., Burke Nanni, S. and Trudeau, L.-E. 2018. On cell loss and selective vulnerability of neuronal populations in Parkinson's disease. *Frontiers in neurology*, p. 455.

Gijtenbeek, J. M., van den Bent, M. J. and Vecht, C. J. 1999. Cyclosporine neurotoxicity: a review. *J Neurol* 246(5), pp. 339-346. doi: 10.1007/s004150050360

Glinka, Y., Gassen, M. and Youdim, M. 1997. Mechanism of 6-hydroxydopamine neurotoxicity. *Advances in Research on Neurodegeneration*, pp. 55-66.

Godwin-Austen, R. B., Frears, C. C., Tomlinson, E. B. and Kok, H. W. L. 1969. EFFECTS OF L-DOPA IN PARKINSON'S DISEASE. *The Lancet* 294(7613), pp. 165-168. doi: https://doi.org/10.1016/S0140-6736(69)91417-2

Goetz, C. G. et al. 2008. Movement Disorder Society-sponsored revision of the Unified Parkinson's Disease Rating Scale (MDS-UPDRS): scale presentation and clinimetric testing results. *Movement disorders : official journal of the Movement Disorder Society* 23(15), pp. 2129-2170. doi: 10.1002/mds.22340

Grace, A. A. 1995. The tonic/phasic model of dopamine system regulation: its relevance for understanding how stimulant abuse can alter basal ganglia function. *Drug Alcohol Depend* 37(2), pp. 111-129. doi: 10.1016/0376-8716(94)01066-t

Graham, R. M. 1994. Cyclosporine: mechanisms of action and toxicity. *Cleve Clin J Med* 61(4), pp. 308-313. doi: 10.3949/ccjm.61.4.308

Grandas, F., Galiano, M. L. and Tabernero, C. 1999. Risk factors for levodopa-induced dyskinesias in Parkinson's disease. *J Neurol* 246(12), pp. 1127-1133. doi: 10.1007/s004150050530

Gray, M. T. and Woulfe, J. M. 2015. Striatal blood-brain barrier permeability in Parkinson's disease. *J Cereb Blood Flow Metab* 35(5), pp. 747-750. doi: 10.1038/jcbfm.2015.32

Gray, R. et al. 2014. Long-term effectiveness of dopamine agonists and monoamine oxidase B inhibitors compared with levodopa as initial treatment for Parkinson's disease (PD MED): a large, open-label, pragmatic randomised trial. *Lancet* 384(9949), pp. 1196-1205. doi: 10.1016/s0140-6736(14)60683-8

Grealish, S. et al. 2014. Human ESC-derived dopamine neurons show similar preclinical efficacy and potency to fetal neurons when grafted in a rat model of Parkinson's disease. *Cell stem cell* 15(5), pp. 653-665. doi: 10.1016/j.stem.2014.09.017

Grealish, S., Jönsson, M. E., Li, M., Kirik, D., Björklund, A. and Thompson, L. H. 2010. The A9 dopamine neuron component in grafts of ventral mesencephalon is an important determinant for recovery of motor function in a rat model of Parkinson's disease. *Brain* 133(Pt 2), pp. 482-495. doi: 10.1093/brain/awp328

Grenn, F. P. et al. 2020. The Parkinson's Disease Genome-Wide Association Study Locus Browser. *Movement disorders : official journal of the Movement Disorder Society* 35(11), pp. 2056-2067. doi: 10.1002/mds.28197

Hameed, A., Hruban, R. H., Gage, W., Pettis, G. and Fox, W. M., 3rd. 1994. Immunohistochemical expression of CD68 antigen in human peripheral blood T cells. *Hum Pathol* 25(9), pp. 872-876. doi: 10.1016/0046-8177(94)90005-1

Han, S. K., Mytilineou, C. and Cohen, G. 1996. L-DOPA up-regulates glutathione and protects mesencephalic cultures against oxidative stress. *J Neurochem* 66(2), pp. 501-510. doi: 10.1046/j.1471-4159.1996.66020501.x

Harms, A. S. et al. 2017. α-Synuclein fibrils recruit peripheral immune cells in the rat brain prior to neurodegeneration. *Acta neuropathologica communications* 5(1), pp. 85-85. doi: 10.1186/s40478-017-0494-9

Harris, M. G. et al. 2014. Immune privilege of the CNS is not the consequence of limited antigen sampling. *Scientific Reports* 4(1), p. 4422. doi: 10.1038/srep04422

Hartig, S. M. 2013. Basic image analysis and manipulation in ImageJ. *Current protocols in molecular biology* 102(1), pp. 14.15. 11-14.15. 12.

Hauser, R. A., Koller, W. C., Hubble, J. P., Malapira, T., Busenbark, K. and Olanow, C. W. 2000. Time course of loss of clinical benefit following withdrawal of levodopa/carbidopa and bromocriptine in early Parkinson's disease. *Movement disorders : official journal of the Movement Disorder Society* 15(3), pp. 485-489. doi: 10.1002/1531-8257(200005)15:3<485::Aid-mds1010>3.0.Co;2-f

Hawkes, C. H., Del Tredici, K. and Braak, H. 2010. A timeline for Parkinson's disease. *Parkinsonism & related disorders* 16(2), pp. 79-84.

Hegarty, S. V., O'Keeffe, G. W. and Sullivan, A. M. 2014. Neurotrophic factors: from neurodevelopmental regulators to novel therapies for Parkinson's disease. *Neural regeneration research* 9(19), pp. 1708-1711. doi: 10.4103/1673-5374.143410

Hegarty, S. V., Sullivan, A. M. and O'Keeffe, G. W. 2013. Midbrain dopaminergic neurons: A review of the molecular circuitry that regulates their development. *Developmental Biology* 379(2), pp. 123-138. doi: https://doi.org/10.1016/j.ydbio.2013.04.014

Heuer, A., Kirkeby, A., Pfisterer, U., Jönsson, M. E. and Parmar, M. 2016. hESC-derived neural progenitors prevent xenograft rejection through neonatal desensitisation. *Exp Neurol* 282, pp. 78-85. doi: 10.1016/j.expneurol.2016.05.027

Hinson, V. K., Goetz, C. G., Leurgans, S., Fan, W., Nguyen, T. and Hsu, A. 2009. Reducing dosing frequency of carbidopa/levodopa: double-blind crossover study comparing twice-daily bilayer formulation of carbidopa/levodopa (IPX054) versus 4 daily doses of standard carbidopa/levodopa in stable Parkinson disease patients. *Clin Neuropharmacol* 32(4), pp. 189-192. doi: 10.1097/WNF.0b013e3181a27fae

Hirsch, E. C., Graybiel, A. M., Duyckaerts, C. and Javoy-Agid, F. 1987. Neuronal loss in the pedunculopontine tegmental nucleus in Parkinson disease and in progressive supranuclear palsy. *Proc Natl Acad Sci U S A* 84(16), pp. 5976-5980. doi: 10.1073/pnas.84.16.5976

Hoban, D. B. et al. 2020. Impact of α-synuclein pathology on transplanted hESC-derived dopaminergic neurons in a humanized α-synuclein rat model of PD. *Proceedings of the National Academy of Sciences* 117(26), pp. 15209-15220.

Holloway, R. G. et al. 2004. Pramipexole vs levodopa as initial treatment for Parkinson disease: a 4-year randomized controlled trial. *Arch Neurol* 61(7), pp. 1044-1053. doi: 10.1001/archneur.61.7.1044

Houser, M. C. and Tansey, M. G. 2017. The gut-brain axis: is intestinal inflammation a silent driver of Parkinson's disease pathogenesis? *NPJ Parkinson's disease* 3(1), pp. 1-9.

Huot, P., Kang, W., Kim, E., Bédard, D., Belliveau, S., Frouni, I. and Kwan, C. 2022. Levodopa-induced dyskinesia: a brief review of the ongoing clinical trials. *Neurodegener Dis Manag* 12(2), pp. 51-55. doi: 10.2217/nmt-2021-0051

Hynes, M., Poulsen, K., Tessier-Lavigne, M. and Rosenthal, A. 1995. Control of neuronal diversity by the floor plate: contact-mediated induction of midbrain dopaminergic neurons. *Cell* 80(1), pp. 95-101. doi: 10.1016/0092-8674(95)90454-9

Iannuzzelli, K. et al. 2020. Gender Differences in Distribution of Lewy Body Pathology in Individuals with Parkinson's Disease (4664). AAN Enterprises.

Imamura, K., Hishikawa, N., Sawada, M., Nagatsu, T., Yoshida, M. and Hashizume, Y. 2003. Distribution of major histocompatibility complex class II-positive microglia and cytokine profile of Parkinson's disease brains. *Acta Neuropathol* 106(6), pp. 518-526. doi: 10.1007/s00401-003-0766-2

Isacson, O. and Kordower, J. H. 2008. Future of cell and gene therapies for Parkinson's disease. *Ann Neurol* 64 Suppl 2(0 2), pp. S122-138. doi: 10.1002/ana.21473

Ishii, T. and Eto, K. 2014. Fetal stem cell transplantation: Past, present, and future. *World J Stem Cells* 6(4), pp. 404-420. doi: 10.4252/wjsc.v6.i4.404

Ishizu, N. et al. 2016. Impaired striatal dopamine release in homozygous Vps35 D620N knock-in mice. *Hum Mol Genet* 25(20), pp. 4507-4517. doi: 10.1093/hmg/ddw279

Ito, D., Amano, T., Sato, H. and Fukuuchi, Y. 2001. Paroxysmal hypertensive crises induced by selegiline in a patient with Parkinson's disease. *J Neurol* 248(6), pp. 533-534. doi: 10.1007/s004150170168

Iwata-Ichikawa, E., Kondo, Y., Miyazaki, I., Asanuma, M. and Ogawa, N. 1999. Glial cells protect neurons against oxidative stress via transcriptional up-regulation of the glutathione synthesis. *J Neurochem* 72(6), pp. 2334-2344. doi: 10.1046/j.1471-4159.1999.0722334.x

Jankovic, J. 2008. Parkinson's disease: clinical features and diagnosis. *Journal of neurology, neurosurgery & psychiatry* 79(4), pp. 368-376.

Jenner, P. 2004. Avoidance of dyskinesia: preclinical evidence for continuous dopaminergic

stimulation. *Neurology* 62(1 Suppl 1), pp. S47-55. doi: 10.1212/wnl.62.1_suppl_1.s47

Jenner, P. 2008. Molecular mechanisms of L-DOPA-induced dyskinesia. *Nature Reviews Neuroscience* 9(9), pp. 665-677. doi: 10.1038/nrn2471

Jonas, R. A., Yuan, T. F., Liang, Y. X., Jonas, J. B., Tay, D. K. and Ellis-Behnke, R. G. 2012. The spider effect: morphological and orienting classification of microglia in response to stimuli in vivo. *PloS one* 7(2), p. e30763. doi: 10.1371/journal.pone.0030763

Joshi, N. and Singh, S. 2018. Updates on immunity and inflammation in Parkinson disease pathology. *J Neurosci Res* 96(3), pp. 379-390. doi: 10.1002/jnr.24185

Jowaed, A., Schmitt, I., Kaut, O. and Wüllner, U. 2010. Methylation regulates alpha-synuclein expression and is decreased in Parkinson's disease patients' brains. *The Journal of neuroscience : the official journal of the Society for Neuroscience* 30(18), pp. 6355-6359. doi: 10.1523/jneurosci.6119-09.2010

Jurga, A. M., Paleczna, M., Kadluczka, J. and Kuter, K. Z. 2021. Beyond the GFAP-Astrocyte Protein Markers in the Brain. *Biomolecules* 11(9), doi: 10.3390/biom11091361

Kaplitt, M. G. et al. 2007. Safety and tolerability of gene therapy with an adeno-associated virus (AAV) borne GAD gene for Parkinson's disease: an open label, phase I trial. *Lancet* 369(9579), pp. 2097-2105. doi: 10.1016/s0140-6736(07)60982-9

Karachi, C. et al. 2010. Cholinergic mesencephalic neurons are involved in gait and postural disorders in Parkinson disease. *J Clin Invest* 120(8), pp. 2745-2754. doi: 10.1172/jci42642

Karschin, C., Dissmann, E., Stühmer, W. and Karschin, A. 1996. IRK(1-3) and GIRK(1-4) inwardly rectifying K+ channel mRNAs are differentially expressed in the adult rat brain. *The Journal of neuroscience : the official journal of the Society for Neuroscience* 16(11), pp. 3559-3570. doi: 10.1523/jneurosci.16-11-03559.1996

Kasten, M. and Klein, C. 2013. The many faces of alpha-synuclein mutations. *Movement disorders : official journal of the Movement Disorder Society* 28(6), pp. 697-701. doi: 10.1002/mds.25499

Katzenschlager, R., Head, J., Schrag, A., Ben-Shlomo, Y., Evans, A. and Lees, A. J. 2008. Fourteen-year final report of the randomized PDRG-UK trial comparing three initial treatments in PD. *Neurology* 71(7), pp. 474-480. doi: 10.1212/01.wnl.0000310812.43352.66

Kefalopoulou, Z. et al. 2014. Long-term clinical outcome of fetal cell transplantation for Parkinson disease: two case reports. *JAMA Neurol* 71(1), pp. 83-87. doi: 10.1001/jamaneurol.2013.4749

Kelly, C. M. et al. 2009. Neonatal desensitization allows long-term survival of neural xenotransplants without immunosuppression. *Nat Methods* 6(4), pp. 271-273. doi:

10.1038/nmeth.1308

Kikuchi, T. et al. 2017. Human iPS cell-derived dopaminergic neurons function in a primate Parkinson's disease model. *Nature* 548(7669), pp. 592-596. doi: 10.1038/nature23664

Kim, S., Wong, Y. C., Gao, F. and Krainc, D. 2021. Dysregulation of mitochondria-lysosome contacts by GBA1 dysfunction in dopaminergic neuronal models of Parkinson's disease. *Nature Communications* 12(1), p. 1807. doi: 10.1038/s41467-021-22113-3

Kimelberg, H. K. 2004. The problem of astrocyte identity. *Neurochem Int* 45(2-3), pp. 191-202. doi: 10.1016/j.neuint.2003.08.015

Kirik, D., Cederfjäll, E., Halliday, G. and Petersén, Å. 2017. Gene therapy for Parkinson's disease: Disease modification by GDNF family of ligands. *Neurobiol Dis* 97(Pt B), pp. 179-188. doi: 10.1016/j.nbd.2016.09.008

Kirik, D. et al. 2002. Parkinson-Like Neurodegeneration Induced by Targeted Overexpression of α-Synuclein in the Nigrostriatal System. *The Journal of Neuroscience* 22(7), pp. 2780-2791. doi: 10.1523/jneurosci.22-07-02780.2002

Kirkeby, A. et al. 2012. Generation of regionally specified neural progenitors and functional neurons from human embryonic stem cells under defined conditions. *Cell reports* 1(6), pp. 703-714.

Kirkeby, A. et al. 2017. Predictive markers guide differentiation to improve graft outcome in clinical translation of hESC-based therapy for Parkinson's disease. *Cell stem cell* 20(1), pp. 135-148.

Klein, C. and Westenberger, A. 2012. Genetics of Parkinson's disease. *Cold Spring Harbor perspectives in medicine* 2(1), pp. a008888-a008888. doi: 10.1101/cshperspect.a008888

Klein, R. L., King, M. A., Hamby, M. E. and Meyer, E. M. 2002. Dopaminergic cell loss induced by human A30P α-synuclein gene transfer to the rat substantia nigra. *Human gene therapy* 13(5), pp. 605-612.

Klein, R. L., Meyer, E. M., Peel, A. L., Zolotukhin, S., Meyers, C., Muzyczka, N. and King, M. A. 1998. Neuron-specific transduction in the rat septohippocampal or nigrostriatal pathway by recombinant adeno-associated virus vectors. *Exp Neurol* 150(2), pp. 183-194. doi: 10.1006/exnr.1997.6736

Kmieciak, M., Gowda, M., Graham, L., Godder, K., Bear, H. D., Marincola, F. M. and Manjili, M. H. 2009. Human T cells express CD25 and Foxp3 upon activation and exhibit effector/memory phenotypes without any regulatory/suppressor function. *Journal of Translational Medicine* 7(1), p. 89. doi: 10.1186/1479-5876-7-89

Kocer, B., Guven, H. and Comoglu, S. S. 2016. Homocysteine Levels in Parkinson's Disease: Is Entacapone Effective? *BioMed research international* 2016, pp. 7563705-7563705. doi: 10.1155/2016/7563705

Konnova, E. A. and Swanberg, M. 2018. Animal models of Parkinson's disease. *Exon Publications*, pp. 83-106.

Kordower, J. H., Chu, Y., Hauser, R. A., Freeman, T. B. and Olanow, C. W. 2008. Lewy body–like pathology in long-term embryonic nigral transplants in Parkinson's disease. *Nature Medicine* 14(5), pp. 504-506.

Kordower, J. H. et al. 1995. Neuropathological evidence of graft survival and striatal reinnervation after the transplantation of fetal mesencephalic tissue in a patient with Parkinson's disease. *New England Journal of Medicine* 332(17), pp. 1118-1124.

Kriks, S. et al. 2011. Dopamine neurons derived from human ES cells efficiently engraft in animal models of Parkinson's disease. *Nature* 480(7378), pp. 547-551. doi: 10.1038/nature10648

Krohn, L. et al. 2020. Comprehensive assessment of PINK1 variants in Parkinson's disease. *Neurobiology of aging* 91, pp. 168. e161-168. e165.

Krüger, R. et al. 1998. Ala30Pro mutation in the gene encoding alpha-synuclein in Parkinson's disease. *Nat Genet* 18(2), pp. 106-108. doi: 10.1038/ng0298-106

Kumar, A., Palfrey, H. A., Pathak, R., Kadowitz, P. J., Gettys, T. W. and Murthy, S. N. 2017. The metabolism and significance of homocysteine in nutrition and health. *Nutr Metab (Lond)* 14, p. 78. doi: 10.1186/s12986-017-0233-z

Kurowska, Z., Englund, E., Widner, H., Lindvall, O., Li, J. Y. and Brundin, P. 2011. Signs of degeneration in 12-22-year old grafts of mesencephalic dopamine neurons in patients with Parkinson's disease. *J Parkinsons Dis* 1(1), pp. 83-92. doi: 10.3233/jpd-2011-11004

Lane, E. L. 2019. L-DOPA for Parkinson's disease—a bittersweet pill. *European Journal of Neuroscience* 49(3), pp. 384-398.

Lane, E. L., Harrison, D. J., Ramos-Varas, E., Hills, R., Turner, S. and Lelos, M. J. 2022. Spontaneous Graft-Induced Dyskinesias Are Independent of 5-HT Neurons and Levodopa Priming in a Model of Parkinson's Disease. *Movement disorders : official journal of the Movement Disorder Society* 37(3), pp. 613-619. doi: 10.1002/mds.28856

Lashuel, H. A. 2020. Do Lewy bodies contain alpha-synuclein fibrils? and Does it matter? A brief history and critical analysis of recent reports. *Neurobiology of disease* 141, p. 104876. doi: https://doi.org/10.1016/j.nbd.2020.104876

Lee, E. S., Chen, H., King, J. and Charlton, C. 2008. The role of 3-O-methyldopa in the side effects of L-dopa. *Neurochem Res* 33(3), pp. 401-411. doi: 10.1007/s11064-007-9442-6

Levite, M., Marino, F. and Cosentino, M. 2017. Dopamine, T cells and multiple sclerosis (MS). *J Neural Transm (Vienna)* 124(5), pp. 525-542. doi: 10.1007/s00702-016-1640-4

LeWitt, P. A. 2009. Levodopa therapeutics for Parkinson's disease: new developments. *Parkinsonism & related disorders* 15, pp. S31-S34.

Li, W. et al. 2016. Extensive graft-derived dopaminergic innervation is maintained 24 years after transplantation in the degenerating parkinsonian brain. *Proc Natl Acad Sci U S A* 113(23), pp. 6544-6549. doi: 10.1073/pnas.1605245113

Licking, N. et al. 2017. Homocysteine and cognitive function in Parkinson's disease. *Parkinsonism Relat Disord* 44, pp. 1-5. doi: 10.1016/j.parkreldis.2017.08.005

Liddelow, S. A. et al. 2017. Neurotoxic reactive astrocytes are induced by activated microglia. *Nature* 541(7638), pp. 481-487. doi: 10.1038/nature21029

Lindgren, H. S. and Lane, E. L. 2011. Rodent models of L-DOPA-induced dyskinesia.*Animal Models of Movement Disorders*. Springer, pp. 337-351.

Lindvall, O. 2016. Clinical translation of stem cell transplantation in Parkinson's disease. *J Intern Med* 279(1), pp. 30-40. doi: 10.1111/joim.12415

Lindvall, O. et al. 1990. Grafts of fetal dopamine neurons survive and improve motor function in Parkinson's disease. *Science* 247(4942), pp. 574-577. doi: 10.1126/science.2105529

Lindvall, O. et al. 1989. Human fetal dopamine neurons grafted into the striatum in two patients with severe Parkinson's disease. A detailed account of methodology and a 6-month follow-up. *Arch Neurol* 46(6), pp. 615-631. doi: 10.1001/archneur.1989.00520420033021

Lindvall, O. et al. 1988. Fetal dopamine-rich mesencephalic grafts in Parkinson's disease. *Lancet* 2(8626-8627), pp. 1483-1484. doi: 10.1016/s0140-6736(88)90950-6

Lipski, J., Nistico, R., Berretta, N., Guatteo, E., Bernardi, G. and Mercuri, N. B. 2011. L-DOPA: a scapegoat for accelerated neurodegeneration in Parkinson's disease? *Progress in neurobiology* 94(4), pp. 389-407.

Liu, Z. and Cheung, H. H. 2020. Stem Cell-Based Therapies for Parkinson Disease. *Int J Mol Sci* 21(21), doi: 10.3390/ijms21218060

Lu, J., Sun, F., Ma, H., Qing, H. and Deng, Y. 2015. Comparison between α-synuclein wild-type and A53T mutation in a progressive Parkinson's disease model. *Biochem Biophys Res Commun* 464(4),

pp. 988-993. doi: 10.1016/j.bbrc.2015.07.007

Lücking, C. B. et al. 2000. Association between early-onset Parkinson's disease and mutations in the parkin gene. *New England Journal of Medicine* 342(21), pp. 1560-1567.

Luquin, M. R., Laguna, J. and Obeso, J. A. 1992. Selective D2 receptor stimulation induces dyskinesia in parkinsonian monkeys. *Ann Neurol* 31(5), pp. 551-554. doi: 10.1002/ana.410310514

Luthman, J., Fredriksson, A., Sundström, E., Jonsson, G. and Archer, T. 1989. Selective lesion of central dopamine or noradrenaline neuron systems in the neonatal rat: motor behavior and monoamine alterations at adult stage. *Behav Brain Res* 33(3), pp. 267-277. doi: 10.1016/s0166-4328(89)80121-4

Lyras, L., Zeng, B. Y., McKenzie, G., Pearce, R. K., Halliwell, B. and Jenner, P. 2002. Chronic high dose L-DOPA alone or in combination with the COMT inhibitor entacapone does not increase oxidative damage or impair the function of the nigro-striatal pathway in normal cynomologus monkeys. *J Neural Transm (Vienna)* 109(1), pp. 53-67. doi: 10.1007/s702-002-8236-2

MacMahon Copas, A. N., McComish, S. F., Fletcher, J. M. and Caldwell, M. A. 2021. The Pathogenesis of Parkinson's Disease: A Complex Interplay Between Astrocytes, Microglia, and T Lymphocytes? *Front Neurol* 12, p. 666737. doi: 10.3389/fneur.2021.666737

Maeda, T., Nagata, K., Yoshida, Y. and Kannari, K. 2005. Serotonergic hyperinnervation into the dopaminergic denervated striatum compensates for dopamine conversion from exogenously administered l-DOPA. *Brain Res* 1046(1-2), pp. 230-233. doi: 10.1016/j.brainres.2005.04.019

Mahmoud, S., Gharagozloo, M., Simard, C. and Gris, D. 2019. Astrocytes Maintain Glutamate Homeostasis in the CNS by Controlling the Balance between Glutamate Uptake and Release. *Cells* 8(2), doi: 10.3390/cells8020184

Mahul-Mellier, A. L. et al. 2020. The process of Lewy body formation, rather than simply α-synuclein fibrillization, is one of the major drivers of neurodegeneration. *Proc Natl Acad Sci U S A* 117(9), pp. 4971-4982. doi: 10.1073/pnas.1913904117

Malek, N. et al. 2019. L-dopa responsiveness in early Parkinson's disease is associated with the rate of motor progression. *Parkinsonism & related disorders* 65, pp. 55-61. doi: https://doi.org/10.1016/j.parkreldis.2019.05.022

Malek, N., Swallow, D., Grosset, K. A., Anichtchik, O., Spillantini, M. and Grosset, D. G. 2014. Alpha-synuclein in peripheral tissues and body fluids as a biomarker for Parkinson's disease - a systematic review. *Acta Neurol Scand* 130(2), pp. 59-72. doi: 10.1111/ane.12247

Marks, W. J., Jr. et al. 2010. Gene delivery of AAV2-neurturin for Parkinson's disease: a double-blind, randomised, controlled trial. *Lancet Neurol* 9(12), pp. 1164-1172. doi: 10.1016/s1474-

4422(10)70254-4

Martín-Flores, N. et al. 2019. MTOR Pathway-Based Discovery of Genetic Susceptibility to L-DOPA-Induced Dyskinesia in Parkinson's Disease Patients. *Molecular Neurobiology* 56(3), pp. 2092-2100. doi: 10.1007/s12035-018-1219-1

Masato, A., Plotegher, N., Boassa, D. and Bubacco, L. 2019. Impaired dopamine metabolism in Parkinson's disease pathogenesis. *Molecular neurodegeneration* 14(1), p. 35. doi: 10.1186/s13024-019-0332-6

Masliah, E. et al. 2000. Dopaminergic loss and inclusion body formation in alpha-synuclein mice: implications for neurodegenerative disorders. *Science* 287(5456), pp. 1265-1269. doi: 10.1126/science.287.5456.1265

Mastroeni, D. et al. 2009. Microglial responses to dopamine in a cell culture model of Parkinson's disease. *Neurobiol Aging* 30(11), pp. 1805-1817. doi: 10.1016/j.neurobiolaging.2008.01.001

Masuda-Suzukake, M. et al. 2013. Prion-like spreading of pathological α-synuclein in brain. *Brain* 136(4), pp. 1128-1138.

Matsuda, N. et al. 2010. PINK1 stabilized by mitochondrial depolarization recruits Parkin to damaged mitochondria and activates latent Parkin for mitophagy. *Journal of Cell Biology* 189(2), pp. 211-221.

McCaffery, P. and Dräger, U. C. 1994. High levels of a retinoic acid-generating dehydrogenase in the meso-telencephalic dopamine system. *Proc Natl Acad Sci U S A* 91(16), pp. 7772-7776. doi: 10.1073/pnas.91.16.7772

McNaught, K. S., Belizaire, R., Isacson, O., Jenner, P. and Olanow, C. W. 2003. Altered proteasomal function in sporadic Parkinson's disease. *Exp Neurol* 179(1), pp. 38-46. doi: 10.1006/exnr.2002.8050

Medina, M., Urdiales, J. L. and Amores-Sánchez, M. I. 2001. Roles of homocysteine in cell metabolism: old and new functions. *Eur J Biochem* 268(14), pp. 3871-3882. doi: 10.1046/j.1432-1327.2001.02278.x

Mehler-Wex, C., Riederer, P. and Gerlach, M. 2006. Dopaminergic dysbalance in distinct basal ganglia neurocircuits: implications for the pathophysiology of Parkinson's disease, schizophrenia and attention deficit hyperactivity disorder. *Neurotoxicity research* 10(3), pp. 167-179.

Mena, M. A., Casarejos, M. J., Carazo, A., Paíno, C. L. and García de Yébenes, J. 1997. Glia protect fetal midbrain dopamine neurons in culture from L-DOPA toxicity through multiple mechanisms. *J Neural Transm (Vienna)* 104(4-5), pp. 317-328. doi: 10.1007/bf01277654

Mena, M. A., Casarejos, M. J., Solano, R. M. and de Yébenes, J. G. 2009. Half a century of L-DOPA. *Curr Top Med Chem* 9(10), pp. 880-893.

Mena, M. A., Pardo, B., Casarejos, M. J., Fahn, S. and García de Yébenes, J. 1992. Neurotoxicity of levodopa on catecholamine-rich neurons. *Movement disorders : official journal of the Movement Disorder Society* 7(1), pp. 23-31. doi: 10.1002/mds.870070105

Mena, M. A., Pardo, B., Paino, C. L. and De Yebenes, J. G. 1993. Levodopa toxicity in foetal rat midbrain neurones in culture: modulation by ascorbic acid. *Neuroreport* 4(4), pp. 438-440. doi: 10.1097/00001756-199304000-00025

Mendez, I. et al. 2005. Cell type analysis of functional fetal dopamine cell suspension transplants in the striatum and substantia nigra of patients with Parkinson's disease. *Brain* 128(7), pp. 1498-1510. doi: 10.1093/brain/awh510

Mendez, I. et al. 2008. Dopamine neurons implanted into people with Parkinson's disease survive without pathology for 14 years. *Nat Med* 14(5), pp. 507-509. doi: 10.1038/nm1752

Mestas, J. and Hughes, C. C. 2004. Of mice and not men: differences between mouse and human immunology. *J Immunol* 172(5), pp. 2731-2738. doi: 10.4049/jimmunol.172.5.2731

Miceli, M. C. and Parnes, J. R. 1991. The roles of CD4 and CD8 in T cell activation. *Semin Immunol* 3(3), pp. 133-141.

Miklya, I., Göltl, P., Hafenscher, F. and Pencz, N. 2014. [The role of parkin in Parkinson's disease]. *Neuropsychopharmacol Hung* 16(2), pp. 67-76.

Mínguez-Castellanos, A. et al. 2007. Carotid body autotransplantation in Parkinson disease: a clinical and positron emission tomography study. *J Neurol Neurosurg Psychiatry* 78(8), pp. 825-831. doi: 10.1136/jnnp.2006.106021

Mitsumoto, A. and Nakagawa, Y. 2001. DJ-1 is an indicator for endogenous reactive oxygen species elicited by endotoxin. *Free Radic Res* 35(6), pp. 885-893. doi: 10.1080/10715760100301381

Mittermeyer, G. et al. 2012. Long-term evaluation of a phase 1 study of AADC gene therapy for Parkinson's disease. *Hum Gene Ther* 23(4), pp. 377-381. doi: 10.1089/hum.2011.220

Miyazaki, I. and Asanuma, M. 2020. Neuron-Astrocyte Interactions in Parkinson's Disease. *Cells* 9(12), p. 2623. doi: 10.3390/cells9122623

Mochizuki, H., Yamada, M. and Mizuno, Y. 2006. Alpha-synuclein overexpression model. *J Neural Transm Suppl* (70), pp. 281-284.

Montoya, C. P., Campbell-Hope, L. J., Pemberton, K. D. and Dunnett, S. B. 1991. The “staircase test”: a measure of independent forelimb reaching and grasping abilities in rats. *Journal of Neuroscience Methods* 36(2), pp. 219-228. doi: https://doi.org/10.1016/0165-0270(91)90048-5

Mor, D. E. et al. 2017. Dopamine induces soluble α-synuclein oligomers and nigrostriatal degeneration. *Nature neuroscience* 20(11), p. 1560.

Morissette, M., Bourque, M., Tremblay, M. and Di Paolo, T. 2022. Prevention of L-Dopa-Induced Dyskinesias by MPEP Blockade of Metabotropic Glutamate Receptor 5 Is Associated with Reduced Inflammation in the Brain of Parkinsonian Monkeys. *Cells* 11(4), doi: 10.3390/cells11040691

Moro, E. 2016. Complications of DBS surgery — insights from large databases. *Nature Reviews Neurology* 12(11), pp. 617-618. doi: 10.1038/nrneurol.2016.163

Mulas, G. et al. 2016. Differential induction of dyskinesia and neuroinflammation by pulsatile versus continuous l-DOPA delivery in the 6-OHDA model of Parkinson's disease. *Exp Neurol* 286, pp. 83-92. doi: 10.1016/j.expneurol.2016.09.013

Murata, M. 2009. Levodopa in the early treatment of Parkinson's disease. *Parkinsonism Relat Disord* 15 Suppl 1, pp. S17-20. doi: 10.1016/s1353-8020(09)70006-9

Murer, M. G., Dziewczapolski, G., Menalled, L. B., García, M. C., Agid, Y., Gershanik, O. and Raisman-Vozari, R. 1998. Chronic levodopa is not toxic for remaining dopamine neurons, but instead promotes their recovery, in rats with moderate nigrostriatal lesions. *Ann Neurol* 43(5), pp. 561-575. doi: 10.1002/ana.410430504

Myall, D. J., Pitcher, T. L., Pearson, J. F., Dalrymple-Alford, J. C., Anderson, T. J. and MacAskill, M. R. 2017. Parkinson's in the oldest old: Impact on estimates of future disease burden. *Parkinsonism Relat Disord* 42, pp. 78-84. doi: 10.1016/j.parkreldis.2017.06.018

Mytilineou, C., Walker, R. H., JnoBaptiste, R. and Olanow, C. W. 2003. Levodopa is toxic to dopamine neurons in an in vitro but not an in vivo model of oxidative stress. *Journal of Pharmacology and Experimental Therapeutics* 304(2), pp. 792-800.

Nakamura, K. et al. 2011. Direct membrane association drives mitochondrial fission by the Parkinson disease-associated protein alpha-synuclein. *J Biol Chem* 286(23), pp. 20710-20726. doi: 10.1074/jbc.M110.213538

Nalls, M. A. et al. 2019. Identification of novel risk loci, causal insights, and heritable risk for Parkinson's disease: a meta-analysis of genome-wide association studies. *Lancet Neurol* 18(12), pp. 1091-1102. doi: 10.1016/s1474-4422(19)30320-5

Navarro-Romero, A., Montpeyó, M. and Martinez-Vicente, M. 2020. The Emerging Role of the Lysosome in Parkinson's Disease. *Cells* 9(11), p. 2399. doi: 10.3390/cells9112399

Niethammer, M. et al. 2018. Gene therapy reduces Parkinson's disease symptoms by reorganizing functional brain connectivity. *Science translational medicine* 10(469),

Nolbrant, S., Heuer, A., Parmar, M. and Kirkeby, A. 2017. Generation of high-purity human ventral midbrain dopaminergic progenitors for in vitro maturation and intracerebral transplantation. *Nature Protocols* 12(9), p. 1962.

Norris, K. L. et al. 2015. Convergence of Parkin, PINK1, and α-synuclein on stress-induced mitochondrial morphological remodeling. *Journal of Biological Chemistry* 290(22), pp. 13862-13874.

Nutt, J. G., Woodward, W. R. and Anderson, J. L. 1985. The effect of carbidopa on the pharmacokinetics of intravenously administered levodopa: the mechanism of action in the treatment of parkinsonism. *Ann Neurol* 18(5), pp. 537-543. doi: 10.1002/ana.410180505

O'Suilleabhain, P. E., Bottiglieri, T., Dewey, R. B., Jr., Sharma, S. and Diaz-Arrastia, R. 2004a. Modest increase in plasma homocysteine follows levodopa initiation in Parkinson's disease. *Movement disorders : official journal of the Movement Disorder Society* 19(12), pp. 1403-1408. doi: 10.1002/mds.20253

O'Suilleabhain, P. E., Sung, V., Hernandez, C., Lacritz, L., Dewey, R. B., Jr., Bottiglieri, T. and Diaz-Arrastia, R. 2004b. Elevated plasma homocysteine level in patients with Parkinson disease: motor, affective, and cognitive associations. *Arch Neurol* 61(6), pp. 865-868. doi: 10.1001/archneur.61.6.865

Ohama, E. and Ikuta, F. 1976. Parkinson's disease: distribution of Lewy bodies and monoamine neuron system. *Acta neuropathologica* 34(4), pp. 311-319.

Olanow, C. W. 2015. Levodopa: effect on cell death and the natural history of Parkinson's disease. *Movement disorders : official journal of the Movement Disorder Society* 30(1), pp. 37-44. doi: 10.1002/mds.26119

Olanow, C. W. et al. 2014. Continuous intrajejunal infusion of levodopa-carbidopa intestinal gel for patients with advanced Parkinson's disease: a randomised, controlled, double-blind, double-dummy study. *Lancet Neurol* 13(2), pp. 141-149. doi: 10.1016/s1474-4422(13)70293-x

Olanow, C. W., Kordower, J. H., Lang, A. E. and Obeso, J. A. 2009. Dopaminergic transplantation for Parkinson's disease: current status and future prospects. *Ann Neurol* 66(5), pp. 591-596. doi: 10.1002/ana.21778

Olsson, M., Nikkhah, G., Bentlage, C. and Björklund, A. 1995. Forelimb akinesia in the rat Parkinson model: differential effects of dopamine agonists and nigral transplants as assessed by a new stepping test. *The Journal of neuroscience : the official journal of the Society for Neuroscience*

15(5 Pt 2), pp. 3863-3875. doi: 10.1523/jneurosci.15-05-03863.1995

Ono, K., Hirohata, M. and Yamada, M. 2007. Anti-fibrillogenic and fibril-destabilizing activities of anti-Parkinsonian agents for alpha-synuclein fibrils in vitro. *J Neurosci Res* 85(7), pp. 1547-1557. doi: 10.1002/jnr.21271

Ono, K., Takasaki, J., Takahashi, R., Ikeda, T. and Yamada, M. 2013. Effects of antiparkinsonian agents on β-amyloid and α-synuclein oligomer formation in vitro. *J Neurosci Res* 91(10), pp. 1371-1381. doi: 10.1002/jnr.23256

Ono, K. and Yamada, M. 2006. Antioxidant compounds have potent anti-fibrillogenic and fibril-destabilizing effects for alpha-synuclein fibrils in vitro. *J Neurochem* 97(1), pp. 105-115. doi: 10.1111/j.1471-4159.2006.03707.x

Orenstein, S. J. et al. 2013. Interplay of LRRK2 with chaperone-mediated autophagy. *Nature neuroscience* 16(4), pp. 394-406. doi: 10.1038/nn.3350

Paisán-Ruiz, C. 2009. LRRK2 gene variation and its contribution to Parkinson disease. *Human mutation* 30(8), pp. 1153-1160.

Pajares, M., I Rojo, A., Manda, G., Boscá, L. and Cuadrado, A. 2020. Inflammation in Parkinson's Disease: Mechanisms and Therapeutic Implications. *Cells* 9(7), p. 1687. doi: 10.3390/cells9071687

Pandey, S. and Srivanitchapoom, P. 2017. Levodopa-induced Dyskinesia: Clinical Features, Pathophysiology, and Medical Management. *Annals of Indian Academy of Neurology* 20(3), pp. 190-198. doi: 10.4103/aian.AIAN_239_17

Pardo, B., Mena, M. A., Casarejos, M. J., Paíno, C. L. and De Yébenes, J. G. 1995. Toxic effects of L-DOPA on mesencephalic cell cultures: protection with antioxidants. *Brain Research* 682(1), pp. 133-143. doi: https://doi.org/10.1016/0006-8993(95)00341-M

Pardo, B., Mena, M. A., Fahn, S. and García de Yébenes, J. 1993. Ascorbic acid protects against levodopa-induced neurotoxicity on a catecholamine-rich human neuroblastoma cell line. *Movement disorders : official journal of the Movement Disorder Society* 8(3), pp. 278-284. doi: 10.1002/mds.870080305

Parish, C. L. and Thompson, L. H. 2021. Embryonic stem cells go from bench to bedside for Parkinson ' s disease. *Cell Reports Medicine* 2(4), p. 100251. doi: https://doi.org/10.1016/j.xcrm.2021.100251

Park, J. et al. 2006. Mitochondrial dysfunction in Drosophila PINK1 mutants is complemented by parkin. *Nature* 441(7097), pp. 1157-1161. doi: 10.1038/nature04788

Park, K. H., Shin, K. S., Zhao, T. T., Park, H. J., Lee, K. E. and Lee, M. K. 2016. L-DOPA modulates cell

viability through the ERK-c-Jun system in PC12 and dopaminergic neuronal cells. *Neuropharmacology* 101, pp. 87-97. doi: https://doi.org/10.1016/j.neuropharm.2015.09.006

Parkkinen, L. et al. 2011. Does levodopa accelerate the pathologic process in Parkinson disease brain? *Neurology* 77(15), pp. 1420-1426. doi: 10.1212/WNL.0b013e318232ab4c

Parmar, M., Grealish, S. and Henchcliffe, C. 2020. The future of stem cell therapies for Parkinson disease. *Nature Reviews Neuroscience* 21(2), pp. 103-115. doi: 10.1038/s41583-019-0257-7

Paus, S., Brecht, H. M., Köster, J., Seeger, G., Klockgether, T. and Wüllner, U. 2003. Sleep attacks, daytime sleepiness, and dopamine agonists in Parkinson's disease. *Movement disorders : official journal of the Movement Disorder Society* 18(6), pp. 659-667. doi: 10.1002/mds.10417

Peng, Q. et al. 2019. The Rodent Models of Dyskinesia and Their Behavioral Assessment. *Front Neurol* 10, p. 1016. doi: 10.3389/fneur.2019.01016

Perlow, M. J., Freed, W. J., Hoffer, B. J., Seiger, A., Olson, L. and Wyatt, R. J. 1979. Brain grafts reduce motor abnormalities produced by destruction of nigrostriatal dopamine system. *Science* 204(4393), pp. 643-647. doi: 10.1126/science.571147

Perry, T. L., Yong, V. W., Ito, M., Foulks, J. G., Wall, R. A., Godin, D. V. and Clavier, R. M. 1984. Nigrostriatal dopaminergic neurons remain undamaged in rats given high doses of L-DOPA and carbidopa chronically. *J Neurochem* 43(4), pp. 990-993. doi: 10.1111/j.1471-4159.1984.tb12834.x

Piccini, P. et al. 1999. Dopamine release from nigral transplants visualized in vivo in a Parkinson's patient. *Nat Neurosci* 2(12), pp. 1137-1140. doi: 10.1038/16060

Piccini, P. et al. 2005. Factors affecting the clinical outcome after neural transplantation in Parkinson's disease. *Brain* 128(12), pp. 2977-2986. doi: 10.1093/brain/awh649

Piquet, A. L., Venkiteswaran, K., Marupudi, N. I., Berk, M. and Subramanian, T. 2012. The immunological challenges of cell transplantation for the treatment of Parkinson's disease. *Brain Research Bulletin* 88(4), pp. 320-331. doi: 10.1016/j.brainresbull.2012.03.001

Poewe, W. et al. 2017. Parkinson disease. *Nature Reviews Disease Primers* 3(1), p. 17013. doi: 10.1038/nrdp.2017.13

Politis, M. et al. 2011. Graft-induced dyskinesias in Parkinson's disease: High striatal serotonin/dopamine transporter ratio. *Movement disorders : official journal of the Movement Disorder Society* 26(11), pp. 1997-2003. doi: 10.1002/mds.23743

Polymeropoulos, M. H. et al. 1997. Mutation in the α-synuclein gene identified in families with Parkinson's disease. *Science* 276(5321), pp. 2045-2047.

Porras, G., Li, Q. and Bezard, E. 2012. Modeling Parkinson's disease in primates: The MPTP model. *Cold Spring Harbor perspectives in medicine* 2(3), pp. a009308-a009308. doi: 10.1101/cshperspect.a009308

Potashkin, J. A., Blume, S. R. and Runkle, N. K. 2010. Limitations of animal models of Parkinson's disease. *Parkinson's disease* 2011, pp. 658083-658083. doi: 10.4061/2011/658083

Putterman, D. B., Munhall, A. C., Kozell, L. B., Belknap, J. K. and Johnson, S. W. 2007. Evaluation of levodopa dose and magnitude of dopamine depletion as risk factors for levodopa-induced dyskinesia in a rat model of Parkinson's disease. *Journal of Pharmacology and Experimental Therapeutics* 323(1), pp. 277-284.

Quiroga-Varela, A., Aguilar, E., Iglesias, E., Obeso, J. A. and Marin, C. 2017. Short- and long-term effects induced by repeated 6-OHDA intraventricular administration: A new progressive and bilateral rodent model of Parkinson's disease. *Neuroscience* 361, pp. 144-156. doi: 10.1016/j.neuroscience.2017.08.017

Rabey, J. M. et al. 2000. Rasagiline mesylate, a new MAO-B inhibitor for the treatment of Parkinson's disease: a double-blind study as adjunctive therapy to levodopa. *Clin Neuropharmacol* 23(6), pp. 324-330. doi: 10.1097/00002826-200011000-00005

Rangasamy, S. B., Soderstrom, K., Bakay, R. A. and Kordower, J. H. 2010. Neurotrophic factor therapy for Parkinson's disease. *Prog Brain Res* 184, pp. 237-264. doi: 10.1016/s0079-6123(10)84013-0

Ren, H., Fu, K., Mu, C., Zhen, X. and Wang, G. 2012. L166P mutant DJ-1 promotes cell death by dissociating Bax from mitochondrial Bcl-X L. *Molecular neurodegeneration* 7(1), pp. 1-11.

Reyes, S., Fu, Y., Double, K., Thompson, L., Kirik, D., Paxinos, G. and Halliday, G. M. 2012. GIRK2 expression in dopamine neurons of the substantia nigra and ventral tegmental area. *J Comp Neurol* 520(12), pp. 2591-2607. doi: 10.1002/cne.23051

Riederer, P. et al. 2019. α-Synuclein in Parkinson's disease: causal or bystander? *Journal of neural transmission* 126(7), pp. 815-840.

Rimoin, D. L., Pyeritz, R. E. and Korf, B. 2013. *Emery and Rimoin's essential medical genetics*. Elsevier.

Rizek, P., Kumar, N. and Jog, M. S. 2016. An update on the diagnosis and treatment of Parkinson disease. *Cmaj* 188(16), pp. 1157-1165. doi: 10.1503/cmaj.151179

Rocca, W. A. 2018. The burden of Parkinson's disease: a worldwide perspective. *The Lancet Neurology* 17(11), pp. 928-929.

Rodriguez-Pallares, J., Parga, J. A., Muñoz, A., Rey, P., Guerra, M. J. and Labandeira-Garcia, J. L.

2007. Mechanism of 6-hydroxydopamine neurotoxicity: the role of NADPH oxidase and microglial activation in 6-hydroxydopamine-induced degeneration of dopaminergic neurons. *J Neurochem* 103(1), pp. 145-156. doi: 10.1111/j.1471-4159.2007.04699.x

Rogers, J., Mastroeni, D., Leonard, B., Joyce, J. and Grover, A. 2007. Neuroinflammation in Alzheimer's disease and Parkinson's disease: are microglia pathogenic in either disorder? *Int Rev Neurobiol* 82, pp. 235-246. doi: 10.1016/s0074-7742(07)82012-5

Rogers, J. D., Sanchez-Saffon, A., Frol, A. B. and Diaz-Arrastia, R. 2003. Elevated plasma homocysteine levels in patients treated with levodopa: association with vascular disease. *Arch Neurol* 60(1), pp. 59-64. doi: 10.1001/archneur.60.1.59

Rolstad, B. 2001. The athymic nude rat: an animal experimental model to reveal novel aspects of innate immune responses? *Immunol Rev* 184, pp. 136-144. doi: 10.1034/j.1600-065x.2001.1840113.x

Roy, N. S., Cleren, C., Singh, S. K., Yang, L., Beal, M. F. and Goldman, S. A. 2006. Functional engraftment of human ES cell-derived dopaminergic neurons enriched by coculture with telomerase-immortalized midbrain astrocytes. *Nat Med* 12(11), pp. 1259-1268. doi: 10.1038/nm1495

Ruggieri, S., Stocchi, F., Denaro, A., Baronti, F. and Agnoli, A. 1986. The role of MAO-b inhibitors in the treatment of Parkinson's disease. *Journal of Neural transmission. Supplementum* 22, pp. 227-233.

Ryu, Y.-K. et al. 2018. Metformin Inhibits the Development of l-DOPA-Induced Dyskinesia in a Murine Model of Parkinson's Disease. *Molecular Neurobiology* 55(7), pp. 5715-5726. doi: 10.1007/s12035-017-0752-7

Sabens, E. A., Distler, A. M. and Mieyal, J. J. 2010. Levodopa deactivates enzymes that regulate thiol− disulfide homeostasis and promotes neuronal cell death: Implications for therapy of parkinson's disease. *Biochemistry* 49(12), pp. 2715-2724.

Sánchez-Danés, A. et al. 2012. Efficient generation of A9 midbrain dopaminergic neurons by lentiviral delivery of LMX1A in human embryonic stem cells and induced pluripotent stem cells. *Hum Gene Ther* 23(1), pp. 56-69. doi: 10.1089/hum.2011.054

Santini, E., Heiman, M., Greengard, P., Valjent, E. and Fisone, G. 2009. Inhibition of mTOR signaling in Parkinson's disease prevents L-DOPA-induced dyskinesia. *Sci Signal* 2(80), p. ra36. doi: 10.1126/scisignal.2000308

Santini, E. et al. 2007. Critical involvement of cAMP/DARPP-32 and extracellular signal-regulated protein kinase signaling in L-DOPA-induced dyskinesia. *The Journal of neuroscience : the official*

journal of the Society for Neuroscience 27(26), pp. 6995-7005. doi: 10.1523/jneurosci.0852-07.2007

Sarkar, C., Basu, B., Chakroborty, D., Dasgupta, P. S. and Basu, S. 2010. The immunoregulatory role of dopamine: an update. *Brain, behavior, and immunity* 24(4), pp. 525-528. doi: 10.1016/j.bbi.2009.10.015

Sarkar, S. and Biswas, S. C. 2021. Astrocyte subtype-specific approach to Alzheimer's disease treatment. *Neurochem Int* 145, p. 104956. doi: 10.1016/j.neuint.2021.104956

Satake, W. et al. 2009. Genome-wide association study identifies common variants at four loci as genetic risk factors for Parkinson's disease. *Nature Genetics* 41(12), pp. 1303-1307.

Sauer, H. and Oertel, W. H. 1994. Progressive degeneration of nigrostriatal dopamine neurons following intrastriatal terminal lesions with 6-hydroxydopamine: a combined retrograde tracing and immunocytochemical study in the rat. *Neuroscience* 59(2), pp. 401-415. doi: 10.1016/0306-4522(94)90605-x

Sbodio, J. I., Snyder, S. H. and Paul, B. D. 2019. Redox Mechanisms in Neurodegeneration: From Disease Outcomes to Therapeutic Opportunities. *Antioxid Redox Signal* 30(11), pp. 1450-1499. doi: 10.1089/ars.2017.7321

Schallert, T., Fleming, S. M., Leasure, J. L., Tillerson, J. L. and Bland, S. T. 2000. CNS plasticity and assessment of forelimb sensorimotor outcome in unilateral rat models of stroke, cortical ablation, parkinsonism and spinal cord injury. *Neuropharmacology* 39(5), pp. 777-787. doi: https://doi.org/10.1016/S0028-3908(00)00005-8

Schmid, M. C. et al. 2018. Integrin CD11b activation drives anti-tumor innate immunity. *Nature Communications* 9(1), p. 5379. doi: 10.1038/s41467-018-07387-4

Schmitt, I. et al. 2015. L-dopa increases α-synuclein DNA methylation in Parkinson's disease patients in vivo and in vitro. *Movement Disorders* 30(13), pp. 1794-1801.

Schnabolk, G., Tomlinson, S. and Rohrer, B. 2014. The complement regulatory protein CD59: insights into attenuation of choroidal neovascularization. *Adv Exp Med Biol* 801, pp. 435-440. doi: 10.1007/978-1-4614-3209-8_55

Schneider, S. A. and Obeso, J. A. 2014. Clinical and pathological features of Parkinson's disease. *Behavioral Neurobiology of Huntington's disease and Parkinson's disease*, pp. 205-220.

Schober, A. 2004. Classic toxin-induced animal models of Parkinson's disease: 6-OHDA and MPTP. *Cell and tissue research* 318(1), pp. 215-224. doi: 10.1007/s00441-004-0938-y

Schweitzer, J. S. et al. 2020. Personalized iPSC-Derived Dopamine Progenitor Cells for Parkinson's

Disease. *N Engl J Med* 382(20), pp. 1926-1932. doi: 10.1056/NEJMoa1915872

Shahmoradian, S. H. et al. 2019. Lewy pathology in Parkinson's disease consists of crowded organelles and lipid membranes. *Nature neuroscience* 22(7), pp. 1099-1109. doi: 10.1038/s41593-019-0423-2

Sharma, M. et al. 2012. Large-scale replication and heterogeneity in Parkinson disease genetic loci. *Neurology* 79(7), pp. 659-667. doi: 10.1212/WNL.0b013e318264e353

Shihabuddin, L. S., Brundin, P., Greenamyre, J. T., Stephenson, D. and Sardi, S. P. 2018. New Frontiers in Parkinson's Disease: From Genetics to the Clinic. *The Journal of neuroscience : the official journal of the Society for Neuroscience* 38(44), pp. 9375-9382. doi: 10.1523/jneurosci.1666-18.2018

Shimozawa, A. et al. 2019. Effect of L-DOPA/Benserazide on Propagation of Pathological α-Synuclein. *Frontiers in Neuroscience* 13(595), doi: 10.3389/fnins.2019.00595

Shin, E., Rogers, J. T., Devoto, P., Björklund, A. and Carta, M. 2014. Noradrenaline neuron degeneration contributes to motor impairments and development of L-DOPA-induced dyskinesia in a rat model of Parkinson's disease. *Experimental Neurology* 257, pp. 25-38.

Shulskaya, M. V. et al. 2018. Whole-Exome Sequencing in Searching for New Variants Associated With the Development of Parkinson's Disease. *Front Aging Neurosci* 10, p. 136. doi: 10.3389/fnagi.2018.00136

Simon-Sanchez, J. et al. 2009. Genome-wide association study reveals genetic risk underlying Parkinson's disease. *Nature Genetics* 41(12), pp. 1308-1312.

Singh, N., Pillay, V. and Choonara, Y. E. 2007. Advances in the treatment of Parkinson's disease. *Progress in neurobiology* 81(1), pp. 29-44.

Singleton, A. B. et al. 2003. alpha-Synuclein locus triplication causes Parkinson's disease. *Science* 302(5646), p. 841. doi: 10.1126/science.1090278

Singleton, A. B., Farrer, M. J. and Bonifati, V. 2013. The genetics of Parkinson's disease: progress and therapeutic implications. *Movement disorders : official journal of the Movement Disorder Society* 28(1), pp. 14-23. doi: 10.1002/mds.25249

Sironi, F. et al. 2010. α-Synuclein multiplication analysis in Italian familial Parkinson disease. *Parkinsonism & related disorders* 16(3), pp. 228-231.

Sloan, D. J., Wood, M. J. and Charlton, H. M. 1991. The immune response to intracerebral neural grafts. *Trends Neurosci* 14(8), pp. 341-346. doi: 10.1016/0166-2236(91)90159-r

Smidt, M. P. and Burbach, J. P. H. 2007. How to make a mesodiencephalic dopaminergic neuron. *Nature Reviews Neuroscience* 8(1), pp. 21-32. doi: 10.1038/nrn2039

Smith, L. A., Jackson, M. J., Hansard, M. J., Maratos, E. and Jenner, P. 2003. Effect of pulsatile administration of levodopa on dyskinesia induction in drug-naïve MPTP-treated common marmosets: effect of dose, frequency of administration, and brain exposure. *Movement disorders : official journal of the Movement Disorder Society* 18(5), pp. 487-495. doi: 10.1002/mds.10394

Snead, D. and Eliezer, D. 2014. Alpha-synuclein function and dysfunction on cellular membranes. *Experimental neurobiology* 23(4), p. 292.

Soliman, M. K., Mazzio, E. and Soliman, K. F. 2002. Levodopa modulating effects of inducible nitric oxide synthase and reactive oxygen species in glioma cells. *Life sciences* 72(2), pp. 185-198.

Song, J., Kim, B. C., Nguyen, D.-T. T., Samidurai, M. and Choi, S.-M. 2017. Levodopa (L-DOPA) attenuates endoplasmic reticulum stress response and cell death signaling through DRD2 in SH-SY5Y neuronal cells under α-synuclein-induced toxicity. *Neuroscience* 358, pp. 336-348.

Spisák, S. et al. 2015. CAUSEL: an epigenome- and genome-editing pipeline for establishing function of noncoding GWAS variants. *Nat Med* 21(11), pp. 1357-1363. doi: 10.1038/nm.3975

Steece-Collier, K., Collier, T. J., Sladek, C. D. and Sladek, J. R., Jr. 1990. Chronic levodopa impairs morphological development of grafted embryonic dopamine neurons. *Exp Neurol* 110(2), pp. 201-208. doi: 10.1016/0014-4886(90)90031-m

Steece-Collier, K., Soderstrom, K. E., Collier, T. J., Sortwell, C. E. and Maries-Lad, E. 2009. Effect of levodopa priming on dopamine neuron transplant efficacy and induction of abnormal involuntary movements in parkinsonian rats. *J Comp Neurol* 515(1), pp. 15-30. doi: 10.1002/cne.22037

Steece-Collier, K., Yurek, D. M., Collier, T. J., Junn, F. S. and Sladek, J. R., Jr. 1995. The detrimental effect of levodopa on behavioral efficacy of fetal dopamine neuron grafts in rats is reversible following prolonged withdrawal of chronic dosing. *Brain Res* 676(2), pp. 404-408. doi: 10.1016/0006-8993(95)00149-k

Stocchi, F. 2005. Optimising levodopa therapy for the management of Parkinson's disease. *Journal of Neurology* 252(4), pp. iv43-iv48. doi: 10.1007/s00415-005-4009-4

Stocchi, F. 2006. The levodopa wearing-off phenomenon in Parkinson's disease: pharmacokinetic considerations. *Expert Opin Pharmacother* 7(10), pp. 1399-1407. doi: 10.1517/14656566.7.10.1399

Stocchi, F. 2009. Dopamine receptor agonists in the treatment of advanced Parkinson's disease. *Parkinsonism Relat Disord* 15 Suppl 4, pp. S54-57. doi: 10.1016/s1353-8020(09)70836-3

Stojkovska, I., Wagner, B. M. and Morrison, B. E. 2015. Parkinson's disease and enhanced

inflammatory response. *Experimental biology and medicine (Maywood, N.J.)* 240(11), pp. 1387-1395. doi: 10.1177/1535370215576313

Stoker, T. B. 2018. Stem Cell Treatments for Parkinson's Disease. In: Stoker, T.B. and Greenland, J.C. eds. *Parkinson's Disease: Pathogenesis and Clinical Aspects*. Brisbane (AU): Codon Publications Copyright: The Authors.

Stott, S. R. W. and Barker, R. A. 2014. Time course of dopamine neuron loss and glial response in the 6-OHDA striatal mouse model of Parkinson's disease. *Eur J Neurosci* 39(6), pp. 1042-1056. doi: 10.1111/ejn.12459

Studer, L. 2017. Chapter 8 - Strategies for bringing stem cell-derived dopamine neurons to the clinic—The NYSTEM trial. In: Dunnett, S.B. and Björklund, A. eds. *Progress in brain research*. Vol. 230. Elsevier, pp. 191-212.

Su, R. and Zhou, T. 2021. Alpha-Synuclein Induced Immune Cells Activation and Associated Therapy in Parkinson's Disease. *Frontiers in Aging Neuroscience* 13, doi: 10.3389/fnagi.2021.769506

Sun, J., Wang, L., Bao, H., Premi, S., Das, U., Chapman, E. R. and Roy, S. 2019. Functional cooperation of α-synuclein and VAMP2 in synaptic vesicle recycling. *Proceedings of the National Academy of Sciences* 116(23), pp. 11113-11115.

Surmeier, D. J., Guzman, J. N., Sanchez-Padilla, J. and Goldberg, J. A. 2011. The origins of oxidant stress in Parkinson's disease and therapeutic strategies. *Antioxid Redox Signal* 14(7), pp. 1289-1301. doi: 10.1089/ars.2010.3521

Sveinbjornsdottir, S. 2016. The clinical symptoms of Parkinson's disease. *Journal of neurochemistry* 139, pp. 318-324.

Swistowski, A., Peng, J., Liu, Q., Mali, P., Rao, M. S., Cheng, L. and Zeng, X. 2010. Efficient generation of functional dopaminergic neurons from human induced pluripotent stem cells under defined conditions. *Stem cells* 28(10), pp. 1893-1904. doi: 10.1002/stem.499

Takahashi, K. and Yamanaka, S. 2006. Induction of pluripotent stem cells from mouse embryonic and adult fibroblast cultures by defined factors. *Cell* 126(4), pp. 663-676. doi: 10.1016/j.cell.2006.07.024

Tambasco, N., Romoli, M. and Calabresi, P. 2018. Levodopa in Parkinson's Disease: Current Status and Future Developments. *Curr Neuropharmacol* 16(8), pp. 1239-1252. doi: 10.2174/1570159x15666170510143821

Tamburrino, A. et al. 2015. Cyclosporin promotes neurorestoration and cell replacement therapy in pre-clinical models of Parkinson's disease. *Acta neuropathologica communications* 3, pp. 84-

84. doi: 10.1186/s40478-015-0263-6

Tan, E.-K., Chao, Y.-X., West, A., Chan, L.-L., Poewe, W. and Jankovic, J. 2020. Parkinson disease and the immune system — associations, mechanisms and therapeutics. *Nature Reviews Neurology* 16(6), pp. 303-318. doi: 10.1038/s41582-020-0344-4

Teo, K. C. and Ho, S.-L. 2013. Monoamine oxidase-B (MAO-B) inhibitors: implications for disease-modification in Parkinson's disease. *Translational Neurodegeneration* 2(1), pp. 1-10.

Thakur, P. et al. 2017. Modeling Parkinson's disease pathology by combination of fibril seeds and α-synuclein overexpression in the rat brain. *Proceedings of the National Academy of Sciences* 114(39), pp. E8284-E8293.

Thanvi, B. R. and Lo, T. C. 2004. Long term motor complications of levodopa: clinical features, mechanisms, and management strategies. *Postgrad Med J* 80(946), pp. 452-458. doi: 10.1136/pgmj.2003.013912

Thiele, S. L., Warre, R. and Nash, J. E. 2012. Development of a unilaterally-lesioned 6-OHDA mouse model of Parkinson's disease. *J Vis Exp* (60), doi: 10.3791/3234

Thompson, L., Barraud, P., Andersson, E., Kirik, D. and Björklund, A. 2005. Identification of dopaminergic neurons of nigral and ventral tegmental area subtypes in grafts of fetal ventral mesencephalon based on cell morphology, protein expression, and efferent projections. *The Journal of neuroscience : the official journal of the Society for Neuroscience* 25(27), pp. 6467-6477. doi: 10.1523/jneurosci.1676-05.2005

Thomson, J. A., Itskovitz-Eldor, J., Shapiro, S. S., Waknitz, M. A., Swiergiel, J. J., Marshall, V. S. and Jones, J. M. 1998. Embryonic stem cell lines derived from human blastocysts. *Science* 282(5391), pp. 1145-1147. doi: 10.1126/science.282.5391.1145

Tiklová, K. et al. 2020. Single cell transcriptomics identifies stem cell-derived graft composition in a model of Parkinson's disease. *Nat Commun* 11(1), p. 2434. doi: 10.1038/s41467-020-16225-5

Tolosa, E., Wenning, G. and Poewe, W. 2006. The diagnosis of Parkinson's disease. *The Lancet Neurology* 5(1), pp. 75-86.

Tomishima, M. and Kirkeby, A. 2021. Bringing Advanced Therapies for Parkinson's Disease to the Clinic: The Scientist's Perspective. *Journal of Parkinson's disease* 11, pp. S135-S140. doi: 10.3233/JPD-212685

Tompkins, M. M., Basgall, E. J., Zamrini, E. and Hill, W. D. 1997. Apoptotic-like changes in Lewy-body-associated disorders and normal aging in substantia nigral neurons. *The American journal of pathology* 150(1), pp. 119-131.

Torres, E. M. and Dunnett, S. B. 2011. 6-OHDA lesion models of Parkinson's disease in the rat.*Animal models of movement disorders*. Springer, pp. 267-279.

Torres, E. M., Lane, E. L., Heuer, A., Smith, G. A., Murphy, E. and Dunnett, S. B. 2011. Increased efficacy of the 6-hydroxydopamine lesion of the median forebrain bundle in small rats, by modification of the stereotaxic coordinates. *J Neurosci Methods* 200(1), pp. 29-35. doi: 10.1016/j.jneumeth.2011.06.012

Torres, P. S., Zapata, D. A., Pacheco-Castro, A., Rodríguez-Fernández, J. L., Cabañas, C. and Regueiro, J. R. 2002. Contribution of CD3 gamma to TCR regulation and signaling in human mature T lymphocytes. *Int Immunol* 14(11), pp. 1357-1367. doi: 10.1093/intimm/dxf095

Trinh, J., Guella, I. and Farrer, M. J. 2014. Disease penetrance of late-onset parkinsonism: a meta-analysis. *JAMA Neurol* 71(12), pp. 1535-1539. doi: 10.1001/jamaneurol.2014.1909

Truong, L., Allbutt, H., Kassiou, M. and Henderson, J. M. 2006. Developing a preclinical model of Parkinson's disease: a study of behaviour in rats with graded 6-OHDA lesions. *Behav Brain Res* 169(1), pp. 1-9. doi: 10.1016/j.bbr.2005.11.026

Tysnes, O.-B. and Storstein, A. 2017. Epidemiology of Parkinson's disease. *Journal of neural transmission* 124(8), pp. 901-905.

Ulusoy, A., Björklund, T., Buck, K. and Kirik, D. 2012. Dysregulated dopamine storage increases the vulnerability to α-synuclein in nigral neurons. *Neurobiology of disease* 47(3), pp. 367-377.

Ulusoy, A., Decressac, M., Kirik, D. and Björklund, A. 2010. Viral vector-mediated overexpression of α-synuclein as a progressive model of Parkinson's disease. *Progress in brain research* 184, pp. 89-111.

Ungerstedt, U. 1968. 6-Hydroxy-dopamine induced degeneration of central monoamine neurons. *Eur J Pharmacol* 5(1), pp. 107-110. doi: 10.1016/0014-2999(68)90164-7

Ungerstedt, U. and Arbuthnott, G. W. 1970. Quantitative recording of rotational behavior in rats after 6-hydroxy-dopamine lesions of the nigrostriatal dopamine system. *Brain Res* 24(3), pp. 485-493. doi: 10.1016/0006-8993(70)90187-3

Uversky, V. N. 2008. α-synuclein misfolding and neurodegenerative diseases. *Current Protein and Peptide Science* 9(5), pp. 507-540.

Valente, E. M. et al. 2004. Hereditary early-onset Parkinson's disease caused by mutations in PINK1. *Science* 304(5674), pp. 1158-1160.

Valkovic, P., Benetin, J., Blazícek, P., Valkovicová, L., Gmitterová, K. and Kukumberg, P. 2005. Reduced plasma homocysteine levels in levodopa/entacapone treated Parkinson patients.

Parkinsonism Relat Disord 11(4), pp. 253-256. doi: 10.1016/j.parkreldis.2005.01.007

Van der Perren, A., Casteels, C., Van Laere, K., Gijsbers, R., Van den Haute, C. and Baekelandt, V. 2016. Development of an Alpha-synuclein Based Rat Model for Parkinson's Disease via Stereotactic Injection of a Recombinant Adeno-associated Viral Vector. *J Vis Exp* (108), p. 53670. doi: 10.3791/53670

Vargas, J. Y., Grudina, C. and Zurzolo, C. 2019. The prion-like spreading of α-synuclein: From in vitro to in vivo models of Parkinson's disease. *Ageing Research Reviews* 50, pp. 89-101. doi: https://doi.org/10.1016/j.arr.2019.01.012

Virameteekul, S., Phokaewvarangkul, O. and Bhidayasiri, R. 2021. Profiling the most elderly parkinson's disease patients: Does age or disease duration matter? *PloS one* 16(12), p. e0261302. doi: 10.1371/journal.pone.0261302

Vivekanantham, S., Shah, S., Dewji, R., Dewji, A., Khatri, C. and Ologunde, R. 2015. Neuroinflammation in Parkinson's disease: role in neurodegeneration and tissue repair. *Int J Neurosci* 125(10), pp. 717-725. doi: 10.3109/00207454.2014.982795

Volpicelli-Daley, L. A., Luk, K. C. and Lee, V. M. 2014. Addition of exogenous α-synuclein preformed fibrils to primary neuronal cultures to seed recruitment of endogenous α-synuclein to Lewy body and Lewy neurite–like aggregates. *Nature Protocols* 9(9), pp. 2135-2146.

Volpicelli-Daley, Laura A. et al. 2011. Exogenous α-Synuclein Fibrils Induce Lewy Body Pathology Leading to Synaptic Dysfunction and Neuron Death. *Neuron* 72(1), pp. 57-71. doi: https://doi.org/10.1016/j.neuron.2011.08.033

Von Coelln, R. et al. 2006. Inclusion body formation and neurodegeneration are parkin independent in a mouse model of α-synucleinopathy. *Journal of Neuroscience* 26(14), pp. 3685-3696.

Wakabayashi, K., Tanji, K., Mori, F. and Takahashi, H. 2007. The Lewy body in Parkinson's disease: molecules implicated in the formation and degradation of α - synuclein aggregates. *Neuropathology* 27(5), pp. 494-506.

Walkinshaw, G. and Waters, C. M. 1995. Induction of apoptosis in catecholaminergic PC12 cells by L-DOPA. Implications for the treatment of Parkinson's disease. *J Clin Invest* 95(6), pp. 2458-2464. doi: 10.1172/jci117946

Wallings, R. L., Herrick, M. K. and Tansey, M. G. 2020. Linking mitochondria to the immune response. *eLife* 9, p. e56214. doi: 10.7554/eLife.56214

Walsh, S., Finn, D. P. and Dowd, E. 2011. Time-course of nigrostriatal neurodegeneration and neuroinflammation in the 6-hydroxydopamine-induced axonal and terminal lesion models of

Parkinson's disease in the rat. *Neuroscience* 175, pp. 251-261. doi: 10.1016/j.neuroscience.2010.12.005

Walz, W. 2016. Experimental Neurosurgery in Animal Models, vol. 116. New York, NY: Springer New York.

Wang, H., Zhao, L., Sun, Z., Sun, L., Zhang, B. and Zhao, Y. 2006. A potential side effect of cyclosporin A: inhibition of CD4(+)CD25(+) regulatory T cells in mice. *Transplantation* 82(11), pp. 1484-1492. doi: 10.1097/01.tp.0000246312.89689.17

Wang, X., Petrie, T. G., Liu, Y., Liu, J., Fujioka, H. and Zhu, X. 2012. Parkinson's disease-associated DJ-1 mutations impair mitochondrial dynamics and cause mitochondrial dysfunction. *Journal of neurochemistry* 121(5), pp. 830-839.

Wang, Z. H. et al. 2002. Therapeutic effects of astrocytes expressing both tyrosine hydroxylase and brain-derived neurotrophic factor on a rat model of Parkinson's disease. *Neuroscience* 113(3), pp. 629-640. doi: https://doi.org/10.1016/S0306-4522(02)00204-X

Watts, R. L. et al. 1997. Effect of stereotaxic intrastriatal cografts of autologous adrenal medulla and peripheral nerve in Parkinson's disease: two-year follow-up study. *Exp Neurol* 147(2), pp. 510-517. doi: 10.1006/exnr.1997.6626

Wenning, G. K. et al. 1997. Short-and long-term survival and function of unilateral intrastriatal dopaminergic grafts in Parkinson's disease. *Annals of Neurology: Official Journal of the American Neurological Association and the Child Neurology Society* 42(1), pp. 95-107.

Whone, A. et al. 2019. Randomized trial of intermittent intraputamenal glial cell line-derived neurotrophic factor in Parkinson's disease. *Brain* 142(3), pp. 512-525. doi: 10.1093/brain/awz023

Winkler, C., Kirik, D., Björklund, A. and Cenci, M. A. 2002. L-DOPA-induced dyskinesia in the intrastriatal 6-hydroxydopamine model of parkinson's disease: relation to motor and cellular parameters of nigrostriatal function. *Neurobiol Dis* 10(2), pp. 165-186. doi: 10.1006/nbdi.2002.0499

Winklhofer, K. F. and Haass, C. 2010. Mitochondrial dysfunction in Parkinson's disease. *Biochimica et Biophysica Acta (BBA)-Molecular Basis of Disease* 1802(1), pp. 29-44.

Wong, Y. C., Kim, S., Peng, W. and Krainc, D. 2019. Regulation and Function of Mitochondria-Lysosome Membrane Contact Sites in Cellular Homeostasis. *Trends Cell Biol* 29(6), pp. 500-513. doi: 10.1016/j.tcb.2019.02.004

Xi, J., Liu, Y., Liu, H., Chen, H., Emborg, M. E. and Zhang, S. C. 2012. Specification of midbrain dopamine neurons from primate pluripotent stem cells. *Stem cells* 30(8), pp. 1655-1663. doi: 10.1002/stem.1152

Yang, K., Zhao, X., Wang, C., Zeng, C., Luo, Y. and Sun, T. 2021. Circuit Mechanisms of L-DOPA-Induced Dyskinesia (LID). *Front Neurosci* 15, p. 614412. doi: 10.3389/fnins.2021.614412

Yasuhara, T., Kameda, M., Sasaki, T., Tajiri, N. and Date, I. 2017. Cell therapy for Parkinson's disease. *Cell transplantation* 26(9), pp. 1551-1559.

Yates, D. 2019. Taking a closer look at PD pathology. *Nature Reviews Neuroscience* 20(9), pp. 511-511. doi: 10.1038/s41583-019-0207-4

Ye, J. et al. 2017. High quality clinical grade human embryonic stem cell lines derived from fresh discarded embryos. *Stem cell research & therapy* 8(1), pp. 1-13.

Yen, G. C. and Hsieh, C. L. 1997. Antioxidant effects of dopamine and related compounds. *Biosci Biotechnol Biochem* 61(10), pp. 1646-1649. doi: 10.1271/bbb.61.1646

Youn, J. et al. 2019. Genetic variants of PARK genes in Korean patients with early-onset Parkinson's disease. *Neurobiol Aging* 75, pp. 224.e229-224.e215. doi: 10.1016/j.neurobiolaging.2018.10.030

Yuan, J., Lei, Z. N., Wang, X., Deng, Y. J. and Chen, D. B. 2015. Interaction between Oc-1 and Lmx1a promotes ventral midbrain dopamine neural stem cells differentiation into dopamine neurons. *Brain Res* 1608, pp. 40-50. doi: 10.1016/j.brainres.2015.02.046

Yun, S. P. et al. 2018. Block of A1 astrocyte conversion by microglia is neuroprotective in models of Parkinson's disease. *Nature Medicine* 24(7), pp. 931-938. doi: 10.1038/s41591-018-0051-5

Yurek, D. M., Steece-Collier, K., Collier, T. J. and Sladek, J. R., Jr. 1991. Chronic levodopa impairs the recovery of dopamine agonist-induced rotational behavior following neural grafting. *Exp Brain Res* 86(1), pp. 97-107. doi: 10.1007/bf00231044

Zarranz, J. J. et al. 2004. The new mutation, E46K, of α-synuclein causes parkinson and Lewy body dementia. *Annals of Neurology: Official Journal of the American Neurological Association and the Child Neurology Society* 55(2), pp. 164-173.

Zhang, M., Chen, L., Wang, S. and Wang, T. 2009. Rab7: roles in membrane trafficking and disease. *Biosci Rep* 29(3), pp. 193-209. doi: 10.1042/bsr20090032

Zhang, W., Zecca, L., Wilson, B., Ren, H. W., Wang, Y. J., Wang, X. M. and Hong, J. S. 2013. Human neuromelanin: an endogenous microglial activator for dopaminergic neuron death. *Front Biosci (Elite Ed)* 5, pp. 1-11. doi: 10.2741/e591

Zhang, Y. and Burock, M. A. 2020. Diffusion Tensor Imaging in Parkinson's Disease and Parkinsonian Syndrome: A Systematic Review. *Frontiers in neurology* 11, doi: 10.3389/fneur.2020.531993

Ziv, I., Zilkha-Falb, R., Offen, D., Shirvan, A., Barzilai, A. and Melamed, E. 1997. Levodopa induces apoptosis in cultured neuronal cells—a possible accelerator of nigrostriatal degeneration in Parkinson's disease? *Movement disorders: official journal of the Movement Disorder Society* 12(1), pp. 17-23.

Zoccolella, S. et al. 2009. Hyperhomocysteinemia in levodopa-treated patients with Parkinson's disease dementia. *Movement disorders : official journal of the Movement Disorder Society* 24(7), pp. 1028-1033. doi: 10.1002/mds.22511